

USING METABOLIC AND BIOCHEMICAL CHARACTERISTICS OF
POSTMORTEM MUSCLE TO INVESTIGATE THE INTERCONNECTEDNESS OF
BEEF COLOR, FLAVOR, AND TENDERNESS

A Dissertation
presented to
the Faculty of the Graduate School
at the University of Missouri-Columbia

In Partial Fulfillment
of the Requirements for the Degree
Doctor of Philosophy

by
JADE VICTORIA COOPER
Dr. Carol L. Lorenzen, Dissertation Supervisor

JULY 2021

The undersigned, appointed by the dean of the Graduate School, have examined the dissertation entitled

USING METABOLIC AND BIOCHEMICAL CHARACTERISTICS OF
POSTMORTEM MUSCLE TO INVESTIGATE THE INTERCONNECTEDNESS OF
BEEF COLOR, FLAVOR, AND TENDERNESS

presented by Jade V. Cooper, a candidate for the degree of Doctor of Philosophy in Animal Science, and hereby certify that, in their opinion, it is worthy of acceptance.

Dr. Carol L. Lorenzen (Chair)

Dr. D. Andy King

Dr. Andrew D. Clarke

Dr. Allison M. Meyer

Dr. Matthew C. Lucy

Acknowledgements:

Thank you to my advisor, Dr. Carol Lorenzen for believing in me, supporting me, encouraging me, and providing me with endless opportunities to become a better version of myself. I am forever grateful for the six years I have been your student. You are truly an inspiration to me.

Dr. Andy King, thank you for allowing me to spend the last year and a half in your lab. I have grown as a scientist and as a person and I appreciate the role you have played in that. Your encouragement and support are things I will always be thankful for.

I would not have made it through this program without Dr. Allison Meyer. Thank you for being in my corner no matter what. You believed in me on days where I didn't believe in myself, and I am eternally grateful for those moments.

Dr. Andrew Clarke, I appreciate your endless support and encouragement no matter the endeavor. You are one heck of an international travel buddy!

Dr. Matt Lucy, I am very grateful you agreed to be on my committee. Your insight, support, and encouragement throughout the process was invaluable to me.

I want to thank Dr. Bryon Wiegand for being a support system for me in all endeavors. Thank you for encouraging me through all the highs and the lows.

Thanks to Dr. Bill Lamberson for allowing me to chase any and all opportunities and dreams that I had. I am a better scientist and individual because you allowed me to grow into one.

Thank you to Rick Disselhorst and the meat lab crew. I would not be near where I am without you all.

Thanks to Zach Callahan and the Weigand lab crew, both past and present, for their help and assistance with any projects.

I want to thank my collaborators Dr. Surendranathan Suman, Dr. Steven Lonergan, and Dr. Peter Sutovsky for their contributions to research done in this dissertation.

Thank you to everyone at US MARC, Dr. Tommy Wheeler, Dr. Steven Shackelford, Dr. Amanda Lindholm-Perry, Dr. Sarah Murray, Patty Beska, Kristen Ostdiek, Casey Trambley, and a huge thank you to Peg Ekren and Megan Landes-Murphy.

I want to thank my friends and support system: Hannah Bingham, Michala Paris, Bria'na Scott, Addison Byrne, Dr. Kelly Vierck, Dr. Karl Kerns, Dr. Harly Durbin, Dr. Troy Rowan, Maggie Nevins, Dr. Deb VanOverbeke, Dr. Shannon Ferrell, Colby Redifer, Josh Zeltwanger, Lindsay Fowler, and Jarmon Stokley. I truly could not have done this without them.

A big thank you to Josh and Tyla Woods for always opening their home to me when I needed a break and for loving and supporting me through all things.

My older sister Emily, for always being one call away.

My Dad and Donna Faye for always believing in me and what I choose to do.

My Mom and Billy, for being my biggest supporters, cheerleaders, and listening ears. I am grateful to have the support at home that I do.

My biggest thank you goes to my three pet children: Lincoln, Roosevelt, and DJ. Thank you for loving me. Thank you for being the reason I got out of bed most days. I need you more than you will ever need me.

Table of Contents

Acknowledgements	ii
List of Tables.....	vi
List of Figures.....	viii
Abstract.....	ix
Chapter 1 - Literature Review.....	1
Post Harvest Factors.....	1
Metabolism and Biochemistry of Beef Color.....	10
Metabolism and Biochemistry of Beef Tenderness.....	22
Metabolism and Biochemistry of Beef Flavor.....	29
Recent Developments and Needs.....	31
Chapter 2 - Muscle color attributes and myoglobin exhibit relationships with tenderness measurements and calpain-1 abundance in beef.....	33
Abstract.....	33
Introduction.....	34
Materials and Methods.....	36
Results and Discussion.....	40
Conclusion.....	47
Chapter 3 - Color stability and tenderness attributes are impacted by metabolic and biochemical characteristics of beef <i>longissimus lumborum</i> steaks at two different aging periods.....	57
Abstract.....	57
Introduction.....	58
Materials and Methods.....	61
Results	77
Discussion.....	85
Conclusion.....	87
Chapter 4 - Aging time and metabolic characteristics impact beef palatability components and flavor attributes in beef <i>longissimus lumborum</i> steaks.....	101
Abstract.....	101
Introduction.....	102

Materials and Methods.....	103
Results	116
Discussion.....	124
Conclusion.....	128
Chapter 5 - Conclusion	140
Appendix A	142
Appendix B	144
Appendix C	228
Appendix D	236
Literature Cited.....	258
Vita.....	282

List of Tables

Table 2.1 Mean (\pm SD) animal and carcass characteristics of Holstein beef carcasses (n = 31).....	49
Table 2.2 Pearson correlation coefficients of carcass characteristics, shear force measurements, and calpain-1 concentrations of LL steaks from Holstein beef carcasses (n =31)	50
Table 2.3 Mean \pm SEM values for objective color, myoglobin redox forms, myoglobin concentration, metmyoglobin reducing activity, shear force, and calpain -1 concentrations at 0, 48, and 336 h postmortem in steaks from Holstein beef carcasses (n = 31).....	51
Table 2.4 Pearson correlation coefficients of metmyoglobin reducing activity, total myoglobin concentration, shear force measurements, and calpain-1 relative abundance of LL steaks from Holstein beef carcasses (n = 31).....	52
Table 2.5. Pearson correlation coefficients of objective color measurements, myoglobin redox forms, shear force measurements and calpain-1 relative abundance of LL steaks from Holstein beef carcasses (n = 31).....	53
Table 3.1. Descriptive attributes of cluster groupings related to color stability and tenderness attributes of beef <i>longissimus lumborum</i> steaks at two aging periods.....	89
Table 3.2. LS Means (SEM) of metabolic and muscle characteristics of beef <i>longissimus lumborum</i> steaks in four clusters aged for 12 or 26 d.....	90
Table 3.3. LS Means (SEM) of tenderness attributes of beef <i>longissimus lumborum</i> steaks in four clusters.....	91
Table 3.4. LS Means (SEM) of muscle biochemical and metabolic attributes of beef <i>longissimus lumborum</i> steaks in four color tenderness groups.....	92
Table 3.5. LS Means of tenderness attributes of beef <i>longissimus lumborum</i> steaks aged for 12 or 26 d.....	93
Table 3.6. LS Means of tenderness attributes of beef <i>longissimus lumborum</i> steaks aged for 12 or 26 d.....	94
Table 3.7. Regression coefficients (SE) for the change in a^* during simulated retail display in beef <i>longissimus lumborum</i> steaks in four clusters aged for 12 or 26 d.....	95

Table 3.8. Correlation coefficients for color and tenderness attributes with metabolic and biochemical attributes in beef <i>longissimus lumborum</i> steaks aged 12 d.....	96
Table 3.9. Correlation coefficients for color and tenderness attributes with metabolic and biochemical attributes in beef <i>longissimus lumborum</i> steaks aged 26 d.....	97
Table 4.1: Least-squares means (SEM) for palatability components, flavor attributes and biochemical characteristics of steaks from the <i>longissimus lumborum</i> from three cluster groupings at 12 or 26 days of aging.....	130
Table 4.2: Least-squares means (SEM) for palatability components ¹ and flavor ² attributes of beef steaks from the <i>longissimus lumborum</i> in three flavor cluster groupings.....	131
Table 4.3: Least-squares means for palatability ¹ and flavor ² attributes of steaks from the <i>longissimus lumborum</i> at 12 or 26 days postmortem.....	132
Table 4.4: Pearson correlation coefficients of palatability components and flavor attributes ³ in beef steaks from the <i>longissimus lumborum</i>	133
Table 4.5: Least-squares means for muscle characteristics and residual metabolism intermediates in beef steaks from the <i>longissimus lumborum</i> in three cluster groupings	134
Table 4.6: Least-squares means for muscle characteristics and residual metabolism intermediates of beef steaks from the <i>longissimus lumborum</i> at 12 or 26 days postmortem	135
Table 4.7: Correlation coefficients of muscle characteristics and residual metabolism intermediates of beef steaks from the <i>longissimus lumborum</i> at both aging periods.....	136
Table 4.8: Pearson correlation coefficients of sensory panel palatability ¹⁵ and flavor attributes ¹⁶ with muscle characteristics and residual metabolism intermediates in beef steaks from the <i>longissimus lumborum</i>	137

List of Figures

Fig. 2.1. Ultimate A.) Temperature and B.) pH decline of Holstein beef carcasses (n = 31) at 0, 24, and 48 h postmortem.....	54
Fig. 2.2. Values for A.) Slice and B.) Warner-Bratzler shear force of LL steaks from Holstein beef carcasses (n = 31) at 48 and 336 h postmortem.....	55
Fig. 2.3. Mean values and example bands for Calpain-1 (80 kDa) relative abundance of LL steaks from Holstein beef carcasses (n = 31) at 0, 48, and 336 h postmortem with representative bands.....	56
Fig. 3.1. Change in a* reflectance values over the duration of retail display for four cluster groups at two different aging periods.....	98
Fig. 3.2. A) Principal Component Analysis of color and tenderness attributes B) Score Plot for Cluster Groupings C.) Loading plot of metabolic and biochemical characteristics of beef <i>longissimus lumborum</i> steaks aged for 12 days.....	99
Fig. 3.3. A) Principal Component Analysis of color and tenderness attributes B) Score Plot for Cluster Groupings C.) Loading plot of metabolic and biochemical characteristics of beef <i>longissimus lumborum</i> steaks aged for 26 days.....	100
Figure 4.1. A) Principal Component Analysis of flavor attributes B) Score Plot for Cluster Groupings C.) Loading plot of metabolic and biochemical characteristics of beef <i>longissimus lumborum</i> steaks aged for 12 days	138
Figure 4.2. A) Principal Component Analysis of flavor attributes B) Score Plot for Cluster Groupings C.) Loading plot of metabolic and biochemical characteristics of beef <i>longissimus lumborum</i> steaks aged for 26 days.....	139

USING METABOLIC AND BIOCHEMICAL CHARACTERISTICS OF
POSTMORTEM MUSCLE TO INVESTIGATE THE INTERCONNECTEDNESS OF
BEEF COLOR, FLAVOR, AND TENDERNESS

Jade Cooper

Dr. Carol Lorenzen, Dissertation Supervisor

ABSTRACT

Understanding relationships between beef palatability and quality components are crucial for continued production of high quality and consistent beef products. Myoglobin concentrations at 48 and 336 h resulted in moderate, negative correlations ($P < 0.05$) to Warner-Bratzler shear force (WBSF) values at 336 h postmortem. Metmyoglobin reducing activity at 336 h exhibited moderate, positive ($P < 0.05$) relationships with slice shear force (SSF) and WBSF values at 48 h. L^* , a^* , and b^* values at 48 h resulted in moderate, positive correlations ($P < 0.05$) with WBSF values at 48 and 336 h. L^* values at 336 h exhibited moderate, positive correlations with SSF values at 336 h and WBSF values at both 48 and 336 h. Values for b^* at 336 h exhibited moderate, positive correlations with calpain-1 concentration at 0 and 336 h. Relationships between glycolytic and oxidative intermediates and color stability and tenderness attributes indicate that muscle metabolic state and biochemical attributes play a role in the animal to animal variation of quality attributes in beef *longissimus lumborum* at two aging periods. Traits associated with increased oxidative capacity such as oxygen consumption and NORA were negatively ($P < 0.05$) related with attributes such as overall tenderness, juiciness, beef, brown and umami and positively ($P < 0.05$) related with attribute such as musty, spoiled, bitter and heated oil. Data indicate that metabolic profile and aging time contribute to color stability, tenderness, flavor profile development and overall palatability.

Chapter 1

Literature Review

1) Conversion of Muscle to Meat and Factors Impacting Meat Quality and Palatability Traits

Extrinsic and Pre-harvest factors

Species, breed, environment/management, genetics, stress:

There are a variety of pre-harvest factors that have a direct impact on the conversion of the muscle to meat process and ultimate meat quality that have been well reviewed. The impacts of chronic stress prior to slaughter on muscle glycogen depletion and ultimate carcass composition has been extensively explored and reviewed (Hedrick et al., 1959; Wismer-Pederson, 1959; Ferguson and Warner, 2008). Increased stress prior to slaughter can deplete glycogen reserves within the muscle. This can result in early cessation of glycolysis postmortem and impact rate and extent of pH decline. Dark, firm, and dry beef is often associated with chronic stress. Genetic and environmental factors impacting meat quality have been reviewed describing the impact on meat color and color stability, tenderness development, intramuscular fat, oxidative stress susceptibility, and energy metabolism (Hocquette et al., 2007; Warner et al., 2010).

Post-harvest factors

Rigor development, metabolism and energy production, pH decline and ultimate pH, temperature decline:

When an animal is exsanguinated, the oxygen supply is terminated and metabolism switches from primarily aerobic to anaerobic. During the conversion of muscle to meat, biochemical metabolism of muscle undergoes significant changes while trying to maintain homeostasis; ATP is primarily generated through anaerobic glycolytic pathways from glucose stored as glycogen. Creatine phosphate is hydrolyzed to buffer ATP level in living muscle and in early postmortem muscle. Reserves of creatine phosphate exhaust rapidly in postmortem muscle leading to a rise in concentration of ADP (Ferguson and Gerrard, 2014). Postmortem ATP is consumed to maintain membrane potential; calcium ion preservation within the sarcoplasmic reticulum (Pösö and Puolanne, 2005). The stiffening of muscle during rigor onset can be attributed to the decrease in ATP and availability for relaxation to occur (Bate-Smith and Bendall, 1947; Kuffi et al., 2018).

Lactate, a byproduct of glycolysis, accumulates in muscle due to halted circulation. Generally, the drop in pH in postmortem muscle from 7.2 to approximately 5.5 has been considered to be due to lactate buildup during anaerobic glycolysis (Przybylski et al., 1994; Apaoblaza et al., 2015). As pH decline is occurring, carcass temperature should be declining as well. Deviations from normal pH and temperature decline can lead to a variety of meat quality issues that will be discussed in later sections.

Metabolic pathways

a) *Glycolysis:*

During the conversion of muscle to meat, ADP is rephosphorylated using phosphagen system glycolysis in an attempt to maintain ATP demands in tissue (Scheffler and Gerrard, 2007). The resulting lactic acid accumulation is considered a reflection of glycogen depletion, thus postmortem metabolism is generally considered anaerobic (England et al., 2013). In postmortem muscle, enzymes involved in energy metabolism remain active in an attempt to meet energy demands. Scopes (1974) indicated that glycolysis was regulated by ATPase activity, and glycolytic enzymes are controlled by ADP levels in the cell. Glycolysis occurring during the postmortem period is impacted by the availability and disappearance of ATP (Scopes, 1974).

Variations in extent and rate of glycolysis is pH and temperature dependent (Marsh, 1954; Bendall, 1973a; England et al., 2014). The rate and extent of pH and temperature decline and ultimate pH have a substantial impact on quality and palatability of fresh meat by way of variations in color, texture, and water holding capacity of muscle (Melody et al., 2004; Scheffler and Gerrard, 2007).

Termination of glycolysis can be attributed to lack of available substrate or pH driven termination of glycolytic enzymes which causes the final or ultimate pH. Studies have shown the average depletion of muscle glycogen is between 44 and 45 mmol/kg over 24 h postmortem (Warriss et al., 1990; Apaoblaza et al., 2015). England et al. (2014) found that phosphofructokinase (PFK) was pH sensitive; activity decreased with a decrease in pH value indicating that loss of

PFK function could be a limiting factor in pH decline in beef carcasses with a normal amount of glycogen. Metabolomic studies have indicated reduction of metabolites involved in glycolytic pathways as time postmortem increases (Mitacek et al., 2019).

b) *Tricarboxylic Acid Cycle/Electron Transport Chain:*

The tricarboxylic acid (TCA) cycle is a set of enzyme-catalyzed reactions occurring in the mitochondrial matrix that are central to oxidative metabolism of beta oxidation, ketones, and pyruvate. Acetyl-CoA from pyruvate enters the cycle and binds with oxaloacetate to form citrate. ATP, three NADH and one FADH₂ are generated with each cycle. The NADH and FADH₂ are then transferred to complex I and II of the electron transport chain for ATP production via oxidative phosphorylation (Martínez-Reyes and Chandel, 2020). Electron donors are oxidized and recycled if ADP is being simultaneously phosphorylated to ATP. If ATP levels are adequate, isocitrate dehydrogenase and α -ketoglutarate dehydrogenase activity ceases (England et al., 2018).

c) *Malate-aspartate and glycerol phosphate shuttles:*

Oxidative phosphorylation may yield more energy via NADH under aerobic conditions. The ETC is located in the inner mitochondrial membrane which is impermeable to NADH. The electron from NADH is transported to the inner mitochondrial membrane by way of glycerol phosphate and malate aspartate shuttles. Glycerol phosphate shuttle uses the glycolytic intermediate dihydroxyacetone phosphate (DHAP) as an electron acceptor. A reaction catalyzed by glycerol - 3 - phosphate dehydrogenase to form glycerol - 3 -

phosphate which diffuses through the membrane and carries the reducing equivalent to mitochondrial FAD. Ultimately electrons are delivered to complex II of the electron transport chain for energy production. The glycerol phosphate shuttle is the primary shuttle in skeletal muscle while the malate-aspartate shuttle is more important in cardiac muscle cells (Blackstock, 1989).

In the malate-aspartate shuttle, oxaloacetate is the acceptor of reducing equivalents. Blackstock (1989) stated that the inner mitochondrial membrane contains a transport system for malate. Malate penetrates the mitochondrial membrane and is oxidized to oxaloacetate and NADH is produced. Malate-aspartate shuttle is responsible for transferring electrons from the cytosolic NADH pool to the NAD⁺ pool in the mitochondria.

Mitochondrial influence in postmortem muscle

Mitochondria are double-membraned cellular organelles responsible for cellular respiration and energy metabolism (Tang et al., 2005a; Mancini and Ramanathan, 2014; Wu et al., 2020). Mitochondria have numerous important functions such as Ca²⁺ regulation and energy production (Scheffler et al., 2015). The outer mitochondrial membrane is a porous, phospholipid bilayer which is readily permeable to small molecules and ions (Wu et al., 2020). The inner mitochondrial membrane is a tight diffusion barrier which consists of transport proteins and complexes which can be involved in the transport of metabolites and intermediates, ATP synthesis, and oxidative phosphorylation (Ramanathan and Mancini, 2018; Wu et al., 2020). The mitochondrial matrix contains various proteins involved in reactions such as lipid oxidation, amino acid

degradation, and the tricarboxylic acid cycle. Four enzyme complexes are responsible for transfer of electrons from reducing equivalents (NADH and FADH₂) to NADH-Coenzyme Q reductase (complex I), succinate dehydrogenase (complex II), cytochrome bc1 (complex III) and cytochrome c oxidase (complex IV) (Ramanathan and Mancini, 2018).

In postmortem muscle, mitochondria continue to metabolize available oxygen in an attempt to meet energy requirements. Recent reports have indicated that mitochondria may play a larger role in postmortem metabolism and pH decline than previously thought (Scheffler et al., 2015; Matarneh et al., 2018). Scheffler et al. (2015) reported that mitochondria function positively influenced maintenance of ATP in an in vitro model. Additionally, Scheffler et al. (2015) found that inhibition of mitochondria enzyme activity contributed to accelerated ATP loss, glycogen degradation and lactate accumulation and rate of pH decline. England et al. (2018) found that O₂ levels decreased gradually in the early hours postmortem and utilizing metabolomic analysis, found that succinate content changed over time indicating mitochondrial function. In vitro glycolysis models indicated that the incorporation of isolated mitochondria influenced the rate of ATP depletion and pH decline (Matarneh et al., 2018; Scheffler et al., 2015).

These changes often impact the prooxidant and antioxidant balance resulting in accumulation of reactive oxygen species. Mitochondria are the first organelles that are subjected to oxidative damage by way of free radicals which can lead to degradation. Oxidative phosphorylation occurs within the inner membrane, producing additional reactive oxygen species (Ke et al., 2017).

The addition of 4-hydroxy-2-nonenal, a product of ω -6-polyunsaturated fatty acid oxidation, to beef heart mitochondria led to lower reduction of metmyoglobin and less metmyoglobin reductase activity as well as less oxygen consumption (Ramanathan et al., 2012) The same study found that mitochondria at pH of 7.4 treated with 4-hydroxy-2-nonenal were swollen and had increased membrane permeability while those treated and lowered to a pH of 5.6 had decreased permeability and volume. Indicating the importance of environmental factors on mitochondria structure and functionality.

Tang et al. (2005a) evaluated the impact of prolonged storage on bovine heart mitochondria functionality and morphology at pH 5.6. and reported that isolated mitochondria could still consume oxygen 60 days postmortem in the presence of succinate. Mitacek et al. (2019) reported that while mitochondria oxygen consumption with the addition of NADH or succinate decreased with aging time, mitochondria continued to consume oxygen after 28 days of aging with substrates added. Maintenance of function and integrity of mitochondria in postmortem muscle is dependent on time and pH (Cheah and Cheah, 1971; Tang et al., 2005b).

Muscle Fibers and Metabolism:

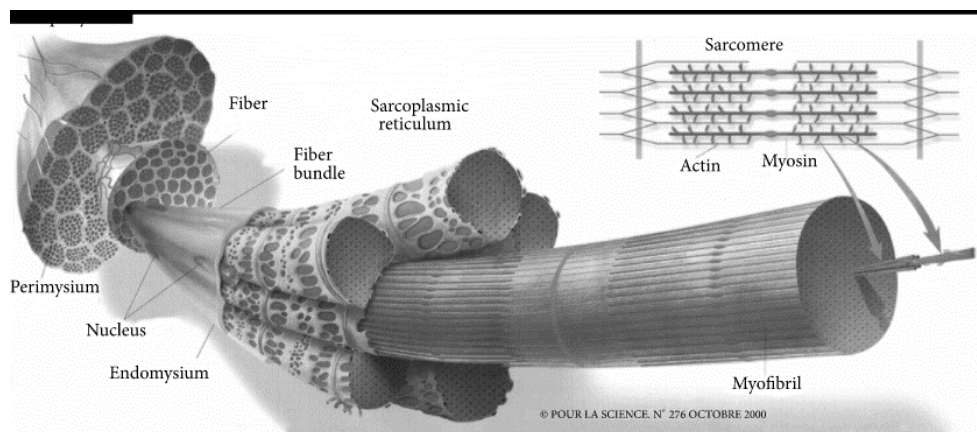


Image credit: (Listrat et al., 2016)

Skeletal muscles are made up of muscle fibers characterized by metabolic properties and morphological traits (Listrat et al., 2016). Myofibrils are the basic unit of a muscle cell and are composed of sarcomeres, the basic contractile unit of the muscle. Hundreds to thousands of myofibrils constitute a muscle fiber. Muscle fibers are surrounded by a connective tissue layer called the endomysium. A muscle bundle is a group of muscle fibers held together by a connective tissue layer called the perimysium. Ultimately, a group of muscle bundles is collectively known as the skeletal muscle which is held together by a connective tissue layer called the epimysium (Listrat et al., 2016).

Morphology is closely related to growth potential and is represented by cross-sectional area and total fiber number. Energy contribution of the primary metabolic pathway which will support contractile abilities of the fiber is important. In general, there are two major pathways to be considered for energy production, aerobic and anaerobic metabolism pathways. Aerobic metabolism has a high oxygen requirement and allows for amino acids, ketones, lipids, glucose, and glycogen to be oxidized in the mitochondria (Ashmore, 1974). Anaerobic metabolism utilizes glycogen stores which are ultimately converted to lactate (Ashmore, 1974).

Contractile characteristics of muscle are differentiated by fiber type and the corresponding metabolism profile of the fiber. Generally, there are four different muscle fiber types: type I, type IIA, and type IIX or type IIB which are categorized as slow-oxidative, fast oxido-glycolytic, and fast-glycolytic, respectively (Schiaffino and Reggiani, 1996). Each fiber type exhibits different morphological, contractile, physiological, metabolic, and chemical characteristics. Classification of muscle fibers

into one of two major types is based on the fiber's specific traits. White or glycolytic, type II muscle fibers possess more glycolytic properties and function by consuming glucose. Red or oxidative, type I muscle fibers exhibit a greater amount of oxidative enzymes and typically display two- to threefold higher mitochondrial density than type II fibers (Picard et al., 2012). Matarneh et al. (2021) reported that mitochondria from type I and type II fibers had different enrichment profiles for α -ketoglutarate and succinate.

Muscles with variations in fiber type composition undergo different patterns of conversion during the conversion of muscle to meat. Chauhan et al. (2019) found that glycolysis and glycogenolysis terminated earlier in primarily oxidative muscles in comparison to glycolytic regardless of glycogen availability. Glycogen content was increased in the beef *masseter* compared to the *cutaneous trunci* from 60 to 1440 min resulting in a higher ultimate pH for the *masseter* than the *cutaneous trunci*. Limited glycolytic flux is speculated to be mediated by pH inactivation of phosphofructokinase. Proteomic research has indicated that the majority of proteins which are differentially abundant between predominantly red and white muscles are metabolic enzymes associated with glycolytic metabolism, TCA, and ETC (Joseph et al., 2012). Yu et al. (2019) found that pyruvate, an important glycolytic metabolite, was more abundant in the *longissimus lumborum* throughout the early postmortem period in comparison to the *psaos major*. This could be attributed to the metabolic patterns associated with their muscle fiber profile as the *longissimus lumborum* is predominantly type II or glycolytic, while the *psaos major* is predominantly red or oxidative.

Oxygen stored in myoglobin can help sustain aerobic metabolism for some time postmortem (Pösö and Puolanne, 2005; Yu et al., 2019). Yu et al. (2019) found that TCA

metabolites were initially more abundant in *longissimus lumborum* than *psoas major* 6 h postmortem with decreases occurring within 24 h. In the *psoas major*, TCA metabolites increased and peaked at 12 h postmortem, indicating different rates at which metabolism occurs within different muscles. Numerous studies have indicated that mitochondrial protein content decreases occur at different rates for muscles containing predominantly type I or predominantly type II (Ke et al., 2017; Mitacek et al., 2019). These differences can impact generation rate and accumulation of reactive oxygen species which can ultimately impact mitochondria degradation and function. Recently, studies have found differences between type I and type II fibers regarding regulation of the permeability transition pore by Ca^{2+} and the metabolism of reactive oxygen species (Picard et al., 2008; Picard et al., 2012).

2) Metabolism and Biochemistry of Beef Color:

Myoglobin / Myoglobin Chemistry:

Myoglobin is a globular protein which consists of a heme group and a surrounding globin moiety found in skeletal and cardiac muscle (Seideman et al., 1984; Liu et al., 2006). In living muscle, myoglobin function is related to oxygen storage and delivery to the mitochondria to facilitate aerobic metabolism when oxygen delivery is ceased for periods of time (Liu et al., 2006). The heme is encompassed within segments of the globin chain protecting the heme iron from oxidation (Ramanathan et al., 2020b). The heme iron can exist in two states, ferric (oxidized, Fe^{3+}) or ferrous (reduced, Fe^{2+}). This iron ion can form six bonds, four of which are with nitrogen atoms of pyrrole groups of the heme ring and one is with a histidine residue of the globin (Ordway and Garry, 2004;

Bekhit and Faustman, 2005) The remaining position is available for binding with oxygen, nitric oxide, carbon monoxide, or other small ligands.

a) *Myoglobin in fresh meat:*

In meat, myoglobin is the primary pigment that contributes to color (Seideman et al., 1984). Meat color intensity is heavily influenced by total myoglobin concentration and myoglobin redox form. Total myoglobin concentration is heavily impacted by species, age, sex, and muscle location and function in an animal. Myoglobin color is determined by the type of ligand attached at the sixth binding site (O_2 , H_2O , CO , NO , etc), the valence state of the iron atom, and protein integrity (Seideman et al., 1984; Yong et al., 2018). The most common myoglobin redox forms found in fresh meat are deoxymyoglobin, oxymyoglobin, and metmyoglobin which are associated with purple, cherry red, and brown meat color, respectively (AMSA, 2012). Deoxymyoglobin is the primary form of myoglobin present in environments where atmospheric O_2 is minimal, such as vacuum packaging. Once O_2 is introduced, through processing or exposure from packaging binding of O_2 molecules to the sixth binding site occurs.

(1) *Oxygenation:* As the iron binds to a free O_2 molecule, oxymyoglobin is formed, this process is known as oxygenation. As oxygenation occurs, the exposed surface of the meat progresses from the deep purple color to a bright cherry red color in a process often referred to as blooming (Jacob, 2020). In both deoxymyoglobin and oxymyoglobin, the heme iron exists in the ferrous, or reduced state. The thickness of the oxymyoglobin layer depends on multiple factors such as temperature, pH, oxygen partial

pressure, and competition for O₂ with other respiratory processes. Oxygen is constantly associating and dissociating with the heme based on the conditions previously mentioned. This disassociation can cause the globin to lose its biological function of protecting the heme from undesirable reactions such as oxidation.

(2) *Oxidation*: Oxidation of the ferrous iron form in both deoxy- and oxymyoglobin to the ferric iron form results in discoloration via the formation of brown metmyoglobin (Faustman and Cassens, 1990). Oxidation and resulting metmyoglobin formation occur based on numerous factors such as temperature, oxygen partial pressure, pH, reducing activity, and, in some cases, microbial growth. Metmyoglobin formation often occurs at subsurface levels of meat products first where oxygen partial pressure is very low. Over time, this layer of metmyoglobin thickens, resulting in surface discoloration of meat products (Bekhit et al., 2001; Mancini and Hunt, 2005)

Metmyoglobin reduction (enzymatic and non-enzymatic):

Metmyoglobin reducing ability is the ability of postmortem muscle to reduce ferric metmyoglobin to ferrous oxy- or deoxymyoglobin. Many pre- and post-harvest factors such as breed (Yin et al., 2011), diet (Faustman et al., 2010), temperature and pH decline rate and extent (Chauhan and England, 2018), lipid oxidation (Mancini and Hunt, 2005), environmental conditions (Suman and Joseph, 2013), and oxygen partial pressure (George and Stratmann, 1952) impact the rate and extent of myoglobin oxidation.

However, meat has an inherent ability to delay metmyoglobin accumulation by way of metmyoglobin reducing activity (Ledward, 1985; Seyfert et al., 2006). Postmortem muscle has three pathways for which metmyoglobin reduction can occur: enzymatic, non-enzymatic, and mitochondria mediated. All metmyoglobin reduction pathways require NADH or an electron from the ETC as an electron donor and an electron carrier such as cytochrome b5 or a NADH-dependent reductase (Ramanathan et al., 2020b).

Enzymatic reduction of metmyoglobin occurs as NADH donates an electron which is transported via an electron transporter, cytochrome b5 reductase, to cytochrome b5, an electron receptor (Bekhit and Faustman, 2005; Elroy et al., 2015). Cytochrome b5 and its reductase are found on the cytosolic surface of mitochondria, nuclear membranes, and the endoplasmic reticulum. Other enzyme systems, such as metmyoglobin reductases require an artificial mediator or activator such as ferrocyanide or methylene blue for reduction (Arihara et al., 1995).

Metmyoglobin can be reduced nonenzymatically in the presence of an electron carrier such as EDTA, which moves an electron from NADH to metmyoglobin (Brown and Snyder, 1969). The concentration of NADH in a muscle is therefore related to color stability as an important reducing equivalent responsible for metmyoglobin reduction (Brown and Snyder, 1969; Denzer et al., 2020). Over time, NADH concentration decreases in postmortem muscle. Mitacek et al. (2018) reported that NADH concentrations in beef *longissimus lumborum* were greater on days 3 and 7 of aging compared to those aged for 14, 21, and 28 days. Mitacek et al. (2019) found that steaks wet aged for 3 days had 29 nmol of NADH per kg of muscle at by 28 days of aging concentration of NADH had decreased to 12 nmol of NADH per kg of muscle.

Glycolytic and tricarboxylic acid substrates including pyruvate, lactate, succinate, and malate have the ability to regenerate NADH (Ramanathan et al., 2014). Enzyme activity such as lactate dehydrogenase is a known method of NADH regeneration which can then be utilized for metmyoglobin reduction (Ramanathan et al., 2014).

Early postmortem, some oxygen is stored in myoglobin in the muscle and can facilitate aerobic metabolism for a period of time (Pösö and Puolanne, 2005). Fatty acids are broken down to enter the TCA cycle when cells are in need of energy. This results in glycerol being available for conversion into glycerol-3-phosphate which can yield NADH for oxygen consumption or metmyoglobin reduction.

pH

As previously mentioned, myoglobin is often the primary research concern and indicator of meat color determination. However, a variety of other factors play a substantial role in meat color and meat color perception. Rate and extent early postmortem pH decline has a substantial impact on structural changes of postmortem muscle (Seideman et al., 1984; Abril et al., 2001). Postmortem metabolism, primarily glycolysis, impacts the decline of pH during the conversion of muscle to meat as previously described. Depending on the extent and rate of pH decline, muscle color and structure are impacted by way of myofilament lattice spacing, myofibril spacing, and rate and extent of protein denaturation (Purslow et al., 2021).

High ultimate pH is usually caused by long term stress exposure prior to slaughter (Ashmore et al., 1971) . This often leads to the depletion of glycogen stores within the animal which impacts availability for postmortem anaerobic metabolism and lactic acid

production needed for normal pH decline. Dark, high pH meat, like that found in dark, firm, and dry beef, is subjected to increased absorption of light in comparison to normal and low ultimate pH meat. This absorption of light and resulting minimal light scattering can be attributed to minimal shrinking of muscle fibers and increased water holding capacity (Seideman et al., 1984; Hughes et al., 2017a; Ponnampalam et al., 2017). Muscle fibers that are associated with meat of a high ultimate pH do not allow for the diffusion of oxygen due to being tightly bound (Wu et al., 2020). This prevents oxygen from binding to myoglobin and oxygenation from occurring.

Apaoblaza et al. (2015) reported that muscle glycogen concentration, glycolytic potential, and lactate were higher in beef carcasses within a normal pH range in comparison to high pH carcasses. In a nontargeted metabolomics study, down regulation of glycolytic metabolites and upregulated TCA substrates were reported in high pH beef in comparison to normal pH beef (Ramanathan et al., 2020a). C nsolo et al. (2021) reported similar findings in muscle within a normal pH range in comparison to high pH. Differences in postmortem glycogenolytic/glycolytic flow in low and high pH muscle could be explained by higher initial muscle glycogen concentration, sustained AMPK activity, and increased glycolytic potential in normal pH carcasses in comparison to high pH carcasses at 24 h postmortem (Apaoblaza et al., 2015; C nsolo et al., 2021).

As mentioned in previous sections, low ultimate pH is primarily caused by the decline of postmortem pH while temperature is still high. The resulting lactic acid buildup is a result of anaerobic metabolism of glycogen and glucose. Differing from high pH meat products, low pH meat products are considered pale with swollen muscle fibers and increased light scattering. Light scattering impact on meat color was hypothesized by

Macdougall (1970) by exhibiting that reflectivity of processed and fresh pork was dependent on light scattering changes which occurred with changes in pH values. Meat with a low ultimate pH can cause myoglobin to be more readily oxidized as lower pH conditions can impact protective effects by altering histidine bonding and orientation (Ramanathan et al., 2020b). Abril et al. (2001) separated beef carcasses into two groups pH > 6.1 and pH < 6.1 to evaluate impact on color development both visually and objectively. They found that beef in the high pH group had less color development over time in comparison to the lower pH group. Increased muscle pH could protect oxymyoglobin from oxidation and denaturation and enhancement of both enzymatic and non-enzymatic mediated metmyoglobin reduction within steaks.

Mitochondria impact:

Both meat color stability and intensity are influenced by mitochondria by way of two mechanisms: metmyoglobin reducing activity and oxygen consumption (Mancini and Ramanathan, 2014). Mitochondria continue to consume oxygen in postmortem muscle and can influence meat color by competing with myoglobin for oxygen, impacting oxygen partial pressure, and ultimately impacting red color development and stability (Ashmore et al., 1971; Ashmore et al., 1972; Ramanathan et al., 2009; Ramanathan et al., 2012; Mancini and Ramanathan, 2014). Wu et al. (2020) saw greater expression of mitochondrial proteins which function to transfer electrons to the primary mitochondrial respiratory chain in high pH muscle in comparison to normal pH.

Tang et al. (2005a) reported that the effect of mitochondria respiration on myoglobin redox status was dependent on both pH and mitochondria density. In a study comparing

mitochondrial density and metmyoglobin formation, the lower the mitochondrial density resulted in the greatest amount of metmyoglobin formation (Tang et al., 2005b). Research has indicated that mitochondria can remain active up to 60 days post-mortem (Tang et al., 2005b). Oxygen consumption by mitochondria promotes anaerobic conditions and the reduction of metmyoglobin and even structurally damaged mitochondria can consume oxygen in the presence of added substrates (Tang et al., 2005b; Ramanathan et al., 2009). (Ramanathan et al., 2013) utilized succinate enhancement and altered pH levels of beef steaks in both vacuum and modified atmosphere packaging. They found that succinate enhanced steaks (pH 5.95) were more red than control (pH 5.65) steaks. Mancini and Ramanathan (2014) found that mitochondrial oxygen consumption decreased over aging time, improving initial bloom color. Additionally, they reported that as aging time increased, mitochondria lost the ability to convert oxymyoglobin to deoxymyoglobin when substrates were added for respiration (Ramanathan et al., 2012)

Mitochondria can increase color stability by transferring available electrons to metmyoglobin by way of complexes III and IV of the ETC and cytochrome c (Tang et al., 2005b). Cytochrome b5 reductase is also found in the outer membrane of the mitochondria and has the ability to produce NADH needed for reduction of metmyoglobin (Tang et al., 2005b; Ramanathan and Mancini, 2018)

The loss of mitochondria related metmyoglobin reduction can have a negative impact on color stability of meat products. Unsaturated fatty acids present in the mitochondria are susceptible to lipid oxidation. Oxidation byproducts such as alkenals, aldehydes, and hydroxyalkenals can inactivate enzymes and NADH dependent metmyoglobin reductase activity (Ramanathan et al., 2012) Mitochondria are very susceptible to damage by way

of oxidative stress and reactive oxygen species. Ke et al. (2017) found increased cytochrome *c* content in the sarcoplasm of color labile *psoas major* in comparison to a more color stable *longissimus lumborum* over 7 days of display. Cytochrome *c* is found in the inner membrane of mitochondria, indicating greater damage to mitochondrial membranes and increased permeability for more color labile muscles. Mitacek et al. (2019) reported that oxygen consumption was more sensitive to aging than metmyoglobin reducing activity. The limited oxidative stress in vacuum packaging could have a protective impact on enzymes involved in metmyoglobin reduction, thus improving ability after aging. Previous research has shown that NADH reductase activity is not impacted by aging time under wet aging conditions although NADH is concentration is; indicating that if NADH is still present post aging period, metmyoglobin reducing ability is still probable (Madhavi and Carpenter, 1993; Mitacek et al., 2019).

Metabolic characteristics

Muscle fiber type and metabolic profile play an important role in meat color and other quality traits. Type I fibers tend to have a greater concentration of myoglobin and mitochondrial protein than type II as red fibers are more oxidative and associated with aerobic metabolism whereas type II are anaerobic and do not require the oxygen red fibers do. Substrates involved in the TCA cycle and glycolysis are utilized at different rates in muscles that are predominantly type I or type II (Abraham et al., 2017). Muscles with increased oxidative metabolic activity tend to be more color labile as oxidative changes will occur more rapidly (Ramanathan et al., 2020b).

Joseph et al. (2012) found differences in the sarcoplasmic proteome of beef *longissimus lumborum* and *psoas major*, which are predominately glycolytic and oxidative, respectively. This study found a greater quantity of glycolytic enzymes in the *longissimus lumborum* in comparison to the *psoas major*. Suman et al. (2014) found that the sarcoplasmic proteome of *longissimus lumborum* exhibited an overabundance of chaperone and antioxidant proteins in comparison to the *psoas major*. Canto et al. (2015) found three glycolytic enzymes to be over abundant in color stable *longissimus* in comparison to color labile. Abraham et al. (2017) utilized untargeted metabolomic analysis to determine differences between metabolite concentrations between beef *psoas major* and *longissimus lumborum* during retail display. They reported greater concentrations of glycolytic compounds in *longissimus lumborum* in comparison to *psoas major* (Abraham et al., 2017). Additionally, they found higher levels of citrate in *longissimus lumborum* at day 7 of display, indicating differences in utilization of citrate for mitochondrial activity between the two muscles. Abraham et al. (2017) found greater levels of succinate in *longissimus lumborum* on days 3 and 7 of display in comparison to *psoas major* indicating less utilization of succinate by mitochondria in the *longissimus lumborum*.

Oxidation

Meat is prone to oxidative deterioration during processing and storage by way of a multitude components such as heme pigments, metal catalyts, unsaturated fatty acids, and other oxidizing agents.

Lipids can be oxidized by three mechanisms including autoxidation, photo-oxidation, and enzymatic-catalyzed oxidation with autoxidation being the main process resulting in meat deterioration (Domínguez et al., 2019). Lipid oxidation results in the production of free radicals or reactive oxygen species (ROS), a highly reactive species containing one or more free electrons, which contribute to the continued oxidation of lipids, or autoxidation (Ayala et al., 2014; Amaral et al., 2018). The two ROS that primarily impact lipids are hydroxyl radical (HO) and hydroperoxyl (HO₂). Hydroxyl radicals are a highly mobile, reactive species of oxygen that can be produced from oxygen in cell metabolism under various stress conditions (Ayala et al., 2014). Primary sources of endogenous ROS production include the mitochondria, endoplasmic reticulum, plasma membrane, and peroxisomes. Lipids in meat products are primarily composed of phospholipids and triglycerides. Triglycerides are considered storage lipids and consist of three fatty acids esterified to a glycerol backbone. Phospholipids are identified as structural lipids consisting of two fatty acids and a phosphate group esterified to a glycerol.

Photo-oxidation is a result of light exposure and serves as a mechanism of initiation for lipid oxidation. Hydroperoxides are formed in the presence of sensitizers, such as myoglobin or hemoglobin, and light. Sensitizers undergo excitation by absorbing light energy and ultimately producing excited triplet sensitizers (Domínguez et al., 2019). Sensitizers react with molecular oxygen to produce singlet oxygen; this singlet oxygen can react directly with electron dense moieties of unsaturated fatty acid double bonds. This reaction can produce hydroperoxide without forming the alkyl radical (Choe and Min, 2006). The excited sensitizer can react with triplet oxygen resulting in the production of superoxide radical anion (O₂⁻) via electron transfer. This ROS has the

ability to abstract hydrogen from unsaturated fatty acids ultimately triggering lipid oxidation or producing an alkyl radical. The alkyl radical can react with molecular oxygen producing a peroxy radical which can abstract hydrogen from a nearby fatty acid initiating a free radical chain reaction (Domínguez et al., 2019).

The enzymatic mechanism behind lipid oxidation is driven by lipoxygenase. Total concentration of lipoxygenase determines the rate and extent of oxidation development by way of this mechanism (Dominguez et al., 2019). Lipoxygenase consists of an active site which contains iron that must be in the ferrous form for enzyme activity to occur. This active site extracts a hydrogen atom from the methylene group of a polyunsaturated fatty acid ultimately forming a conjugated diene system that reacts with molecular oxygen. A peroxy radical removes hydrogen from an additional unsaturated fatty acid molecule and an alkyl radical and conjugated hydroperoxy diene are generated.

Meats containing greater quantities of polyunsaturated fatty acids are more prone to lipid oxidation in comparison to monounsaturated and saturated fatty acids. Lipid autoxidation is a chain reaction of free radicals reacting with unsaturated fatty acids and occurs in three stages: initiation, propagation, and termination (Amaral et al., 2018; Domínguez et al., 2019). The role that lipid oxidation plays in meat color is attributed to the byproducts of lipid oxidation directly impacting myoglobin molecules and the consumption of O₂ during lipid oxidation which lowers the partial pressure impacting myoglobin state (Lynch and Faustman, 2000; Allen and Cornforth, 2006). Ramanathan et al. (2014) found that secondary lipid oxidation products such as 4-hydroxy-2-nonenal (HNE) can bind to cysteine, lysine, and histidine residues. The binding of HNE to

histidine residues on myoglobin can alter the tertiary structure of myoglobin and promote heme release (Faustman et al., 1999; Suman et al., 2006)

Reactive oxygen species derived from lipid oxidation have been identified as potential indicators of protein oxidation and can play a role in the oxidation of proteins during aging and postmortem storage (Park et al., 2006; Estévez et al., 2008). Myoglobin is also a natural promoter of protein oxidation and carbonylation in meat systems (Estévez and Heinonen, 2010). Park et al. (2006) found carbonyl formation by way of metmyoglobin occurred to a greater extent than metal catalyzed oxidizing systems. Oxidation of oxy-to metmyoglobin forms a superoxide radical that follows a similar redox cycle to transition metals (Estévez, 2011). Myoglobin has been reported to be a predictive marker for formation of carbonyls in proteomic studies (Promeyrat et al., 2011). Beef has been reported to be more susceptible to protein oxidation than other species which authors speculate is due to the increased iron and myoglobin content found in beef muscles (Lund et al., 2007).

- 3) **Metabolism and Biochemistry of Beef Tenderness:** Consumers have long rated tenderness as the most important trait when it comes to eating experience and are willing to pay premiums to purchase guaranteed tender products (Shackelford et al., 2001). Determination of tenderness involves three major factors: collagen solubility and content, extent of muscle shortening, and proteolysis that occurs during aging (Koochmaraie and Geesink, 2006a).

Muscle Characteristics:

The sarcomere is the basic contractile unit of muscle and is the bulk of muscle fibers. Alignment of filaments in the sarcomere are precise and alternate between light and dark bands, giving skeletal muscle its striated appearance. Sarcomeres consist of contractile, cytoskeletal, and regulatory proteins that play a key role in contraction. Muscle shortening is a result of sarcomere shortening during rigor development (Koochmaraie, 1996).

Collagen, elastin, and reticulin are connective tissue proteins found in meat animals. Collagen is the connective tissue that is most responsible for impacting tenderness by way of background toughness. Collagen content varies between 1 – 15% of dry muscle weight in cattle (Listrat et al., 2016). Within the muscle, collagen is found in three specific regions: the epimysium surrounding the entire muscle, the perimysium surrounding muscle bundles, and the endomysium surrounding muscle fibers. The perimysium is the main contributor to connective tissue related tenderness issues. As animals mature, cross-links between collagen fibrils become increasingly heat stable and increase overall toughness (McCormick, 1994).

Temperature and pH

Temperature in the early postmortem period can substantially impact shortening. Both cold and heat shortening can occur if rigor is developed outside of the ideal range of 14-20 °C (Locker and Hagyard, 1963; Devine et al., 1999) Rate and extent of shortening is likely based on the impact that muscle temperature has on its metabolism both pre- and post-rigor (Marsh, 1954; Bendall, 1973a; Bhat et al., 2018).

A variety of biochemical mechanisms that play a key role in postmortem tenderization are pH driven. Postmortem pH decline plays a substantial role in the activation of enzyme systems impacting proteolysis and ultimate tenderization (Dransfield, 1994; Melody et al., 2004). Watanabe et al. (1996) found that meat with high ultimate pH values was more tender initially than meat at normal pH values, but as aging time progressed tenderness levels became more similar. This indicates a more rapid initial tenderization rate for higher pH meat products, which can be attributed to proteolysis enzymes being more functional within specific pH ranges (Lomiwes et al., 2014b; Wicks et al., 2019) Low pH also decreases water holding capacity and increases drip and cook loss which can produce meat with less overall palatability.

Proteolysis and underlying systems

Proteolysis of key structural proteins such as desmin, titin, troponin-T, and nebulin has a substantial impact on tenderization that occurs during postmortem aging (Huff-Lonergan et al., 1996; Koohmaraie, 1996; Anderson et al., 2012a). The calpain system consists of calcium activated calpains (calpain-1 and calpain-2) which are endogenous proteases, and their inhibitor calpastatin. This system is predominantly involved in proteolysis with calpain-1 having the greatest impact on degradation of myofibrillar and cytoskeletal proteins (Huff-Lonergan et al., 1996; Koohmaraie, 1996; Ji and Takahashi, 2006; Koohmaraie and Geesink, 2006a). During aging, a variety of proteins are broken down by calpain-1 beginning in the early postmortem periods (Baron et al., 2004). Calpain activity is regulated by numerous factors such as decline in pH, oxidation, protein denaturation, and calpastatin activity (Rowe et al., 2004) A positive correlation

has been reported between calpastatin activity and meat toughness (Shackelford et al., 1994; Kemp et al., 2010). Over time, calpain-1 increasingly continues to autolyze and ultimately become inactive (Maddock et al., 2005). Calpain-1 in high pH samples has been shown to autolyze faster than low pH samples, indicating earlier activation and increased activity early postmortem (Lomiwes et al., 2014b)

Cathepsin involvement in meat tenderization is a lesser-known entity than other protease systems. Cathepsins are capable of hydrolyzing myofibrillar proteins and degrading proteins within the A- and Z- band regions (Zeece and Katoh, 1989). Cathepsins are a group of proteases located within the lysosomes. Muscle pH decline postmortem leads to the destabilization of lysosomal membranes, ultimate cathepsin release to the sarcoplasm, and cathepsin activity (Lomiwes et al., 2014b). Etherington (1984) found that cathepsins remain active between a pH of 3.0 and 6.0 indicating their primary contribution to tenderization occurs after that of calpain-1. Baron et al. (2004) reported degradation of myofilaments by cathepsins occurred at a later stage of postmortem storage. The study further indicated that after intermediate filaments were initially depolymerized, cathepsins were able to further degrade larger fragments. Lomiwes et al. (2014b) reported that cathepsin B activity was consistently lower in high pH beef in comparison to low pH beef.

Apoptosis involvement in postmortem proteolysis is orchestrated by the caspase protease system (Kemp and Parr, 2012). There are three activation pathways involved in caspase mediated apoptosis: intrinsic, extrinsic, and endoplasmic reticulum mediated. Kemp et al. (2006) found high levels of caspase 9 activity in muscle cells. Caspase 9 activity has been found to correlate with caspase 3/7 activity (Kemp et al., 2006; Kemp et

al., 2009). Caspase activity is highest in the early stages of the postmortem period with a greater amount of activity being associated with lower shear force values (Kemp et al., 2006). Lana and Zolla (2016) reported that caspase 3 was associated with calpastatin inhibition and functions in tandem with reactive oxygen species and calpain-1.

Metabolic Characteristics

Muscles with a greater proportion of oxidative, type I fibers have been shown to have higher ultimate pH and decreased rate of pH decline than more glycolytic muscles, or those with predominantly type II fibers (Choi et al., 2007; Anderson et al., 2012b). Studies have indicated that muscles that are more prone to oxidative metabolism are more tender than muscles that are primarily glycolytic (Hwang et al., 2010; Chriki et al., 2012; Kim et al., 2018). Muscle fiber size can play a role in tenderness as larger fibers are associated with toughness in comparison to smaller fibers (Maltin et al., 1998). Type II fibers are substantially larger than type I fibers which has been shown to contribute to variations in tenderness among different muscles (Renand et al., 2001; Hwang et al., 2010; Beline et al., 2020)

Anderson et al. (2012a) compared the proteome of muscles with varying tenderness levels to identify proteins that could serve as predictors of tenderness. The study found that myosin light chain 1 differed in abundance in the sarcoplasm of high and low star probe samples and could be useful as an indicator of early postmortem proteolysis (Anderson et al., 2012a). Myosin light chain 1 is more abundant in oxidative compared to glycolytic fibers and proteomics work have indicated a greater abundance of myosin light chain 1 in less tender meat (Dang et al., 2020). Anderson et al. (2014) utilized proteomics

to evaluate posttranslational modifications of proteins in steaks of various tenderness levels. Six isoforms of the glycolytic enzyme phosphoglucomutase were found and the least phosphorylated isoform had a greater abundance in the less tender steaks indicating the amount of phosphorylation of individual phosphoglucomutase isoforms are important in establishing the relationship between tenderness and phosphoglucomutase (Anderson et al., 2014).

Antonelo et al. (2020) identified acetyl-carnitine, adenine, anserine, creatine, glutamine, glucose, and lactate as the metabolites most associated with differences in tenderness. King et al. (2019) identified glucose, glucose-6-phosphate, malic acid, glycerol- 3- phosphate and 3-phosphoglyceric acid as metabolites associated with differences in tenderness. Variations of metabolite profile between tough and tender beef in these studies indicate the importance metabolic pathways such as glycolysis, the TCA cycle, D-glutamine and D-glutamate metabolism, and other energy production shuttles have on tenderness (King et al., 2019; Antonelo et al, 2020).

Oxidation

As in lipid oxidation, components of muscle tissues such as transition metals, heme pigments, unsaturated fatty acids, and oxidative enzymes are precursors for the formation of ROS and play a role in protein oxidation initiation (Estévez, 2011). During oxidative stress, the imbalance of anti- and pro-oxidant species results in damage to a variety of cellular components. Protein oxidation has been shown to have an impact on proteolysis enzyme activity and thus impacting tenderness (Rowe et al., 2004). Oxidative stress is

known to induce cellular protein damage by compromising function and structure ultimately leading to cell death (Ouali et al., 2013; Picard and Gagaoua, 2017).

Protein carbonylation results in the irreversible conversion of amino acid side chains into carbonyl groups (Lund et al., 2007; Estévez, 2011). These modified proteins serve as indicators of oxidative stress in postmortem muscle (Malheiros et al., 2019). Carbonyl formation in meat proteins occurs by way of direct oxidation of susceptible amino acid side chains such as threonine, lysine, proline, and arginine (Estévez and Heinonen, 2010; Estévez, 2011). Numerous studies have reported a relationship between carbonyl formation and decreased tenderness in beef (Rowe et al., 2004; Zakrys et al., 2009). Protein oxidation's influence on tenderness is driven by decreasing proteolysis during aging and promoting the formation of protein crosslinks via disulfide bonding (Lund et al., 2007; Lametsch et al., 2008; Huff Lonergan et al., 2010; Estévez, 2011)

Antonelo et al. (2020) found that increased oxidative metabolism led to increased oxidative stress in early postmortem periods, leading to myofibrillar proteins being more susceptible to proteolysis and increased tenderization. Pro- and anti-apoptotic proteins are released from the mitochondria and the ratio of these proteins impacts the rate and extent of apoptosis (Lomiwes et al., 2014a). Oxidative muscles undergo apoptosis earlier than glycolytic due to cellular stress (Antonelo et al., 2020). Pro-apoptotic proteins in the mitochondria, such as cytochrome c have shown to induce and enhance caspase activation which can contribute to proteolysis (Ouali et al., 2013; Lomiwes et al., 2014a) Studies have indicated that oxidized myofibrillar proteins are more susceptible to degradation by way of caspases (Chen et al., 2014). Anti-apoptotic proteins, such as heat shock proteins (HSP), increase activity and expression to prevent oxidative stress related

damage and protein denaturation(Kemp et al., 2010; Lomiwes et al., 2014c; Picard and Gagaoua, 2020) Heat shock proteins prevent apoptosis onset by mechanisms such as prevention of caspase activity or binding to cytochrome *c*, ultimately delaying proteolysis (Picard and Gagaoua, 2020). In a proteomics study, Bernard et al. (2007) found a negative correlation between Hsp27 and meat tenderness and juiciness.

Cao et al. (2010) studied the biochemical and morphological alterations in the cell associated with apoptosis in *longissimus*, *psaos major*, and *semitendinosus*. The biochemical indicator of apoptosis is degradation of genomic DNA by way of endogenous DNAases into DNA fragments and strand breaks (Cao et al., 2010). The *psaos* had greater nucleotide concentration than both the *longissimus* and *semitendinosus* at day 7. This could be attributed to the increased mitochondria content in the *psaos* due to type I fiber concentration. Degens et al. (2007) reported increased apoptosis in oxidative muscles in comparison to glycolytic muscles. Authors speculate that the increased mitochondrial volume in oxidative muscles lead to increased susceptibility to mitochondrial associated apoptosis (Zhang et al., 2020)

4) Metabolism and Biochemistry of Beef Flavor:

Meat Flavor Chemistry

Hundreds of compounds exist in meat that contribute to flavor and aroma. These compounds are often altered through storage and cooking method, adding to the increased complexity surrounding meat flavor. Maillard's reaction, lipid oxidation, interaction between byproducts of lipid oxidation and Maillard's reaction, and vitamin

degradation produce volatile flavor components during cooking responsible for meat aroma (Khan et al., 2015).

Flavor precursors

Development of flavor in meat has been related to flavor precursors such as sugars, free fatty acids, free amino acids, and nucleotides (Mottram, 1998). Flavor precursors are categorized as water-soluble (sugar, sugar phosphates, free amino acids, peptides, nucleotides and nucleotide-bound sugars, and nitrogenous compounds) or lipids (Hornstein et al., 1960; Hornstein and Crowe, 1960; Mottram, 1998; Resconi et al., 2013). Werkhoff et al. (1990) reported that cysteine and methionine are the largest contributors to meat flavor. Endogenous enzymes involved in proteolysis, glycolysis, and lipolysis produce non-volatile compounds which ultimately contribute to meat flavor (Toldrá and Flores, 2000).

Lipid derived

As established, postmortem aging results in numerous biochemical changes to improve meat tenderness. It is important to note that flavor development occurs over the duration of the aging period (Kim et al., 2018). During the aging period, unsaturated fatty acids oxidize and produce a variety of compounds contributing to both characteristic and undesirable flavors (Stetzer et al., 2007). Degradation of lipids results in the formation of aldehydes, ketones, carboxylic acids, and alcohols (Kerth and Miller, 2015). When these compounds are formed during prolonged storage, they can lead to undesirable flavors but during cooking the reaction occurs rapidly and a different volatile profile is established

(Mottram, 1998). Unsaturated fatty acids in the phospholipids are highly susceptible to autoxidation and play a substantial role in flavor development. Foraker et al. (2020) reported a shift in flavor profile of beef between 35 and 49 d of wet aging, moving toward a more sour and musty profile. Stetzer et al. (2007) found that beef flavor was negatively correlated with pentanal, indicating a decrease in beef flavor with an increase in lipid oxidation byproducts. Setyabrata et al. (2021) utilized UPLC-MS metabolomic analysis to determine metabolite differences in flavor profiles of beef loins aged with varying methods.

Maillard Reaction

Sugars, amino acids, nucleotides and peptides go through the Maillard reaction. The Maillard reaction plays a substantial role in browning of meat surfaces during cooking and flavor development. Under most circumstances, the Maillard reaction is divided into three stages. The first stage begins with a condensation between a reducing sugar and an amino group leading to an N-glycosamine. The intermediate stage sees the release of the amino group and resulting sugar fragmentation products. In the final stage, a combination of fragmentation, dehydration, cyclization, and polymerization of amino groups reactions occur. In particular, the Strecker reaction which sees amino acids degraded by dicarbonyls formed in the Maillard reaction leading to decarboxylation and deamination of the amino acid, is particularly important to flavor development. Reaction paths of the Maillard reaction are temperature, pH, time, water content, and reactant dependent (Martins and van Boekel, 2005; van Boekel, 2006).

Metabolic Characteristics

Due to different metabolic and physiological properties of oxidative and glycolytic muscles, it has been shown that muscles undergo different processes during the postmortem aging period resulting in different byproducts available for flavor development (Yu et al., 2019a). Chikuni et al. (2010) reported greater carbonyl content and free fatty acids in oxidative muscles.

5) Recent Developments and Needs

With a growing number of new and innovative technologies available, meat quality research is at a pivotal point. The development and implementation of high throughput technologies such as transcriptomics, genomics, proteomics, and metabolomics allow for increasingly detailed information and data regarding meat quality attributes. However, these technologies and their use in meat science research is still quite novel and development of predictive technologies using data from these findings is still quite far off. Gagaoua et al. (2020) proposed a six-stage process for industry-implementation of predictive biomarkers: protein discovery/identification, qualification, verification, optimization of research assays, industrial validation, and commercialization.

Current use of these technologies allows for a greater understanding of the pathways and mechanisms involved in the development of meat quality attributes such as color, tenderness, and flavor. Additionally, there is a great need for understanding interactions and relationships between factors impacting meat quality traits and attributes.

Chapter 2

Muscle color attributes and myoglobin exhibit relationships with tenderness measurements and calpain-1 abundance in beef

Abstract: The objective of this study was to determine the extent to which myoglobin and beef color are associated with calpain-1 concentration and tenderness. *Longissimus lumborum* (LL) samples from the left side of Holstein beef carcasses (n = 31) were collected immediately post-evisceration on the harvest floor for 0 h analyses. After USDA quality and yield grading, six steaks were removed from the right side of each carcass for analyses at 48 and 336 h postmortem. Myoglobin concentrations at 48 and 336 h resulted in moderate, negative correlations ($P < 0.05$) to Warner-Bratzler shear force (WBSF) values at 336 h postmortem. Metmyoglobin reducing activity at 336 h exhibited moderate, positive ($P < 0.05$) relationships with slice shear force (SSF) and WBSF values at 48 h. L^* , a^* , and b^* values at 48 h resulted in moderate, positive correlations ($P < 0.05$) with WBSF values at 48 and 336 h. L^* values at 336 h exhibited moderate, positive correlations with SSF values at 336 h and WBSF values at both 48 and 336 h. Values for b^* at 336 h exhibited moderate, positive correlations with calpain-1 concentration at 0 and 336 h. Data from this study indicate a potential connection between myoglobin concentration and meat color with tenderness aspects and calpain-1 concentration. Results from this study warrant further investigation of the relationship between myoglobin and beef tenderness.

INTRODUCTION

Tenderness and color are two of the most important traits for determining overall consumer perception of meat quality (Neely et al., 1998; Suman et al., 2014). Demand for high quality, consistent beef products in the U.S. continues to grow. Variability in quality traits of fresh beef products can be impacted by numerous pre- and post-harvest factors. U.S. consumers are willing to pay a premium for beef products that are guaranteed tender (Boleman et al., 1997; Shackelford et al., 2001). Current direct tenderness evaluation methods are invasive and time consuming. There is an inherent need for rapid tenderness prediction technologies to segment beef carcasses to take advantage a tenderness marketing advantage.

Three primary factors determine meat tenderness: background toughness, toughening phase, and tenderization phase (Koochmaraie and Geesink, 2006). Tenderization that occurs during the aging process can be primarily attributed to the calpain system. The calpain system is a calcium dependent endogenous protease system responsible for proteolysis of myofibrillar proteins within muscle fibers (Kemp et al., 2006; Huff Lonergan et al., 2010; Nowak, 2011; Colle et al., 2018). In skeletal muscle, the calpain system primarily consists of three isoforms: calpain-1, calpain- 2 and calpain- 3, along with calpastatin; an inhibitor of calpain (Kemp et al., 2010). Calpain-1 is the primary endopeptidase responsible for tenderization of beef during aging (Rosell et al., 1996; Koochmaraie and Geesink, 2006)When calcium is present, the intact 80 kDa catalytic subunit of calpain-1 autolyzes to an intermediate (78 kDa) and finally to an active subunit (76 kDa) (Wright et al., 2018)Binding of calcium ions to specific domains results in a conformational shift and the dissociation of a calpain subunit. Activation and autolysis of

calpain -1 occurs during the early stages of postmortem aging with most activity lost within the first 7 days (Camou et al., 2007). An intricate system of intermediate filaments in skeletal muscle interconnect myofibrils at Z-disks. Desmin is the primary protein making up the filaments and its degradation has a substantial impact on tenderization by way of calpain mediated proteolysis (Huff-Lonergan et al., 1996; Baron et al., 2004). Additionally, proteins such as titin, nebulin, filamin, and troponin T are also impacted by calpain mediated proteolysis (Huff-Lonergan et al., 1996). Degradation of these proteins also contributes to tenderization that occurs during the aging process.

The main sarcoplasmic protein in skeletal muscle is myoglobin (Mb), the pigment responsible for meat color. In living muscle, Mb serves as an oxygen storage protein and delivers oxygen to mitochondria (Wittenberg and Wittenberg, 2003; Ordway and Garry, 2004). In postmortem muscle, oxidation of the central iron atom is responsible for fresh meat color (Mancini and Hunt, 2005). Previous research has indicated that Mb may serve as an efficient inhibitor of endopeptidases such as calpains (Rosell et al., 1996; Volle et al., 1999).

Previous research has resulted in a variety of findings related to objective color and tenderness measurements. Moderate negative and positive correlations between objective color measurements and Warner-Bratzler shear force (WBSF) values in beef steaks have been reported (Wulf et al., 1996; Wulf et al., 1997; Wulf and Page, 2000; Goñi et al., 2007). Therefore, the objective of this study was to determine the relationship between objective meat color measurements, myoglobin concentrations, myoglobin state, and calpain-1 abundance on beef tenderness.

MATERIALS AND METHODS

Animal Harvest and Sample Collection

Holstein heifers (n = 31) were slaughtered under USDA inspection at the University of Missouri red meat abattoir. Immediately post evisceration, a portion of the *longissimus lumborum* (LL) was removed from the left side of each carcass and immediately transported to the lab for 0 h analyses. At 48 h postmortem, the right side of each carcass was ribbed between the 12th and 13th rib and carcasses were subjected to USDA yield and quality grading (United States Department of Agriculture, 2017). After grading, LL were removed, and six steaks, each 2.54 cm thick, were fabricated. Three steaks were randomly delegated for 48 h analyses and three were vacuum packaged and wet aged for an ultimate aging period of 336 h postmortem.

Carcass pH and Temperature

Carcass pH and temperature measurements were collected at 0, 24, and 48 h postmortem on the left side of each carcass in triplicate and were averaged. The pH measurements were collected using a waterproof portable meat pH meter (Hannah Instruments, HI98163, Smithfield, RI, USA). Temperature readings were collected using a handheld thermometer (Omega Microprocessor, Model HH21, Stamford, CT, USA).

Total Myoglobin Concentration

Triplicate, 2.5 g minced steak samples were homogenized for 60 s using a Polytron homogenizer (Polytron 10–35 GT, Kinematica, Bohemia, NY) in 22.5 mL of sodium phosphate buffer, pH 6.8. Homogenate was then filtered through filter paper with particle retention of 4 to 8 µm and a flow rate of 25 mL/min (Fisherbrand P4 Grade, Fisher Scientific, Suwanee, GA) into clean tubes. Filtrate absorbance was read at 525 nm on a

Genesys 20 spectrophotometer (Thermo Fisher Scientific, Waltham, MA). Myoglobin concentrations (mg/g) were calculated utilizing the equation provided in AMSA (2012).

Objective Color Determination

Samples collected for both 48 and 336 h analyses were evaluated for objective color determination. Triplicate readings were taken on steak surfaces immediately following a 20 min bloom time. L^* (lightness), a^* (redness), and b^* (yellowness) were measured on the steak surface using a HunterLab MiniScan 45/0 LAV (Hunter Associates Laboratory, Weston, VA) equipped with a D65 light source, 2.5 cm aperture, and 10° standard observer. Physical standards were used for calibration prior to readings being taken each day. Additionally, instrumental color readings were utilized to calculate a/b ratio (ab), saturation index (SI), and hue angle (HA) values according to AMSA (2012).

Myoglobin Redox Forms

Percentages of Mb redox forms, i.e., deoxymyoglobin (DMb), oxymyoglobin (OMb), and metmyoglobin (MMb), on steak surfaces were determined at the conclusion of each aging time point according to methods described in AMSA (2012). A 20 min minimum bloom time was allotted for before measurements were taken. Reflectance was measured at wavelengths of 470, 530, 570, and 700 nm on the light-exposed steak surfaces employing a HunterLab MiniScan 45/0 LAV (Hunter Associates Laboratory, VA), and the percentage of Mb redox forms were determined utilizing the equations according to AMSA (2012).

Metmyoglobin Reducing Activity

Metmyoglobin reducing ability (MRA) was measured using a method described by Sammel et al. (2002). Triplicate cubes, 4-cm × 4-cm × 0.64-cm deep, from the center of

each steaks surface were removed on each designated postmortem period. Upon removal, samples were bathed in a 0.3% sodium nitrite solution for 20 min to induce MMb formation. After 20 min, samples were removed from the solution, blotted dry, and vacuum sealed (Multivac, Chamber Machine P200, Kansas City, MO) in labeled individual packages. Readings of each sample were taken immediately after packaging utilizing a HunterLab MiniScan in triplicate to obtain reflectance data. Samples were incubated at room temperature for 120 min to induce MMb reduction. After the incubation period, samples were rescanned in triplicate with a HunterLab MiniScan. Surface MMb values were calculated using K/S ratios and formulas provided in AMSA (2012).

Slice and Warner-Bratzler Shear Force

Shear force measurements were obtained according to protocols outlined in Callahan et al. (2013) Prior to cooking, raw weights were obtained for each steak. Steaks were cooked on a grated non-stick electric grill (Indoor/Outdoor Grill, Hamilton Beach, Southern Pines, NC, USA) to an internal temperature of 35 °C, flipped, and finished at a final temperature of 71 °C. After cooking, steaks were individually weighed and immediately wrapped in tin foil and stored at refrigerated temperatures (4 °C) for 24 h prior to sampling. After refrigeration, steaks were subjected to WBSF and slice shear force (SSF) sampling. A 1 cm x 5 cm slice was removed from the lateral end of the steak parallel to the muscle fibers for SSF analysis. Additionally, five 1.27 cm cores were removed parallel to muscle fiber orientation for WBSF. All shears were performed by the United STM Smart-1 Test System SSTM-550 with a test speed of 250 mm/min for WBSF and 500 mm/min for SSF. (United Calibration Corp, Huntington Beach, CA, USA).

Calpain-1 Relative Abundance

Calpain-1 relative abundance was determined using methods outlined in Carlson et al. (2017) with modifications. 0.5 g tissue was homogenized (Polytron 10–35 GT, Kinematica, Bohemia, NY, USA) in 5 ml of 10mM phosphate buffer with 2% SDS, pH 7. Protein content was determined using a Bradford assay. Samples were diluted to a final protein concentration of 4 mg/ml. Samples were heated for denaturation at 70 °C for 10 minutes prior to electrophoresis and vortexed for 5 min. Electrophoresis was completed using MOPS SDS Running Buffer (50 mM MOPS, 50mM Tris Base, 0.1% SDS, 1 mM EDTA, pH 7.7) and 4-12% Bis-Tris gels (RunBlue 4-12% Bis-Tris Gel, NBT41227; Expedeon, San Diego, CA, USA). After electrophoresis, gels were transferred to polyvinylidene difluoride (PVDF) membranes. Gels were transferred onto membranes using the Owl™ VEP-2 Mini Tank Electroblotting System running at a constant voltage of 65 V for 1.5 h with a 1X Bis-Tris transfer buffer with 10% methanol (per gel) content. Membranes were then blocked in a PBS-Tween solution containing 5% nonfat dry milk (NFDm). Membranes were blocked for approximately 1 h at room temperature. Primary antibodies were diluted in PBS-Tween and were added to the blots immediately after blocking and incubated overnight. Primary antibody dilutions contained (1:10,000) calpain-1 using monoclonal mouse anti-calpain-1(MA3-940; Thermo Scientific, Rockford, IL, USA). After incubation, blots were washed in PBS-Tween 5 times for 5-min intervals. Blots were then incubated for 1 h at room temperature with a secondary goat anti-mouse-HRP antibody (1:10,000) (31430; Thermo Scientific, Rockford, IL, USA). After secondary incubation, blots were washed with PBS-Tween. Membranes were reacted with a chemiluminescent substrate (Immobilon® Crescendo Western HRP Substrate, Millipore Corporation, Billerica, MA, USA). Images of blots were obtained using a ChemiDoc

Touch Imaging System (Bio-Rad, Hercules, CA, USA) and analyzed by Image Lab™ Software (ver, 5.2.1, Bio-Rad, Hercules, CA, USA).

Statistical Analysis

All statistical analyses were performed using SAS statistical software (SAS Version 9.4, SAS Inst. Inc., Cary, NC, USA). The GLM function of SAS was used to produce LS Means and standard errors of pH, temperature, objective color, myoglobin redox forms, myoglobin concentration, metmyoglobin reducing activity, intact calpain-1 relative abundance, and shear force values. Data were analyzed with the model using time (h postmortem) as a fixed effect. T-tests were performed to determine differences among means at each time point with the COCHRAN approximation applied. PROC CORR was utilized to determine correlations. Significance was determined at $P < 0.05$.

RESULTS AND DISCUSSION

Carcass Characteristics

Average carcass characteristics can be found in Table 2.1. Mean hot carcass weight (HCW) of 188.79 kg was determined among the sample set. Moderate, positive correlations were present between HCW and calpain-1 relative abundance at 0 ($P < 0.05$) and 48 h ($P < 0.05$) postmortem (0.44 and 0.39, respectively; Table 2.2). There were moderate, negative correlations present between HCW and SSF ($P < 0.05$) and WBSF ($P < 0.01$) at 48 h. Additionally, HCW was moderately, negatively correlated to WBSF values ($P < 0.05$) at 336 h (-0.38, -0.50, and -0.46, respectively). Mean USDA Yield Grade of carcasses was 1.7 and Quality Grade was USDA Choice³⁴. Moderate, negative correlations ($P < 0.05$) were present between calpain-1 abundance at 0, 48, and 336 h postmortem and carcass yield grade (-0.37, -0.45, and -0.40, respectively; Table 2.2). Carcass insulation, or lack

thereof, provided by subcutaneous fat can impact rate of temperature decline on beef carcasses. Shortening can occur if rigor occurs outside of the ideal temperature range of 14 – 20 °C (Devine et al., 1999). Mean ultimate pH of carcasses at 48 h was 5.69 and mean temperature was 1.14 °C at 48h (Fig. 2.1.) indicating normal temperature and pH decline and normal rigor development. Ultimate pH at 48 h and WBSF values at 336 h exhibited a moderate, positive correlation ($P < 0.01$) (Table 2.2) indicating a relationship between ultimate pH and ultimate tenderness of steaks from the LL. A moderate, negative correlation ($P < 0.05$) between carcass temperature at 24 and SSF at 336 h was also found. Extent and rate of pH and temperature decline in early postmortem muscle is known to play a critical role in various meat quality traits such as color (Abril et al., 2001; Hughes et al., 2017b), tenderness (Jeremiah et al., 1991; Zhang et al., 2018) water holding capacity, and flavor (Wulf et al., 2002) Dransfield (1994) found that meat with a high ultimate pH were more tender than meat at a normal pH early postmortem. Lomiwes et al. (2014) reported that calpain-1 in high pH samples have been shown to autolyze at a more rapid rate than normal and low pH meat indicating increased activity early postmortem.

Total Myoglobin Concentration

Color of meat is primarily determined by the total concentration and chemical state of the protein Mb (Mancini and Hunt, 2005). Total Mb concentrations decreased ($P < 0.05$) in steaks sampled at 0 compared to those sampled 48 h postmortem (Table 2.3). This initial decrease in myoglobin could be attributed to shrinkage and moisture loss during initial chilling of carcasses after harvest. No differences ($P > 0.05$) were seen between total Mb concentration of steaks sampled at 48 or 336 h postmortem (Fig. 2.2). Moderate, negative correlations were found between Mb concentration 48 h postmortem and WBSF values at

336 h ($P < 0.05$) as well as Mb concentrations at 336 and WBSF values at 336 h ($P < 0.05$) (-0.36 and -0.41, respectively) (Table 2.4). Myoglobin concentration is impacted by a variety of factors such as muscle location and type, animal age, and species (Abril et al., 2001). A possible explanation for this relationship between Mb concentration and tenderness could be the fiber type composition of muscle. Muscle fiber composition has a substantial impact on numerous biochemical and ultimate quality and palatability factors of meat products (Klont et al., 1998; Wright et al., 2018). Muscles with a greater proportion of oxidative fibers tend to have a greater concentration of myoglobin and are more susceptible to oxidative metabolism and are more tender (Kim et al., 2018)

Rosell et al. (1996) reported that calpain-1 activity decreased in the presence of 1 mg/ml of Mb indicating a potential role as an inhibitor of endogenous proteases within the muscle. Conversely, Volle et al. (1999) stated that the inhibition of proteases by Mb was an “artifact” and that no relationship between the extent of postmortem muscle proteolysis and Mb should be expected. No correlations ($P > 0.05$) were found between Mb content and calpain-1 relative abundance at any timepoint in this study.

Objective Color Measurements

Mean values for objective color measurements can be found in Table 2.3. No differences ($P > 0.05$) were found in L^* values of LL steaks at 48 or 336 h postmortem. Indicating no differences in lightness over the duration of aging. Mean values for a^* were greater ($P < 0.05$) at 48 h postmortem in comparison to 336 h. Decreases in a^* values could indicate oxidation of myoglobin over the duration of aging leading to a loss of red color contributed from deoxy- and oxymyoglobin. No differences ($P > 0.05$) were observed in b^* values of steaks from the LL between 48 and 336 h postmortem. No differences ($P >$

0.05) were observed between 48 and 336 h steaks for SI values. Values for hue angle were greater ($P < 0.0001$) in 336 h samples in comparison to 48 h steaks. A greater HA value is indicative of a loss of redness or discoloration of fresh beef products. Since a decrease in a^* was reported for 336 h samples, an increased HA value would be expected.

As seen in Table 2.5, moderate, positive correlations occurred between L^* values at 48 h postmortem and WBSF values at both 48 h ($P < 0.05$) and 336 h ($P < 0.01$) postmortem (0.40 and 0.49, respectively). Values for L^* at 336 h exhibited moderate positive correlations with SSF values at 336 h ($P < 0.05$) (0.36) and WBSF values at both 48 and 336 h postmortem ($P < 0.05$) (0.42 and 0.45, respectively). Values for a^* at 48 h postmortem exhibited moderate, positive correlations with WBSF values at both 48 and 336 h postmortem ($P < 0.05$) (0.40 and 0.39, respectively). Moderate, positive correlations were found between b^* values at 48 h and WBSF values at 48 h ($P < 0.05$) and 336 h ($P < 0.01$) (0.41 and 0.46, respectively). Calpain-1 relative abundance at both 0 and 336 h exhibited moderate positive correlations with b^* values at 336 h (0.39 and 0.37, respectively). Wulf et al. (1997) reported correlations between tenderness measurements and objective color measurements with b^* having the strongest relationship with tenderness. Wulf and Page (2000) found that higher L^* and b^* values were associated with decreased shear force values in beef longissimus muscle. Goñi et al. (2007) reported positive correlations between L^* values and shear force and negative correlations between both a^* and b^* values. Conversely, in this study we found positive correlations between objective color values and shear force measurements.

Correlations between objective color measurements and tenderness factors can be found in Table 2.5. Moderate, positive correlations ($P < 0.05$) were found between SI

values at 48 h and WBSF values at 48 and 336 h (0.42 and 0.44, respectively). Hue angle values at 48 h exhibited moderate, positive correlations ($P < 0.05$) with WBSF values at 336 h (0.45). Increased HA values are indicative of discoloration, which could be due to oxidation and MMb formation (Trinderup and Kim, 2015). Previous relationships between protein oxidation and increased WBSF values has been reported (Rowe et al., 2004; Zakrys-Waliwander et al., 2012). Hue angle values at 336 h exhibited a moderate, positive correlation ($P < 0.05$) with calpain-1 concentrations at 0 h (0.36). Values for a/b ratios at both 48 and 336 h exhibited moderate, negative correlations ($P < 0.05$) with WBSF values at 336 h (-0.47 and -0.36, respectively). Data indicate that the relationship between objective color measurements and ultimate tenderness attributes need to be further evaluated.

Surface Myoglobin Redox Forms

Deoxymyoglobin concentration of steaks sampled 48 h postmortem were greater ($P < 0.0001$) than those evaluated at 336 h postmortem as seen in Table 2.3. Conversely, concentrations of OMb were greater ($P < 0.0001$) in steaks evaluated at 336 h postmortem in comparison to those evaluated at 48 h. A similar trend was seen in MMb concentrations with steaks evaluated at 336 h having greater ($P < 0.0001$) concentrations than those evaluated at 48 h. A loss of DMb indicates oxygenation into OMb or oxidation to MMb, this could be attributed to less competition for O₂ between myoglobin and mitochondria with extended postmortem aging allowing for more oxygenation and less reducing ability (Mancini and Ramanathan, 2014)

No apparent correlations ($P > 0.05$) were found between surface DMb or OMb and shear force or calpain-1 concentrations at all time periods (Table 2.5). Surface MMb at 48

h exhibited moderate, positive correlations ($P < 0.05$) with calpain-1 concentration at 0, 48, and 336 h (0.36, 0.47, and 0.38, respectively) (Table 2.5). Rowe et al. (2004) reported positive correlations between protein carbonyl content and WBSF values. Additionally, Zakrys-Waliwander et al. (2012) reported that beef LD steaks with increased carbonyl content led to increased formation of intermolecular crosslinks and ultimately higher WBSF values. Positive correlations between MMB and calpain-1 concentration over the duration of aging could be attributed to oxidative conditions early postmortem impacting calpain-1 autolysis and resulting proteolysis, potentially decreasing overall tenderness.

Metmyoglobin Reducing Activity

Metmyoglobin reducing activity impacts color stability of muscles by the reduction of metmyoglobin to its ferrous redox forms. As seen in Table 2.3, MRA increased ($P < 0.0001$) in steaks produced from the LL between 0 and 48 h postmortem. No differences ($P > 0.05$) were seen between steaks between 48 and 336 h postmortem. Moderate, positive correlations were found between MRA at 336 h postmortem and SSF ($P < 0.05$) and WBSF values ($P < 0.05$) at 48 h (0.39 and 0.43, respectively) (Table 2.4). No apparent correlations ($P > 0.05$) were present between MRA and calpain-1 abundance.

Slice and Warner-Bratzler Shear Force

Aging of beef products is a widely used industry practice to improve tenderness and overall palatability. Values for both SSF and WBSF (Fig. 2.2) decreased ($P < 0.0004$, $P < 0.0001$, respectively) between 48 and 336 h postmortem. This was to be expected as proteolysis occurs during aging leading to expected tenderization. Colle et al. (2015) reported decreases in WBSF values for steaks produced from the LL between 2 and 14 d of aging. Moderate, positive correlations ($P < 0.01$) were reported between SSF values at

48 and 336 h. Additionally, SSF values at 48 h had moderate positive correlations with WBSF values at 48 ($P < 0.001$) and 336 h ($P < 0.01$) (0.49, 0.69, and 0.55, respectively) (Table 2.5). Slice shear force values at 336 h exhibited moderate positive correlations between WBSF values at both 48 ($P < 0.01$) and 336 h ($P < 0.001$) (0.61 and 0.70, respectively). Shackelford et al. (1999) reported correlations ranging from moderate to strong between SSF and WBSF values in the *longissimus*. Lorenzen et al. (2010) found that WBSF and SSF measurements among *longissimus* steaks ranged from moderate to strong positive correlations. Furthermore, Lorenzen et al. (2010) found that WBSF and SSF values taken from the same steak resulted in moderate to strong positive correlations. Warner-Bratzler shear force values at 48 h exhibited a moderate, positive correlation ($P < 0.001$) with WBSF values at 336 h (0.64) (Table 2.5). Interestingly, no correlations ($P > 0.05$) were found between calpain-1 relative abundance and shear force values at any time point (Table 2.5). While calpain-1 activity was not measured in this study, variations in activity of calpain-1 over time could explain the relationship between tenderness measurements and calpain-1 in this study.

Calpain-1 Relative Abundance and Autolysis

The calpain system plays a substantial role in proteolysis of postmortem muscle and is known to be heavily regulated by the endogenous inhibitor calpastatin (Huff-Lonergan et al., 1996; Geesink and Koohmaraie, 1999). In the presence of calcium, calpain-1 activates and begins autolyzing, initiating proteolytic abilities ((Koohmaraie and Geesink, 2006; Huff Lonergan et al., 2010). Calpain-1 relative abundance values for intact (80 kDa) calpain-1 decreased ($P < 0.05$) in steaks sampled at 0 and 48 h postmortem, indicating autolysis (Fig. 2.3). Calpain-1 activity is thought to be limited postmortem due

to the rate of decline in muscle pH and temperature (Dang et al., 2020). No difference in calpain-1 relative abundance ($P > 0.05$) was seen in steaks sampled at 48 and 336 h postmortem (Fig. 2.3). As expected, calpain-1 relative abundance at 0 h exhibited strong, positive correlations with calpain-1 concentrations at both 48 h ($P < 0.001$) and 336 h ($P < 0.001$) (0.87 and 0.81, respectively). Additionally, calpain-1 concentrations at 48 h exhibited a strong, positive correlation ($P < 0.001$) with concentrations at 336 h (0.95) (Table 2.2).

CONCLUSION

Correlations between tenderness measurements such as calpain-1 concentration and SSF and WBSF with carcass measurements such as ultimate pH and temperature were apparent. This confirms that the conversion of muscle to meat and the ultimate rigor endpoint have substantial roles in tenderness aspects of meat quality. In this study, positive relationships between calpain-1 concentration and HCW were reported while a negative relationship between HCW and shear force was found indicating that carcass size could have an impact on calpain-1 concentration and resulting proteolysis. Objective color measurements such as L^* , a^* , b^* , SI, and HA at 48 h postmortem were positively related to shear force values at the end of aging. While a/b values and total myoglobin concentration negatively correlated with WBSF values. Data from this study further indicate a relationship between meat color parameters and tenderness levels. More research is needed to determine mechanisms behind these relationships.

Acknowledgements: This work was funded in part by the Beef Checkoff through the Missouri Beef Industry Council. The authors would like to thank Dr. Mark Ellersieck, Dr.

Karl Kerns and Dr. Michal Zigo for their help and guidance with lab work and their expertise.

Table 2.1: Mean (\pm SD) animal and carcass characteristics of Holstein beef carcasses (n = 31)

Hot Carcass Wt (kg)	USDA Yield Grade	USDA Quality Grade ¹
188.79	1.71	534.84
± 14.66	± 0.35	± 150.24

100 = Practically devoid⁰⁰; 300 = Slight⁰⁰; 400 = Small⁰⁰; 500 = Modest⁰⁰; 700 = Slightly Abundant⁰⁰; 900 = Abundant⁰⁰

Table 2.2. Pearson correlation coefficients of carcass characteristics, shear force measurements, and calpain-1 concentrations of LL steaks from Holstein beef carcasses (n =31)

	HCW	YG	QG	pH 0	pH 24	pH 48	Temp 0	Temp 24	Temp 48	SSF 48	SSF 336	WBSF 48	WBSF 336	Calp 0	Calp 48	Calp 336
HCW ¹	-	-0.39*	0.22	-	0.12	0.23	0.14	0.33	0.20	-0.28	-0.38*	-0.50**	-0.46*	0.44*	0.39*	0.27
YG ²		-	-0.36*	0.20	0.24	0.04	-0.11	-0.45*	0.16	0.19	0.19	0.09	0.18	-0.37*	-0.45*	-0.40*
QG ³			-	0.25	-0.68***	-0.55**	-0.35	0.04	0.00	0.14	0.19	-0.06	0.04	-0.01	-0.07	-0.07
pH 0				-	0.12	-0.10	-0.08	-0.08	0.35	-0.14	0.15	-0.11	0.21	-0.29	-0.40*	-0.29
pH 24					-	0.80***	0.41*	-0.23	-0.06	-0.40*	-0.18	-0.43*	-0.24	-0.12	-0.19	-0.14
pH 48						-	0.32	-0.24	-0.02	-0.36*	-0.32	-0.37*	0.49**	-0.14	-0.17	-0.19
Temp 0							-	0.28	-0.20	-0.10	-0.20	-0.46**	-0.19	0.05	0.00	-0.02
Temp 24								-	-0.18	-0.06	-0.42*	-0.39*	-0.17	0.43*	0.43*	0.32
Temp 48									-	0.03	0.11	0.19	0.09	-0.31	-0.43*	-0.49**
SSF ⁴ 48										-	0.49**	0.69***	0.55**	0.04	-0.02	-0.11
SSF 336											-	0.61***	0.70***	-0.16	-0.17	-0.15
WBSF ⁵ 48												-	0.64***	-0.10	-0.12	-0.13
WBSF 336													-	-0.08	-0.13	-0.10
Calp ⁶ 0														-	0.87***	0.81***
Calp 48															-	0.95***
Calp 336																-

¹ Hot carcass weight (kg), ² USDA yield grade, ³ USDA Quality Grade, ⁴ Slice shear force (N), ⁵ Warner-Bratzler shear force (N), ⁶ Calpain-1 relative abundance, * $P < 0.05$, ** $P < 0.01$, *** $P < 0.001$

Table 2.3. Mean \pm SEM values for objective color, myoglobin redox forms, myoglobin concentration, metmyoglobin reducing activity, shear force, and calpain -1 concentrations at 0, 48, and 336 h postmortem in steaks from Holstein beef carcasses (n = 31).

	0 Hr	48 Hr	336 Hr	P-Value
<i>L</i> *	-	36.02 \pm 0.45	37.48 \pm 0.61	0.06
<i>a</i> *	-	15.84 \pm 0.23 ^a	13.93 \pm 0.45 ^b	0.0004
<i>b</i> *	-	12.04 \pm 0.27	12.67 \pm 0.43	0.22
SI ¹	-	19.91 \pm 0.34	18.87 \pm 0.57	0.13
HA ²	-	37.13 \pm 0.32 ^b	42.28 \pm 0.70 ^a	<0.0001
a/b ³	-	1.33 \pm 0.02 ^a	1.11 \pm 0.03 ^b	<0.0001
OMb ⁴	-	45.77 \pm 0.43 ^b	49.46 \pm 0.44 ^a	<0.0001
MMb ⁵	-	34.75 \pm 0.09 ^b	40.19 \pm 0.61 ^a	<0.0001
DMb ⁶	-	19.49 \pm 0.47 ^a	10.92 \pm 1.03 ^b	<0.0001
MYO ⁷	4.63 \pm 0.07 ^a	3.68 \pm 0.08 ^b	3.71 \pm 0.09 ^b	<0.0001
MRA ⁸	20.52 \pm 2.08 ^b	40.28 \pm 2.31 ^a	38.98 \pm 2.96 ^a	<0.0001
WBSF ⁹	-	71.32 \pm 4.23 ^a	50.07 \pm 2.71 ^b	<0.0001
SSF ¹⁰	-	374.62 \pm 16.81 ^a	283.26 \pm 17.39 ^b	0.0004

¹ Saturation index, ² Hue angle, ³ a/b ratio, ⁴ Oxymyoglobin (%), ⁵ Metmyoglobin (%), ⁶ Deoxymyoglobin (%), ⁷ Myoglobin concentration (mg/g), ⁸ Metmyoglobin reducing activity (%), ⁹ Warner-Bratzler shear force (N), ¹⁰ Slice Shear Force (N)
^{a-b} Means lacking a common superscript differ ($P < 0.05$)

Table 2.4. Pearson correlation coefficients of metmyoglobin reducing activity, total myoglobin concentration, shear force measurements, and calpain-1 relative abundance of LL steaks from Holstein beef carcasses (n = 31)

	MRA 0	MRA 48	MRA 336	MYO 0	MYO 48	MYO 336	SSF 48	SSF 336	WBSF 48	WBSF 336	Calp 0	Calp 48	Calp 336
MRA ¹ 0	-	-0.23	0.35	0.28	0.07	-0.01	0.27	0.20	0.20	0.11	0.16	0.26	0.25
MRA 48		-	0.39*	-0.17	-0.23	-0.31	0.08	-0.02	0.30	0.15	0.06	-0.07	-0.13
MRA 336			-	0.37	0.05	0.08	0.39*	0.20	0.43*	0.13	0.14	0.14	0.09
MYO ² 0				-	0.52**	0.61***	0.29	0.11	0.25	-0.05	0.10	0.14	0.08
MYO 48					-	0.81***	0.01	-0.24	0.04	-0.36*	-0.21	-0.09	-0.13
MYO 336						-	-0.06	-0.23	-0.03	-0.41*	-0.22	-0.08	-0.09
SSF ³ 48							-	0.49**	0.69***	0.55**	0.04	-0.02	-0.11
SSF 336								-	0.61**	0.70***	-0.16	-0.17	-0.15
WBSF ⁴ 48									-	0.64***	-0.10	-0.12	-0.13
WBSF 336										-	-0.08	-0.13	-0.10
Calp ⁵ 0											-	0.87***	0.81***
Calp 48												-	0.95***
Calp 336													-

¹ Metmyoglobin reducing ability (%), ² Myoglobin concentration (mg/g), ³ Slice shear force (N), ⁴ Warner-Bratzler shear force (N), ⁵ Calpain-1 relative abundance, * $P < 0.05$, ** $P < 0.01$, *** $P < 0.001$

Table 2.5. Pearson correlation coefficients of objective color measurements, myoglobin redox forms, shear force measurements and calpain-1 relative abundance of LL steaks from Holstein beef carcasses (n = 31)

	L* 48	L* 336	a* 48	a* 336	b* 48	b* 336	SI 48	SI 336	HA 48	HA 336	ab 48	ab 336	OMb 48	OMb 336	MMb 48	MMb 336	DMb 48	DMb 336	SSF 48	SSF 336	WBSF 48	WBSF 336	Calp 0	Calp 48	Calp 336
L* 48	-	0.71**	0.01	0.91**	0.45*	0.83***	0.23	0.93**	0.68**	-	0.94***	-	0.27	0.66**	-0.15	0.43*	-0.22	-0.59**	0.26	0.29	0.40*	0.49**	0.03	-0.05	-0.02
L* 336		-	0.60**	-	0.71**	-0.09	-	0.67**	0.65*	-	0.68***	0.67***	0.30	0.42*	-0.12	0.64***	-0.25	-0.53**	0.21	0.36*	0.42*	0.45*	-0.01	-0.06	-0.08
a* 48			-	-0.03	0.90**	0.39*	0.98***	0.17	0.54**	0.62*	-0.56**	-	0.65**	0.77**	0.43*	0.52**	-	-0.61***	0.27	0.20	0.40*	0.39*	0.25	0.27	0.24
a* 336				-	-0.02	0.74**	-0.03	0.94***	0.00	-0.30	-0.01	0.27	-0.08	0.15	-0.13	-0.69***	0.10	0.23	0.00	0.07	-0.13	-0.04	0.07	0.07	0.14
b* 48					-	0.44*	0.97***	0.20	0.85**	0.69*	-	-	0.53**	0.69**	0.07	0.47**	-0.50**	-0.59***	0.25	0.26	0.41*	0.46**	0.16	0.12	0.11
b* 336						-	0.42***	0.92***	0.40*	0.70**	-0.42*	-	0.86***	0.72***	-0.03	0.48**	0.02	-0.10	0.03	0.08	-0.01	0.16	0.39*	0.32	0.37*
SI 48							-	0.19	0.71**	0.67*	-	-	0.61**	0.75**	0.27	0.51**	-	0.62**	0.27	0.23	0.42*	0.44*	0.21	0.20	0.18
SI 336								-	0.20	0.03	-0.21	-0.06	0.72***	0.71***	-0.06	0.32	-0.07	-0.45	0.07	0.07	-0.08	0.05	0.24	0.21	0.26
HA ² 48									-	0.60*	-	-0.62**	0.21	0.45*	-0.37*	0.30	-0.12	-0.43*	0.19	0.29	0.33	0.45*	0.02	-0.08	-0.07
HA 336										-	0.99***	-	0.09	0.52**	0.18	0.81***	-0.12	-0.67***	0.20	0.07	0.22	0.32	0.36*	0.27	0.25
ab ³ 48											-	0.99***	-0.21	-0.47**	0.36*	-0.31	0.12	0.44*	-	-0.30	-0.34	-0.47**	-0.02	0.08	0.07
ab 336												-	0.64***	-0.11	-0.58**	-0.19	-0.80***	0.13	0.69***	-	-0.11	-0.26	-0.36*	-0.35	-0.26
OMb ⁴ 48													-	0.45*	0.40*	0.12	-	-0.28	0.13	0.09	0.23	0.07	0.01	0.01	-0.07
OMb 336														-	0.41*	0.42*	0.98***	-0.49**	0.25	0.04	0.23	0.23	0.17	0.17	0.17
MMb ⁵ 48															-	0.40*	-0.56**	-0.34	0.07	-0.34	0.01	-0.25	0.36*	0.47**	0.38*
MMb 336																-	0.40*	-0.65***	0.14	-0.09	0.20	0.13	0.21	0.23	0.17
DMb ⁶ 48																	-	0.32	-	-0.13	-0.01	-0.21	-0.08	-0.09	-0.01
DMb 336																		-	0.07	0.04	-0.14	-0.18	-0.24	-0.14	-0.16
SSF ⁷ 48																			-	0.49**	0.69***	0.55**	0.04	-0.02	-0.11
SSF 336																				-	0.61**	0.70***	-0.16	-0.17	-0.15
WBS F ⁸ 48																					-	0.64***	-0.10	-0.12	-0.13
WBS F 336																						-	-0.08	-0.13	-0.10
Calp ⁹ 0																							-	0.87***	0.81**
Calp 48																								-	0.95**
Calp 336																									-

* P < 0.05, ** P < 0.01, *** P < 0.001, ¹Saturation index, ²Hue angle, ³a/b ratio, ⁴Oxymyoglobin (%), ⁵Metmyoglobin (%), ⁶Deoxymyoglobin (%), ⁷Slice shear force (N), ⁸Warner-Bratzler shear force (N), ⁹Calpain-1 relative abundance

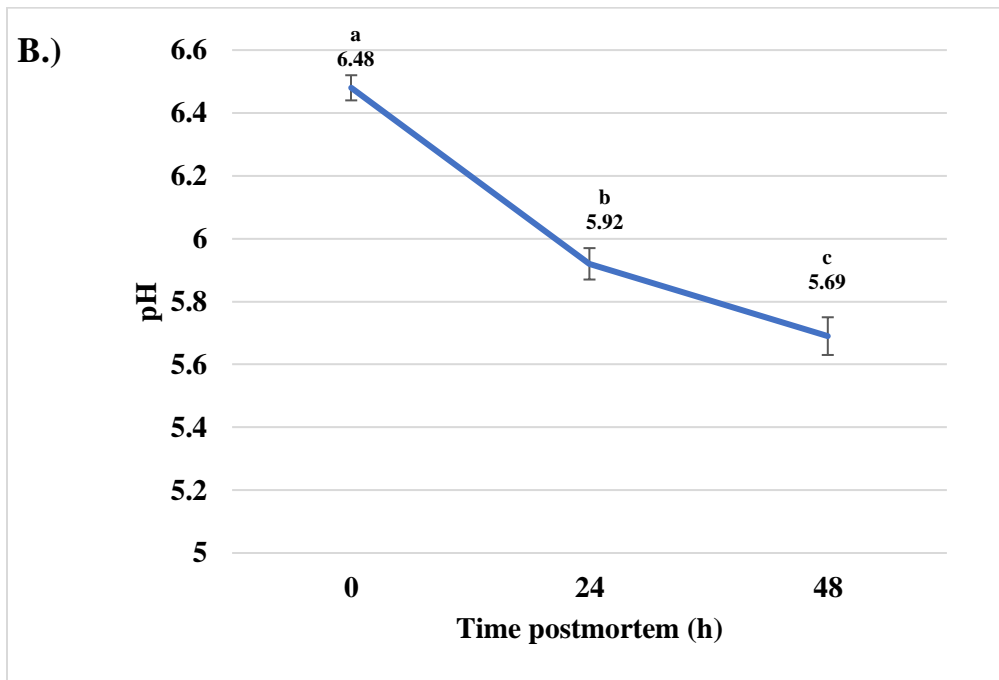
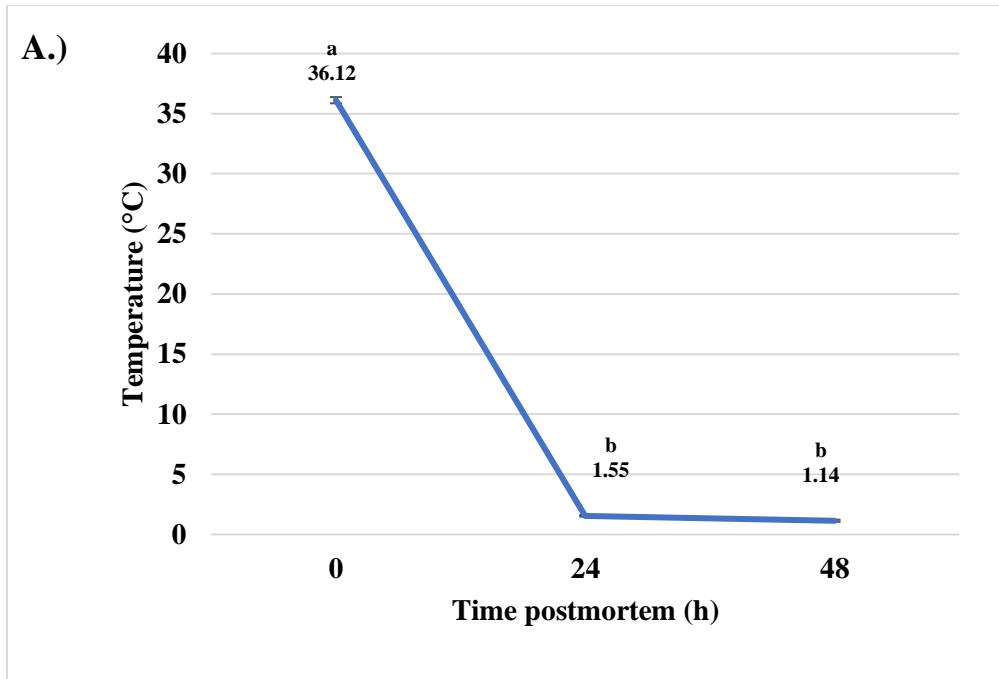


Fig. 2.1. Ultimate A.) Temperature and B.) pH decline of Holstein beef carcasses (n = 31) at 0, 24, and 48 h postmortem. ^{abc} Means lacking a common superscript differ ($P < 0.05$).

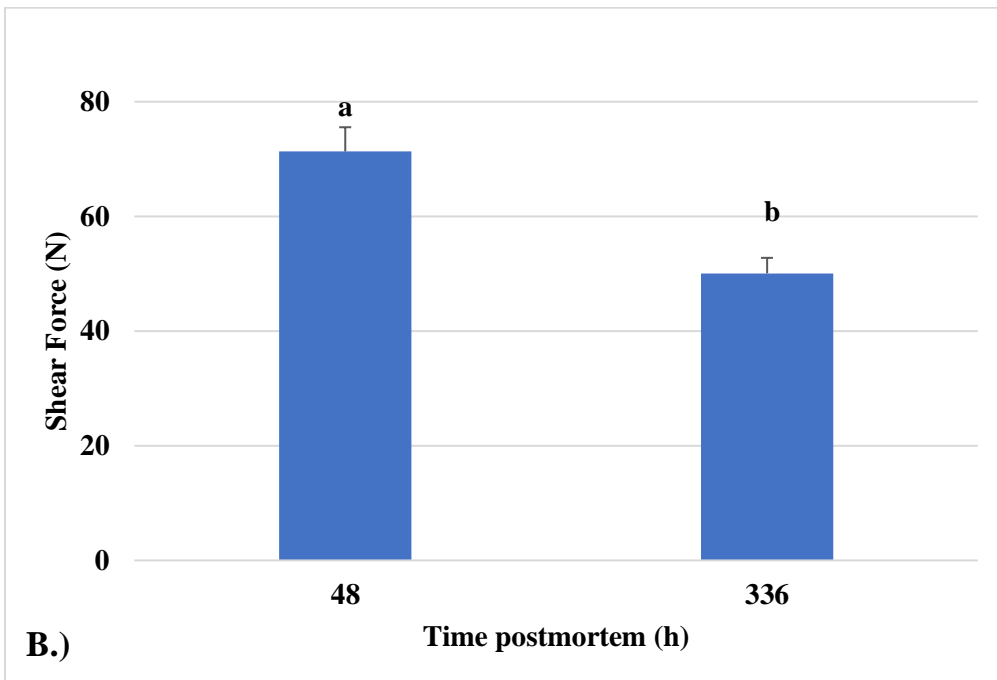
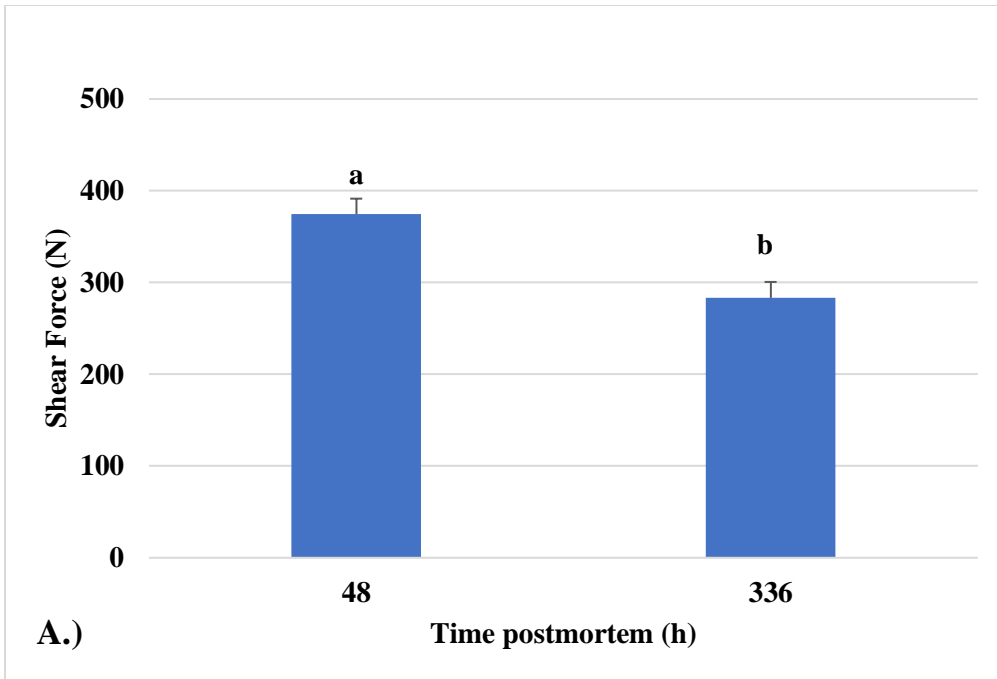


Fig. 2.2. Values for A.) Slice and B.) Warner-Bratzler shear force of LL steaks from Holstein beef carcasses (n = 31) at 48 and 336 h postmortem. ^{a-b} Means lacking a common superscript differ ($P < 0.05$)

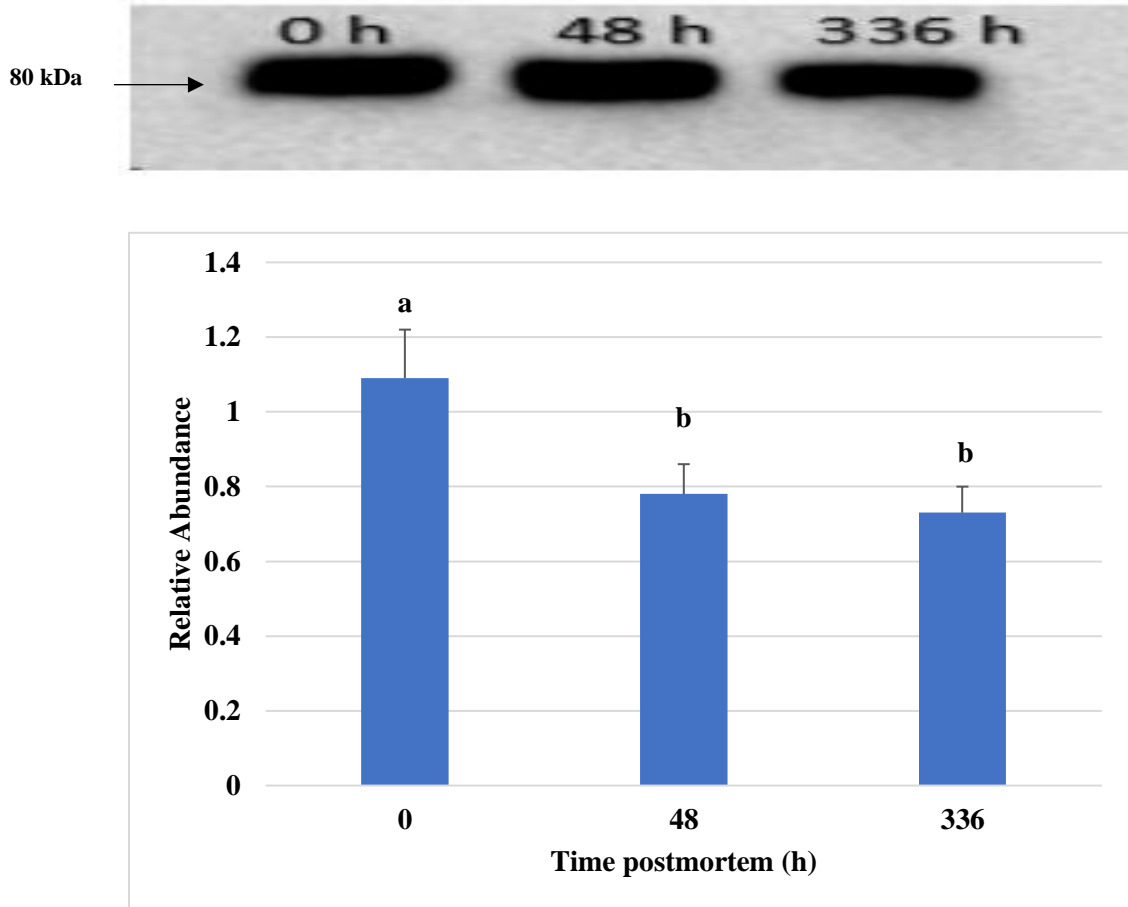


Fig. 2.3. Mean values and example bands for Calpain-1 (80 kDa) relative abundance of LL steaks from Holstein beef carcasses ($n = 31$) at 0, 48, and 336 h postmortem with representative bands. ^{a-b} Means lacking a common superscript differ ($P < 0.05$)

Chapter 3

Color stability and tenderness attributes are impacted by metabolic and biochemical characteristics of beef *longissimus lumborum* steaks at two different aging periods

Abstract: Beef color and tenderness are two of the most important attributes contributing to perception of meat quality and palatability. Studies have indicated specific proteins and metabolites are associated with color stability and tenderness. Many of these studies are done utilizing muscles with known variation in muscle attributes. Very few studies have evaluated differences in attributes within the same muscle to determine animal to animal variation in these components, as well as the relationship between color and tenderness within a specific muscle. Therefore, the objective of this study was to evaluate biochemical and metabolic variation in beef *longissimus lumborum* steaks of four color stability and tenderness classifications. Beef carcasses (n = 96) were selected based on tenderness and color stability predictions at grading. Strip loins were removed from both sides of each carcass and the *longissimus lumborum* was isolated and aged for 12 or 26 d. Four cluster groupings were formed to reflect both tough and tender classifications as well as stabile or labile classifications. A cluster grouping x aging time interaction ($P < 0.05$) for overall tenderness (OT), post-reduction metmyoglobin (PRM), nitric oxide reducing activity (NORA), carbonyl formation in the insoluble fraction, and residual lactate concentration. Differences ($P < 0.05$) were found between cluster groups for slice shear force (SSF), sarcomere length, and percent desmin degradation. Values for SSF decreased ($P < 0.05$) with aging time whereas sarcomere length and desmin degradation increased ($P < 0.05$) with aging. Differences ($P < 0.05$) in cluster groups were found in

total myoglobin (TMYO) concentration, residual malate, and myosin heavy chain (MHC) isoforms. Residual glycogen (GLY) and glucose-6-phosphate (G6P) concentration decreased ($P < 0.05$) with aging time whereas glucose (GLU) concentration increased ($P < 0.05$). A cluster group x aging time interaction ($P < 0.05$) was present for regression coefficients for simulated retail display data with L^* , a^* and chroma (CHR) all having a cubic effect. Cluster groups had a cubic effect ($P < 0.05$) on b^* and hue angle (HA) data and a quadratic effect ($P < 0.05$) on ΔE values. Relationships between glycolytic and oxidative intermediates and color stability and tenderness attributes indicate that muscle metabolic state and biochemical attributes play a role in the animal to animal variation of quality attributes in beef *longissimus lumborum* at two aging periods.

INTRODUCTION

Color is the primary indicator of freshness and quality of beef at consumer point of purchase (Mancini and Hunt, 2005). Deviations in acceptable color can lead to consumer discrimination and refusal to buy products. Beef color stability is a factor impacted by numerous intrinsic and extrinsic factors. Color stability is impacted by muscle source (McKenna et al., 2005; King et al., 2011b; Joseph et al., 2012; S. P. Suman et al., 2014; Canto et al., 2016; Nair et al., 2018a), physiological age and sex (Faustman et al., 1992; Cho et al., 2015), ultimate pH (Page et al., 2001; McKeith et al., 2016; Zhang et al., 2018; Ramanathan et al., 2020a), myoglobin (Suman and Joseph, 2013; Wang et al., 2021), mitochondrial abundance and functionality (Seyfert et al., 2006; McKeith et al., 2016; Mitacek et al., 2019; Wu et al., 2020; Ramanathan et al., 2021), metmyoglobin reducing activity (Madhavi and Carpenter, 1993; Bekhit and Faustman, 2005; Seyfert et al., 2006), oxygen consumption (Tang et al., 2005a), aging time and method (Mancini

and Ramanathan, 2014; Wyrwicz et al., 2016; Callahan et al., 2017; Nair et al., 2018a), packaging and display characteristics (Cooper et al., 2016; Cooper et al., 2017; Cooper et al., 2018; Mitacek et al., 2018), and oxidation (Greene and Price, 1975; Faustman and Cassens, 1990; Faustman et al., 1999; Lynch and Faustman, 2000; Faustman et al., 2010). Research efforts are continuously being made to understand the mechanisms impacting color stability in order to improve and prolong beef display life.

Historically, tenderness has primarily been deemed the most important palatability trait for consumer eating satisfaction. Consumers have indicated they are willing to pay premiums for guaranteed tender beef products. Beef tenderness is impacted by a variety of intrinsic and extrinsic factors such as animal breed (Marino et al., 2013; Wright et al., 2018), physiological age and sex (Huff-Lonergan et al., 1995; Girard et al., 2012; Cruzen et al., 2014), muscle type and location (Calkins et al., 1981; Anderson et al., 2012a; Picard et al., 2014; Dang et al., 2020; Vierck et al., 2020), ultimate pH of muscle (Watanabe et al., 1996; Maddock et al., 2005; Lomiwes et al., 2014b; Grayson et al., 2016), sarcomere length (Koohmaraie et al., 2002; White et al., 2006), connective tissue (Weston et al., 2002; Vierck et al., 2018; Listrat et al., 2020) postmortem aging time and proteolysis extent (Koohmaraie, 1992; Koohmaraie, 1994; Huff-Lonergan et al., 1996; Koohmaraie et al., 2002; Kemp et al., 2010; Anderson et al., 2012b; Marino et al., 2013; Lomiwes et al., 2014a), oxidation (Warner et al., 2005; Malheiros et al., 2019), cooking method and degree of doneness (Lucherker et al., 2016). While these factors have been proven to impact beef tenderness, they do not fully explain tenderness development and variability (Shackelford et al., 2012). As tenderness plays such a crucial role in

consumer eating satisfaction, a more in-depth understanding of tenderness and the mechanisms behind it is of great importance.

Previous and ongoing proteomics and metabolomics work in both color and tenderness studies have indicated that specific proteins and metabolites associated with various biological and metabolic pathways are correlated with beef color stability (Joseph et al., 2012; Canto et al., 2015; Yu et al., 2017; Nair et al., 2018b; Nair et al., 2018a; Yu et al., 2019b; Ramanathan et al., 2020a; Wu et al., 2020; Ramanathan et al., 2021) and beef tenderness traits (D'Alessandro et al., 2012; Picard et al., 2014; Picard and Gagaoua, 2017; King et al., 2019; Malheiros et al., 2019; Antonelo et al., 2020; Picard and Gagaoua, 2020; Gagaoua et al., 2021). Many of these specific systems and their products have been found to be correlated with both color stability and tenderness attributes indicating potential mechanisms behind relationships these traits.

While the relationships between meat quality attributes such as color stability and tenderness are continually becoming more evident, the underlying mechanisms behind these relationships are yet to be fully determined or understood. Additionally, many of the current studies utilize different muscles known for substantial variation in color and tenderness traits as opposed to a singular muscle to assess animal to animal variation in metabolic and biochemical characteristics. Therefore, the objective of this study was to evaluate biochemical and metabolic variation in beef *longissimus lumborum* steaks of four color stability and tenderness classifications.

MATERIALS AND METHODS

Carcasses used in this experiment were selected and obtained from a commercial packing facility. Therefore, animal care and use approval was not obtained for this experiment.

Sample Selection and Fabrication

Beef carcasses (n = 96) were selected at a commercial processing facility. All carcasses selected for this study exhibited A maturity scores. An image-analysis based grading system was used to collect carcass grade characteristics and evaluated using the VBG 2000 GigE beef grading system (Shackelford et al., 2003). Evaluation of carcasses occurred as they were presented for grading and were selected based on predicted tenderness and color stability attributes. The beef, loin, strip loin (similar to IMPS #180 [USDA, 2014]) from both sides of each carcass were designated to an aging period of 12 or 26 d in a complete block so that each aging time and carcass side combination was represented equally in each predicted class. Post-fabrication subprimals were vacuum packaged, sorted by aging time, boxed, and transported back to the US Meat Animal Research Center abattoir via refrigerated truck (-2°C). Upon arrival, subprimals were wet aged at 1°C for the designated time period.

After aging, the *longissimus lumborum* was cut into 2.54 cm steaks using a Grasselli NSL400 (Grasselli-SSI, Throop, PA). Steaks (n = 4) were immediately placed in a simulated retail display setting for a concurrent project. Steaks (n = 2) were vacuum sealed and frozen at -20°C for use with a trained sensory panel. Immediately post fabrication, a steak was trimmed free of external fat and connective tissue to measure oxygen

consumption (OC) and nitric oxide metmyoglobin reducing ability (NORA). An additional steak was trimmed free of connective tissue and external fat, diced and frozen in liquid nitrogen for storage at -80°C for lab analyses including measuring pH, protein oxidation, myosin heavy-chain isoform quantification for fiber type determination, and determination of residual glycogen (GLY), glucose (GLU), glucose-6-phosphate (G6P), lactate, and malate.

Simulated Retail Display

Individual steaks were placed on a polystyrene tray lined with a soaker pad and overwrapped with oxygen permeable polyvinylchloride (PVC) film [stretchable meat film 55003815; Prime Source, St Louis, MO, USA; Oxygen transmission rate = 1.4 mL/(cm² x 24 h) at 23 °C]. Steaks were placed in simulated retail display under continuous fluorescent lighting [3500 K color temperature; CRI = 86; 32W; T8 Ecolux bulb model no. F32T8/SPX35, GE, GE Lighting, Cleveland, OH, USA] for an 11 d period. Light intensity at steak surface was approximately 2000 lx. Simulated retail display occurred at approximately 1°C.

After steaks were packaged, a minimum bloom time of 2 h was allotted before initial color (d 0) measurements were obtained. Color readings were taken utilizing a Hunter MiniScan XE Plus Colorimeter (Hunter-Lab, Reston, VA, USA) equipped with a 25-mm port. Spectral data was collected with Illuminant A and a 10° observer. Color data was additionally collected on d 1, 4, 7, and 11 of display. Color readings were done in duplicate on the steaks surface and values were averaged together to give an overall CIE values for *L** (lightness), *a** (redness), and *b** (yellowness). Additionally, spectral data was utilized to calculate chroma (CH), or color intensity and hue angle (HA) according to

AMSA (2012). Additionally, overall color change was calculated and reported as ΔE which was calculated as $[(\Delta L^* + \Delta a^* + \Delta b^*)^{0.5}]$. ΔL^* Δa^* Δb^* were calculated as the differences in values between d 1, 4, 7, and 11 of display.

pH

Muscle pH was determined as described by (Bendall, 1973) on samples collected at 2 (pHd2), 12, and 26 d postmortem, depending on allocated aging period (pHu). A 2.5 (± 0.05) g powdered sample was measured into a 50 ml plastic tube. Twenty-five ml of Iodoacetate potassium chloride (5 mM Iodoacetic Acid, 150 mM Potassium Chloride, pH 7.0) was added to tubes and samples were homogenized for 10 seconds. Homogenates were allowed to rest at room temperature (approximately 20°C) for 1 h, mixed via vortexing, and pH of the suspension was recorded using a Corning 125 pH meter equipped with a semi-micro combination electrode (Corning, Inc. Corning, NY, USA) that had been calibrated using two standards.

Myoglobin Content Determination

Steaks utilized for myoglobin content (TMYO) determination were trimmed free of external fat and connective tissue before being pulverized in liquid nitrogen to produce a homogenous powder. A method described by (AMSA, 2012) with modifications was utilized to determine myoglobin concentration. A 2.5 (± 0.05) g powdered sample was weighed into a 35 ml centrifuge tube. Twenty-five mL of cold 40mM potassium phosphate buffer was added to each tube. Samples were homogenized for 30 seconds each and placed on ice immediately post homogenization. Once all samples were homogenized, samples were transferred to refrigerated storage for 1 h to allow for

pigment extraction. Samples were centrifuged for 35 min at 15,000 x g at 4°C. Supernatant was poured off centrifuged samples into a 50 mL conical. Supernatants were filtered using a syringe filter (Nalgene surfactant-free cellulose acetate membrane 0.45µm) into a 1.5 ml tube. Using a multichannel pipette, 200µl of each supernatant was plated, in triplicate, in a clear 96 well plate. Samples were read against a blank sample of cold sodium phosphate buffer and absorbance spectra were collected at 525 and 700 nm using a Spectramax plus 96-well plate reader (Molecular Devices, Sunnydale, CA, USA). Myoglobin content was calculated using equations provided in (AMSA, 2012) and reported as mg/g of myoglobin. Samples were done in triplicate and values were averaged.

Nitric oxide metmyoglobin reducing ability and oxygen consumption

Steaks that were allocated for nitric oxide reducing activity (NORA) and oxygen consumption (OC) were sampled by the removal of a 2.54 cm x 2.54 cm x steak thickness cube from the center of each steak. Cubes were then divided in half horizontally to expose the interior portion of the muscle. The interior portion of the steak, which had never been exposed to light or oxygen was used for OC while the exterior portion of the cube which contained the surface previously exposed to light and oxygen was used for NORA. Cube samples used for NORA were oxidized in 50 ml of 0.3% sodium nitrite solution for 30 min at 20 °C as described by (AMSA, 2012). After 30 min, samples were removed from the sodium nitrite solution, blotted, and individually vacuum packaged. Samples were then immediately scanned in duplicate with a Hunter MiniScan colorimeter with settings as previously described. Samples were allowed to reduce at room

temperature for 2 h before being scanned again with identical settings as the initial scan. Equations provided by AMSA (2012) were used to quantify surface metmyoglobin.

Oxygen consumption was determined by methods described in (AMSA, 2012). The top surface of the bottom portion of the cube, or interior of the steak, was allowed to oxygenate, or bloom, for 2 h at 4°C. After the oxygenation period, samples were individually vacuum packaged and immediately scanned with a Hunter MiniScan equipped with the previous settings and calibrated through the film of a vacuum bag. Vacuum packaged samples were incubated for 20 min at 25°C and rescanned with the colorimeter for spectral data collection. Proportion of oxymyoglobin on the deoxygenated and oxygenated samples was determined and OC was reported as the percentage of oxymyoglobin pre-incubation minus the percentage of oxymyoglobin post-incubation.

Slice Shear Force

Steaks utilized for slice shear force (SSF) were thawed at 5 °C for 24 h before cooking. Cooking was done as described above utilizing methods described in Wheeler et al. (1998) on an electric conveyor belt grill to achieve an internal temperature of 70 °C. Shear force values were determined using methods described in Shackelford et al. (1999) Internal steak temperatures were monitored pre- and post-cooking with a handheld thermometer equipped with a thermocouple probe (Cole-Parmer, Vernon Hills, IL, USA) placed in the geometric center of each steak. A 1-cm-thick, 5-cm-long slice was removed from each cooked steak parallel to muscle fibers. Slices were sheared with a flat, blunt-end blade using an electronic testing machine (Model 4411, Instron Corp, Norwood, MA, USA) with a crosshead speed of 500 mm/min. Slice shear force values are reported in kg.

Sarcomere Length Determination

Sarcomere length (Sarc) was determined utilizing a helium-neo laser diffraction method described in Cross et al. (1981). Cooked slices from SSF determination were trimmed of all hard, cooked edges from each slice. Samples were finely diced and snap frozen in liquid nitrogen before being pulverized in a pre-cooled Waring blender to the consistency of a fine powder. Powdered sample was immediately transferred to a pre-cooled conical tube and placed in freezer storage until use. Each day before beginning measurements, microscope stage was checked to ensure that it was set properly at 10 cm above the top of the stage where diffraction bands would be measured. Using a cold metal spatula, a small amount of powdered tissue was placed on a microscope slide. Approximately 100 μ l of sucrose buffer (0.2 M Sucrose in 0.1 M NaHPO₄, pH 7.4) was added to the top of the sample to moisten the powder. In a dark room, the slide was placed on the stage so that the laser beam passed through the sample. The slide was moved around the stage until a diffraction pattern of three parallel lines appeared. Six diffraction patterns were traced on a single piece of paper for each sample. Thirty-six diffraction patterns were traced for each sample. Patterns were scanned into JPEG images and Image Pro software (Media Cybernetics, Inc., Rockville, MD) was used to measure the diffraction bands. Sarcomere length was determined by the following equation:

$$\text{sarcomere length, } \mu\text{m} = \frac{0.6328 \times D \times \sqrt{\left(\frac{T}{D}\right)^2 + 1}}{T}$$

Desmin Degradation

One g of sample was homogenized in 10 ml of TRIS-EDTA (50 mM Tris, 10 mM EDTA, pH 8.3) for 20 seconds. After homogenizing, a 0.5 ml aliquot was transferred into a microcentrifuge tube. 0.5 ml of 2X treatment buffer (0.125 M Tris, 4% SDS, 20% Glycerol, H₂O, pH 6.8) was added to the microcentrifuge tube and samples were vortexed. Samples were heated in a 50°C water bath for 20 min, mixed again to shear nucleic acids, and were heated for an additional 5 min. After heating samples were centrifuged for 20 min at 16,000 x g. Protein concentration was determined using a bicinchoninic acid (BCA) assay (Pierce micro-BCA-assay, Thermo Scientific, Waltham, MA, USA). After protein concentration was determined samples could be diluted to the concentrations needed.

Desmin degradation was determined using the WES Protein Separation Module (Protein Simple, San Jose, CA, USA). Protein concentrations from extracted samples were determined and utilized to determine dilutions needed to reach 0.3 mg/ml for desmin degradation determination. Additionally, samples collected from LD at 0 h postmortem were diluted and utilized throughout samples on each WES plate to serve as a standard to determine degradation against. Using the WES kits, 0.1x sample buffer was made from 10X sample buffer provided in the WES kit and samples were diluted to the intermediate dilution step. Separation modules were prepared from the WES kit containing DTT, fluorescent 5X master mix and a biotinylated ladder and were immediately stored on ice upon mixing. Primary antibody (Rabbit monoclonal desmin, clone RM234, Novus Biologicals, Centennial, CO, USA) was then diluted (1:50) and immediately stored on ice. Final samples were diluted using 1-part 5X master mix and 4-

parts sample (1µl 5X, 4µl sample) into a 0.5 ml microcentrifuge tube. Samples were immediately vortexed and placed into a multiblock heater at 95°C for 5 min. After heating, samples were mixed and placed into a microcentrifuge at max speed for 15 seconds. Samples were stored on ice after centrifugation until plated. Immediately prior to plating the assay, HRP solution was made by combining 200µl of peroxide solution and 200µl of luminol supplied in the WES assay kit. Secondary antibody (Anti-Rabbit, WES Detection Kit, Protein Simple, San Jose, CA, USA) was utilized in each plate. Plates were pipetted from bottom to top to avoid evaporation according to kit insert provided. After pipetting, plates were centrifuged at 1000 x g for 5 min. Immediately prior to placing the plate in the WES system, 500 µl of wash buffer was added to the first three rows of wells below sample wells. Plates were placed into the WES system and a new capillary cartridge was inserted into the cartridge holder for each plate. The WES system was started and ran until completion. Once a run was complete, peaks were measured using the WES system software to determine percent desmin degradation on samples versus the 0 h postmortem standards. Each peak was individually evaluated to ensure desmin degradation was correctly accounted for in each sample.

Soluble and Insoluble Protein Carbonyl

Extraction of soluble and insoluble fractions along with carbonyl determination was completed using methods provided in (Rowe et al., 2004) with modifications. Five g of finely diced muscle was placed in a 35 ml centrifuge tube and 15 ml of cold post rigor extraction buffer (100 mM Tris, 10 mM EDTA, MCE) was added to each tube. Samples were homogenized for 10 seconds at medium speed and then incubated in refrigeration for 10 min. This process was repeated 3 times for each sample. After the final incubation,

samples were centrifuged at 27,000 x g for 30 min at 4°C. Supernatants were filtered through cheesecloth and total filtered volume was recorded as the soluble fraction. A 4 g portion of the remaining pellet was removed from each centrifuge tube and placed into a new 35 ml centrifuge tube, 10 ml of salt solution (100 mM KCl, 2 mM MgCl₂, 1 mM EGTA, 1 mM NaN₃, 20 mM K₂HPO₄, pH 7.0) was immediately added to each tube and samples were homogenized for 10 seconds at medium speed. Samples were incubated in refrigeration for 30 min with vigorous vortexing occurring every 10 min. After incubation, samples were centrifuged at 27,000 x g for 20 min at 4 °C. Supernatant was poured off and pellets were washed with 10 ml KCl/MCE solution (50 mM KCl, 5 mM MCE). Post-wash samples were centrifuged at 27, 000 x g for 10 min at 4 °C. Supernatant was poured off and pellet was washed with 10 ml of sodium phosphate buffer (200 mM Na₂HPO₄, pH 7.4). Samples were again centrifuged at 27,000 x g for 10 min at 4 °C. Supernatant was poured off and samples were homogenized with 25 ml of sodium phosphate buffer. The remaining pellet suspension was the insoluble fraction. Protein concentration of both soluble and insoluble fractions were determined using a BCA protein assay kit (Pierce micro-BCA-assay, Thermo Scientific, Waltham, MA, USA) utilizing a BSA standard curve.

Samples were diluted to 6 mg/ml using a sodium phosphate EDTA solution (1mM EDTA, 50mM Na₂HPO₄) into 15 ml plastic conicals. Two dilutions were made for each sample, one for the DNPH treated sample and the other for the HCL treated blank. Once all dilutions were completed, 4 ml of DNPH was added to its respective tube and 4 ml 2M HCL was added to each tube designated as a blank. Samples were vortexed and placed into dark storage for a 1 h incubation with vortexing occurring at 15 min intervals.

After incubation, 5 ml of 20% TCA was added to each tube and samples were placed in refrigeration for 10 min. Samples were centrifuged using a benchtop centrifuge at 1000 x g for 8 min. After centrifugation, supernatant was poured off to leave a remaining pellet. Four ml of 10% TCA was added to each tube and pellets were broken up with glass rods before vortexing. Samples were centrifuged using a benchtop centrifuge at 1000 x g for 8 min. Supernatant was discarded and pellets were washed three times with 50:50 ethyl alcohol:ethyl acetate. Pellets were centrifuged at 1000 x g for 8 min after each wash and supernatant was discarded each time. After the final wash, samples were dissolved in 6M Guanidine hydrochloride and incubated at 37 °C for 10 min. Protein concentration was determined for final samples using a BCA protein assay as previously described. Carbonyl content was determined using absorbance of DNPH treated samples vs blanks serving as reference samples at 360 nm on a Spectramax plus spectrophotometer (Molecular Devices, Sunnydale, CA, USA). Carbonyl content (nmol/mg protein) for both the soluble and insoluble fractions were calculated using the molar extinction coefficient for DNPH $22,000 \text{ M}^{-1}\text{cm}^{-1}$ and the formula: carbonyl content = (absorbance \times 106/22,000)/mg protein.

Myosin Heavy Chain Isoform Separation and Quantification using Polyacrylamide Gel Electrophoresis (PAGE)

Myosin heavy chain (MHC) isoforms were separated and quantified using methods described in Picard et al. (2011) with modifications. One g of sample was homogenized in 10 ml of TRIS-EDTA (50 mM Tris, 10 mM EDTA, pH 8.3) for 20 sec at medium speed. Immediately after homogenizing, a 0.5 ml aliquot was transferred into a microcentrifuge tube. 0.5 ml of 2X treatment buffer (0.125 M Tris, 4% SDS, 20%

Glycerol, H₂O, pH 6.8) was added to the microcentrifuge tube and samples were vortexed. Samples were heated in a 50°C water bath for 20 min, mixed again to shear nucleic acids, and heated for an additional 5 min. After heating samples were centrifuged for 20 min at 16,000 x g. Protein concentration of samples was determined using a BCA assay (Pierce micro-BCA-assay, Thermo Fisher Scientific, Waltham, MA, USA). Once protein concentration of samples was determined, samples were diluted to 3 mg/ml using a 2X treatment buffer containing MCE and bromophenol blue (0.5M Tris, 10% SDS, Glycerol, H₂O, MCE, 0.8% bromophenol blue, pH 6.8). After dilution, samples were heated for 10 min at 50 °C. Once heating was complete, samples were vortexed once more and frozen until use.

Bio-rad Mini-Protean gels (Bio-Rad, Hercules, CA, USA) were poured with a 6% stacking (30% Acrylamide (50:1), 0.04% SDS, 47% Glycerol, 6mM EDTA, 115mM Glycine, 110mM Tris (pH 6.7), H₂O, 0.1% APS, 0.05% TEMED) and a 9% separating (30% Acrylamide (50:1), 0.4% SDS, 35% Glycerol, 115 mM Glycine, 230mM Tris (pH 8.8), H₂O, 0.1% APS, 0.05% TEMED). Separating gels were poured and allowed to polymerize for 1 h before stacking gel was poured. Combs were placed into stacking gels and gels were sealed in plastic bags and placed in refrigeration until needed for electrophoresis.

Samples were removed from freezer storage and placed in a 37 °C water bath for 5-10 min to allow samples to thaw and SDS buffer to go back into solution. Upper and lower chamber running buffers were made fresh daily. Upper chamber running buffer contained 5X running buffer (100mM Tris, 150mM Glycine) diluted to 1X running buffer with H₂O, 0.1% SDS, and 0.07% MCE. Lower chamber running buffer contained

5X running buffer (50mM Tris, 75mM Glycine) diluted to 1X running buffer with H₂O, and 0.05% SDS. Gels were removed from the refrigerator, combs were removed, and gels were washed with distilled H₂O immediately prior to loading. Gels were loaded into the electrophoresis modules were placed inside tanks. Upper chamber running buffer was added to the inside assembly of the module and lower chamber buffer was added to the tank. Wells were washed with running buffer prior to loading. Samples were vortexed immediately prior to loading. Using a 10 µl pipette, 2.7 µl of sample was added to each well. Once all samples were loaded into their respective gels, modules were placed into a refrigerated room to run at 70 v for 30 h.

After the 30 h run, gels were removed from glass plates, stackers were removed, and gels were placed into shallow individual containers and washed for 5 min with dd H₂O. Three washes were done for each individual gel. After initial washes gels were covered with Imperial Protein Stain (Thermo Fisher Scientific, Waltham, MA, USA) and stained for a minimum of 1 h with gentle shaking. After staining, gels were washed with dd H₂O for 30 min with gentle shaking. After the initial wash, water was discarded, and gels were washed in fresh dd H₂O overnight with gentle shaking. After overnight wash, gels were imaged using the Bio-Rad GelDoc Go Imaging System (Bio-Rad, Hercules, CA, USA) and gels were analyzed using Image Lab Software (Version 6.1, Bio-Rad, Hercules, CA, USA) to determine percent myosin heavy chain type of samples. Samples were analyzed in duplicate and values were averaged to determine value (%) of MHC-1 (type I fibers) and MHC-2 (type II fibers) in each sample.

Residual Metabolic Intermediate Determination

Extractions and residual metabolic components were completed via methods described in Hammelman et al. (2003) with modifications. One g of powdered tissue was homogenized and deprotonated with 4 ml of 2 M HCl. One ml of homogenate was immediately removed and placed into a 1.6 ml microcentrifuge tube for use with amyloglucosidase (AGS) digestion for residual glycogen (GLY) determination. The remaining homogenate was centrifuged at 30,000 x g for 20 min at 4 °C. After centrifugation, samples were neutralized with approximately 800 µl of 5.4 M KOH to a pH of approximately 7.0. Neutralized samples were stored in refrigeration until use for malate assay.

A 200 µl aliquot of homogenate was added to a 35 ml centrifuge tube and combined with 1 ml of AGS and 50 µl of potassium hydroxide (KOH). The pH was measured and adjusted to be approximately 4.8. Samples were incubated for 3 h at 37°C with inverting occurring once every hour. After incubation, samples were placed in refrigeration for 10 min and 100 µl of 2M HCl was added to each tube. After hydrolysis was stopped, 40µl of 5.4 M KOH was added to each tube to neutralize the sample. Samples were incubated for an additional 10 min in refrigeration before being centrifuged at 30,000 x g for 20 min at 4°C. Supernatant was removed with a pipette and placed into a 1.5 ml centrifuge tube for residual GLY content determination. A 400 µl aliquot of sample was added to a glass test tube and combined with 200 µl of ATP/NADP solution, and 1.7 ml of 0.3 M triethanolamine (TEA) buffer. Tubes were vortexed and samples were plated in triplicate 210 µl aliquots into a 96 well plate. Initial absorbance was read at 340 nm on a Spectramax plus 96-well plate reader (Molecular Devices, Sunnydale, CA, USA) and values were recorded (OD1). After plating samples, 40 µl of glucose-6-

phosphate dehydrogenase and 40 μ l of hexokinase were added to each tube. Tubes were vortexed and incubated at room temperature for 20 min. After incubation, tubes were vortexed again and immediately plated in triplicate 210 μ l aliquots into a 96 well plate. Absorbance was read at 340 nm on a 96-well plate reader and absorbance values were recorded (OD2). Final absorbance values associated with glycogen content were determined by $OD2 - OD1$. The quantity of residual glycogen was determined by way of standard curves of 1mmol, 900, 600, 300, and 0 μ M glucose standard. Glucose and G6P concentration from additional assays were subtracted from overall glycogen content to determine the final GLY content. Residual GLY content is reported as μ mol/g of muscle.

A 200 μ l aliquot of extracted and neutralized sample was added to a glass tube and combined with 200 μ l of NAD and 3 ml of reaction buffer (0.4 M Hydrazine, 0.5 M Glycine, pH 9.0) and immediately vortexed. Samples were plated in triplicate 210 μ l aliquots into a 96 well plate. Absorbance was read at 340 nm on a Spectramax plus 96-well plate reader and initial absorbance values were recorded (OD1). After reading the initial plate, 40 μ l of malate dehydrogenase was added to each tube and immediately vortex. Tubes incubated in a 25°C water bath for 2 hr. After incubation, samples were plated in triplicate 210 μ l aliquots into a 96 well plate and absorbance was read again at 340 nm (OD2). Absorbance values for determination of residual malate was calculated as $OD2 - OD1$. Residual malate was calculated using standard curves of 600, 400, 200, 100, and 0 μ M malic acid. Malate is reported as μ mol/g of muscle.

An additional extraction was completed utilizing 0.5 g of powdered tissue which was homogenized and deprotonated with 10 ml of 2 M HCl. Homogenates were incubated in refrigeration for 15 minutes before being centrifuged at 30,000 x g for 20

min at 4 °C. After centrifugation, supernatant was poured into a 50 ml conical and neutralized with 3.5 ml of 5.4 M KOH to an approximate pH of 7.0. After extraction and neutralization, samples were stored in refrigeration until used for determination of residual lactate, glucose (GLU), and glucose-6-phosphate (G6P).

A 400 µl aliquot of extracted and neutralized sample was added to a glass tube and combined with 200 µl of ATP/NADP solution and 1.7 ml of 0.3 triethanolamine (TEA) buffer. Tubes were vortexed and samples were immediately plated in 210 µl aliquots in triplicate, on a 96 well plate. Plates were read at 340 nm on a Spectramax plus 96-well plate reader and initial absorbance values (OD1) were recorded. After initial plate reading, 40 µl of glucose-6-phosphate dehydrogenase was added to each tube. Tubes were vortexed and incubated at room temperature for 20 min. After incubation, samples were plated in triplicate 210 µl aliquots on a 96 well plate. Plates were read at 340 nm and absorbance values were recorded (OD2). After reading, 40 µl of hexokinase was added to each tube. Tubes were vortexed and incubated at room temperature for 20 min. After incubation, samples were plated in triplicate 210 µl aliquots into a 96 well plate. Plates were read again at 340 nm on a plate reader and absorbance values were recorded (OD3). Absorbance values for calculating G6P were determined by $OD2 - OD1$ and GLU was determined by $OD3 - OD2$. Residual GLU and G6P were calculated utilizing standard curves of 1mmol, 900, 600, 300, and 0 µM GLU and G6P standards. Glucose and G6P are reported as µmol/g of muscle.

A 50 µl aliquot of extracted and neutralized sample was added to a glass tube and combined with 150µl of an HCL/KOH solution. 200µl of NAD and 3 ml of reaction buffer (0.4 M Hydrazine, 0.5 M Glycine, pH 9.0) were added to the tubes and tubes were

immediately vortexed. Samples were plated in triplicate 210 μ l aliquots into a 96 well plate. Absorbance was read at 340 nm on Spectramax plus 96-well plate reader and initial absorbance values were recorded (OD1). After reading initial values, 40 μ l of lactate dehydrogenase was added into each sample tube and tubes were immediately vortexed. Samples were incubated in a 25°C water bath for 2 h before tubes were removed and vortexed again. After incubation, samples were plated in triplicate 210 μ l aliquots into a 96 well plate. Absorbance was measured at 340 nm on a 96-well plate reader and values were recorded (OD2). Absorbance values to determine residual lactate was calculated as $OD2 - OD1$. Residual lactate concentration was determined by way of lactate standard curves of 2 mmol, 1.4 mmol, 1 mmol, 400, and 0 μ M. Lactate is reported as μ mol/g of muscle.

Statistical Analysis

Four color stability and tenderness attribute component cluster groupings were created using Agglomerative hierarchical clustering using the factoextra package Kassambara and Mundt (2020) in R statistical software R Core Team (2020) to represent variation in flavor profile and palatability components. Clustering was done utilizing all retail display data as well as overall tenderness (OT), SSF, desmin degradation, and sarcomere length. Data were scaled using the scale() function and the Euclidean distance matrix was calculated using the dist() function. Dendrograms were generated using the hclust() function. Thus, the four resulting clusters represented samples differing in color stability and tenderness attributes. Data was analyzed as a split plot design using the GLIMMIX function of SAS version 9.4 (SAS Institute Inc., Cary, NC, USA) with carcass serving as whole plot experimental unit and cluster as the whole plot treatment and

carcass side serving as the split plot experimental unit and aging time as the split plot treatment. Cluster, aging period and their interaction were included as fixed effects in the model. Carcass nested within collection trip was included as a random effect in the model. Additionally, color stability data collected during simulated retail display were analyzed including the squared and cubed day of display terms to the model to describe trends in color change. Regression equations were generated for changes in color attributes throughout retail display using contrasts to determine intercept (d_0) values and β -coefficients and to describe color change occurring during simulated retail display. Orthogonal contrasts were used to make pair-wise comparisons when differences were indicated. The Kenward-Roger approximation was utilized to estimate degrees of freedom. The PRINCOMP function of SAS was utilized to identify color and tenderness attributes into principal components at both aging periods score plots and loading plots were produced to determine relationships between attributes and metabolic data. Pearson correlation coefficients of flavor attributes and muscle metabolic characteristics were determined using the PROC CORR procedure in SAS. A level of $\alpha < 0.05$ was used to determine differences among traits.

RESULTS

General color and tenderness profile for each cluster grouping is presented in Table 3.1. Among variation in carcasses selected for this study, cluster 1 is identified as tender with moderate color stability attributes. Cluster 2 is considered tender and color stable. Cluster 3 is considered tough and color labile. Cluster 4 is identified as moderate tenderness and moderate color stability.

A cluster by aging time interaction occurred for OT, NORA, insoluble fraction carbonyl, and residual lactate concentration (Table 3.2). Overall tenderness scores increased for all clusters with increasing aging time ($P = 0.01$). While still the least tender, cluster 3 OT scores increased substantially between aging periods in comparison to the remaining clusters. Values for NORA decreased ($P < 0.05$) with increased aging time for clusters 1 and 3. No differences between 12 and 26 d of aging were reported for NORA values for clusters 2 and 4. Although values for nitric oxide reducing ability were greater for cluster 1 at 12 d of aging, values decreased by over 17% between aging periods for resulting in similar NORA among all clusters with extended aging times. Carbonyl formation in the insoluble fraction increased ($P < 0.05$) substantially for cluster 2 with increasing aging time. No other differences in carbonyl content ($P > 0.05$) were found among clusters at both aging time points. Residual lactate content decreased ($P < 0.05$) substantially between aging periods for cluster 1. While cluster 4 also decreased, no differences ($P > 0.05$) were present among aging periods. By 26 d of aging, residual lactate was similar ($P > 0.05$) among all clusters.

Table 3.3 contains tenderness attributes for all clusters. Slice shear force values were higher ($P < 0.0001$) in cluster 3 than all other CT groups indicating cluster 3 was less tender than other groups. Sarcomere length was greater in cluster 1 ($P = 0.01$) than clusters 3 and 4. Longer sarcomeres indicate less actomyosin crosslinks and are associated with increased tenderness. No differences ($P > 0.05$) were found between cluster 2 and all other groups for sarcomere length. Desmin degradation was greater ($P = 0.01$) in clusters 1 and 2 than clusters 3 and 4 indicating increased proteolysis for clusters 1 and 2.

Biochemical and metabolic attributes for beef *longissimus lumborum* steaks for each cluster are depicted in Table 3.4. Total myoglobin concentration was greater ($P < 0.0001$) in clusters 3 and 4 than clusters 1 and 2. Ultimate pH values were greater ($P = 0.003$) in cluster 4 than pH_u values in clusters 1 and 2. Additionally, pH_u values were higher ($P = 0.003$) in both clusters 2 and 3 than cluster 1. However, all pH_u values are within 0.05 units of one another which would be expected to have minimal impact. Residual malate concentration was lower ($P = 0.05$) in cluster 1 than clusters 2 and 4. Residual malate values for cluster 3 did not differ ($P > 0.05$) among any of the groups. Myosin heavy chain-1 isoforms, or type I muscle fibers, were greater ($P = 0.01$) in clusters 3 and 4 than cluster 2. Conversely, MHC-2 isoforms, or type II muscle fibers were greater in cluster 2 than clusters 3 and 4. No differences ($P > 0.05$) were present between cluster 1 and all other groups for MHC isoforms. While differences in percent MHC isoforms were present between groups in this study, differences were very small. No differences ($P > 0.05$) were found among CT groups for OC, IMF, pH d2, soluble fraction carbonyl formation, residual GLY, residual GLU, or residual G6P concentrations.

Postmortem aging is a key tool in development of tenderness in beef. As seen in Table 3.5, aging period had a substantial impact on tenderness attributes on steaks from the *longissimus lumborum*. Slice shear force values decreased ($P < 0.0001$) as aging time increased. Sarcomere length ($P = 0.003$) and percent desmin degradation ($P < 0.0001$) were greater after 26 d of aging in comparison to 12 d.

Table 3.6 contains mean biochemical and metabolic attribute values at both aging periods for beef *longissimus lumborum* steaks. Total myoglobin was greater ($P = 0.03$) in

steaks aged for 12 d than those aged for 26. Initial metmyoglobin formation was greater in steaks ($P = 0.02$) after 12 days of aging in comparison to 26 d of aging. Residual GLY concentration was greater ($P < 0.002$) in steaks aged for 12 d than those with 26 d of aging. Residual GLU concentration was lower ($P < 0.0001$) in steaks aged 12 d than steaks aged 26 d. Conversely, residual G6P concentration was higher ($P < 0.0001$) in steaks aged for 12 d in comparison to those aged 26 d. No differences ($P > 0.05$) in malate concentration were found between aging periods. Additionally, no differences were found in MHC isoforms between aging periods.

Regression coefficients for change in a^* values for clusters at both 12 and 26 days are presented in Table 3.7 and graphically in Fig 3.1. Differences were reported at the cubic term ($P = 0.003$) for changes in a^* over the duration of retail display. A slight increase in a^* values occurred at the early stages of retail display for all CT groups at both aging periods. As display lengthened, a^* values decreased more substantially for steaks within cluster 3 at both 12 and 26 d. Steaks from clusters 1 and 4 aged for 26 d did not decrease in a^* value to the level cluster 3 steaks did but did not end up with a^* values like all other CT groups and aging periods. Chroma values followed the same pattern as a^* values for all CT groups at both aging periods (data not shown).

Correlation coefficients between color and tenderness attributes with biochemical and metabolic attributes at 12 d of aging are presented in Table 3.8. Nitric oxide reducing ability exhibited no relationships ($P > 0.05$) with any color attributes after 12 d of aging. Sarcomere length (0.40) was positively related to NORA while percent desmin degradation was negatively related to NORA (-0.21). In the present study, oxygen consumption after 12 d of aging was negatively related to L^* (-0.33) and a^* (-0.42) color

values at d 0 of simulated retail display. By d 11 of simulated display, OC and L^* values were negatively related (-0.31) while no other ($P > 0.05$) relationships were present with color attribute values. A negative relationship between OC and OT (-0.26) was reported. Conversely, a positive relationship between OC and SSF (0.26) was present. No relationships ($P > 0.05$) were present between OC and percent desmin degradation or sarcomere length. Total myoglobin concentration was negatively related to L^* values at d 0 of simulated display (-0.81). Positive relationships between TMYO and a^* (0.23) were present at d 0 of simulated display. By d 11 of simulated display, TMYO was negatively related to L^* and a^* (-0.79 and -0.35, respectively). Myoglobin concentration was negatively related to overall tenderness scores and desmin degradation (-0.28 and -0.22, respectively). The pH values at 2 d postmortem were negatively related to L^* values (-0.24) at the onset of simulated retail display. Additionally, pH_{d2} values were positively correlated to SSF values at 12 d of aging. Ultimate pH values were negatively related to L^* and a^* values at d 0 of simulated display (-0.42, and -0.22, respectively). After 11 d of simulated retail display only a negative relationship (-0.39) with L^* remained for pH_u. No relationships ($P > 0.05$) between pH_u and tenderness attributes at 12 d of aging were present in this study. No relationships ($P > 0.05$) were present between color or tenderness attributes and carbonyl formation in the soluble fraction of beef *longissimus lumborum* steaks. Similarly, no relationships ($P > 0.05$) were present between carbonyl formation in the insoluble fraction and color or tenderness attributes. Residual GLY concentration was negatively related to a^* values at 11 d of simulated display (-0.25) and SSF values (-0.28). A positive relationship (0.22) between GLY and OT scores occurred in steaks aged for 12 d. Residual GLU was positively related to a^* values (0.35) at d 0 of

retail display. Positive relationships between GLU and OT (0.20) was present while a negative relationship with SSF (-0.24) was also present at 12 d of aging. Relationships between color and tenderness attributes for residual G6P followed the same trends as residual GLU. No relationships ($P > 0.05$) were found between residual lactate concentrations and any color or tenderness attributes of beef *longissimus lumborum* steaks aged for 12 d. Malate concentration was not ($P > 0.05$) related to any color attributes at d 0 of simulated retail display. Positive relationships were present at d 11 of simulated display between residual malate concentration and a^* (0.29) values. A negative relationship (-0.23) occurred between malate concentration and SSF values. Percent MHC-1, or type I muscle fibers, was negatively related to L^* (-0.36) at the onset of retail display. By d 11 of simulated retail display, MHC-1 was negatively related to L^* (-0.35), and a^* (-0.24) values. Conversely, percent MHC-2, or type-II muscle fibers, was positively related to L^* values (0.35) at d 0 of simulated retail display. By 11 d of display, percent MHC-2 was positively related to L^* (0.35) and a^* (0.24) values. No relationships ($P > 0.05$) between MHC isoforms and tenderness attributes were present in the current study.

Correlation coefficients between color and tenderness traits and metabolic and biochemical attributes at 26 d of aging are presented in Table 3.9. Nitric oxide reducing ability was negatively related to a^* values at onset of simulated retail display as well as OT scores (-0.20 and -0.29, respectively). Oxygen consumption was negatively related to both L^* and a^* (-0.43 and -0.28, respectively) at the onset of retail display. Additionally, OC was negatively related to L^* values at d 11 of retail display (-0.35) and positively related to SSF (0.25). Myoglobin concentration was negatively related to L^* values at

both d0 and d11 of simulated display (-0.86 and -0.77, respectively). At d0 of display MYO was positively related to a^* values (0.41) but by d11 of display that relationship was negative (-0.25). Myoglobin concentration was positively related to SSF values (0.23) and negatively related to OT scores (-0.28) after 26 d of aging. Values for pHd2 were negatively related to L^* and a^* values at d0 of simulated display (-0.30 and -0.25, respectively). At d11 of simulated display pHd2 values were negatively related to L^* values (-0.24). Additionally, pHd2 values were negatively related to OT (-0.28) and positively related to SSF (0.32). Ultimate pH values were negatively associated with L^* values at both d0 (-0.44) and d11 (-0.32) of simulated display. Values for pHu were negatively related to OT scores (-0.29) and positively related to SSF values (0.22). No relationships ($P > 0.05$) between carbonyl content in the soluble fraction and any color or tenderness traits were present after 26 d of aging. Carbonyl content in the insoluble fraction was positively related to L^* values at d11 of retail display. Residual glycogen, GLU, and G6P were positively related to OT (0.31, 0.35, and 0.28, respectively) and negatively related to SSF (-0.30, -0.40, and -0.26, respectively). Residual GLU, G6P, and Lactate were positively related to a^* values at d0 of display (0.22, 0.22, and 0.20, respectively). No relationships ($P > 0.05$) were present between malate and any color or tenderness traits at 26 d of aging. Myosin heavy chain-1 isoform was negatively related to L^* values at d0 and d11 of simulated display (-0.31 and -0.24, respectively). Additionally, MHC-1 was negatively related to a^* values at d11 of display (-0.24). Positive relationships between MHC-2 and L^* values at d0 and d11 (0.31 and 0.24, respectively) as well as a^* values at d11 (0.24) were present.

Principal component analysis of tenderness and color stability traits at 12 d of aging is presented in Fig. 3.2. Principal component 1 accounts for 52.92% of the variation among samples and is heavily influenced by a^* , b^* , and chroma values at 11 d of display. Negative correlations between these attributes and ΔE and hue angle values at d 11 of display are present indicating that principal component 1 is heavily driven by color stability. Principal component two accounts for 20.41% of variation and is heavily influenced by desmin degradation and OT scores. Negative correlations between these attributes and SSF indicate that component two is driven by tenderness attributes. A score plot for all four clusters is depicted in Fig. 2 B. Cluster 2 is primarily associated with color stability attributes and positively related to desmin degradation and overall tenderness scores. Cluster 1 trended more toward color stability and tenderness attributes whereas cluster 4 trended more toward color labile attributes but was fairly similar to cluster 1 in relation to tenderness traits. Cluster 3 was heavily related to color labile attributes. Loading plots for metabolic and biochemical data are presented in Fig. 2 C. Malate and MHC-2 or type II fibers are positively related to principal component 1. Whereas MHC-1 or type I fibers and total myoglobin are negatively related to principal component 1. Residual GLY, GLU, and G6P are positively related to principal component 2. Conversely, OC appears to be negatively related to component 2.

Figure 3.3 contains the principal component analysis at 26 d of aging. Overall, the principal component analysis between 12 and 26 d are rather similar. Principal component 1 accounts for 49.22% of variation and, like d12, is heavily influenced by color stability attributes. Principal component 2 is heavily influenced by OT scores and accounts for 19.02% of variation. Score plots indicate that clusters 2 and 3 are still

heavily related to the respective traits established at 12d (Fig .3.3 B.) Cluster 1 appears to trend toward more color labile attributes at d 26 in comparison to d 12. Cluster 4 appears to trend slightly more toward tenderness attributes after 26 d of aging. However, both cluster 1 and cluster 4 primarily group around the origin with no obvious major influence in variation among those specific groups. Loading plots in Fig 3.3 C. indicate that principal component 1 is positively related to MHC-2 or type II fibers and malate and is negatively related to total myoglobin concentration. Loading plots additionally indicate that residual GLY, GLU, and G6P are still positively related to principal component 2 whereas total myoglobin, pH values, NORA, and OC are negatively related.

DISCUSSION

Proteolysis of myofibrillar and cytoskeletal, proteins, such as desmin, during aging is a key component of tenderness development in beef (Koohmaraie, 1992; Huff-Lonergan et al., 1996; Baron et al., 2004; Huang et al., 2011; Lana and Zolla, 2016). Previous studies have shown increased desmin degradation during aging of beef at up to 42 d (King et al., 2009; King et al., 2019). Decreased SSF values along with increased sarcomere length and percent desmin degradation are all indicative of increased tenderness at 26 d of aging. Desmin degradation was positively related to both OT scores and sarcomere length in principal component analysis done at both aging periods. Furthermore, SSF was negatively related to all other tenderness attributes. Sarcomere length in steaks from the *longissimus lumborum* in this study were similar to previous reported values (Koohmaraie et al., 2002; Chun et al., 2020). While sarcomere length increased ($P = 0.003$) with increasing aging period in this study, differences were slight amongst both groups, these differences may not have a substantial impact on tenderness

variation at both aging periods. Recent studies in beef tenderness have found no differences in sarcomere length across tenderness classifications or aging period, indicating other tenderness factors may be of greater importance in tenderization (King et al., 2019; Chun et al., 2020). In the current study, sarcomere length was not different among clusters with differences in both SSF and desmin degradation percentages.

Historically, the role that muscle fiber type plays on meat tenderness has not been totally understood. In this study, differences in fiber type were reported among clusters. However, differences were less than 2% among all clusters so little to no impact would be expected. Many studies have indicated that more oxidative, or type I fibers, are more tender than their more glycolytic counterparts as oxidative fibers are more susceptible to oxidative stress which can lead to apoptosis occurring at earlier timepoints than glycolytic fibers (Picard and Gagaoua, 2017). (Antonelo et al., 2020) found that tender beef underwent oxidative stress at an earlier time point than tough beef. In the current study, no relationships were present between fiber type and tenderness attributes. However, NORA was negatively related to OT scores and OC was positively related to SSF values indicating negative impacts on tenderness.

Type I muscle fibers are associated with greater mitochondria and myoglobin concentrations, making them more susceptible to oxidation, contributing to lack of color stability (McKenna et al., 2005; Salim et al., 2019). Oxidation of oxymyoglobin to metmyoglobin contributes to loss of red color (a^*) and discoloration over the duration of retail display (Baron and Andersen, 2002; Faustman et al., 2010). Increased oxygen consumption has been associated with decreased color stability (Madhavi and Carpenter, 1993; McKenna et al., 2005). In this study, total myoglobin concentration was negatively

related to color attributes by d11 of simulated retail display, indicating a decrease in color stability as myoglobin concentration increased. Furthermore, myoglobin concentration was positively related to SSF values indicating less tenderness with increased myoglobin content. Differences in myoglobin concentration among clusters was present as cluster 3 and cluster 4 both had greater myoglobin concentration and are associated with decreased tenderness and color stability in comparison to clusters 1 and 2.

The mechanisms and impact that protein oxidation has on meat quality and palatability traits is still being heavily researched. Rowe et al. (2004) reported that oxidation of beef muscle proteins had a negative impact on tenderization and contributed this impact to inactivation of calpain-1. Carbonylation of proteins is additionally thought to potentially impact tenderness formation of crosslinks and strengthening and shrinking of myofibrils (Morzel et al., 2006; Estévez, 2011). No relationships between carbonyls and tenderness attributes were found at either aging period in this study.

King et al. (2019) reported that glucose concentration increased in steaks between 7 and 14 d of aging but did not report increases between 14 and 28 d of aging. Residual GLU increased from d 12 to 26 in the current study. Previous reports have also indicated decreases in G6P concentrations as aging time increased (King et al., 2019). Conversely, King et al. (2019) reported a positive relationship between malic acid and desmin degradation in a metabolomics study. Antonelo et al. (2020) reported that lactate was one of the compounds most associated with differences in tender and tough beef from the *longissimus thoracis*. King et al. (2019) also reported negative correlations between glucose and SSF values. Antonelo et al. (2020) reported a negative correlation between glucose and Warner-Bratzler shear force values. Positive relationships in this study

between glycolytic intermediates GLY, GLU, and G6P with overall tenderness and negative relationships with slice shear force indicate benefits between glycolytic muscle attributes and tenderness.

CONCLUSION

Data from this study indicate that variation in color stability and tenderness in the *longissimus lumborum* at two different aging times is impacted by both biochemical and metabolic characteristics. Color stability attributes were negatively related to total myoglobin concentration as well as oxygen consumption and reducing ability.

Additionally, ultimate pH played a role in initial color as well as color after extended simulated display. MHC-2, or type II muscle fibers, were positively related to objective color measurements at the end of retail display indicating greater color stability than MHC-1, or type I muscle fibers. Residual GLY and GLU concentrations were negatively related to SSF measurements and positively related to OT scores indicating glycolytic intermediates may play a role in tenderization. Conversely, attributes associated with mitochondria function such as oxygen consumption and reducing ability were showed to have a negative impact on both OT scores and SSF. Data from this study indicate that metabolic characteristics of beef *longissimus lumborum* play a role in both color stability and tenderness. More research is warranted to further understand the relationships behind the mechanisms driving these relationships within the *longissimus lumborum* in beef animals.

Table 3.1. Descriptive attributes of cluster groupings related to color stability and tenderness attributes of beef *longissimus lumborum* steaks at two aging periods.

Attributes ¹	
Cluster Group	
Cluster 1 ²	Tender with moderate color stability
Cluster 2 ³	Tender and color stable
Cluster 3 ⁴	Tough and color labile
Cluster 4 ⁵	Moderate tenderness and color stability

¹Descriptive color stability and tenderness attributes

²n = 29

³n = 38

⁴n = 14

⁵n = 15

Table 3.2. LS Means (SEM) of metabolic and muscle characteristics of beef *longissimus lumborum* steaks in four clusters aged for 12 or 26 d.

Color Tenderness Group ¹ Variable	Aging Period (d)								P-Value
	12				26				
	Cluster 1 ⁶	Cluster 2 ⁷	Cluster 3 ⁸	Cluster 4 ⁹	Cluster 1	Cluster 2	Cluster 3	Cluster 4	
OT ²	6.18 ^{bcd} (0.14)	5.84 ^{de} (0.12)	4.80 ^f (0.20)	5.61 ^e (0.19)	6.74 ^a (0.14)	6.37 ^b (0.12)	5.87 ^{ede} (0.20)	6.31 ^{bc} (0.19)	0.01
NORA ³	69.56 ^a (2.74)	51.61 ^b (2.39)	54.78 ^b (3.94)	52.73 ^b (3.81)	42.20 ^c (2.74)	45.79 ^{bc} (2.39)	41.60 ^c (3.94)	45.51 ^{bc} (3.81)	0.0004
Insol Carb ⁴	3.80 ^a (0.34)	2.27 ^b (0.30)	3.94 ^a (0.49)	3.06 ^{ab} (0.47)	3.47 ^a (0.34)	3.65 ^a (0.30)	3.45 ^a (0.49)	3.57 ^a (0.47)	0.0093
Lactate ⁵	160.73 ^a (3.71)	144.57 ^b (3.24)	150.16 ^{ab} (5.33)	149.09 ^{ab} (5.15)	143.65 ^b (3.76)	146.45 ^b (3.24)	146.75 ^b (5.33)	138.66 ^b (5.15)	0.0086

^{abdef} Values within a row lacking a common superscript differ (P < 0.05)

¹Cluster 1 Tender with moderate color stability, Cluster 2 Tender and color stable, Cluster 3 Tough and color labile, Cluster 4 Moderate tenderness and color stability

²Overall Tenderness ranked on an 8 point scale where 1 = extremely tough and 8 = extremely tender

³Nitric Oxide Reducing Activity- IMF-PRM= NORA (%)

⁴Carbonyl formation in the insoluble fraction (µmol/mg)

⁵Residual lactate (µmol/g)

⁶n = 29

⁷n = 38

⁸n = 14

⁹n = 15

Table 3.3. LS Means (SEM) of tenderness attributes of beef *longissimus lumborum* steaks in four clusters.

Variable	Color Tenderness Cluster Group ¹				P-Value
	Cluster 1 ⁵	Cluster 2 ⁶	Cluster 3 ⁷	Cluster 4 ⁸	
SSF ²	12.41 ^b (0.61)	13.49 ^b (0.53)	18.57 ^a (0.88)	13.65 ^b (0.85)	<0.0001
Sarc Length ³	1.76 ^a (0.01)	1.74 ^{ab} (0.01)	1.71 ^b (0.01)	1.72 ^b (0.01)	0.01
Desmin ⁴	91.88 ^a (1.48)	93.27 ^a (1.30)	86.60 ^b (2.13)	86.70 ^b (2.06)	0.01

^{ab} Values within a row lacking a common superscript differ (P < 0.05)

¹ Cluster 1 Tender with moderate color stability, Cluster 2 Tender and color stable, Cluster 3 Tough and color labile, Cluster 4 Moderate tenderness and color stability

² Slice Shear Force (kg)

³ Sarcomere length (μm)

⁴ Desmin degradation (%)

⁵ n = 29

⁶ n = 38

⁷ n = 14

⁸ n = 15

Table 3.4. LS Means (SEM) of muscle biochemical and metabolic attributes of beef *longissimus lumborum* steaks in four color tenderness groups.

Variable	Cluster Group ¹				P-Value
	Cluster 1 ¹³	Cluster 2 ¹⁴	Cluster 3 ¹⁵	Cluster 4 ¹⁶	
TMYO ²	3.98 ^b (0.12)	3.92 ^b (0.10)	5.01 ^a (0.17)	5.33 ^a (0.16)	<0.0001
OC ³	34.03 (1.73)	33.17 (1.51)	37.44 (2.49)	39.24 (2.40)	0.25
pHd ⁴	5.50 (0.01)	5.53 (0.01)	5.51 (0.01)	5.53 (0.01)	0.55
pHu ⁵	5.51 ^c (0.01)	5.53 ^b (0.01)	5.54 ^{ab} (0.01)	5.56 ^a (0.01)	0.003
Sol Carb ⁶	1.47 (0.14)	1.76 (0.12)	1.54 (0.20)	1.44 (0.18)	0.30
GLY ⁷	13.90 (1.52)	11.29 (1.33)	14.95 (2.19)	14.35 (2.11)	0.37
GLU ⁸	8.94 (0.32)	8.18 (0.28)	8.62 (0.46)	8.37 (0.45)	0.35
G6P ⁹	7.65 (0.35)	7.21 (0.30)	7.52 (0.50)	6.59 (0.49)	0.33
Malate ¹⁰	0.80 ^b (0.06)	1.03 ^a (0.05)	0.86 ^{ab} (0.09)	1.09 ^a (0.09)	0.05
MHC-1 ¹¹	31.08 ^{ab} (0.35)	30.29 ^b (0.30)	31.99 ^a (0.50)	31.84 ^a (0.48)	0.01
MHC-2 ¹²	68.92 ^{ab} (0.35)	69.71 ^a (0.30)	68.01 ^b (0.50)	68.16 ^b (0.48)	0.01

^{ab}-Values within a row lacking a common superscript differ (P < 0.05)

¹ Cluster 1 Tender with moderate color stability, Cluster 2 Tender and color stable, Cluster 3 Tough and color labile, Cluster 4 Moderate tenderness and color stability

²Total myoglobin (mg/g)

³Oxygen Consumption (%)

⁴pH of striploin at 2 days postmortem

⁵Ultimate pH after aging period

⁶Carbonyl formation in the soluble fraction (μmol/mg)

⁷Residual glycogen (μmol/mg)

⁸Residual glucose (μmol/mg)

⁹Residual glucose-6-phosphate (μmol/mg)

¹⁰Residual malate (μmol/mg)

¹¹Myosin heavy chain isoform-1 (%)

¹²Myosin heavy chain isoform-2 (%)

¹³n = 29

¹⁴n = 38

¹⁵n = 14

¹⁶n = 15

Table 3.5. LS Means of tenderness attributes of beef *longissimus lumborum* steaks aged for 12 or 26 d.

Variable	Aging Period (d)		SEM ⁴	P-Value
	12	26		
SSF ¹	15.90 ^a	13.16 ^b	0.44	<0.0001
Sarc Length ²	1.72 ^b	1.75 ^a	0.01	0.003
Desmin ³	84.80 ^b	94.42 ^a	1.06	<0.0001

^{ab} Values within a row lacking a common superscript differ (P < 0.05)

¹ Slice shear force (kg)

² Sarcomere length (μm)

³ Desmin degradation (%)

⁴ Standard Error of the Mean

Table 3.6. LS Means of tenderness attributes of beef *longissimus lumborum* steaks aged for 12 or 26 d.

Variable	Aging Period (d)		SEM ¹²	P-Value
	12	26		
MYO ¹	4.52 ^b	4.60 ^a	0.04	0.03
OC ²	35.64	36.30	1.16	0.55
pHd ³	5.51	5.52	0.01	0.16
pHu ⁴	5.53	5.54	0.01	0.20
Sol Carb ⁵	1.55	1.55	0.10	0.99
GLY ⁶	14.67 ^a	12.58 ^b	0.97	0.002
GLU ⁷	7.31 ^b	9.74 ^a	0.23	<0.0001
G6P ⁸	8.07 ^a	6.41 ^b	0.23	<0.0001
Malate ⁹	0.95	0.97	0.04	0.65
MHC-1 ¹⁰	31.42	31.18	0.23	0.23
MHC-2 ¹¹	68.58	68.82	0.23	0.23

^{ab}-Values within a row lacking a common superscript differ (P < 0.05)

¹ Total myoglobin (mg/g)

² Oxygen Consumption (%)

³ pH of striploin at 2 days postmortem

⁴ Ultimate pH after aging period

⁵ Carbonyl formation in the soluble fraction (μmol/mg)

⁶ Residual glycogen (μmol/mg)

⁷ Residual glucose (μmol/mg)

⁸ Residual glucose-6-phosphate (μmol/mg)

⁹ Residual malate (μmol/mg)

¹⁰ Myosin heavy chain isoform-1 (%)

¹¹ Myosin heavy chain isoform-2 (%)

¹² Standard error of the mean

Table 3.7. Regression coefficients (SE) for the change in a^* during simulated retail display in beef *longissimus lumborum* steaks in four clusters aged for 12 or 26 d.

Cluster x Aging Period (d)	β_0^1	β_1^2	β_2^3	β_3^4
a^*				
CLUSTER 1 x 12	33.69 (0.46)	1.32 (1.22)	-3.41 ^{ab} (2.35)	-0.07 ^{bc} (1.32)
CLUSTER 2 x 12	33.32 (0.40)	4.65 (1.06)	-6.65 ^b (2.05)	1.83 ^b (1.16)
CLUSTER 3 x 12	33.75 (0.66)	0.60 (1.75)	-3.94 ^{ab} (3.38)	-2.58 ^c (1.90)
CLUSTER 4 x 12	33.53 (0.63)	5.99 (1.69)	-10.50 ^{bc} (3.26)	3.33 ^{ab} (1.84)
CLUSTER 1 x 26	33.27 (0.46)	-2.87 (1.22)	1.18 ^a (2.35)	-2.77 ^c (1.32)
CLUSTER 2 x 26	33.20 (0.40)	3.06 (1.06)	-6.40 ^b (2.05)	1.91 ^b (1.16)
CLUSTER 3 x 26	33.35 (0.66)	2.40 (1.75)	-15.90 ^c (3.38)	6.58 ^a (1.90)
CLUSTER 4 x 26	33.78 (0.63)	2.67 (1.69)	-6.37 ^{ab} (3.26)	0.87 ^{bc} (1.84)
$P > F$	0.93	0.23	0.03	0.003

^{abc} β - coefficients within a column and attribute lacking a common superscript differ ($P < 0.05$)

¹ β -coefficient for the intercept of the regression equation describing change in the attribute over simulated retail display, which is equal to the 0 d value for the attribute

² β -coefficient for the linear term of the regression equation describing change in the attribute over simulated retail display

³ β -coefficient for the quadratic term of the regression equation describing change in the attribute over simulated retail display

⁴ β -coefficient for the cubic term of the regression equation describing change in the attribute over simulated retail display

⁵ Cluster 1 Tender with moderate color stability, Cluster 2 Tender and color stable, Cluster 3 Tough and color labile, Cluster 4 Moderate tenderness and color stability

⁶ n = 29

⁷ n = 38

⁸ n = 14

⁹ n = 15

Table 3.8. Correlation coefficients for color and tenderness attributes with metabolic and biochemical attributes in beef *longissimus lumborum* steaks aged 12 d.

Variable	L* 0d	a* 0d	L* 11d	a* 11d	OT ¹	SSF ²	Desmin ³	Sarc ⁴
NORA ⁵	0.18	0.03	0.08	0.08	0.02	0.11	-0.21*	0.40***
OC ⁶	-0.33**	-0.42***	-0.26**	-0.02	-0.26**	0.26*	-0.07	-0.05
TMYO ⁷	-0.81***	0.23*	-0.79***	-0.35**	-0.28**	0.09	-0.22*	-0.18
pHd ²	-0.24*	-0.19	-0.18	-0.02	-0.11	0.23*	-0.10	-0.05
pHu ⁹	-0.44***	-0.22*	-0.39***	-0.05	-0.10	0.12	-0.07	-0.14
Sol Carb ¹⁰	0.00	-0.05	0.11	0.02	-0.11	0.15	-0.15	-0.01
Insol Carb ¹¹	-0.08	0.04	-0.11	-0.24	0.05	0.02	0.06	-0.07
GLY ¹²	0.05	0.16	-0.01	-0.26*	0.25*	-0.28**	0.16	0.04
GLU ¹³	0.18	0.35**	0.11	-0.03	0.20*	-0.24*	0.09	0.15
G6P ¹⁴	0.19	0.35*	0.14	-0.09	0.20*	-0.24*	0.15	0.13
Lactate ¹⁵	0.03	0.06	-0.08	-0.05	0.03	-0.12	-0.11	0.11
Malate ¹⁶	0.05	-0.06	0.15	0.29**	0.19	-0.23**	0.17	0.14
MHC -1 ¹⁷	-0.36**	0.10	-0.35**	-0.24*	0.00	-0.01	-0.07	0.01
MHC -2 ¹⁸	0.36**	-0.10	0.35**	0.24*	0.00	0.01	0.07	-0.01

*P < 0.05, ** P < 0.01, *** P < 0.0001

¹Overall Tenderness ranked on an 8 point scale where 1 = extremely tough and 8 = extremely tender

²Slice shear force (kg)

³Desmin degradation (%)

⁴Sarcomere length (μm)

⁵Nitric Oxide Reducing Activity- IMF-PRM= NORA (%)

⁶Oxygen Consumption (%)

⁷Total myoglobin (mg/g)

⁸pH of strip loin at 2 days post-mortem

⁹Ultimate pH after aging period

¹⁰Carbonyl formation in the soluble fraction (μmol/mg)

¹¹Carbonyl formation in the insoluble fraction (μmol/mg)

¹²Residual glycogen (μmol/g)

¹³Residual glucose (μmol/g)

¹⁴Residual glucose-6-phosphate (μmol/g)

¹⁵Residual malate (μmol/g)

¹⁶Residual lactate (μmol/g)

¹⁷Myosin heavy chain isoform- 1 (%)

¹⁸Myosin heavy chain isoform-2 (%)

Table 3.9. Correlation coefficients for color and tenderness attributes with metabolic and biochemical attributes in beef *longissimus lumbarum* steaks aged 26 d.

Variable	L* 0d	a* 0d	L* 11d	a* 11d	OT ¹	SSF ²	Desmin ³	Sarc ⁴
NORA ⁵	-0.09	-0.20*	-0.08	0.17	-0.29**	0.06	0.05	-0.01
OC ⁶	-0.43***	-0.28**	-0.35**	-0.10	-0.13	0.25*	0.03	-0.12
TMYO ⁷	-0.86***	0.41***	-0.77***	-0.25*	-0.28**	0.23*	-0.11	-0.13
pHd ⁸	-0.30**	-0.25*	-0.24*	-0.08	-0.28**	0.32**	-0.02	-0.01
pHu ⁹	-0.44***	-0.03	-0.32**	0.15	-0.29**	0.22*	0.15	0.07
Sol Carb ¹⁰	0.03	0.08	0.06	0.18	0.04	0.05	-0.05	-0.12
Insol Carb ¹¹	0.15	-0.20	0.21*	0.09	0.18	-0.05	0.13	0.03
GLY ¹²	-0.01	0.10	-0.08	-0.05	0.31**	-0.30**	-0.05	0.01
GLU ¹³	0.04	0.22*	0.04	-0.17	0.35**	-0.40***	-0.06	0.07
G6P ¹⁴	0.13	0.22*	0.14	-0.14	0.28**	-0.26**	0.00	-0.12
Lactate ¹⁵	-0.01	0.20*	-0.06	0.05	0.08	-0.09	0.01	0.03
Malate ¹⁶	-0.10	0.07	-0.05	0.20	-0.04	0.08	0.11	-0.19
MHC -1 ¹⁷	-0.31**	0.18	-0.24*	-0.22*	0.04	0.00	0.17	-0.02
MHC -2 ¹⁸	0.31**	-0.18	0.24*	0.22*	-0.04	0.00	-0.17	0.02

*P < 0.05, ** P < 0.01, *** P < 0.0001

¹Overall Tenderness ranked on an 8 point scale where 1 = extremely tough and 8 = extremely tender

²Slice shear force (kg)

³Desmin degradation (%)

⁴Sarcomere length (μ m)

⁵Nitric Oxide Reducing Activity- IMF-PRM= NORA (%)

⁶Oxygen Consumption (%)

⁷Total myoglobin (mg/g)

⁸pH of striploin at 2 days post-mortem

⁹Ultimate pH after aging period

¹⁰Carbonyl formation in the soluble fraction (μ mol/mg)

¹¹Carbonyl formation in the insoluble fraction (μ mol/mg)

¹²Residual glycogen (μ mol/g)

¹³Residual glucose (μ mol/g)

¹⁴Residual glucose-6-phosphate (μ mol/g)

¹⁵Residual malate (μ mol/g)

¹⁶Residual lactate (μ mol/g)

¹⁷Myosin heavy chain isoform- 1 (%)

¹⁸Myosin heavy chain isoform-2 (%)

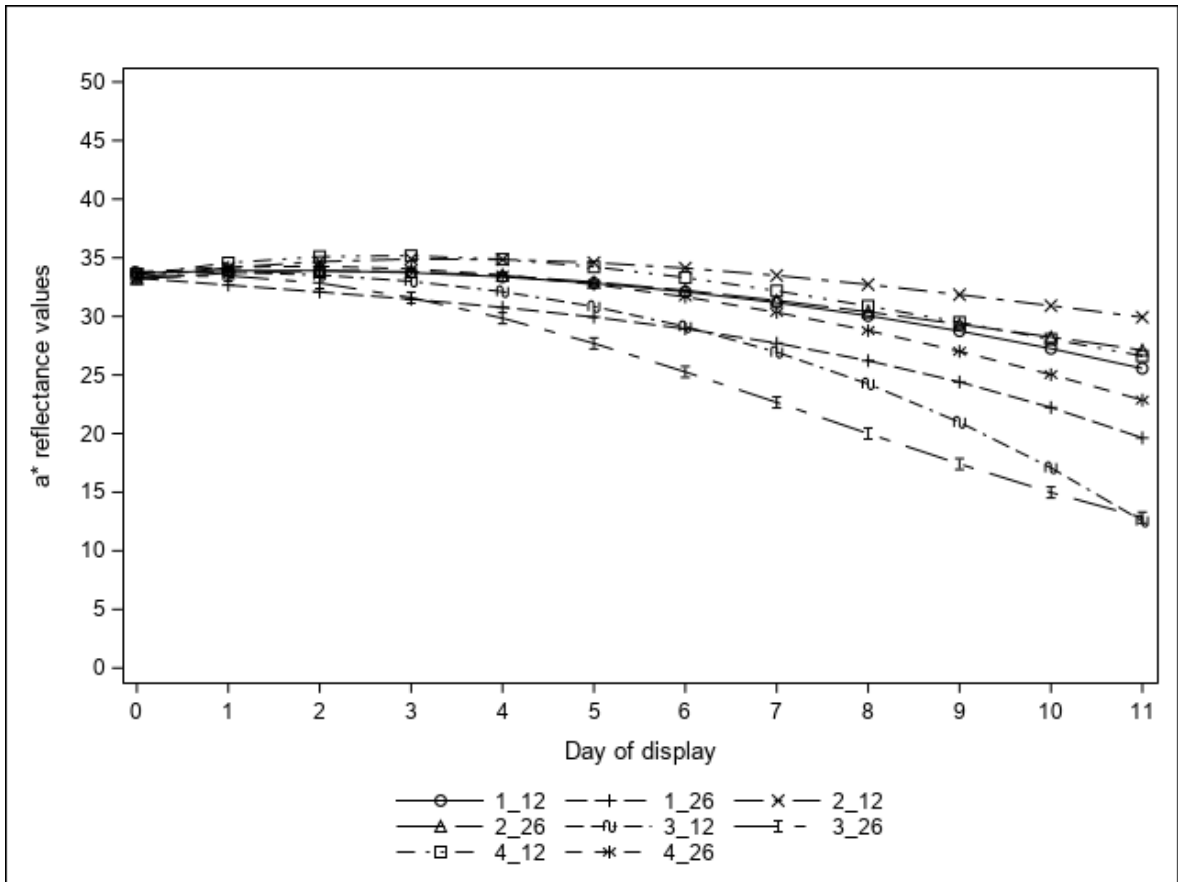


Fig. 3.1. Change in a* reflectance values over the duration of retail display for four cluster groups at two different aging periods.

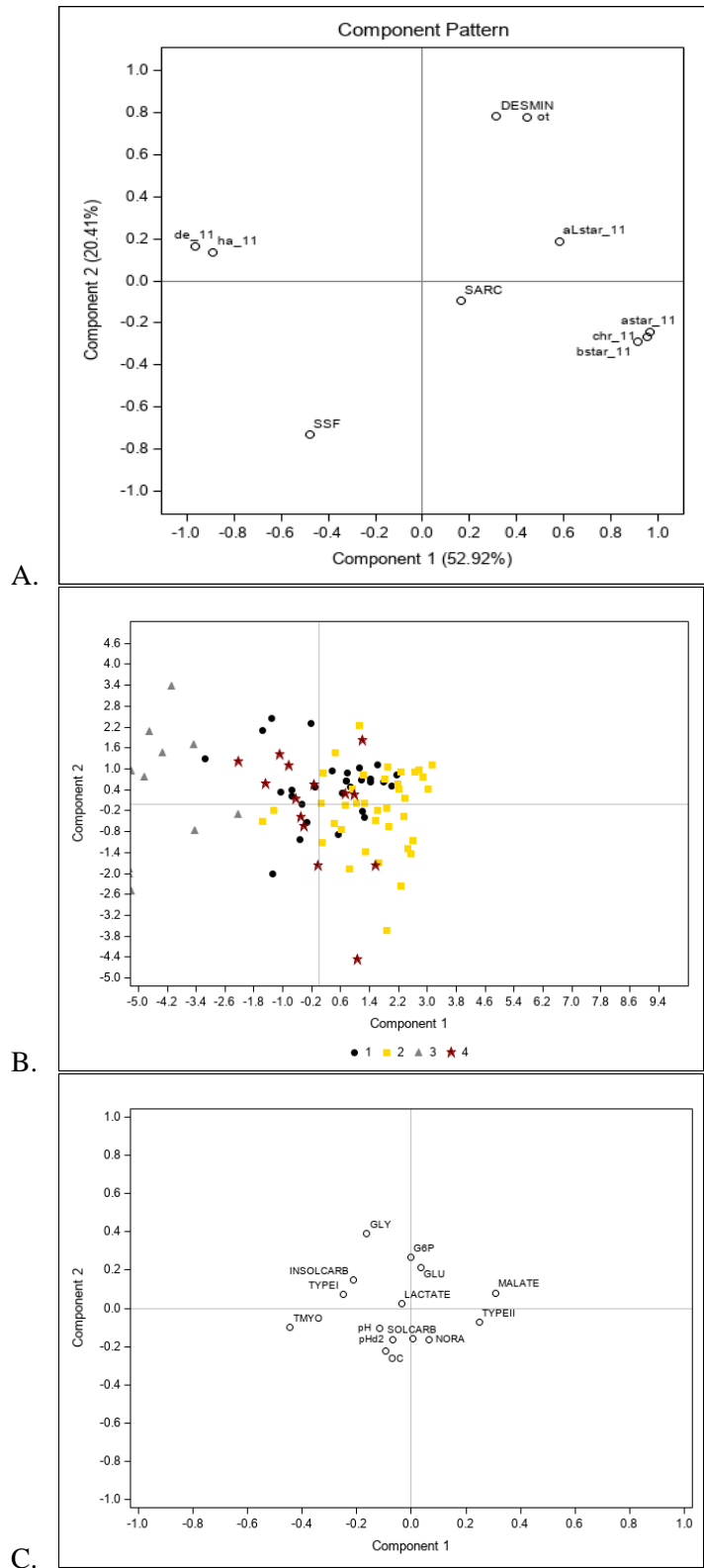


Fig. 3.2. A) Principal Component Analysis of color and tenderness attributes B) Score Plot for Cluster Groupings C.) Loading plot of metabolic and biochemical characteristics of beef *longissimus lumborum* steaks aged for 12 days

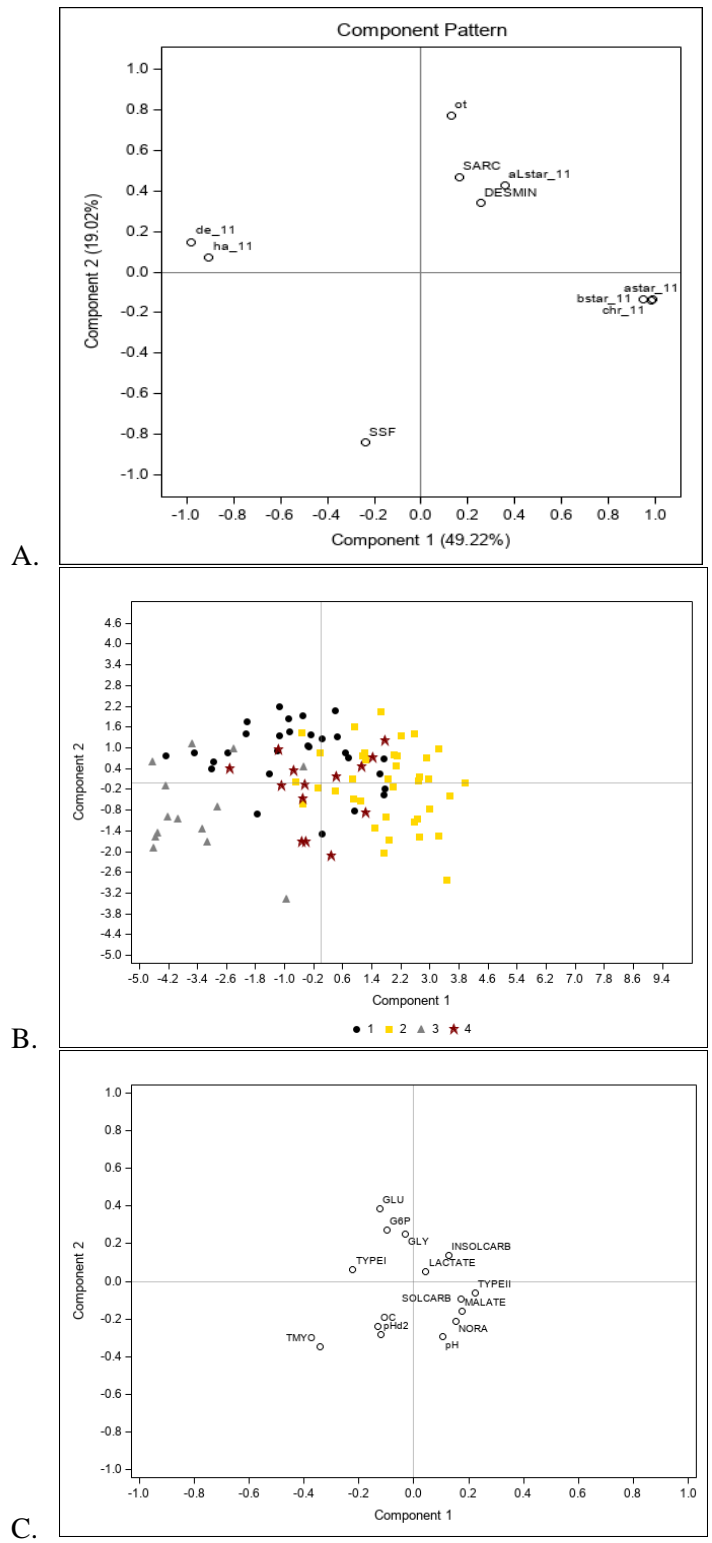


Fig. 3.3. A) Principal Component Analysis of color and tenderness attributes B) Score Plot for Cluster Groupings C.) Loading plot of metabolic and biochemical characteristics of beef *longissimus lumborum* steaks aged for 26 days

Chapter 4

Aging time and metabolic characteristics impact beef palatability components and flavor attributes in beef *longissimus lumborum* steaks

ABSTRACT: Flavor is one of the most important palatability attributes when determining consumer satisfaction. It is important to gain a better understanding of flavor attributes, factors that influence flavor, and the mechanisms behind variation in flavor profile. Therefore, the objective of this study was to determine the impact variation in metabolic traits had on flavor and palatability components of beef *longissimus lumborum* aged for 12 or 26 d. Beef carcasses (n = 96) were selected at grading for utilization in this study. After aging, 2.54 cm steaks were sliced from each *longissimus lumborum* and utilized for trained sensory panel and lab analyses. Muscle and metabolic traits were measured after both aging periods to determine pH, reducing ability, oxygen consumption, muscle fiber type via gel electrophoresis, and residual metabolism intermediates. Utilizing trained sensory panel data, clusters (n = 3) were created based on variation in flavor profile among carcasses. An aging time x cluster grouping interaction was reported for traits such as overall tenderness ($P = 0.02$), salt ($P = 0.02$), and nitric oxide reducing ability (NORA) ($P < 0.0001$). Flavor and palatability traits including juiciness ($P = 0.002$), umami ($P = 0.01$), heated oil ($P = 0.05$), chemical ($P = 0.01$), and butter ($P = 0.01$) were different among cluster groups. Increased aging time resulted in increased juiciness ($P < 0.0001$), beef ($P < 0.0001$), umami ($P < 0.0001$), sweet ($P = 0.01$), and butter ($P = 0.001$) flavor attributes. Conversely, increased aging times decreased rancid ($P = 0.0051$) and spoiled ($P = 0.003$) flavors. Longer aging periods resulted in increased residual glucose (GLU) ($P < 0.0001$)

concentrations and decreased residual glucose-6-phosphate (G6P) ($P < 0.0001$) and lactate ($P = 0.03$). Type I, or oxidative, muscle fibers were positively related ($P < 0.05$) to beef brown and bloody flavor attributes. Residual GLY and GLU were positively ($P < 0.05$) palatability components overall tenderness and juiciness. Residual GLY was positively related ($P < 0.05$) to brown, bloody, fat, umami, and rancid flavor attributes and negatively related ($P < 0.05$) to chemical flavor. Residual G6P was positively related ($P < 0.05$) to metallic and sour flavor attributes and negatively related to beef flavor identity and butter flavor attributes. Lactate exhibited positive relationships ($P < 0.05$) with bitter and rancid flavor attributes. Traits associated with increased oxidative capacity such as oxygen consumption and NORA were negatively ($P < 0.05$) related with attributes such as overall tenderness, juiciness, beef, brown and umami and positively ($P < 0.05$) related with attribute such as musty, spoiled, bitter and heated oil. Data indicate that metabolic profile and aging time contribute to flavor profile development and overall palatability.

INTRODUCTION

Development of meat quality and palatability characteristics are impacted by the physiological changes and resulting biochemical and metabolic processes muscle undergoes during the conversion to meat. While tenderness has often been regarded as the most important factor related to meat palatability, flavor has continued to increase in importance over time (Miller et al., 2001; Sitz et al., 2005; Legako et al., 2015; Lucherk et al., 2016; O'Quinn et al., 2018). A variety of extrinsic and intrinsic factors are known to influence flavor and palatability characteristics of beef such as genetics (Koutsidis et al., 2008), diet (Larick et al., 1987; Vasta and Priolo, 2006; Koutsidis et al., 2008), pre-harvest stress (Wulf et al., 2002), intramuscular fat (Legako et al., 2015; Nyquist et al., 2018),

postmortem aging (Watanabe et al., 2015; Vierck et al., 2020), packaging type (Ponce et al., 2019; Vierck et al., 2020), oxidation (Greene and Price, 1975; Greene and Cumuze, 1982), and cooking method (Gardner and Legako, 2018; Olson et al., 2019; Vierck et al., 2019).

The development of flavor during cooking happens through a variety of processes and is heavily dependent on the amount and type of flavor precursors present in beef (Batzer et al., 1960; Kerth and Miller, 2015; Khan et al., 2015). During the postmortem aging process, meat flavor precursors are developed by way of free amino acids, oxidation by-products, and reducing sugars (Khan et al., 2015). In recent years, the relationship between muscle metabolic attributes and meat quality and palatability traits has become a necessary focus. New and innovative technologies and research advancements have led to improvements in management, selection, and postmortem processing resulting in improved meat quality attributes. However, there is limited knowledge behind the relationships between postmortem muscle metabolic characteristics and meat quality attributes, specifically flavor profile. Further understanding of intrinsic factors impacting flavor attributes will allow for continued improvements in flavor and production of a consistent beef product. Therefore, the objective of this study was to evaluate relationships between variations in flavor profile and muscle metabolic characteristics in beef *longissimus lumborum* steaks at two different aging periods.

MATERIALS AND METHODS

Carcasses used in this experiment were selected and obtained from a commercial packing facility. Therefore, animal care and use approval was not obtained for this experiment.

Sample Selection and Fabrication

Beef carcasses (n = 96) were selected at a commercial processing facility. All carcasses selected for this study exhibited A maturity scores. An image-analysis based grading system was used to collect carcass grade characteristics and evaluated using the VBG 2000 GigE beef grading system (Shackelford et al., 2003). Evaluation of carcasses occurred as they were presented for grading and were selected based on predicted tenderness and color stability attributes utilizing visible and near-infrared spectroscopy (VISNIR; Shackelford et al., 2003). The beef, loin, strip loin (similar to IMPS #180 [USDA, 2017]) from both sides of each carcass were designated to an aging period of 12 or 26 d in a complete block so that each aging time and carcass side combination was represented equally in each predicted class. Post-fabrication subprimals were vacuum packaged, sorted by aging time, boxed, and transported back to the US Meat Animal Research Center abattoir via refrigerated truck (-2°C). Upon arrival, subprimals were wet aged at 1°C for the designated time period.

After aging, the *longissimus lumborum* was cut into 2.54 cm steaks using a Grasselli NSL400 (Grasselli-SSI, Throop, PA, USA). Steaks (n = 4) were immediately placed in a simulated retail display setting for a concurrent project. Steaks (n = 2) were vacuum sealed and frozen at -20°C for use with a trained sensory panel. Immediately post fabrication, a steak was trimmed free of external fat and connective tissue to measure oxygen consumption and metmyoglobin reducing ability. An additional steak was trimmed free of connective tissue and external fat, diced and frozen in liquid nitrogen for storage at -80°C for lab analyses including measuring pH, protein oxidation, myosin heavy-chain isoform

quantification for fiber type determination, and determination of residual glycogen (GLY), glucose (GLU), glucose-6-phosphate (G6P), lactate, and malate.

Trained Descriptive Panel Analysis

On each day of sensory panel evaluation, panels were presented samples from each of the prediction classes. Samples were thawed at 5 °C for 24 h before cooking. Cooking was done as described by (Wheeler et al., 1998) on an electric conveyor belt grill to achieve an internal temperature of 700. Internal steak temperatures were monitored pre- and post-cooking with a handheld thermometer equipped with a thermocouple probe (Cole-Parmer, Vernon Hills, IL, USA) placed in the geometric center of the steak. Once cooking was complete, exterior fat and connective tissue were discarded and steaks were cut into 1.27 cm x 1.27 cm x steak thickness cubes. Cubes were mixed before randomly being selected and assigned to each panelist. Steaks were processed and served immediately after reaching max temperature. On each panel day, panelists were given a warm-up sample before formal evaluation began.

A highly experienced descriptive attribute panel trained in accordance with guidelines provided by (Cross et al., 1978) and the American Meat Science Association (2016) with additional training in beef flavor evaluation by way of the beef lexicon (Adhikari et al., 2011) was utilized in this study. Overall tenderness (OT) and juiciness were rated on an 8-point scale (1 = extremely tough or dry, 8=extremely tender or juicy). A 15-point scale (0=not detectable, 15=extremely strong) was utilized for evaluation of flavor attributes such as beef flavor identity, brown/roasted, fat-like, bloody/serummy, liver-like, metallic, green-hay-like, umami, overall sweet, sweet, sour, salty, bitter, burnt, rancid,

heated oil, barnyard, chemical, apricot, asparagus, green, cumin, chocolate/cocoa, dairy, buttery, cooked milk, sour milk/dairy, floral, beet, stale refrigerator, and warmed over.

pH

Muscle pH was determined as described by (Bendall, 1973b) on samples collected at 2, 12, and 26 d postmortem. 2.5 (\pm 0.05) g of powdered sample was measured into a 50 ml plastic tube. Twenty-five ml of Iodoacetate potassium chloride (5 mM Iodoacetic Acid, 150 mM Potassium Chloride, pH 7.0) was added to tubes and samples were homogenized for 10 seconds. Homogenates were allowed to rest at room temperature (approximately 20°C) for 1 h, mixed via vortexing, and pH of the suspension was recorded using a Corning 125 pH meter equipped with a semi-micro combination electrode (Corning, Inc. Corning, NY, USA) that had been calibrated using two standards.

Nitric Oxide Metmyoglobin Reducing Activity and Oxygen Consumption

Steaks that were allocated for nitric oxide reducing activity and oxygen consumption were sampled by the removal of a 2.54 cm x 2.54 cm x steak thickness cube from the center of each steak. Cubes were then divided in half horizontally to expose the interior portion of the muscle. The interior portion of the steak, which had never been exposed to light or oxygen was used for oxygen consumption while the exterior portion of the cube which contained the surface previously exposed to light and oxygen was used for nitric oxide metmyoglobin reducing ability. Cube samples used for nitric oxide reducing activity (NORA) were oxidized in 50 ml of 0.3% sodium nitrite solution for 30 min at room temperature (approximately 20 °C) as described by (AMSA, 2012). After 30 min, samples were removed from the sodium nitrite solution, blotted and individually vacuum packaged.

Samples were then immediately scanned in duplicate with a Hunter MiniScan colorimeter (HunterLab, Reston, VA, USA) equipped with a 25 mm port. Spectral data was collected with Illuminant A and a 10° observer. Samples were allowed to reduce at 30°C for 2 h before being scanned again with identical settings as the initial scan. Equations provided by AMSA (2012) were used to quantify surface metmyoglobin. Metmyoglobin reducing activity is the absolute difference in surface metmyoglobin proportions between IMF and the reduced readings. Proportion of surface metmyoglobin after the reducing period was reported as post-reduction metmyoglobin (PRM).

Oxygen consumption (OC) was determined by methods described in (AMSA, 2012). The top surface of the bottom portion of the cube, or interior of the steak, was allowed to oxygenate, or bloom, for 2 h at 4°C. After the oxygenation period, samples were individually vacuum packaged and immediately scanned with a Hunter MiniScan equipped with the previous settings and calibrated through the film of a vacuum bag. Vacuum packaged samples were incubated for 20 min at 25°C and rescanned with the colorimeter for spectral data collection. Proportion of oxymyoglobin on the deoxygenated and oxygenated samples was determined and oxygen consumption was reported as the percentage of oxymyoglobin pre-incubation minus the percentage of oxymyoglobin post-incubation.

Soluble and Insoluble Protein Carbonyl

Extraction of soluble and insoluble fractions along with carbonyl determination was completed using methods provided in (Rowe et al., 2004) with modifications. Five g of finely diced muscle was placed in a 35 ml centrifuge tube and 15 ml of cold post rigor extraction buffer (100 mM Tris, 10 mM EDTA, MCE) was added. Samples were

homogenized for 10 sec at medium speed and then incubated in refrigeration for 10 min. This process was repeated 3 times. After the final incubation, samples were centrifuged at 27,000 x g for 30 min at 4°C. Supernatants were filtered through cheesecloth and volume was recorded as the soluble fraction. A 4 g portion of the remaining pellet was removed from each centrifuge tube and placed into a new 35 ml centrifuge tube, 10 ml of salt solution (100 mM KCl, 2 mM MgCl₂, 1 mM EGTA, 1 mM NaN₃, 20 mM K₂HPO₄, pH 7.0) was added to each tube and samples were homogenized for 10 sec at medium speed. Samples were incubated in refrigeration for 30 min with vortexing occurring every 10 min. After incubation, samples were centrifuged at 27,000 x g for 20 min at 4°C. Supernatant was poured off and pellet was washed with 10 ml KCl/MCE solution (50 mM KCl, 5 mM MCE). Samples were centrifuged at 27,000 x g for 10 min at 4°C. Supernatant was poured off and pellet was washed with 10 ml of sodium phosphate buffer (200 mM Na₂HPO₄, pH 7.4). Samples were centrifuged at 27,000 x g for 10 min at 4°C. Supernatant was poured off and samples were homogenized with 25 ml of sodium phosphate buffer. The remaining pellet suspension was the insoluble fraction. Protein concentration of both soluble and insoluble fractions were determined using a bicinchoninic acid (BCA) protein assay kit (Thermo Scientific, Pierce micro-BCA-assay) utilizing a BSA standard curve.

Samples were diluted to 6 mg/ml using a sodium phosphate EDTA solution (1mM EDTA, 50mM Na₂HPO₄) into 15 ml plastic conicals. Two dilutions were made for each sample, one to be used as a blank and the other as a DNPH treated sample. Once all dilutions were completed, 4 ml of DNPH was added to its respective tube and 4 ml 2M HCL was added to each tube designated as a blank. Samples were vortexed and placed into dark storage for 1 h incubation with vortexing occurring at 15 min intervals. After

incubation, 5 ml of 20% TCA was added to each tube. Samples were placed in refrigeration for 10 min. Samples were centrifuged using a benchtop centrifuge at 1000 x g for 8 min. After centrifugation, supernatant was poured off to leave a remaining pellet. Four ml of 10% TCA was added to each tube and pellets were broken up with glass rods before vortexing. Samples were centrifuged using a benchtop centrifuge at 1000 x g for 8 min. Supernatant was discarded and pellets were washed three times with 50:50 ethyl alcohol:ethyl acetate. Pellets were centrifuged at 1000 x g for 8 min and afterward supernatant was discarded. After the final wash, samples were dissolved in 6M Guanidine hydrochloride and incubated at 37°C for 10 min. Protein concentration was determined for final samples using a BCA protein assay as previously described. Carbonyl content was determined using absorbance of DNPH treated samples vs blanks serving as reference samples at 360 nm on a Spectramax plus spectrophotometer (Molecular Devices, Sunnydale, CA, USA). Carbonyl content (nmol/mg protein) for both the soluble and insoluble fractions were calculated using the molar extinction coefficient for DNPH 22,000 $M^{-1}cm^{-1}$ and the formula: carbonyl content = (absorbance \times 106/22,000)/mg protein.

Myosin Heavy Chain Isoform Separation and Quantification using Polyacrylamide Gel Electrophoresis (PAGE)

Myosin heavy chain (MHC) isoforms were separated and quantified using methods described in Picard et al. (2011) with modifications. One g of sample was homogenized in 10 ml of TRIS-EDTA (50 mM Tris, 10 mM EDTA, pH 8.3) for 20 sec at medium speed. Immediately after homogenizing, a 0.5 ml aliquot was transferred into a microcentrifuge tube. 0.5 ml of 2X treatment buffer (0.125 M Tris, 4% SDS, 20% Glycerol, H₂O, pH 6.8) was added to the microcentrifuge tube and samples were vortexed. Samples were heated

in a 50°C water bath for 20 min, mixed again to shear nucleic acids, and were heated for an additional 5 min. After heating samples were centrifuged for 20 min at 16,000 x g. Protein concentration was determined using a BCA assay (Pierce micro-BCA-assay, Thermo Fisher Scientific, Waltham, MA, USA). After protein concentration of samples were determined, samples were diluted to 3 mg/ml using a 2X treatment buffer containing MCE and bromophenol blue (0.5M Tris, 10% SDS, Glycerol, H₂O, MCE, 0.8% bromophenol blue, pH 6.8). After dilution, samples were heated for 10 min at 50°C. After heating, samples were frozen until gels were run.

Bio-rad Mini-Protean gels were poured with a 6% stacking (30% Acrylamide (50:1), 0.04% SDS, 47% Glycerol, 6mM EDTA, 115mM Glycine, 110mM Tris (pH 6.7), H₂O, 0.1% APS, 0.05% TEMED) and a 9% separating (30% Acrylamide (50:1), 0.4% SDS, 35% Glycerol, 115 mM Glycine, 230mM Tris (pH 8.8), H₂O, 0.1% APS, 0.05% TEMED). Separating gels were poured and allowed to polymerize for an hour before stacking gel was poured. Combs were placed into stacking gels and gels were sealed in plastic bags and placed in refrigeration until needed for electrophoresis.

Samples were removed from freezer storage and placed in a 37°C water bath for 5-10 minutes to allow samples to thaw and SDS buffer to go back into solution. Upper and lower chamber running buffers were made fresh daily. Upper chamber running buffer contained 5X running buffer (100mM Tris, 150mM Glycine) diluted to 1X running buffer with H₂O, 0.1% SDS, and 0.07% MCE. Lower chamber running buffer contained 5X running buffer (50mM Tris, 75mM Glycine) diluted to 1X running buffer with H₂O, and 0.05% SDS. Gels were removed from the refrigerator, combs were removed, and gels were washed with distilled H₂O immediately prior to loading. Gels were loaded into the

electrophoresis modules were placed inside tanks. Upper chamber running buffer was added to the inside assembly of the module and lower chamber buffer was added to the tank. Wells were washed with running buffer prior to loading. Using a 10 μ l pipette, 2.7 μ l of sample was added to each well. Once all samples were loaded modules were placed into a refrigerated room and run at 70 v for 30 h.

After the 30 h run, gels were removed from glass plates, stackers were removed, gels were placed into shallow individual containers and washed 3 times for 5 min with dd H₂O. After initial washes gels were covered with Imperial Protein Stain (Thermo Fisher Scientific, Waltham, MA) and stained for 1 hr with gentle shaking. After staining, gels were washed with dd H₂O for 30 min, water was discarded, and gels were washed in fresh dd H₂O overnight with gentle shaking. After overnight wash, gels were imaged using the Bio-Rad GelDoc Go Imaging System (Bio-Rad, Hercules, CA, USA) and gels were analyzed using Image Lab Software (Version 6.1, Bio-Rad, Hercules, CA, USA) to determine percent myosin heavy chain type of samples. Samples were analyzed in duplicate and values were averaged to determine value (%) of MHC-1 (Type I fibers) and MHC-2 (Type II fibers) in each sample. MHC-2 isoforms did not sufficiently separate; therefore, they were considered collectively.

Residual Metabolic Intermediate Determination

Extractions and residual metabolic components were completed via methods described in Hammelman et al. (2003) with modifications. One g of powdered tissue was homogenized and deprotonated with 4 ml of 2M HCl. One ml of homogenate was immediately removed and placed into a 1.6 ml microcentrifuge tube for use with amyloglucosidase (AGS) digestion for residual glycogen (GLY) determination. The

remaining homogenate was centrifuged at 30,000 x g for 20 min at 4°C. After centrifugation, samples were neutralized with approximately 800 µl of 5.4 M KOH to a pH of approximately 7.0. Neutralized samples were stored in refrigeration until use for malate assay.

An additional extraction was completed utilizing 0.5 g of powdered tissue which was homogenized and deprotonated with 10 ml of 2M HCl. Homogenates were incubated in refrigeration for 15 min before being centrifuged at 30,000 x g for 20 min at 4°C. After centrifugation, supernatant was poured into a 50 ml conical and neutralized with 3.5 ml of 5.4 M KOH to an approximate pH of 7.0. After extraction and neutralization, samples were stored in refrigeration until used for determination of residual lactate, GLU, and G6P.

A 200 µl aliquot of homogenate was added to a 35 ml centrifuge tube and combined with 1 ml of AGS and 50 µl of potassium hydroxide (KOH). The pH was measured and adjusted to be approximately 4.8. Samples were incubated for 3 h at 37°C with inverting occurring once every hour. After incubation, samples were placed in refrigeration for 10 min and 100 µl of 2M HCl was added to each tube. After hydrolysis was stopped, 40µl of 5.4 M KOH was added to each tube to neutralize the sample. Samples were incubated for an additional 10 min in refrigeration before being centrifuged at 30,000 x g for 20 min at 4°C. Supernatant was removed with a pipette and placed into a 1.5 ml centrifuge tube for residual GLY content determination. A 400 µl aliquot of sample was added to a glass test tube and combined with 200 µl of ATP/NADP solution, and 1.7 ml of 0.3 M triethanolamine (TEA) buffer. Tubes were vortexed and samples were plated in triplicate 210 µl aliquots into a 96 well plate. Initial absorbance was read at 340 nm on a Spectramax plus 96-well plate reader (Molecular Devices, Sunnydale, CA, USA) and values were

recorded (OD1). After plating samples, 40 μ l of glucose-6-phosphate dehydrogenase and 40 μ l of hexokinase were added to each tube. Tubes were vortexed and incubated at room temperature for 20 min. After incubation, tubes were vortexed again and immediately plated in triplicate 210 μ l aliquots into a 96 well plate. Absorbance was read at 340 nm on a 96-well plate reader and absorbance values were recorded (OD2). Final absorbance values associated with glycogen content were determined by $OD2 - OD1$. The quantity of residual glycogen was determined by way of standard curves of 1mmol, 900, 600, 300, and 0 μ M glucose standard. Glucose and G6P concentration from additional assays were subtracted from overall glycogen content to determine the final GLY content. Residual GLY content is reported as μ mol/g of muscle.

A 400 μ l aliquot of extracted and neutralized sample was added to a glass tube and combined with 200 μ l of ATP/NADP solution and 1.7 ml of 0.3 triethanolamine (TEA) buffer. Tubes were vortexed and samples were immediately plated in 210 μ l aliquots in triplicate, on a 96 well plate. Plates were read at 340 nm on a Spectramax plus 96-well plate reader (Molecular Devices, Sunnydale, CA) and initial absorbance values (OD1) were recorded. After initial plate reading, 40 μ l of glucose-6-phosphate dehydrogenase was added to each tube. Tubes were vortexed and incubated at room temperature for 20 min. After incubation, samples were plated in triplicate 210 μ l aliquots on a 96 well plate. Plates were read at 340 nm and absorbance values were recorded (OD2). After reading, 40 μ l of hexokinase was added to each tube. Tubes were vortexed and incubated at room temperature for 20 min. After incubation, samples were plated in triplicate 210 μ l aliquots into a 96 well plate. Plates were read again at 340 nm on a plate reader and absorbance values were recorded (OD3). Absorbance values for calculating G6P were determined by

$OD2 - OD1$ and GLU was determined by $OD3 - OD2$. Residual GLU and G6P were calculated utilizing standard curves of 1mmol, 900, 600, 300, and 0 μ M GLU and G6P standards. Glucose and G6P are reported as μ mol/g of muscle.

A 50 μ l aliquot of extracted and neutralized sample was added to a glass tube and combined with 150 μ l of an HCL/KOH solution. A 200 μ l aliquot of NAD and 3 ml of reaction buffer (0.4 M Hydrazine, 0.5 M Glycine, pH 9.0) were added to the tubes and tubes were immediately vortexed. Samples were plated in triplicate 210 μ l aliquots into a 96 well plate. Absorbance was read at 340 nm on Spectramax plus 96-well plate reader (Molecular Devices, Sunnydale, CA, USA) and initial absorbance values were recorded (OD1). After reading initial values, 40 μ l of lactate dehydrogenase was added into each sample tube and tubes were immediately vortexed. Samples were incubated in a 25°C water bath for 2 h before tubes were removed and vortexed again. After incubation, samples were plated in triplicate 210 μ l aliquots into a 96 well plate. Absorbance was measured at 340 nm on a 96-well plate reader and values were recorded (OD2). Absorbance values to determine residual lactate was calculated as $OD2 - OD1$. Residual lactate concentration was determined by way of lactate standard curves of 2 mmol, 1.4 mmol, 1 mmol, 400, and 0 μ M. Lactate is reported as μ mol/g of muscle.

A 200 μ l aliquot of extracted and neutralized sample was added to a glass tube and combined with 200 μ l of NAD and 3 ml of reaction buffer (0.4 M Hydrazine, 0.5 M Glycine, pH 9.0) and immediately vortexed. Samples were plated in triplicate 210 μ l aliquots into a 96 well plate. Absorbance was read at 340 nm on a Spectramax plus 96-well plate reader (Molecular Devices, Sunnydale, CA, USA) and initial absorbance values were recorded (OD1). After reading the initial plate, 40 μ l of malate dehydrogenase was added

to each tube and immediately vortex. Tubes incubated in a 25°C water bath for 2 hr. After incubation, samples were plated in triplicate 210 µl aliquots into a 96 well plate and absorbance was read again at 340 nm (OD2). Absorbance values for determination of residual malate was calculated as $OD2 - OD1$. Residual malate was calculated using standard curves of 600, 400, 200, 100, and 0 µM malic acid. Malate is reported as µmol/g of muscle.

Statistical Analysis

Three flavor palatability component cluster groupings were created using Agglomerative hierarchical clustering using the factoextra package Kassambara and Mundt (2020) in R statistical software (R Core Team, 2020) to represent variation in flavor profile and palatability components. Clustering used overall tenderness, juiciness, and all flavor attributes. Data were scaled using the scale() function and the Euclidean distance matrix was calculated using the dist() function. Dendrograms were generated using the hclust() function. Thus, the three resulting clusters represented samples differing in flavor profile and palatability components. Data was analyzed as a split plot design using the GLIMMIX function of SAS version 9.4 (SAS Institute Inc., Cary, NC) with carcass serving as whole plot experimental unit and cluster grouping as the whole plot treatment and carcass side serving as the split plot experimental unit and aging time being the split plot treatment. Aging time, flavor cluster grouping, and their interaction served as fixed effects in the model. The interaction between trip and flavor cluster grouping served as random effects. The Kenward-Roger approximation was utilized to estimate degrees of freedom. The PRINCOMP function of SAS was utilized to identify flavor attribute scores into principal components independently for both aging periods.

Pearson correlation coefficients of flavor attributes and muscle metabolic characteristics were determined using the PROC CORR procedure in SAS. Significance was determined when P values were less than or equal to $\alpha = 0.05$ for all analyses.

RESULTS

As seen in Table 4.1, a cluster grouping by aging time interaction occurred for overall tenderness of steaks from the *longissimus lumborum* ($P = 0.02$). Overall tenderness scores increased between d 12 and 26 for all groups with flavor spoiled/musty Cluster being less tender ($P < 0.05$) than both liver/metallic and beef/brown clusters after both aging periods. However, it is important to note that while all three cluster groups OT scores increased between aging periods, OT for the spoiled/musty cluster increased an entire unit while both the liver/metallic and beef/brown groups saw approximately half a unit increase in OT score. Data would indicate that while tenderness was still lower in the spoiled/musty cluster, perhaps tenderization occurred in greater amounts during prolonged aging for this cluster group than both the liver/metallic and beef/brown cluster groups. A cluster grouping by aging time treatment interaction occurred for the salt flavor attribute ($P = 0.02$) (Table 4.1). Spoiled/musty flavor cluster had lower salt scores after d 12 of aging than flavor cluster three while salt scores in flavor clusters one and three did not differ at either aging period. By d 26 of aging, spoiled/musty cluster salt scores had increased to similar levels of both liver/metallic and beef/brown. While no differences ($P > 0.05$) were found between salt flavor scores in the liver/metallic and beef/brown salt flavor scores between aging periods, scores increased ($P < 0.05$) tremendously in comparison for the spoiled/musty clusters over the aging period. A cluster grouping by aging time interaction ($P < 0.0001$) occurred for nitric oxide reducing ability (Table 4.1). Values for NORA were greater ($P <$

0.05) for liver/metallic cluster was greater at 12 d than NORA values beef/brown cluster. Ultimately, NORA values did not change ($P > 0.05$) between aging periods for both the spoiled/musty or beef/brown flavor clusters. However, NORA values decreased ($P < 0.05$) substantially for the liver/metallic flavor cluster. Values for NORA ($P > 0.05$) were within a 5% range of d 12 values for the spoiled/musty and beef/brown cluster groupings. Whereas values for the liver/metallic cluster group decreased ($P < 0.05$) by approximately 26%, indicating a substantial decrease in reducing ability with prolonged aging of carcasses included in the liver/metallic cluster.

Table 4.2 contains mean values for flavor attributes and palatability components within all flavor clusters. Juiciness was lower ($P = 0.002$) in the spoiled/musty cluster than both liver/metallic and beef/brown clusters. Umami ($P = 0.01$) and flavor attributes were greater in the beef/brown cluster than both the liver/metallic and spoiled/musty clusters. Heated oil flavor attributes were greater ($P = 0.05$) in flavor liver/metallic cluster than both spoiled/musty and beef/brown flavor clusters. Chemical flavor attributes were greater ($P = 0.01$) in the spoiled/musty cluster than both liver/metallic and beef/brown clusters. Butter flavor attributes were greater ($P = 0.01$) in the beef/brown cluster as opposed to both the liver/metallic and spoiled/musty cluster groupings. While beef flavor identity ($P = 0.07$) and metallic ($P = 0.07$) flavor attributes tended to differ among flavor clusters, there were no differences within clusters for flavor attributes including brown ($P = 0.09$), bloody ($P = 0.20$), fat ($P = 0.44$), liver ($P = 0.18$), sweet ($P = 0.85$), sour ($P = 0.97$), bitter ($P = 0.22$), rancid ($P = 0.42$), musty ($P = 0.37$) or spoiled ($P = 0.36$).

Overall juiciness ($P < 0.0001$) as well as flavor attributes including beef flavor identity ($P < 0.0001$), umami ($P < 0.0001$), sweet ($P = 0.01$), and butter ($P = 0.001$) all

followed the same pattern of greater panel score as aging time increased with d 26 being greater than d 12 indicating continued flavor and palatability development with increased aging times (Table 4.3). Conversely, both rancid ($P = 0.01$) and spoiled ($P = 0.003$) flavor scores decreased with increased aging time with d 12 being higher than d 26. Flavor attributes such as bloody ($P = 0.43$), fat ($P = 0.33$), metallic ($P = 0.91$), liver ($P = 0.10$), sour ($P = 0.16$), bitter ($P = 0.46$), heated oil ($P = 0.45$), chemical ($P = 0.25$), and musty ($P = 0.77$) did not differ between aging periods in this experiment.

Correlation coefficients for palatability components and flavor attributes from both aging periods are depicted in Table 4.4, only meaningful relationships among attributes ($P < 0.05$) are presented and discussed. Overall tenderness and juiciness components exhibited a strong positive relationship (0.89). Overall tenderness was positively related to beef flavor identity (0.16), fat (0.17), liver (0.17), umami (0.27), sweet (0.14), heated oil (0.18), and butter (0.35) flavor attributes while being negatively related to brown (-0.16), rancid (0.18), chemical (-0.18), and spoiled (-0.22) flavor attributes. Relationships between juiciness and flavor attributes were very similar to OT with the lack of a relationship with liver flavor and the addition of a positive relationship (0.23) with bloody flavor. Beef flavor identity was positively related to brown (0.69), fat (0.22), umami (0.66), sweet (0.29), salt (0.21), and butter (0.43) flavor attributes. Negative relationships between beef flavor identity and bloody (-0.29), metallic (-0.40), liver (-0.48), sour (-0.30), bitter (-0.24), rancid (-0.28), musty (-0.20), and spoiled (-0.37) attributes. Brown flavor followed a very similar trend with no relationship being present with rancid or musty flavors and a negative relationship present with heated oil flavor (-0.15). Conversely, bloody flavor attributes resulted in opposite relationships with flavor attributes associated with beef flavor identity

with the exception of no relationship present with fat flavor attributes. Fat flavor was positively related to umami (0.30), sweet (0.25), and butter (0.28) attributes and negatively related to chemical (-0.15) flavor. Metallic flavor attributes were positively related to liver (0.42), bitter (0.44), rancid (0.18), heated oil (0.17), musty (0.15), spoiled (0.16), and butter (0.36) flavor attributes and negatively related to umami (-0.33), and salt (-0.17) flavor attributes. Liver flavor attribute was positively related to sour (0.15), bitter (0.34), heated oil (0.28), musty (0.17), and spoiled (0.24) flavor attributes and negatively related to umami (-0.40), sweet (-0.19), and butter (-0.39) attributes. Sour flavor attributes were positively related to bitter (0.24), rancid (0.36), musty (0.23), and spoiled (0.20) attributes while negatively related to heated oil (-0.15) and butter (-0.34) attributes. Bitter and rancid flavor attributes exhibited similar relationships with attributes as their sour counterpart. Salt flavor attribute was positively related to butter (0.15) flavor and negatively related to bitter (-0.24) and rancid (-0.15). Heated oil flavor attribute was negatively related to musty (-0.17) flavor and chemical flavor was negatively related to butter (-0.19) flavor attribute. Musty flavor was positively related to spoiled (0.25) flavor and both musty and spoiled flavor attributes were negatively related to butter flavor (-0.37 and -0.32, respectively).

No differences ($P < 0.05$) were determined among biochemical and metabolic components among flavor clusters (Table 4.5). However, an aging effect was present for various glycolytic intermediates and end products biochemical and metabolic attributes (Table 4.6). Residual GLU increased ($P < 0.0001$) as aging time increased. Conversely, G6P and lactate concentration decreased with increasing aging time. No differences ($P > 0.05$) were determined for OC, pHd2, pHu, MYO, carbonyl content in the soluble or insoluble fraction, malate, or MHC isoforms between aging periods.

Correlation coefficients among biochemical and metabolic attributes from both aging periods are presented in Table 4.7. Only meaningful relationships among traits will be reported and discussed. Oxygen consumption was positively related to MYO (0.18), pHd2 (0.31), pHu (0.43), and MHC-1 (0.15) while negative relationships with G6P (-0.28) and MHC-2 (-0.15) were present. Nitric oxide reducing ability was positively related to residual G6P (0.22) and lactate (0.21) while exhibiting negative relationships with GLU (-0.17), pHu (-0.15), and MYO (-0.20). Total myoglobin concentration was positively related to pHu (0.35) and MHC-1 (0.43). Conversely, as expected, MYO exhibited a negative relationship with MHC-2 (-0.43). Values for pH at 2 dpm were positively (0.50) related to pHu values. Additionally, pHd2 was negatively related to residual glycolytic intermediates GLY (-0.19), GLU (-0.24), G6P (-0.40), and lactate (-0.21). As expected, ultimate pH values followed the same trend exhibiting negative relationships with residual glycolytic intermediates GLY (-0.16), GLU (-0.28), G6P (-0.41), and lactate (-0.23). Additionally, pHu was positively related to more oxidative MHC-1 (0.17) and conversely negatively related to glycolytic MHC-2 isoforms (-0.17). Carbonyl content in the soluble fraction was positively related to carbonyl content in the insoluble fraction (0.19). Furthermore, carbonyl content in the insoluble fraction was negatively related to residual malate (-0.17). Additional relationships among residual glycolytic intermediates and other metabolic components were present. Positive relationships were found between GLY and residual GLU (0.17), G6P (0.26), and residual malate (0.14). A positive relationship was found between GLY and MHC-2 (0.17) resulting in a negative relationship with MHC-1 (-0.17). Positive relationships between residual GLU and G6P (0.32) and residual G6P and lactate (0.22) were also reported.

Correlation coefficients for biochemical and metabolic components with palatability components and flavor attributes at both aging periods are presented in Table 4.8. Only meaningful relationships will be discussed. Oxygen consumption was negatively related to OT (-0.19) and juiciness (-0.20) palatability components as well as butter flavor attribute (-0.17). A positive relationship between OC and musty (0.15) and spoiled (0.20) was present. Nitric oxide reducing ability was positively related to flavor attributes including bloody (0.20), metallic (0.23), liver (0.26), bitter (0.15), heated oil (0.14), and spoiled (0.16). Negative relationships between NORA and OT (-0.22), beef (-0.33), brown (-0.32), umami (-0.30), and butter (-0.31) were also present. Total myoglobin concentration was negatively related to both palatability components OT (-0.24) and juiciness (-0.19). Additionally, MYO was negatively related to sweet (-0.18) and heated oil (-0.18) flavor attributes. Positive relationships between MYO and beef flavor identity (0.18), brown (0.37), bloody (0.21), fat (0.16), and rancid (0.22) flavor attributes were present. Values for pH_{d2} were negatively related to OT (-0.15) scores and sour (-0.16) flavor. Ultimate pH was positively related to both beef flavor identity (0.18) and brown (0.19) flavor while exhibiting negative relationships with metallic (-0.36), liver (-0.35), sour (-0.19), bitter (-0.24), and heated oil (-0.24) flavor attributes. Carbonyl formation in the soluble fraction was positively related to salt (0.18) flavor while carbonyl formation in the insoluble fraction was positively related to juiciness (0.16), sweet (0.21), and butter (0.28) flavor attributes. Residual glycogen was positively related to palatability components OT (0.21) and juiciness (0.19) as well as brown (0.19), bloody (0.15), fat (0.15), umami (0.20), and rancid flavor attributes. A negative relationship between GLY and chemical (-0.17) flavor was also present. Residual GLU was also positively related to palatability components OT

(0.40) and juiciness (0.28) as well as liver (0.21) and bitter (0.16) flavor attributes. Glucose-6-phosphate was negatively related to beef flavor identity (-0.15), umami (-0.18), and butter (-0.15) flavor attributes and positively related to sour (0.20) flavor. Residual lactate was positively related to both bitter and rancid flavor attributes (0.15 and 0.18, respectively). MHC isoforms were related to beef flavor identity, brown, and bloody flavor attributes with positive relationships with MHC-1 (0.17, 0.15, and 0.18, respectively) and negative relationships with MHC-2 (-0.17, -0.15, and -0.18, respectively).

Principal component analysis was performed on flavor attributes at both aging periods. Principal component one explained 34.39% of the variation in flavor attributes in *longissimus lumborum* steaks after 12 d of aging (Fig. 4.1 A.). Metallic, liver and bloody flavor attributes explain a large portion of principal component one. Principal component two explained 14.54% of variation and was largely impacted by brown, rancid, musty, and sour flavor attributes after 12 d of aging. Score plots (Fig. 4.1 B.) were created to determine differentiating flavor attributes for each of the three cluster groupings in order to determine defining flavor characteristics for each cluster grouping based on PCA output. Plots at d 12 indicated that one flavor grouping was defined primarily by liver, metallic, bloody, and heated oil flavor attributes. An additional flavor group was mostly related to spoiled, musty, bitter, rancid, and sweet flavor attributes. A third flavor group was primarily associated with beef, brown and umami, and butter flavor attributes. A loading plot containing all metabolic and biochemical attributes (Fig. 4.1 C.) was then produced to visualize relationships between metabolic attributes and flavor attributes associated with principal components 1 and 2. Nitric oxide reducing ability was positively related to principal component one indicating positive relationships with bloody, metallic, bitter, and

liver flavor attributes and negative relationships with brown, beef, umami, and butter flavor attributes. Component two was negatively related to NORA resulting in positive relationships between NORA and heated oil flavor attributes. Component two was positively related to TMYO resulting in positive relationships with brown and rancid flavor attributes as well as negative relationships with sweet flavor attributes.

Principal component 1 for *longissimus lumborum* steaks aged 26 d explained 30.47% of variation in flavor attributes (Fig. 4.2 A.). Bitter, liver, rancid, and musty flavor attributes explained a large portion of principal component one at 26 d of aging. Heated oil and sweet flavor attributes explain a large portion of principal component two, which explains 14.16% of variation in steaks aged for 26 d. Score plots for 26 d of aging indicate that metallic, liver, bloody, and heated oil flavor attributes were still the defining attributes for that respective flavor cluster (Fig 4.2 B.). Additionally, the beef, umami, brown, and butter cluster remained. The cluster defined by spoiled, musty, bitter, rancid and sweet flavors while still obvious became less defined. As stated earlier, rancid, and spoiled flavor attributes scores decreased as aging time increased, therefore development of other flavor attributes could impact distribution at 26 d. A loading plot containing all metabolic and biochemical attributes (Fig. 4.2 C.) was then produced to visualize relationships between metabolic attributes and flavor attributes influencing principal components 1 and 2. Ultimate pH values were negatively related to principal component 1 indicating positive relationships with brown, beef flavor identity and umami flavor attributes and negative relationships with metallic, liver, bitter flavor attributes at 26 d. Ultimate pH was also negatively related to principal component two indicating a negative relationship with heated oil flavor attributes.

DISCUSSION

Tenderization that occurs during aging is a result of proteolysis of myofibrillar proteins within the muscle fibers (Koochmaraie, 1996; Koochmaraie and Geesink, 2006b; Kemp et al., 2009; Cruzen et al., 2014). In agreement with results from the current study, King et al. (2021) reported increasing panel scores for tenderness in steaks from the *longissimus lumborum* as aging time increased. Postmortem aging also plays a key role in the production of flavor precursors by way of proteolysis and oxidation (Yancey et al., 2005). Vierck et al. (2020) reported that steaks not exposed to aging conditions had lower concentrations of flavor contributing free amino acids than their aged counterparts as many of these amino acids are freed by way of postmortem proteolysis during aging. Similarly, (Foraker et al., 2020) reported an increase in concentration of free amino acids and sugars as aging time increased. In this study, GLU concentration increased with increasing aging time whereas G6P and lactate decreased as aging time increased. Aging time had an impact on some flavor attribute scores. King et al. (2021) reported a cubic trend with the rancid flavor attribute in steaks from the *longissimus lumborum* over a 35 d aging period with d 21 having the highest score and d 28 being the lowest. Foraker et al. (2020) found that flavor notes in beef *longissimus lumborum* did not differentiate until d 35 of aging, followed by an increase in sour and musty flavor attributes. It is evident that while panelists are trained to evaluate each individual flavor attribute, ratings for specific flavor attributes can be dependent on ratings of others, also deemed a “halo effect” of flavor attributes. Foraker et al., (2020) reported similar findings in beef steaks from the *longissimus lumborum* utilizing different aging treatments.

Muscle fiber composition plays a substantial role in the determination of muscle metabolic capacity and characteristics (Lefaucheur, 2010). Yu et al. (2019) found higher levels of glycolytic enzyme lactate dehydrogenase activity in the *longissimus lumborum* in comparison to the *psoas major*, a muscle with predominantly type I fibers. Conversely, they found higher levels of tricarboxylic cycle enzymes succinate dehydrogenase and malate dehydrogenase activity in the *psoas major*. No differences were found in the current study among flavor cluster groupings and metabolic components. The *longissimus lumborum* is classified as a more glycolytic muscle and in this experiment the longissimus was comprised of around 70% type II or glycolytic fibers therefore no major differences in fiber type among cluster groups is not totally surprising. As previously mentioned, an aging effect was present for metabolic intermediates with GLU increasing with aging time while G6P and lactate decreased. Glucose was positively related to overall tenderness and juiciness scores which concurrently increased with aging time. Lactate was positively related to bitter and rancid flavor attributes whereas G6P was positively related to sour and metallic flavors. Furthermore, G6P was negatively related to beef, umami, and butter flavor attributes; indicating a decrease in residual lactate and G6P could be beneficial to flavor profile. Previous metabolomics research has indicated a potential relationship between tenderness and malate concentration in beef longissimus steaks (King et al., 2019). No relationships between malate and palatability components or flavor attributes were present in this study.

Variation in muscle fiber type results in variation in rate and extent of postmortem glycolysis. Muscles with a greater number of oxidative, or type I fibers, display a quickened rate of initial pH decline and an earlier cessation of postmortem glycolysis.

Data from this study indicated positive relationship between pH values and oxygen consumption. This is thought to be attributed to greater initial glycogen content in type II fibers or increased demand for ATP due to increased hydrolysis of ATP by way of mitochondrial ATPases (England et al., 2013). In the current study, no differences were reported between flavor clusters for fiber type or pHu values. Positive relationships between pHu values and beef flavor identity and brown flavor attribute coincide with positive correlations between type I muscle fibers and these flavor attributes.

Metmyoglobin reducing ability has been identified as a substantial determinant in meat quality traits related to color stability (Mancini and Hunt, 2005; Ramanathan et al., 2010; King et al., 2011). Very little data is available evaluating the potential relationship between reducing activity and flavor profile of beef. Positive relationships between NORA and metallic, liver, spoiled, heated oil, and bloody flavor attributes were present in this study. Conversely, NORA was negatively related to beef, brown, umami and butter flavor attributes as well as overall tenderness scores. After 12 days of aging, NORA was related to attributes impacting both principal component one and principal component two indicating that reducing ability attributes may play a role in flavor development at the earlier stages of aging.

Oxygen consumption in meat is an important biochemical factor influenced by mitochondrial function known to play a role in myoglobin redox state (Ramanathan and Mancini, 2018). Increased mitochondrial density and myoglobin concentration results in increased competition for O₂ (Faustman and Cassens, 1990). Increased consumption of O₂ by mitochondria can decrease the oxygen partial pressure of the environment which plays a substantial role the oxidation of red oxymyoglobin to brown metmyoglobin

(Ramanathan and Mancini, 2018). While OC has been shown to decrease over time, mitochondria have been shown to metabolize oxygen up to 60 days postmortem under vacuum packaging (Tang et al., 2005a). Muscles with more aerobic capacity and oxidative, type I fibers are likely to have increased mitochondria density (Hunt and Hedrick, 1977; Picard et al., 2012). (McKenna et al., 2005) found that the *longissimus lumborum* in beef had a very low oxygen consumption rate which contributes to its color stability. In the current study, OC was negatively related to panel scores for palatability components overall tenderness and juiciness. Additionally, OC was positively associated with musty and spoiled flavor attributes.

Muscle fiber composition and resulting metabolic state does play a substantial role on eating quality of beef products. Research has shown that muscles with predominantly oxidative fibers are more susceptible to lipid and protein oxidation than their glycolytic counterparts (Canto et al., 2016; Ke et al., 2017). Type I fibers contain a higher concentration of mitochondria and myoglobin. Approximately 50% of the lipids in the mitochondrial membrane are unsaturated fatty acids (Schenkel and Bakovic, 2014). These unsaturated fatty acids are susceptible to oxidation resulting in the formation of alkenals, aldehydes, and hydroxyalkenals (Ramanathan and Mancini, 2018). Lipid oxidation is a known contributor to meat quality deterioration. However, lipid oxidation also plays a substantial role in the development of meat flavor. A known relationship is present between lipid and myoglobin oxidation (Faustman et al., 2010). Increased myoglobin content as well as increased unsaturated fatty acid content in mitochondrial membranes can have an impact on flavor development depending on fiber type composition and metabolic capacity (Hwang et al., 2010). In the current study,

myoglobin concentration was negatively related to overall tenderness and juiciness palatability components and positively related to beef flavor identity, brown bloody, fat and rancid flavor attributes. Additionally, type I fibers were also positively related to beef flavor identity, brown and bloody flavor attributes. Indicating that characteristics of type I muscle fibers do play a role in influencing flavor profile of beef *longissimus lumborum* steaks.

Protein oxidation has been shown to have a negative impact on tenderness of beef products (Rowe et al., 2004). No relationships were present between carbonyl formation and tenderness in the current study. Carbonyl formation in the sarcoplasmic fraction was positively related to salt flavor attributes whereas carbonyls in the insoluble fraction were positively related to juiciness, sweet, and umami flavors. The impact that protein carbonylation has on meat flavor is yet to be fully understood (Estévez, 2011). Estévez et al. (2011) proposed that specific protein carbonyls could react with free amino acids and ultimately form Strecker aldehydes, but more research is needed to fully understand the full impact protein oxidation has on specific aldehyde formation and mechanisms behind the reactions.

CONCLUSION

Findings in this study indicate that aging time and muscle metabolic characteristics can play a role in the flavor and palatability attributes of beef *longissimus lumborum* steaks. Increased aging times in this study resulted in increased juiciness, beef flavor, umami, sweet and butter attribute scores while decreasing rancid and spoiled scores. Indicating that flavor development in the *longissimus lumborum* was still occurring in a desirable direction at 26 d of aging. Components relating to both oxidative

and glycolytic metabolism contributed to palatability and flavor profiles at both aging periods. Relationships between metabolism intermediates and characteristics and flavor attributes were present in the study, although not totally elucidated. This study indicates that metabolic profile and aging period play a role in flavor profile of beef, but more research is needed to fully understand the mechanisms driving them.

Table 4.1: Least-squares means (SEM) for palatability components, flavor attributes and biochemical characteristics of steaks from the *longissimus lumborum* from three cluster groupings at 12 or 26 days of aging

Attribute	Aging Time (d) x Flavor Cluster Group						P-Value
	12			26			
	LIVER/METALLIC CLUSTER ⁴	SPOILED/MUSTY CLUSTER ⁵	BEEF/BROWN CLUSTER ⁶	LIVER/METALLIC CLUSTER ⁴	SPOILED/MUSTY CLUSTER ⁵	BEEF/BROWN CLUSTER ⁶	
OT ¹	5.94 ^{bc} (0.21)	4.50 ^d (0.19)	6.17 ^b (0.19)	6.61 ^a (0.21)	5.50 ^c (0.19)	6.60 ^a (0.19)	0.02
Salt ²	1.91 ^{bc} (0.06)	1.85 ^c (0.06)	2.06 ^{ab} (0.05)	1.99 ^{abc} (0.06)	2.09 ^a (0.06)	2.02 ^{ab} (0.05)	0.02
NORA ³	70.51 ^a (5.24)	57.45 ^{ab} (4.69)	47.34 ^{bc} (4.84)	34.26 ^c (5.24)	52.05 ^b (4.69)	42.91 ^{bc} (4.84)	<0.0001

abcd means within a row lacking a common superscript differ ($P < 0.05$)

1 Overall Tenderness ranked on an 8 point scale where 1 = extremely tough and 8 = extremely tender

2 Salt flavor attribute ranked on a 16 point scale, where 0 = none and 15 = extremely high

3 Nitric Oxide Reducing Activity- IMF-PRM= NORA (%)

4 n= 27

5 n= 24

6 n= 45

Table 4.2: Least-squares means (SEM) for palatability components¹ and flavor² attributes of beef steaks from the *longissimus lumborum* in three flavor cluster groupings

Attribute	Flavor Cluster Grouping			P-Value
	LIVER/METALLIC CLUSTER ³	SPOILED/MUSTY CLUSTER ⁴	BEEF/BROWN CLUSTER ⁵	
Juiciness	6.07 ^a (0.13)	5.27 ^b (0.11)	6.11 ^a (0.12)	0.0024
Beef	4.46 (0.13)	4.55 (0.12)	4.95 (0.12)	0.07
Brown	3.59 (0.22)	4.23 (0.19)	4.32 (0.20)	0.09
Bloody	2.29 (0.13)	1.99 (0.12)	1.93 (0.12)	0.20
Fat	1.17 (0.12)	1.68 (0.11)	1.87 (0.10)	0.44
Metallic	0.93 (0.11)	0.81 (0.09)	0.53 (0.10)	0.07
Liver	0.75 (0.17)	0.51 (0.15)	0.24 (0.16)	0.18
Umami	2.81 ^b (0.07)	2.90 ^b (0.06)	3.22 ^a (0.05)	0.01
Sweet	0.83 (0.08)	0.79 (0.07)	0.85 (0.07)	0.85
Sour	1.38 (0.09)	1.36 (0.08)	1.35 (0.07)	0.97
Bitter	0.37 (0.07)	0.34 (0.06)	0.21 (0.06)	0.22
Rancid	0.86 (0.14)	1.06 (0.12)	0.82 (0.13)	0.42
Heated Oil	0.80 ^a (0.08)	0.49 ^b (0.07)	0.51 ^b (0.07)	0.05
Chemical	0.29 ^b (0.04)	0.42 ^a (0.04)	0.28 ^b (0.03)	0.01
Musty	0.21 (0.08)	0.34 (0.07)	0.19 (0.07)	0.37
Spoiled	0.12 (0.05)	0.14 (0.04)	0.05 (0.04)	0.36
Butter	0.86 ^b (0.10)	0.69 ^b (0.09)	1.21 ^a (0.09)	0.01

ab means within a row lacking a common superscript differ ($P < 0.05$)

1 Juiciness ranked on an 8 point scale, where 1 = extremely dry and 8 = extremely juicy

2 Flavor attributes ranked on a 16 point scale, where 0 = none and 15 = extremely high

3 n= 27

4 n= 24

5 n= 45

Table 4.3: Least-squares means for palatability¹ and flavor² attributes of steaks from the *longissimus lumborum* at 12 or 26 days postmortem

Attribute	Aging Time (d)		SEM ³	P-Value
	12	26		
Juiciness	5.67 ^b	5.96 ^a	0.07	<0.0001
Beef	4.48 ^b	4.83 ^a	0.08	<0.0001
Brown	3.88 ^b	4.21 ^a	0.12	0.0002
Bloody	2.13	2.04	0.08	0.43
Fat	1.72	1.78	0.07	0.33
Metallic	0.75	0.76	0.06	0.91
Liver	0.46	0.54	0.10	0.10
Umami	2.84 ^b	3.11 ^a	0.04	<0.0001
Sweet	0.76 ^b	0.88 ^a	0.05	0.01
Sour	1.41	1.31	0.06	0.16
Bitter	0.29	0.32	0.04	0.46
Rancid	1.00 ^a	0.82 ^b	0.08	0.01
Heated Oil	0.58	0.61	0.05	0.45
Chemical	0.35	0.31	0.03	0.25
Musty	0.25	0.24	0.05	0.77
Spoiled	0.14 ^a	0.07 ^b	0.03	0.003
Butter	0.84 ^b	1.00 ^a	0.06	0.001

ab means within a row lacking a common superscript differ ($P < 0.05$)

1 Juiciness ranked on an 8 point scale, where 1 = extremely dry and 8 = extremely juicy

2 Flavor attributes ranked on a 16 point scale, where 0 = none and 15 = extremely high

3 Standard Error of the Mean

Table 4.4: Pearson correlation coefficients of palatability components and flavor attributes³ in beef steaks from the *longissimus lumborum*

Variable	OT	Juiciness	Beef	Brown	Bloody	Fat	Metallic	Liver	Umami	Sweet	Sour	Salt	Bitter	Rancid	Heated oil	Chemical	Musty	Spoiled	Butter
OT ¹	-	0.89***	0.16*	-0.16*	0.10	0.17*	-0.03	0.17*	0.27**	0.14*	-0.03	0.05	-0.01	-0.18*	0.18*	-0.18*	-0.14	-0.22*	0.35***
Juiciness ²		-	0.21**	-0.16*	0.23**	0.26**	-0.07	0.08	0.28***	0.21**	-0.09	-0.03	-0.01	-0.20**	0.24**	-0.21**	-0.14	-0.27**	0.41***
Beef			-	0.69***	-0.29***	0.22**	-0.40***	-0.48***	0.66***	0.29***	-0.30***	0.21**	-0.24**	-0.28***	0.04	0.02	-0.20**	-0.37***	0.43***
Brown				-	-0.30***	0.17*	-0.44***	-0.47***	0.51***	0.12	-0.14	0.21**	-0.21**	-0.07	-0.15*	0.04	-0.06	-0.18*	0.32***
Bloody					-	0.07	0.35***	0.42***	-0.16*	-0.03	0.09	-0.19**	0.33***	0.32***	0.13	-0.08	0.14*	0.20*	-0.14*
Fat						-	-0.10	-0.07	0.30***	0.25**	-0.03	0.05	0.09	-0.03	0.03	-0.15*	0.12	-0.05	0.28***
Metallic							-	0.42***	-0.33***	0.02	0.10	-0.17*	0.44***	0.18*	0.17*	-0.01	0.15*	0.16*	0.36***
Liver								-	-0.40***	-0.19**	0.15*	-0.08	0.34***	0.12	0.28***	-0.04	0.17*	0.24**	-0.39***
Umami									-	0.43***	-0.33***	0.31***	-0.22**	-0.32***	0.08	-0.09	-0.21**	-0.28**	0.53***
Sweet										-	-0.52***	0.17*	-0.17*	-0.31***	0.22**	-0.06	-0.25**	-0.21**	0.39***
Sour											-	0.05	0.24**	0.36***	-0.15*	0.13	0.23**	0.20**	-0.34***
Salt												-	-0.24**	-0.15*	0.02	0.00	-0.01	-0.09	0.15*
Bitter													-	0.34***	-0.01	-0.05	0.45***	0.20**	-0.30***
Rancid														-	-0.34***	-0.06	0.32***	0.31***	-0.32***
Heated Oil															-	-0.03	-0.17*	-0.04	0.03
Chemical																-	0.05	-0.01	-0.19*
Musty																	-	0.25**	-0.37**
Spoiled																		-	-0.32***
Butter																			-

* P < 0.05, ** P < 0.01, *** P < 0.0001

1 OT= Overall Tenderness ranked on an 8 point scale where 1 = extremely tough and 8 = extremely tender

2 Juiciness ranked on a 8 point scale where 1 = extremely dry and 8 = extremely juicy

3 Flavor attributes ranked on a 15 point scale where 0 = not detectable and 15 = extremely strong

Table 4.5: Least-squares means for muscle characteristics and residual metabolism intermediates in beef steaks from the *longissimus lumborum* in three cluster groupings

Attribute	Flavor Cluster Grouping			P-Value
	LIVER/METALLIC CLUSTER ¹⁴	SPOILED/MUSTY CLUSTER ¹⁵	BEEF/BROWN CLUSTER ¹⁶	
OC ¹	34.14 (2.92)	40.51 (2.57)	32.47 (2.55)	0.14
pH d2 ²	5.52 (0.02)	5.52 (0.02)	5.50 (0.02)	0.56
pHu ³	5.51 (0.03)	5.54 (0.02)	5.53 (0.03)	0.81
MYO ⁴	4.05 (0.21)	4.55 (0.18)	4.39 (0.17)	0.24
Sol Carb ⁵	1.58 (0.20)	1.57 (0.18)	1.68 (0.16)	0.89
Insol Carb ⁶	3.38 (0.26)	2.95 (0.27)	3.50 (0.20)	0.25
GLY ⁷	11.17 (2.61)	11.12 (2.30)	14.39 (2.34)	0.57
GLU ⁸	8.97 (0.43)	7.77 (0.38)	8.55 (0.33)	0.22
G6P ⁹	7.69 (0.52)	6.68 (0.45)	7.37 (0.41)	0.43
Lactate ¹⁰	148.14 (4.56)	145.31 (4.02)	147.91 (3.61)	0.86
Malate ¹¹	0.98 (0.15)	0.86 (0.13)	1.03 (0.14)	0.68
MHC-1 ¹²	30.80 (0.29)	30.73 (0.31)	31.31 (0.23)	0.22
MHC-2 ¹³	69.20 (0.29)	69.27 (0.31)	68.69 (0.23)	0.22

¹ Oxygen Consumption (%)

² pH of striploin at 2 days post-mortem

³ Ultimate pH after aging period

⁴ Total myoglobin concentration (mg/g)

⁵ Carbonyl formation in the soluble fraction (μmol/mg)

⁶ Carbonyl formation in the insoluble fraction (μmol/mg)

⁷ Residual glycogen (μmol/g)

⁸ Residual glucose (μmol/g)

⁹ Residual glucose-6-phosphate (μmol/g)

¹⁰ Residual lactate (μmol/g)

¹¹ Residual malate (μmol/g)

¹² Myosin heavy chain isoform- 1 (%)

¹³ Myosin heavy chain isoform-2 (%)

¹⁴ n= 27

¹⁵ n= 24

¹⁶ n= 45

Table 4.6: Least-squares means for muscle characteristics and residual metabolism intermediates of beef steaks from the *longissimus lumborum* at 12 or 26 days postmortem

Attribute	Aging Time (d)		SEM ¹⁴	P-Value
	12	26		
OC ¹	36.05	35.36	1.71	0.64
pH d2 ²	5.51	5.52	0.01	0.20
pHu ³	5.52	5.53	0.02	0.26
MYO ⁴	91.36	92.07	0.78	0.40
Sol Carb ⁵	1.61	1.62	0.12	0.93
Insol Carb ⁶	3.06	3.50	0.20	0.12
GLY ⁷	13.11	11.35	1.52	0.14
GLU ⁸	7.28 ^b	9.59 ^a	0.27	<0.0001
G6P ⁹	8.17 ^a	6.32 ^b	0.31	<0.0001
Lactate ¹⁰	150.34 ^a	143.90 ^b	2.79	0.03
Malate ¹¹	0.95	0.97	0.09	0.66
MHC-1 ¹²	31.11	30.78	0.23	0.31
MHC-2 ¹³	68.89	69.22	0.23	0.31

¹ Oxygen Consumption (%)

² pH of striploin at 2 days post-mortem

³ Ultimate pH after aging period

⁴ Total myoglobin concentration (mg/g)

⁵ Carbonyl formation in the soluble fraction (μmol/mg)

⁶ Carbonyl formation in the insoluble fraction (μmol/mg)

⁷ Residual glycogen (μmol/g)

⁸ Residual glucose (μmol/g)

⁹ Residual glucose-6-phosphate (μmol/g)

¹⁰ Residual lactate (μmol/g)

¹¹ Residual malate (μmol/g)

¹² Myosin heavy chain isoform- 1 (%)

¹³ Myosin heavy chain isoform-2 (%)

¹⁴ Standard Error of the Mean

Table 4.7: Correlation coefficients of muscle characteristics and residual metabolism intermediates of beef steaks from the *longissimus lumborum* at both aging periods

Var	OC ¹	NORA ²	MYO ³	pH d2 ⁴	pHu ⁵	Sol Carb ⁶	Insol Carb ⁷	GLY ⁸	GLU ⁹	G6P ¹⁰	Lactate ¹¹	Malate ¹²	MHC-1 ¹³	MHC-2 ¹⁴
OC	-	0.12	0.18*	0.31***	0.43***	-0.04	0.02	-0.10	-0.16*	-0.28***	-0.13	-0.06	0.15*	-0.15*
NORA		-	-0.20**	0.05	-0.15*	-0.01	-0.06	0.01	-0.17*	0.22**	0.21**	-0.02	-0.02	0.02
TMYO				0.07	0.35***	-0.08	0.00	0.11	0.05	-0.10	0.03	0.03	0.43***	-0.43***
pH d2				-	0.50***	-0.06	-0.05	-0.19**	-0.24**	-0.40***	-0.21**	0.04	0.03	-0.03
pHu					-	-0.10	0.01	-0.16*	-0.28***	-0.41***	-0.23**	0.11	0.17*	-0.17*
Sol Carb						-	0.19**	0.01	-0.10	0.13	0.06	0.01	-0.02	0.02
Insol Carb							-	0.01	0.06	0.04	0.12	-0.17*	0.03	-0.03
GLY								-	0.17*	0.26**	0.09	0.14*	-0.17*	0.17*
GLU									-	0.32***	0.09	0.09	0.02	-0.02
G6P										-	0.22**	0.05	0.01	-0.01
Lactate											-	0.01	0.08	-0.08
Malate												-	-0.02	0.02
MHC-1													-	-1.00***
MHC-2														-

* P < 0.05, ** P < 0.01, *** P < 0.0001

¹ Oxygen Consumption (%)

² Nitric Oxide Reducing Activity- IMF-PRM= NORA (%)

³ Total myoglobin (mg/g)

⁴ pH of striploin at 2 days post-mortem

⁵ Ultimate pH after aging period

⁶ Carbonyl formation in the soluble fraction (µmol/mg)

⁷ Carbonyl formation in the insoluble fraction (µmol/mg)

⁸ Residual glycogen (µmol/g)

⁹ Residual glucose (µmol/g)

¹⁰ Residual glucose-6-phosphate (µmol/g)

¹¹ Residual lactate (µmol/g)

¹² Residual malate (µmol/g)

¹³ Myosin heavy chain isoform- 1 (%)

¹⁴ Myosin heavy chain isoform-2 (%)

Table 4.8: Pearson correlation coefficients of sensory panel palatability¹⁵ and flavor attributes¹⁶ with muscle characteristics and residual metabolism intermediates in beef steaks from the *longissimus lumborum*

	OC ¹	NORA ²	MYO ³	pH d2 ⁴	pHu ⁵	Sol Carb ⁶	Insol Carb ⁷	GLY ⁸	GLU ⁹	G6P ¹⁰	Lactate ¹¹	Malate ¹²	MHC-1 ¹³	MHC-2 ¹⁴
OT	-0.19**	-0.22**	-0.24**	-0.15*	-0.13	-0.02	0.13	0.21**	0.40***	0.05	-0.01	0.09	0.00	0.00
Juiciness	-0.20**	-0.14	-0.19**	-0.10	-0.06	-0.06	0.16*	0.19**	0.28***	0.05	0.00	0.04	0.05	-0.05
Beef	-0.06	-0.33***	0.18*	0.01	0.18*	0.05	0.10	0.14	0.07	-0.15*	-0.05	0.09	0.17*	-0.17*
Brown	-0.07	-0.32***	0.37***	0.01	0.19**	0.09	0.08	0.19**	0.09	-0.14	0.02	0.02	0.15*	-0.15*
Bloody	0.10	0.20**	0.21**	0.05	-0.09	-0.05	0.09	0.15*	0.06	0.07	0.08	0.00	0.18*	-0.18*
Fat	-0.06	-0.09	0.16*	-0.13	-0.01	-0.05	-0.03	0.15*	0.06	-0.09	0.04	0.00	0.14	-0.14
Metallic	-0.09	0.23**	-0.09	-0.04	-0.36***	-0.01	0.01	-0.09	0.11	0.15*	0.06	-0.02	0.08	0.08
Liver	0.12	0.26**	-0.09	0.01	-0.35***	-0.07	-0.04	-0.01	0.21**	0.04	0.05	-0.08	0.02	0.02
Umami	-0.08	-0.30***	0.04	-0.04	0.16*	0.02	0.09	0.20**	0.03	-0.18*	0.00	0.14	0.04	-0.04
Sweet	-0.03	-0.11	-0.18*	-0.05	-0.03	0.07	0.21**	-0.04	-0.04	-0.11	-0.04	-0.07	-0.06	0.06
Sour	0.00	0.09	0.04	-0.16*	-0.19**	0.05	-0.11	0.11	0.13	0.20**	0.14	0.06	-0.07	0.07
Salt	-0.05	-0.06	-0.07	-0.01	0.03	0.18*	0.01	0.07	0.01	-0.03	0.02	0.15	0.00	0.00
Bitter	-0.01	0.15*	0.04	-0.03	-0.24**	-0.06	-0.06	-0.08	0.16*	0.03	0.15*	-0.09	-0.07	0.07
Rancid	0.02	0.08	0.22**	0.06	-0.04	0.07	-0.12	0.16*	-0.08	0.00	0.18*	0.02	0.13	-0.13
Heated Oil	-0.07	0.14*	-0.18*	-0.12	-0.24**	0.09	0.07	-0.01	0.12	0.12	-0.03	0.00	-0.06	0.06
Chemical	-0.13	-0.06	0.02	-0.14	-0.08	0.10	-0.05	-0.17*	-0.03	0.11	-0.09	-0.07	-0.10	0.10
Musty	0.15*	0.05	0.13	0.07	0.00	-0.03	-0.05	-0.02	-0.03	-0.07	0.01	0.04	0.06	-0.06
Spoiled	0.20**	0.16**	0.06	0.06	-0.08	0.08	-0.04	0.08	-0.08	0.07	0.12	0.03	0.13	-0.13
Butter	-0.17*	-0.31***	-0.06	-0.07	0.13	0.09	0.28***	0.07	0.01	-0.15*	0.06	0.01	0.08	-0.08

* P < 0.05, ** P < 0.01, *** P < 0.0001

1 Oxygen Consumption (%)

2 Nitric Oxide Reducing Activity- IMF-PRM= NORA (%)

3 Total myoglobin (mg/g)

4 pH of striploin at 2 days post-mortem

5 Ultimate pH after aging period

6 Carbonyl formation in the soluble fraction (µmol/mg)

7 Carbonyl formation in the insoluble fraction (µmol/mg)

8 Residual glycogen (µmol/g)

9 Residual glucose (µmol/g)

10 Residual glucose-6-phosphate (µmol/g)

11 Residual lactate (µmol/g)

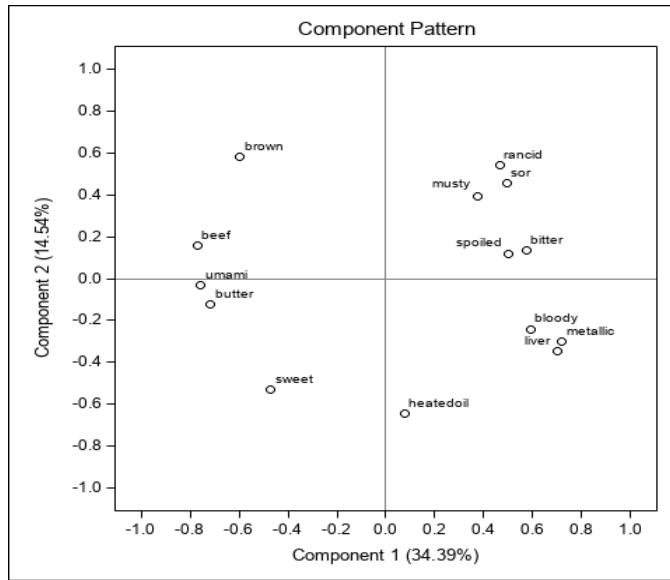
12 Residual malate (µmol/g)

13 Myosin heavy chain isoform- 1 (%)

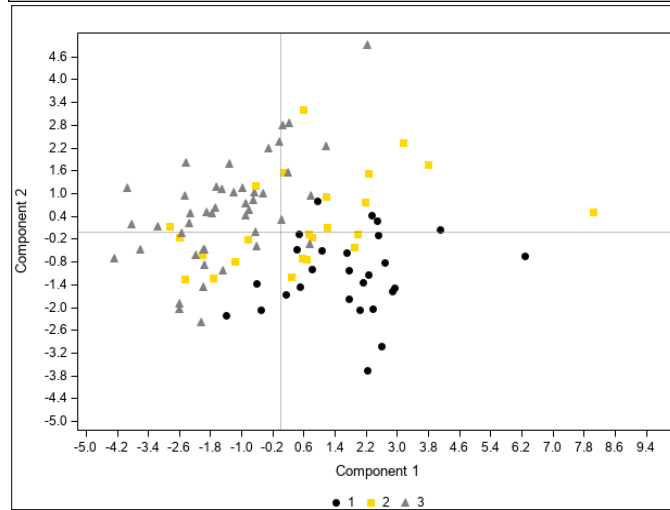
14 Myosin heavy chain isoform-2 (%)

15 Overall Tenderness and juiciness s ranked on an 8 point scale where 1 = extremely tough/dry and 8 = extremely tender/juicy

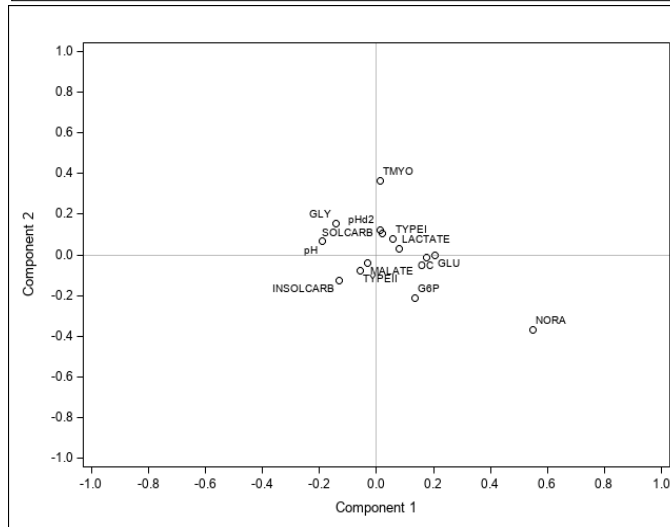
16 Flavor attributes ranked on a 15 point scale where 0 = not detectable and 15 = extremely strong



A.



B.



C.

Figure 4.1. A) Principal Component Analysis of flavor attributes B) Score Plot for Cluster Groupings C.) Loading plot of metabolic and biochemical characteristics of beef *longissimus lumbrorum* steaks aged for 12 days

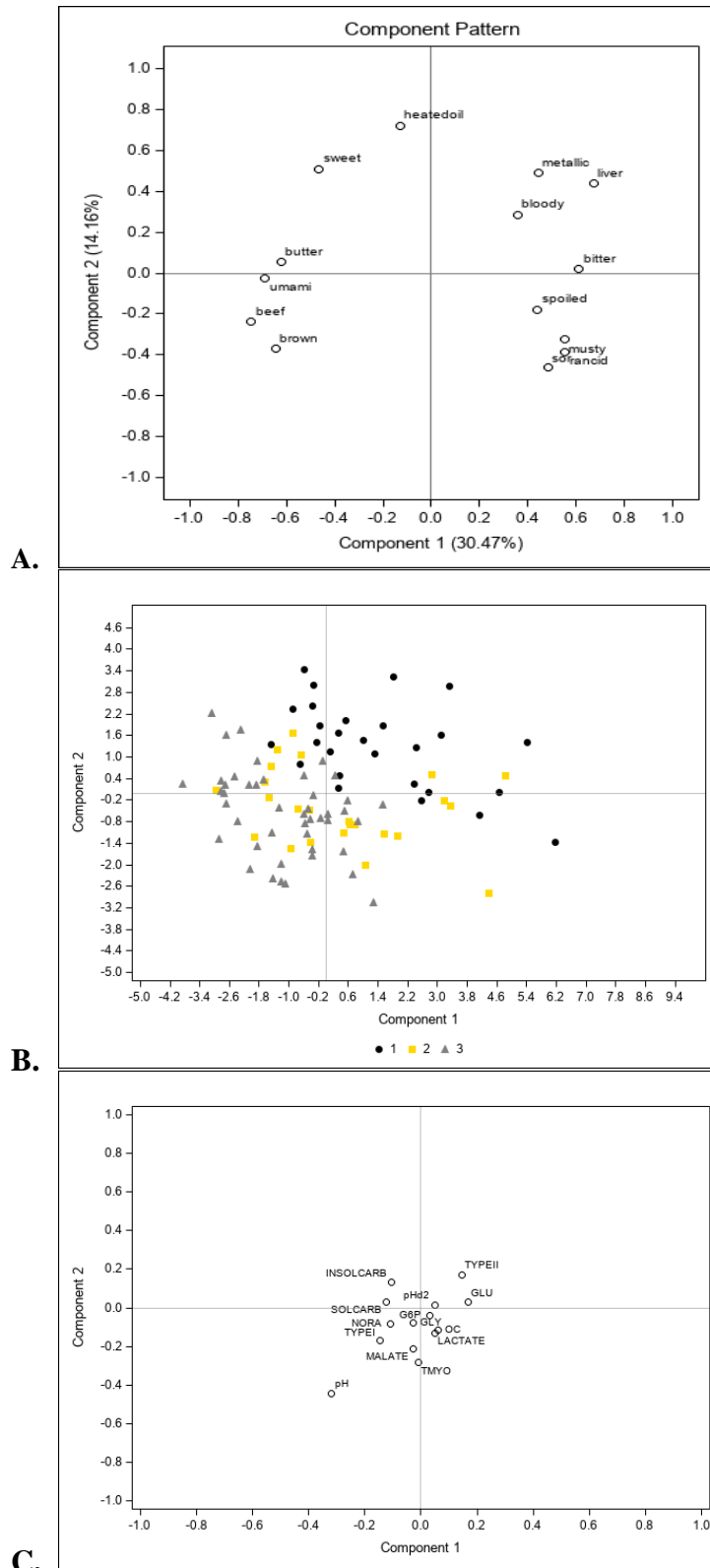


Figure 4.2. A) Principal Component Analysis of flavor attributes B) Score Plot for Cluster Groupings C.) Loading plot of metabolic and biochemical characteristics of beef *longissimus lumborum* steaks aged for 26 days

Chapter 5

Conclusion

It is well established that the conversion of muscle to meat and muscle characteristics have substantial roles in various aspects of meat quality. However, further understanding the mechanisms behind these roles and contributions is necessary for continued improvement in quality and palatability of beef. Relationships between metabolism intermediates and biochemical characteristics and meat quality and palatability traits in *longissimus lumborum* were present, although not totally elucidated. Data from this study indicate that variation in palatability components and quality attributes of beef is impacted by biochemical and metabolic characteristics of the muscle. Type II, or glycolytic, muscle fibers were positively related to color stability in comparison to their oxidative counterparts. Furthermore, glycolytic intermediates were associated with increased tenderness and color stability. Residual glycogen and glucose were positively related to overall tenderness and juiciness scores. Type II muscle fibers were negatively related to beef flavor identity, brown, and bloody flavor attributes. Color stability attributes were negatively related to total myoglobin concentration as well as oxygen consumption and reducing ability. Furthermore, attributes associated with mitochondrial function such as oxygen consumption and reducing ability had a negative impact on both overall tenderness scores and slice shear force. Attributes associated with mitochondrial function were negatively related to juiciness scores as well as desirable flavor attributes. Myoglobin concentration was related to a variety of flavor and

palatability attributes exhibiting negative relationships with overall tenderness and juiciness scores and positive relationships with beef flavor identity, brown, bloody, fat, and rancid flavor attributes. Additionally, myoglobin concentration influenced shear force values. However, the relationships were not always similar. Further indicating need for a greater understanding of mechanisms behind the relationships between color and tenderness attributes at various aging times. While it is clear that metabolic attributes and aging period play a role in flavor profile development in beef, but more research is needed to fully understand the impact that these specific attributes have on flavor attributes and palatability components in beef.

Overall tenderness, juiciness, beef flavor identity, umami, sweet, and butter attribute scores increased as aging time increased, indicating positive flavor development still occurring during prolonged aging periods. Furthermore, rancid and spoiled attribute scores decreased. Components relating to both oxidative and glycolytic metabolism were related to palatability and flavor profiles at both aging periods.

Moving forward, gaining a further understanding of the relationships between quality and palatability traits themselves as well as their relationship with metabolic and biochemical characteristics is imperative for continued improvement of beef products. Utilization of omics technologies will allow for a more detailed snapshot of the metabolic or biochemical state of the beef muscle at any specific time point. Gaining more detailed and specific knowledge about the inner workings within the muscle will allow researchers to identify relationships among traits, the factors impacting those traits, and more importantly, the mechanisms behind them.

Appendix A. SAS Input for Chapter 2

```

run;
options ls=95 ps=70;
data one; infile 'C:\Users\jvc3w3\Downloads\MBICfinal0620.csv' dsd firstobs=2 missover;
input ID HCW YG QG pH0 pH24 pH48 Temp0 Temp24 Temp48 SSf48Hr
SSF336Hr WBSF48Hr WBSF336Hr
CookLoss48Hr CookLoss336Hr Myo0 Myo48 Myo336 MRA0 MRA48
MRA336 L48 a48 b48 L336 a336
b336 ab48 si48 ha48 ab336 si336 ha336 MMb48
Dmb48 Omb48 MMb336 DMb336 Omb336 calp0 calp48 calp336;
proc print;
proc corr;
proc means stderr;

proc glm;
model pH24 pH48 Temp24 Temp48 SSf48Hr SSF336Hr WBSF48Hr WBSF336Hr
CookLoss48Hr CookLoss336Hr Myo0 Myo48 Myo336 MRA0 MRA48
MRA336 L48 a48 b48 L336 a336
b336 ab48 si48 ha48 ab336 si336 ha336 MMb48
Dmb48 Omb48 MMb336 DMb336 Omb336 =calp0 /p predicted;
proc glm;
model pH24 pH48 Temp24 Temp48 SSf48Hr SSF336Hr WBSF48Hr WBSF336Hr
CookLoss48Hr CookLoss336Hr Myo0 Myo48 Myo336 MRA0 MRA48
MRA336 L48 a48 b48 L336 a336
b336 ab48 si48 ha48 ab336 si336 ha336 MMb48
Dmb48 Omb48 MMb336 DMb336 Omb336=calp0 calp0*calp0 /p predicted;
run;

data two; set one;
ph=pH0; temp=Temp0; tm=0; output;
ph=pH24; temp=temp24; tm=24; output;
ph= pH48; temp=temp48; tm=48; output;
data two; set two;
keep id ph temp tm;
proc print;
proc glm; class tm;
model ph temp=tm;
means tm/lines;
lsmeans tm/pdiff;
run;

data three; set one;
myo=myo0; mra=mra0; calp=calp0; tm=0; output;
myo=myo48; mra=mra48; calp=calp48; tm=48; output;
myo=myo336; mra=mra336; calp=calp336; tm=336; output;
proc print;
proc glm; class tm;
model myo mra calp=tm;
means tm/lines;
lsmeans tm/pdiff;
run;

data four; set one;

```



```
l=l48; a=a48; b=b48;ssf=ssf48hr; wbsf=wbsf48hr; cookloss=cookloss48hr; si=si48; ha=ha48; ab=ab48;
omb=omb48; mmb=mmb48; dmb=dmb48; calp=calp48; tm=48; output;
l=l336; a=a336; b=b336; ssf=ssf336hr; wbsf=wbsf336hr; cookloss=cookloss336hr; si=si336; ha=ha336;
ab=ab336; omb=omb336; mmb=mmb336; dmb=dmb336; calp=calp336; tm=336; output;
proc print;
proc ttest cochran;
var l a b ssf wbsf cookloss si ha ab omb mmb dmb calp;
class tm;
run;
```

Appendix B. SAS input for Chapter 3

```
ods trace on;
```

```
data dummy;
```

```
do dpm = 12, 26;  
do coltend4 = 1 to 4;  
cx = coltend4 + 600;  
STK_ID = dpm*1000 + cx;  
do i=0 to 11;  
d=i;  
    day1 = d;  
    d2 = d*d;  
    d3 = d2*d;  
trip = 2.5;  
output;  
end;  
end;  
end;  
run;
```

```
data long;
```

```
set metdata;
```

```
array aLstar(5) aLstar_00 -- aLstar_11 ;  
array aLstar(5) aLstar_00 -- aLstar_11 ;  
array aLstar(5) aLstar_00 -- aLstar_11 ;  
array aLstar(5) aLstar_00 -- aLstar_11 ;  
array aLstar(5) aLstar_00 -- aLstar_11 ;  
array aLstar(5) aLstar_00 -- aLstar_11 ;  
array aLstar(5) aLstar_00 -- aLstar_11 ;
```

```
DO day = 1 to 5;
```

```
    Lstar = aLstar(day);  
    astar = aLstar(day);  
    bstar = aLstar(day);  
    chr = aLstar(day);  
    ha = aLstar(day);  
    de = aLstar(day);
```

```
    OUTPUT;
```

```
    END;
```

```
    DROP
```

```
    aLstar_00--aLstar_11
```

```
    astar_00--astar_11
```

```
    bstar_00--bstar_11
```

```
    chr_00--chr_11
```

```
    ha_00--ha_11
```

```
    de_00--de_11
```

```
    ;
```

```
run;
```

```

data long; set long;
if day = 1 then d = 0;
if day = 2 then d = 1;
if day = 3 then d = 4;
if day = 4 then d = 7;
if day = 5 then d = 11;
d2 = d*d;
d3 = d2*d;
day1 = d;
run;

```

```

data long; merge long dummy; by STK_ID; run;

```

```

proc glimmix data = long ;          *noprofile ;
class STK_ID cx trip coltend4 dpm day1;
model lstar = coltend4 dpm coltend4*dpm
d coltend4*d dpm*d coltend4*dpm*d
d2 coltend4*d2 dpm*d2 coltend4*dpm*d2
d3 coltend4*d3 dpm*d3 coltend4*dpm*d3
/ solution ddfm = kr ; * ;
random trip(cx) ;
random day1/ TYPE = sp(pow) (day1) sub = STK_ID residual ; * ;
output out =predval predicted = pred;;
lsmeans coltend4*dpm/ e;
estimate '          Coltend 1 12 d      12      Interceptbeta      '          Intercept1      coltend4 1
           0          0          0      dpm      1          0      coltend4*dpm      1      0          0
           0          0          0          0          0          ;
estimate '          Coltend 1          26      Interceptbeta      '          Intercept1      coltend4 1
           0          0          0      dpm      0          1      coltend4*dpm      0      1          0
           0          0          0          0          0          ;
estimate '          Coltend 2          12      Interceptbeta      '          Intercept1      coltend4 0
           1          0          0      dpm      1          0      coltend4*dpm      0      0          1
           0          0          0          0          0          ;
estimate '          Coltend 2          26      Interceptbeta      '          Intercept1      coltend4 0
           1          0          0      dpm      0          1      coltend4*dpm      0      0          0
           1          0          0          0          0          ;
estimate '          Coltend3          12      Interceptbeta      '          Intercept1      coltend4 0
           0          1          0      dpm      1          0      coltend4*dpm      0      0          0
           0          1          0          0          0          ;
estimate '          Coltend 3          26      Interceptbeta      '          Intercept1      coltend4 0
           0          1          0      dpm      0          1      coltend4*dpm      0      0          0
           0          0          1          0          0          ;
estimate '          Coltend4          12      Interceptbeta      '          Intercept1      coltend4 0
           0          0          1      dpm      1          0      coltend4*dpm      0      0          0
           0          0          0          1          0          ;
estimate '          Coltend 4          26      Interceptbeta      '          Intercept1      coltend4 0
           0          0          1      dpm      0          1      coltend4*dpm      0      0          0
           0          0          0          0          1          ;
estimate '          Coltend 1          Interceptbeta      '          Intercept1      coltend4 1
           0          0          0      dpm      0.5      0.5      coltend4*dpm      0.5      0.5      0
           0          0          0          0          0          ;

```

```

estimate '      Coltend 2      Interceptbeta      Intercept1      coltend4 0
      1      0      0      dpm      0.5      0.5      coltend4*dpm      0      0      0.5
      0.5      0      0      0      0      ;
estimate '      Coltend 3      Interceptbeta      Intercept1      coltend4 0
      0      1      0      dpm      0.5      0.5      coltend4*dpm      0      0      0
      0      0.5      0.5      0      0      ;
estimate '      Coltend 4      Interceptbeta      Intercept1      coltend4 0
      0      0      1      dpm      0.5      0.5      coltend4*dpm      0      0      0
      0      0      0      0.5      0.5      ;
estimate '      12      Interceptbeta      Intercept1      coltend4 0.25      0.25
      0.25      0.25      dpm      1      0      coltend4*dpm      0.25      0      0.25      0
      0.25      0      0.25      0      ;
estimate '      26      Interceptbeta      Intercept1      coltend4 0.25      0.25
      0.25      0.25      dpm      0      1      coltend4*dpm      0      0.25      0      0.25
      0      0.25      0      0.25      ;

```

```

estimate '      Coltend 1 12 d      12      linear      beta      '      d      4.6      d*coltend4
      4.6      0      0      0      d*dpm      4.6      0      d*coltend4*dpm      4.6      0
      0      0      0      0      0      0      ;
estimate '      Coltend 1      26      linear      beta      '      d      4.6      d*coltend4
      4.6      0      0      0      d*dpm      0      4.6      d*coltend4*dpm      0      4.6
      0      0      0      0      0      0      ;
estimate '      Coltend 2      12      linear      beta      '      d      4.6      d*coltend4
      0      4.6      0      0      d*dpm      4.6      0      d*coltend4*dpm      0      0
      4.6      0      0      0      0      0      ;
estimate '      Coltend 2      26      linear      beta      '      d      4.6      d*coltend4
      0      4.6      0      0      d*dpm      0      4.6      d*coltend4*dpm      0      0
      0      4.6      0      0      0      0      ;
estimate '      Coltend3      12      linear      beta      '      d      4.6      d*coltend4
      0      0      4.6      0      d*dpm      4.6      0      d*coltend4*dpm      0      0
      0      0      4.6      0      0      0      ;
estimate '      Coltend 3      26      linear      beta      '      d      4.6      d*coltend4
      0      0      4.6      0      d*dpm      0      4.6      d*coltend4*dpm      0      0
      0      0      0      4.6      0      0      ;
estimate '      Coltend4      12      linear      beta      '      d      4.6      d*coltend4
      0      0      0      4.6      d*dpm      4.6      0      d*coltend4*dpm      0      0
      0      0      0      0      4.6      0      ;
estimate '      Coltend 4      26      linear      beta      '      d      4.6      d*coltend4
      0      0      0      4.6      d*dpm      0      4.6      d*coltend4*dpm      0      0
      0      0      0      0      0      4.6      ;
estimate '      Coltend 1      linear      beta      '      d      4.6      d*coltend4
      4.6      0      0      0      d*dpm      2.3      2.3      d*coltend4*dpm      2.3      2.3
      0      0      0      0      0      0      ;
estimate '      Coltend 2      linear      beta      '      d      4.6      d*coltend4
      0      4.6      0      0      d*dpm      2.3      2.3      d*coltend4*dpm      0      0
      2.3      2.3      0      0      0      0      ;
estimate '      Coltend 3      linear      beta      '      d      4.6      d*coltend4
      0      0      4.6      0      d*dpm      2.3      2.3      d*coltend4*dpm      0      0
      0      0      2.3      2.3      0      0      ;
estimate '      Coltend 4      linear      beta      '      d      4.6      d*coltend4
      0      0      0      4.6      d*dpm      2.3      2.3      d*coltend4*dpm      0      0
      0      0      0      0      2.3      2.3      ;

```

```

estimate '          12  linear  beta  '      d      4.6  d*coltend4  1.15
      1.15  1.15  1.15  d*dpm  4.6  0      d*coltend4*dpm  1.15  0  1.15
      0      1.15  0      1.15  0      ;
estimate '          26  linear  beta  '      d      4.6  d*coltend4  1.15
      1.15  1.15  1.15  d*dpm  0      4.6  d*coltend4*dpm  0  1.15  0
      1.15  0      1.15  0      1.15  ;

estimate '          Coltend 1 12 d  12  quadratic  beta  '      d2  37.4
      d2*coltend4  37.4  0  0  0  d2*dpm  37.4  0
      d2*coltend4*dpm  37.4  0  0  0  0  0  0  0  0
;
estimate '          Coltend 1  26  quadratic  beta  '      d2  37.4
      d2*coltend4  37.4  0  0  0  d2*dpm  0  37.4
      d2*coltend4*dpm  0  37.4  0  0  0  0  0  0  0
;
estimate '          Coltend 2  12  quadratic  beta  '      d2  37.4
      d2*coltend4  0  37.4  0  0  d2*dpm  37.4  0
      d2*coltend4*dpm  0  0  37.4  0  0  0  0  0  0
;
estimate '          Coltend 2  26  quadratic  beta  '      d2  37.4
      d2*coltend4  0  37.4  0  0  d2*dpm  0  37.4
      d2*coltend4*dpm  0  0  0  37.4  0  0  0  0  0
;
estimate '          Coltend3  12  quadratic  beta  '      d2  37.4
      d2*coltend4  0  0  37.4  0  d2*dpm  37.4  0
      d2*coltend4*dpm  0  0  0  0  0  37.4  0  0  0
;
estimate '          Coltend 3  26  quadratic  beta  '      d2  37.4
      d2*coltend4  0  0  37.4  0  d2*dpm  0  37.4
      d2*coltend4*dpm  0  0  0  0  0  0  37.4  0  0
;
estimate '          Coltend4  12  quadratic  beta  '      d2  37.4
      d2*coltend4  0  0  0  37.4  d2*dpm  37.4  0
      d2*coltend4*dpm  0  0  0  0  0  0  0  37.4  0
;
estimate '          Coltend 4  26  quadratic  beta  '      d2  37.4
      d2*coltend4  0  0  0  37.4  d2*dpm  0  37.4
      d2*coltend4*dpm  0  0  0  0  0  0  0  0  37.4
;
estimate '          Coltend 1  quadratic  beta  '      d2  37.4
      d2*coltend4  37.4  0  0  0  d2*dpm  18.7  18.7
      d2*coltend4*dpm  18.7  18.7  0  0  0  0  0  0  0
;
estimate '          Coltend 2  quadratic  beta  '      d2  37.4
      d2*coltend4  0  37.4  0  0  d2*dpm  18.7  18.7
      d2*coltend4*dpm  0  0  18.7  18.7  0  0  0  0  0
;
estimate '          Coltend 3  quadratic  beta  '      d2  37.4
      d2*coltend4  0  0  37.4  0  d2*dpm  18.7  18.7
      d2*coltend4*dpm  0  0  0  0  0  18.7  18.7  0  0
;
estimate '          Coltend 4  quadratic  beta  '      d2  37.4
      d2*coltend4  0  0  0  37.4  d2*dpm  18.7  18.7

```

```

d2*coltend4*dpm      0      0      0      0      0      0      0      18.7  18.7
;
estimate'           12      quadratic      beta      '      d2      37.4      d2*coltend4
9.35      9.35      9.35      9.35      d2*dpm 37.4      0      d2*coltend4*dpm      9.35
0      9.35      0      9.35      0      9.35      0      ;
estimate'           26      quadratic      beta      '      d2      37.4      d2*coltend4
9.35      9.35      9.35      9.35      d2*dpm 0      37.4      d2*coltend4*dpm      0
9.35      0      9.35      0      9.35      0      9.35      ;

estimate'           Coltend 1 12 d      12      cubic      beta      '      d3      347.8      d3*coltend4
347.8      0      0      0      d3*dpm 347.8      0      d3*coltend4*dpm      347.8
0      0      0      0      0      0      0      ;
estimate'           Coltend 1      26      cubic      beta      '      d3      347.8      d3*coltend4
347.8      0      0      0      d3*dpm 0      347.8      d3*coltend4*dpm      0
347.8      0      0      0      0      0      0      ;
estimate'           Coltend 2      12      cubic      beta      '      d3      347.8      d3*coltend4
0      347.8      0      0      d3*dpm 347.8      0      d3*coltend4*dpm      0
0      347.8      0      0      0      0      0      ;
estimate'           Coltend 2      26      cubic      beta      '      d3      347.8      d3*coltend4
0      347.8      0      0      d3*dpm 0      347.8      d3*coltend4*dpm      0
0      0      347.8      0      0      0      0      ;
estimate'           Coltend3      12      cubic      beta      '      d3      347.8      d3*coltend4
0      0      347.8      0      d3*dpm 347.8      0      d3*coltend4*dpm      0
0      0      0      347.8      0      0      0      ;
estimate'           Coltend 3      26      cubic      beta      '      d3      347.8      d3*coltend4
0      0      347.8      0      d3*dpm 0      347.8      d3*coltend4*dpm      0
0      0      0      0      347.8      0      0      ;
estimate'           Coltend4      12      cubic      beta      '      d3      347.8      d3*coltend4
0      0      0      347.8      d3*dpm 347.8      0      d3*coltend4*dpm      0
0      0      0      0      0      347.8      0      ;
estimate'           Coltend 4      26      cubic      beta      '      d3      347.8      d3*coltend4
0      0      0      347.8      d3*dpm 0      347.8      d3*coltend4*dpm      0
0      0      0      0      0      0      347.8      ;
estimate'           Coltend 1      cubic      beta      '      d3      347.8      d3*coltend4
347.8      0      0      0      d3*dpm 173.9      173.9      d3*coltend4*dpm      173.9
173.9      0      0      0      0      0      0      ;
estimate'           Coltend 2      cubic      beta      '      d3      347.8      d3*coltend4
0      347.8      0      0      d3*dpm 173.9      173.9      d3*coltend4*dpm      0
0      173.9      173.9      0      0      0      0      ;
estimate'           Coltend 3      cubic      beta      '      d3      347.8      d3*coltend4
0      0      347.8      0      d3*dpm 173.9      173.9      d3*coltend4*dpm      0
0      0      0      173.9      173.9      0      0      ;
estimate'           Coltend 4      cubic      beta      '      d3      347.8      d3*coltend4
0      0      0      347.8      d3*dpm 173.9      173.9      d3*coltend4*dpm      0
0      0      0      0      0      173.9      173.9      ;
estimate'           12      cubic      beta      '      d3      347.8      d3*coltend4      86.95
86.95      86.95      86.95      d3*dpm 347.8      0      d3*coltend4*dpm      86.95      0
86.95      0      86.95      0      86.95      0      ;
estimate'           26      cubic      beta      '      d3      347.8      d3*coltend4      86.95
86.95      86.95      86.95      d3*dpm 0      347.8      d3*coltend4*dpm      0      86.95
0      86.95      0      86.95      0      86.95      ;
contrast' Coltend1 vs Coltend2      Interceptbeta      '      Intercept0      coltend4
1      -1      0      0      dpm      0      0      coltend4*dpm      0.5      0.5
-0.5      -0.5      0      0      0      0      ;

```

contrast' Coltend1 vs	Coltend3	Intercept	beta	'	Intercept	0	coltend4
1 0	-1 0	dpm	0 0	coltend4*dpm	0.5	0.5	0.5
0 0	-0.5 -0.5	0	0 ;				
contrast' Coltend1 vs	Coltend4	Intercept	beta	'	Intercept	0	coltend4
1 0	0 -1	dpm	0 0	coltend4*dpm	0.5	0.5	0.5
0 0	0 0	-0.5	-0.5 ;				
contrast' Coltend2 vs	Coltend3	Intercept	beta	'	Intercept	0	coltend4
0 1	-1 0	dpm	0 0	coltend4*dpm	0	0	0
0.5 0.5	-0.5 -0.5	0	0 ;				
contrast' Coltend2 vs	Coltend4	Intercept	beta	'	Intercept	0	coltend4
0 1	0 -1	dpm	0 0	coltend4*dpm	0	0	0
0.5 0.5	0 0	-0.5	-0.5 ;				
contrast' Coltend3 vs	Coltend4	Intercept	beta	'	Intercept	0	coltend4
0 0	-1 1	dpm	0 0	coltend4*dpm	0	0	0
0 0	-0.5 -0.5	0.5	0.5 ;				
contrast' 12 vs	26	Intercept	beta	'	Intercept	0	coltend4
0 0	dpm	1 -1	coltend4*dpm	0.25	-0.25	0.25	-0.25
0.25 -0.25	0.25 -0.25						
contrast' 1_12	1_26	Intercept	beta	'	Intercept	0	coltend4
0 0	dpm	1 -1	coltend4*dpm	1	-1	0	0
0 0	0 0						
contrast' 1_12	2_12	Intercept	beta	'	Intercept	0	coltend4
0 0	dpm	0 0	coltend4*dpm	1	0	-1	0
0 0	0 0						
contrast' 1_12	2_26	Intercept	beta	'	Intercept	0	coltend4
0 0	dpm	1 -1	coltend4*dpm	1	0	0	-1
0 0	0 0						
contrast' 1_12	3_12	Intercept	beta	'	Intercept	0	coltend4
-1 0	dpm	0 0	coltend4*dpm	1	0	0	0
-1 0	0 0						
contrast' 1_12	3_26	Intercept	beta	'	Intercept	0	coltend4
-1 0	dpm	1 -1	coltend4*dpm	1	0	0	0
0 -1	0 0						
contrast' 1_12	4_12	Intercept	beta	'	Intercept	0	coltend4
0 -1	dpm	0 0	coltend4*dpm	1	0	0	0
0 0	-1 0						
contrast' 1_12	4_26	Intercept	beta	'	Intercept	0	coltend4
0 -1	dpm	1 -1	coltend4*dpm	1	0	0	0
0 0	0 -1						
contrast' 1_26	2_12	Intercept	beta	'	Intercept	0	coltend4
0 0	dpm	-1 1	coltend4*dpm	0	1	-1	0
0 0	0 0						
contrast' 1_26	2_26	Intercept	beta	'	Intercept	0	coltend4
0 0	dpm	0 0	coltend4*dpm	0	1	0	-1
0 0	0 0						
contrast' 1_26	3_12	Intercept	beta	'	Intercept	0	coltend4
-1 0	dpm	-1 1	coltend4*dpm	0	1	0	0
-1 0	0 0						
contrast' 1_26	3_26	Intercept	beta	'	Intercept	0	coltend4
-1 0	dpm	0 0	coltend4*dpm	0	1	0	0
0 -1	0 0						
contrast' 1_26	4_12	Intercept	beta	'	Intercept	0	coltend4
0 -1	dpm	-1 1	coltend4*dpm	0	1	0	0
0 0	-1 0						

contrast' 1_26	4_26		Intercept	beta	'	Intercept	0	coltend4	1	0
0	-1	dpm	0	0		coltend4*dpm	0	1	0	0
0	0	0	-1		;					
contrast' 2_12	2_26		Intercept	beta	'	Intercept	0	coltend4	0	0
0	0	dpm	1	-1		coltend4*dpm	0	0	1	-1
0	0	0	0		;					
contrast' 2_12	3_12		Intercept	beta	'	Intercept	0	coltend4	0	1
-1	0	dpm	0	0		coltend4*dpm	0	0	1	0
-1	0	0	0		;					
contrast' 2_12	3_26		Intercept	beta	'	Intercept	0	coltend4	0	1
-1	0	dpm	1	-1		coltend4*dpm	0	0	1	0
0	-1	0	0		;					
contrast' 2_12	4_12		Intercept	beta	'	Intercept	0	coltend4	0	1
0	-1	dpm	0	0		coltend4*dpm	0	0	1	0
0	0	-1	0		;					
contrast' 2_12	4_26		Intercept	beta	'	Intercept	0	coltend4	0	1
0	-1	dpm	1	-1		coltend4*dpm	0	0	1	0
0	0	0	-1		;					
contrast' 2_26	3_12		Intercept	beta	'	Intercept	0	coltend4	0	1
-1	0	dpm	-1	1		coltend4*dpm	0	0	0	1
-1	0	0	0		;					
contrast' 2_26	3_26		Intercept	beta	'	Intercept	0	coltend4	0	1
-1	0	dpm	0	0		coltend4*dpm	0	0	0	1
0	-1	0	0		;					
contrast' 2_26	4_12		Intercept	beta	'	Intercept	0	coltend4	0	1
0	-1	dpm	-1	1		coltend4*dpm	0	0	0	1
0	0	-1	0		;					
contrast' 2_26	4_26		Intercept	beta	'	Intercept	0	coltend4	0	1
0	-1	dpm	0	0		coltend4*dpm	0	0	0	1
0	0	0	-1		;					
contrast' 3_12	3_26		Intercept	beta	'	Intercept	0	coltend4	0	0
0	0	dpm	1	-1		coltend4*dpm	0	0	0	0
1	-1	0	0		;					
contrast' 3_12	4_12		Intercept	beta	'	Intercept	0	coltend4	0	0
1	-1	dpm	0	0		coltend4*dpm	0	0	0	0
1	0	-1	0		;					
contrast' 3_12	4_26		Intercept	beta	'	Intercept	0	coltend4	0	0
1	-1	dpm	1	-1		coltend4*dpm	0	0	0	0
1	0	0	-1		;					
contrast' 3_26	4_12		Intercept	beta	'	Intercept	0	coltend4	0	0
1	-1	dpm	-1	1		coltend4*dpm	0	0	0	0
0	1	-1	0		;					
contrast' 3_26	4_26		Intercept	beta	'	Intercept	0	coltend4	0	0
1	-1	dpm	0	0		coltend4*dpm	0	0	0	0
0	1	0	-1		;					
contrast' 4_12	4_26		Intercept	beta	'	Intercept	0	coltend4	0	0
0	0	dpm	1	-1		coltend4*dpm	0	0	0	0
0	0	1	-1		;					
contrast' Coltend1 vs	Coltend2		linear	beta	'	d	0			
d*coltend4	4.6	-4.6	0	0		d*dpm	0	0	d*coltend4*dpm	
2.3	2.3	-2.3	-2.3	0		0	0	0		
contrast' Coltend1 vs	Coltend3		linear	beta	'	d	0			
d*coltend4	4.6	0	-4.6	0		d*dpm	0	0	d*coltend4*dpm	
2.3	2.3	0	0	-2.3		-2.3	0	0		

contrast' Coltend1 vs		Coltend4		linear	beta	'	d	0	
d*coltend4	4.6	0	0	-4.6	d*dpm	0	0	d*coltend4*dpm	
2.3	2.3	0	0	0	-2.3	-2.3	;		
contrast' Coltend2 vs		Coltend3		linear	beta	'	d	0	
d*coltend4	0	4.6	-4.6	0	d*dpm	0	0	d*coltend4*dpm	
0	0	2.3	2.3	-2.3	-2.3	0	0	;	
contrast' Coltend2 vs		Coltend4		linear	beta	'	d	0	
d*coltend4	0	4.6	0	-4.6	d*dpm	0	0	d*coltend4*dpm	
0	0	2.3	2.3	0	0	-2.3	-2.3	;	
contrast' Coltend3 vs		Coltend4		linear	beta	'	d	0	
d*coltend4	0	0	-4.6	4.6	d*dpm	0	0	d*coltend4*dpm	
0	0	0	0	-2.3	-2.3	2.3	2.3	;	
contrast' 12 vs 26				linear	beta	'	d	0	d*coltend4
0	0	0	0	d*dpm	4.6	-4.6	d*coltend4*dpm	1.15	-1.15
-1.15	1.15	-1.15	1.15	-1.15	-1.15	;			0
contrast' 1_12 1_26				linear	beta	'	d	0	d*coltend4
0	0	0	0	d*dpm	4.6	-4.6	d*coltend4*dpm	4.6	-4.6
0	0	0	0	0	0	;			0
contrast' 1_12 2_12				linear	beta	'	d	0	d*coltend4
-4.6	0	0	0	d*dpm	0	0	d*coltend4*dpm	4.6	0
0	0	0	0	0	0	;			-4.6
contrast' 1_12 2_26				linear	beta	'	d	0	d*coltend4
-4.6	0	0	0	d*dpm	4.6	-4.6	d*coltend4*dpm	4.6	0
-4.6	0	0	0	0	0	;			0
contrast' 1_12 3_12				linear	beta	'	d	0	d*coltend4
0	-4.6	0	0	d*dpm	0	0	d*coltend4*dpm	4.6	0
0	-4.6	0	0	0	0	;			0
contrast' 1_12 3_26				linear	beta	'	d	0	d*coltend4
0	-4.6	0	0	d*dpm	4.6	-4.6	d*coltend4*dpm	4.6	0
0	0	-4.6	0	0	0	;			0
contrast' 1_12 4_12				linear	beta	'	d	0	d*coltend4
0	0	-4.6	0	d*dpm	0	0	d*coltend4*dpm	4.6	0
0	0	0	-4.6	0	0	;			0
contrast' 1_12 4_26				linear	beta	'	d	0	d*coltend4
0	0	-4.6	0	d*dpm	4.6	-4.6	d*coltend4*dpm	4.6	0
0	0	0	0	0	-4.6	;			0
contrast' 1_26 2_12				linear	beta	'	d	0	d*coltend4
-4.6	0	0	0	d*dpm	-4.6	4.6	d*coltend4*dpm	0	4.6
0	0	0	0	0	0	;			-4.6
contrast' 1_26 2_26				linear	beta	'	d	0	d*coltend4
-4.6	0	0	0	d*dpm	0	0	d*coltend4*dpm	0	4.6
-4.6	0	0	0	0	0	;			0
contrast' 1_26 3_12				linear	beta	'	d	0	d*coltend4
0	-4.6	0	0	d*dpm	-4.6	4.6	d*coltend4*dpm	0	4.6
0	-4.6	0	0	0	0	;			0
contrast' 1_26 3_26				linear	beta	'	d	0	d*coltend4
0	-4.6	0	0	d*dpm	0	0	d*coltend4*dpm	0	4.6
0	0	-4.6	0	0	0	;			0
contrast' 1_26 4_12				linear	beta	'	d	0	d*coltend4
0	0	-4.6	0	d*dpm	-4.6	4.6	d*coltend4*dpm	0	4.6
0	0	0	-4.6	0	0	;			0
contrast' 1_26 4_26				linear	beta	'	d	0	d*coltend4
0	0	-4.6	0	d*dpm	0	0	d*coltend4*dpm	0	4.6
0	0	0	0	0	-4.6	;			0

```

contrast' 2_12 2_26 linear beta ' d 0 d*coltend4 0
0 0 0 d*dpm 4.6 -4.6 d*coltend4*dpm 0 0 4.6
-4.6 0 0 0 0 ;
contrast' 2_12 3_12 linear beta ' d 0 d*coltend4 0
4.6 -4.6 0 d*dpm 0 0 d*coltend4*dpm 0 0 4.6
0 -4.6 0 0 0 ;
contrast' 2_12 3_26 linear beta ' d 0 d*coltend4 0
4.6 -4.6 0 d*dpm 4.6 -4.6 d*coltend4*dpm 0 0 4.6
0 0 -4.6 0 0 ;
contrast' 2_12 4_12 linear beta ' d 0 d*coltend4 0
4.6 0 -4.6 d*dpm 0 0 d*coltend4*dpm 0 0 4.6
0 0 0 -4.6 0 ;
contrast' 2_12 4_26 linear beta ' d 0 d*coltend4 0
4.6 0 -4.6 d*dpm 4.6 -4.6 d*coltend4*dpm 0 0 4.6
0 0 0 0 -4.6 ;
contrast' 2_26 3_12 linear beta ' d 0 d*coltend4 0
4.6 -4.6 0 d*dpm -4.6 4.6 d*coltend4*dpm 0 0 0
4.6 -4.6 0 0 0 ;
contrast' 2_26 3_26 linear beta ' d 0 d*coltend4 0
4.6 -4.6 0 d*dpm 0 0 d*coltend4*dpm 0 0 0
4.6 0 -4.6 0 0 ;
contrast' 2_26 4_12 linear beta ' d 0 d*coltend4 0
4.6 0 -4.6 d*dpm -4.6 4.6 d*coltend4*dpm 0 0 0
4.6 0 0 -4.6 0 ;
contrast' 2_26 4_26 linear beta ' d 0 d*coltend4 0
4.6 0 -4.6 d*dpm 0 0 d*coltend4*dpm 0 0 0
4.6 0 0 0 -4.6 ;
contrast' 3_12 3_26 linear beta ' d 0 d*coltend4 0
0 0 0 d*dpm 4.6 -4.6 d*coltend4*dpm 0 0 0
0 4.6 -4.6 0 0 ;
contrast' 3_12 4_12 linear beta ' d 0 d*coltend4 0
0 4.6 -4.6 d*dpm 0 0 d*coltend4*dpm 0 0 0
0 4.6 0 -4.6 0 ;
contrast' 3_12 4_26 linear beta ' d 0 d*coltend4 0
0 4.6 -4.6 d*dpm 4.6 -4.6 d*coltend4*dpm 0 0 0
0 4.6 0 0 -4.6 ;
contrast' 3_26 4_12 linear beta ' d 0 d*coltend4 0
0 4.6 -4.6 d*dpm -4.6 4.6 d*coltend4*dpm 0 0 0
0 0 4.6 -4.6 0 ;
contrast' 3_26 4_26 linear beta ' d 0 d*coltend4 0
0 4.6 -4.6 d*dpm 0 0 d*coltend4*dpm 0 0 0
0 0 4.6 0 -4.6 ;
contrast' 4_12 4_26 linear beta ' d 0 d*coltend4 0
0 0 0 d*dpm 4.6 -4.6 d*coltend4*dpm 0 0 0
0 0 0 4.6 -4.6 ;
contrast' Coltend1 vs Coltend2 quadratic beta ' d2 0
d2*coltend4 37.4 -37.4 0 0 d2*dpm 0 0
d2*coltend4*dpm 18.7 18.7 -18.7 -18.7 0 0 0 0
;
contrast' Coltend1 vs Coltend3 quadratic beta ' d2 0
d2*coltend4 37.4 0 -37.4 0 d2*dpm 0 0
d2*coltend4*dpm 18.7 18.7 0 0 -18.7 -18.7 0 0
;
contrast' Coltend1 vs Coltend4 quadratic beta ' d2 0
d2*coltend4 37.4 0 0 -37.4 d2*dpm 0 0

```

```

d2*coltend4*dpm      18.7  18.7  0  0  0  0  0  -18.7  -18.7
;
contrast' Coltend2 vs  Coltend3      quadratic  beta  '  d2  0
d2*coltend4      0  37.4  -37.4  0  d2*dpm  0  0
d2*coltend4*dpm  0  0  18.7  18.7  -18.7  -18.7  0  0
;
contrast' Coltend2 vs  Coltend4      quadratic  beta  '  d2  0
d2*coltend4      0  37.4  0  -37.4  d2*dpm  0  0
d2*coltend4*dpm  0  0  18.7  18.7  0  0  -18.7  -18.7
;
contrast' Coltend3 vs  Coltend4      quadratic  beta  '  d2  0
d2*coltend4      0  0  -37.4  37.4  d2*dpm  0  0
d2*coltend4*dpm  0  0  0  0  -18.7  -18.7  18.7  18.7
;
contrast' 12 vs 26      quadratic  beta  '  d2  0  d2*coltend4
0  0  0  0  d2*dpm  37.4  -37.4  d2*coltend4*dpm  9.35
-9.35  9.35  -9.35  9.35  -9.35  9.35  -9.35  ;
contrast' 1_12 1_26      quadratic  beta  '  d2  0  d2*coltend4
0  0  0  0  d2*dpm  37.4  -37.4  d2*coltend4*dpm  37.4
-37.4  0  0  0  0  0  0  ;
contrast' 1_12 2_12      quadratic  beta  '  d2  0  d2*coltend4
37.4  -37.4  0  0  d2*dpm  0  0  d2*coltend4*dpm  37.4
0  -37.4  0  0  0  0  0  ;
contrast' 1_12 2_26      quadratic  beta  '  d2  0  d2*coltend4
37.4  -37.4  0  0  d2*dpm  37.4  -37.4  d2*coltend4*dpm  37.4
0  0  -37.4  0  0  0  0  ;
contrast' 1_12 3_12      quadratic  beta  '  d2  0  d2*coltend4
37.4  0  -37.4  0  d2*dpm  0  0  d2*coltend4*dpm  37.4
0  0  0  -37.4  0  0  0  ;
contrast' 1_12 3_26      quadratic  beta  '  d2  0  d2*coltend4
37.4  0  -37.4  0  d2*dpm  37.4  -37.4  d2*coltend4*dpm  37.4
0  0  0  0  -37.4  0  0  ;
contrast' 1_12 4_12      quadratic  beta  '  d2  0  d2*coltend4
37.4  0  0  -37.4  d2*dpm  0  0  d2*coltend4*dpm  37.4
0  0  0  0  0  -37.4  0  ;
contrast' 1_12 4_26      quadratic  beta  '  d2  0  d2*coltend4
37.4  0  0  -37.4  d2*dpm  37.4  -37.4  d2*coltend4*dpm  37.4
0  0  0  0  0  0  -37.4  ;
contrast' 1_26 2_12      quadratic  beta  '  d2  0  d2*coltend4
37.4  -37.4  0  0  d2*dpm  -37.4  37.4  d2*coltend4*dpm  0
37.4  -37.4  0  0  0  0  0  ;
contrast' 1_26 2_26      quadratic  beta  '  d2  0  d2*coltend4
37.4  -37.4  0  0  d2*dpm  0  0  d2*coltend4*dpm  0
37.4  0  -37.4  0  0  0  0  ;
contrast' 1_26 3_12      quadratic  beta  '  d2  0  d2*coltend4
37.4  0  -37.4  0  d2*dpm  -37.4  37.4  d2*coltend4*dpm  0
37.4  0  0  -37.4  0  0  0  ;
contrast' 1_26 3_26      quadratic  beta  '  d2  0  d2*coltend4
37.4  0  -37.4  0  d2*dpm  0  0  d2*coltend4*dpm  0
37.4  0  0  0  -37.4  0  0  ;
contrast' 1_26 4_12      quadratic  beta  '  d2  0  d2*coltend4
37.4  0  0  -37.4  d2*dpm  -37.4  37.4  d2*coltend4*dpm  0
37.4  0  0  0  0  -37.4  0  ;
contrast' 1_26 4_26      quadratic  beta  '  d2  0  d2*coltend4
37.4  0  0  -37.4  d2*dpm  0  0  d2*coltend4*dpm  0
37.4  0  0  0  0  0  -37.4  ;

```

```

contrast' 2_12 2_26 quadratic beta ' d2 0 d2*coltend4
0 0 0 0 d2*dpm 37.4 -37.4 d2*coltend4*dpm 0
0 37.4 -37.4 0 0 0 0 ;
contrast' 2_12 3_12 quadratic beta ' d2 0 d2*coltend4
0 37.4 -37.4 0 d2*dpm 0 0 d2*coltend4*dpm 0
0 37.4 0 -37.4 0 0 0 ;
contrast' 2_12 3_26 quadratic beta ' d2 0 d2*coltend4
0 37.4 -37.4 0 d2*dpm 37.4 -37.4 d2*coltend4*dpm 0
0 37.4 0 0 -37.4 0 0 ;
contrast' 2_12 4_12 quadratic beta ' d2 0 d2*coltend4
0 37.4 0 -37.4 d2*dpm 0 0 d2*coltend4*dpm 0
0 37.4 0 0 0 -37.4 0 ;
contrast' 2_12 4_26 quadratic beta ' d2 0 d2*coltend4
0 37.4 0 -37.4 d2*dpm 37.4 -37.4 d2*coltend4*dpm 0
0 37.4 0 0 0 0 -37.4 ;
contrast' 2_26 3_12 quadratic beta ' d2 0 d2*coltend4
0 37.4 -37.4 0 d2*dpm -37.4 37.4 d2*coltend4*dpm 0
0 0 37.4 -37.4 0 0 0 ;
contrast' 2_26 3_26 quadratic beta ' d2 0 d2*coltend4
0 37.4 -37.4 0 d2*dpm 0 0 d2*coltend4*dpm 0
0 0 37.4 0 -37.4 0 0 ;
contrast' 2_26 4_12 quadratic beta ' d2 0 d2*coltend4
0 37.4 0 -37.4 d2*dpm -37.4 37.4 d2*coltend4*dpm 0
0 0 37.4 0 0 -37.4 0 ;
contrast' 2_26 4_26 quadratic beta ' d2 0 d2*coltend4
0 37.4 0 -37.4 d2*dpm 0 0 d2*coltend4*dpm 0
0 0 37.4 0 0 0 -37.4 ;
contrast' 3_12 3_26 quadratic beta ' d2 0 d2*coltend4
0 0 0 0 d2*dpm 37.4 -37.4 d2*coltend4*dpm 0
0 0 0 37.4 -37.4 0 0 ;
contrast' 3_12 4_12 quadratic beta ' d2 0 d2*coltend4
0 0 37.4 -37.4 d2*dpm 0 0 d2*coltend4*dpm 0
0 0 0 37.4 0 -37.4 0 ;
contrast' 3_12 4_26 quadratic beta ' d2 0 d2*coltend4
0 0 37.4 -37.4 d2*dpm 37.4 -37.4 d2*coltend4*dpm 0
0 0 0 37.4 0 0 -37.4 ;
contrast' 3_26 4_12 quadratic beta ' d2 0 d2*coltend4
0 0 37.4 -37.4 d2*dpm -37.4 37.4 d2*coltend4*dpm 0
0 0 0 0 37.4 -37.4 0 ;
contrast' 3_26 4_26 quadratic beta ' d2 0 d2*coltend4
0 0 37.4 -37.4 d2*dpm 0 0 d2*coltend4*dpm 0
0 0 0 0 37.4 0 -37.4 ;
contrast' 4_12 4_26 quadratic beta ' d2 0 d2*coltend4
0 0 0 0 d2*dpm 37.4 -37.4 d2*coltend4*dpm 0
0 0 0 0 0 37.4 -37.4 ;
contrast' Coltend1 vs Coltend2 cubic beta ' d3 0
d3*coltend4 347.8 -347.8 0 0 d3*dpm 0 0
d3*coltend4*dpm 173.9 173.9 -173.9 -173.9 0 0 0 0
;
contrast' Coltend1 vs Coltend3 cubic beta ' d3 0
d3*coltend4 347.8 0 -347.8 0 d3*dpm 0 0
d3*coltend4*dpm 173.9 173.9 0 0 -173.9 -173.9 0 0
;
contrast' Coltend1 vs Coltend4 cubic beta ' d3 0
d3*coltend4 347.8 0 0 -347.8 d3*dpm 0 0

```

```

d3*coltend4*dpm      173.9  173.9  0    0    0    0    0    -173.9 -173.9
;
contrast' Coltend2 vs Coltend3      cubic beta ' d3 0
d3*coltend4      0    347.8 -347.8 0    d3*dpm 0    0
d3*coltend4*dpm      0    0    173.9 173.9 -173.9 -173.9 0    0
;
contrast' Coltend2 vs Coltend4      cubic beta ' d3 0
d3*coltend4      0    347.8 0    -347.8 d3*dpm 0    0
d3*coltend4*dpm      0    0    173.9 173.9 0    0    -173.9 -173.9
;
contrast' Coltend3 vs Coltend4      cubic beta ' d3 0
d3*coltend4      0    0    -347.8 347.8 d3*dpm 0    0
d3*coltend4*dpm      0    0    0    0    -173.9 -173.9 173.9 173.9
;
contrast' 12 vs 26      cubic beta ' d3 0    d3*coltend4 0
0    0    0    d3*dpm 347.8 -347.8 d3*coltend4*dpm 86.95 -86.95
86.95 -86.95 86.95 -86.95 86.95 -86.95 ;
contrast' 1_12 1_26      cubic beta ' d3 0    d3*coltend4 0
0    0    0    d3*dpm 347.8 -347.8 d3*coltend4*dpm 347.8 -347.8
0    0    0    0    0    0 ;
contrast' 1_12 2_12      cubic beta ' d3 0    d3*coltend4 347.8
-347.8 0    0    d3*dpm 0    0    d3*coltend4*dpm 347.8 0
-347.8 0    0    0    0    0 ;
contrast' 1_12 2_26      cubic beta ' d3 0    d3*coltend4 347.8
-347.8 0    0    d3*dpm 347.8 -347.8 d3*coltend4*dpm 347.8 0
0    -347.8 0    0    0    0 ;
contrast' 1_12 3_12      cubic beta ' d3 0    d3*coltend4 347.8
0    -347.8 0    d3*dpm 0    0    d3*coltend4*dpm 347.8 0
0    0    -347.8 0    0    0 ;
contrast' 1_12 3_26      cubic beta ' d3 0    d3*coltend4 347.8
0    -347.8 0    d3*dpm 347.8 -347.8 d3*coltend4*dpm 347.8 0
0    0    0    -347.8 0    0 ;
contrast' 1_12 4_12      cubic beta ' d3 0    d3*coltend4 347.8
0    0    -347.8 d3*dpm 0    0    d3*coltend4*dpm 347.8 0
0    0    0    0    -347.8 0 ;
contrast' 1_12 4_26      cubic beta ' d3 0    d3*coltend4 347.8
0    0    -347.8 d3*dpm 347.8 -347.8 d3*coltend4*dpm 347.8 0
0    0    0    0    0    -347.8 ;
contrast' 1_26 2_12      cubic beta ' d3 0    d3*coltend4 347.8
-347.8 0    0    d3*dpm -347.8 347.8 d3*coltend4*dpm 0    347.8
-347.8 0    0    0    0    0 ;
contrast' 1_26 2_26      cubic beta ' d3 0    d3*coltend4 347.8
-347.8 0    0    d3*dpm 0    0    d3*coltend4*dpm 0    347.8
0    -347.8 0    0    0    0 ;
contrast' 1_26 3_12      cubic beta ' d3 0    d3*coltend4 347.8
0    -347.8 0    d3*dpm -347.8 347.8 d3*coltend4*dpm 0    347.8
0    0    -347.8 0    0    0 ;
contrast' 1_26 3_26      cubic beta ' d3 0    d3*coltend4 347.8
0    -347.8 0    d3*dpm 0    0    d3*coltend4*dpm 0    347.8
0    0    0    -347.8 0    0 ;
contrast' 1_26 4_12      cubic beta ' d3 0    d3*coltend4 347.8
0    0    -347.8 d3*dpm -347.8 347.8 d3*coltend4*dpm 0    347.8
0    0    0    0    -347.8 0 ;
contrast' 1_26 4_26      cubic beta ' d3 0    d3*coltend4 347.8
0    0    -347.8 d3*dpm 0    0    d3*coltend4*dpm 0    347.8
0    0    0    0    0    -347.8 ;

```

```

contrast' 2_12 2_26 cubic beta ' d3 0 d3*coltend4 0
0 0 0 d3*dpm 347.8 -347.8 d3*coltend4*dpm 0 0
347.8 -347.8 0 0 0 0 ;
contrast' 2_12 3_12 cubic beta ' d3 0 d3*coltend4 0
347.8 -347.8 0 d3*dpm 0 0 d3*coltend4*dpm 0 0
347.8 0 -347.8 0 0 0 ;
contrast' 2_12 3_26 cubic beta ' d3 0 d3*coltend4 0
347.8 -347.8 0 d3*dpm 347.8 -347.8 d3*coltend4*dpm 0 0
347.8 0 0 -347.8 0 0 ;
contrast' 2_12 4_12 cubic beta ' d3 0 d3*coltend4 0
347.8 0 -347.8 d3*dpm 0 0 d3*coltend4*dpm 0 0
347.8 0 0 0 -347.8 0 ;
contrast' 2_12 4_26 cubic beta ' d3 0 d3*coltend4 0
347.8 0 -347.8 d3*dpm 347.8 -347.8 d3*coltend4*dpm 0 0
347.8 0 0 0 0 -347.8 ;
contrast' 2_26 3_12 cubic beta ' d3 0 d3*coltend4 0
347.8 -347.8 0 d3*dpm -347.8 347.8 d3*coltend4*dpm 0 0
0 347.8 -347.8 0 0 0 ;
contrast' 2_26 3_26 cubic beta ' d3 0 d3*coltend4 0
347.8 -347.8 0 d3*dpm 0 0 d3*coltend4*dpm 0 0
0 347.8 0 -347.8 0 0 ;
contrast' 2_26 4_12 cubic beta ' d3 0 d3*coltend4 0
347.8 0 -347.8 d3*dpm -347.8 347.8 d3*coltend4*dpm 0 0
0 347.8 0 0 -347.8 0 ;
contrast' 2_26 4_26 cubic beta ' d3 0 d3*coltend4 0
347.8 0 -347.8 d3*dpm 0 0 d3*coltend4*dpm 0 0
0 347.8 0 0 0 -347.8 ;
contrast' 3_12 3_26 cubic beta ' d3 0 d3*coltend4 0
0 0 0 d3*dpm 347.8 -347.8 d3*coltend4*dpm 0 0
0 0 347.8 -347.8 0 0 ;
contrast' 3_12 4_12 cubic beta ' d3 0 d3*coltend4 0
0 347.8 -347.8 d3*dpm 0 0 d3*coltend4*dpm 0 0
0 0 347.8 0 -347.8 0 ;
contrast' 3_12 4_26 cubic beta ' d3 0 d3*coltend4 0
0 347.8 -347.8 d3*dpm 347.8 -347.8 d3*coltend4*dpm 0 0
0 0 347.8 0 0 -347.8 ;
contrast' 3_26 4_12 cubic beta ' d3 0 d3*coltend4 0
0 347.8 -347.8 d3*dpm -347.8 347.8 d3*coltend4*dpm 0 0
0 0 0 347.8 -347.8 0 ;
contrast' 3_26 4_26 cubic beta ' d3 0 d3*coltend4 0
0 347.8 -347.8 d3*dpm 0 0 d3*coltend4*dpm 0 0
0 0 0 347.8 0 -347.8 ;
contrast' 4_12 4_26 cubic beta ' d3 0 d3*coltend4 0
0 0 0 d3*dpm 347.8 -347.8 d3*coltend4*dpm 0 0
0 0 0 0 347.8 -347.8 ;

```

run;

```

data predval; set predval;
if cx <=599 then delete;
trt = catx('_', coltend4, dpm);
run;
proc sort data = predval; by coltend4 d; run;

```

```

proc means data = predval mean ;
by coltend4;

```

```

var pred;
OUTPUT OUT=cluster MEAN=;
run;

proc sgplot data=predval ;
    title ' ';
series x = d y = pred/ group = trt markers name = "series";
*scatter x=d y=pred/ group = dcc2 name="fit" ;
    xaxis label = "Day of display" values=(0 to 11 by 1) ;
    yaxis label = "1* reflectance values" values = (0 to 55 by 5) ;
keylegend "series" / across = 3 noborder location = outside position = bottom ;
*keylegend "fit" / location=outside position=bottomleft;

run;

proc means data = predval mean ;
by coltend4 d;
var pred;
OUTPUT OUT=cluster MEAN=;
run;

proc sgplot data=cluster ;
    title ' ';
series x = d y = pred/ group = coltend4 markers name = "series";
*scatter x=d y=pred/ group = dcc2 name="fit" ;
    xaxis label = "Day of display" values=(0 to 11 by 1) ;
    yaxis label = "1* reflectance values" values = (0 to 50 by 5) ;
keylegend "series" / across = 3 noborder location = outside position = bottom ;
*keylegend "fit" / location=outside position=bottomleft;

run;

proc sort data = predval; by dpm d; run;

proc means data = predval mean ;
by dpm ;
var pred;
OUTPUT OUT=dpm MEAN=;
run;

proc means data = predval mean ;
by dpm d;
var pred;
OUTPUT OUT=dpm MEAN=;
run;

proc sgplot data=dpm ;
    title ' ';
series x = d y = pred/ group = dpm markers name = "series";
    xaxis label = "Day of display" values=(0 to 11 by 1) ;
    yaxis label = "1* reflectance values" values = (0 to 50 by 5) ;
keylegend "series" / across = 3 noborder location = outside position = bottom ;
*keylegend "fit" / location=outside position=bottomleft;

```

run;

```
proc glimmix data = long ;          *noprofile ;
class STK_ID cx trip coltend4 dpm day1;
model astar = coltend4 dpm coltend4*dpm
d coltend4*d dpm*d coltend4*dpm*d
d2 coltend4*d2 dpm*d2 coltend4*dpm*d2
d3 coltend4*d3 dpm*d3 coltend4*dpm*d3
/ solution ddfm = kr ; * ;
random trip(cx) ;
random day1/ TYPE = sp(pow) (day1) sub = STK_ID residual ; * ;
output out =predval predicted = pred;;
lsmeans coltend4*dpm/ e;
estimate '          Coltend 1 12 d 12 Interceptbeta '          Intercept1 coltend4 1
0 0 0 dpm 1 0 coltend4*dpm 1 0 0
0 0 0 0 0 ;
estimate '          Coltend 1 26 Interceptbeta '          Intercept1 coltend4 1
0 0 0 dpm 0 1 coltend4*dpm 0 1 0
0 0 0 0 0 ;
estimate '          Coltend 2 12 Interceptbeta '          Intercept1 coltend4 0
1 0 0 dpm 1 0 coltend4*dpm 0 0 1
0 0 0 0 0 ;
estimate '          Coltend 2 26 Interceptbeta '          Intercept1 coltend4 0
1 0 0 dpm 0 1 coltend4*dpm 0 0 0
1 0 0 0 0 ;
estimate '          Coltend3 12 Interceptbeta '          Intercept1 coltend4 0
0 1 0 dpm 1 0 coltend4*dpm 0 0 0
0 1 0 0 0 ;
estimate '          Coltend 3 26 Interceptbeta '          Intercept1 coltend4 0
0 1 0 dpm 0 1 coltend4*dpm 0 0 0
0 0 1 0 0 ;
estimate '          Coltend4 12 Interceptbeta '          Intercept1 coltend4 0
0 0 1 dpm 1 0 coltend4*dpm 0 0 0
0 0 0 1 0 ;
estimate '          Coltend 4 26 Interceptbeta '          Intercept1 coltend4 0
0 0 1 dpm 0 1 coltend4*dpm 0 0 0
0 0 0 0 1 ;
estimate '          Coltend 1 Interceptbeta '          Intercept1 coltend4 1
0 0 0 dpm 0.5 0.5 coltend4*dpm 0.5 0.5 0
0 0 0 0 0 ;
estimate '          Coltend 2 Interceptbeta '          Intercept1 coltend4 0
1 0 0 dpm 0.5 0.5 coltend4*dpm 0 0 0.5
0.5 0 0 0 0 ;
estimate '          Coltend 3 Interceptbeta '          Intercept1 coltend4 0
0 1 0 dpm 0.5 0.5 coltend4*dpm 0 0 0
0 0.5 0.5 0 0 ;
estimate '          Coltend 4 Interceptbeta '          Intercept1 coltend4 0
0 0 1 dpm 0.5 0.5 coltend4*dpm 0 0 0
0 0 0 0.5 0.5 ;
estimate '          12 Interceptbeta '          Intercept1 coltend4 0.25 0.25
0.25 0.25 dpm 1 0 coltend4*dpm 0.25 0 0.25 0
0.25 0 0.25 0 ;
```



```

estimate '          26 Interceptbeta ' Intercept1 coltend4 0.25 0.25
         0.25 0.25 dpm 0 1 coltend4*dpm 0 0.25 0 0.25
         0 0.25 0 0.25 ;

estimate ' Coltend 1 12 d 12 linear beta ' d 4.6 d*coltend4
         4.6 0 0 0 d*dpm 4.6 0 d*coltend4*dpm 4.6 0
         0 0 0 0 0 0 ;
estimate ' Coltend 1 26 linear beta ' d 4.6 d*coltend4
         4.6 0 0 0 d*dpm 0 4.6 d*coltend4*dpm 0 4.6
         0 0 0 0 0 0 ;
estimate ' Coltend 2 12 linear beta ' d 4.6 d*coltend4
         0 4.6 0 0 d*dpm 4.6 0 d*coltend4*dpm 0 0
         4.6 0 0 0 0 0 ;
estimate ' Coltend 2 26 linear beta ' d 4.6 d*coltend4
         0 4.6 0 0 d*dpm 0 4.6 d*coltend4*dpm 0 0
         0 4.6 0 0 0 0 ;
estimate ' Coltend3 12 linear beta ' d 4.6 d*coltend4
         0 0 4.6 0 d*dpm 4.6 0 d*coltend4*dpm 0 0
         0 0 4.6 0 0 0 ;
estimate ' Coltend 3 26 linear beta ' d 4.6 d*coltend4
         0 0 4.6 0 d*dpm 0 4.6 d*coltend4*dpm 0 0
         0 0 0 4.6 0 0 ;
estimate ' Coltend4 12 linear beta ' d 4.6 d*coltend4
         0 0 0 4.6 d*dpm 4.6 0 d*coltend4*dpm 0 0
         0 0 0 0 4.6 0 ;
estimate ' Coltend 4 26 linear beta ' d 4.6 d*coltend4
         0 0 0 4.6 d*dpm 0 4.6 d*coltend4*dpm 0 0
         0 0 0 0 0 4.6 ;
estimate ' Coltend 1 linear beta ' d 4.6 d*coltend4
         4.6 0 0 0 d*dpm 2.3 2.3 d*coltend4*dpm 2.3 2.3
         0 0 0 0 0 0 ;
estimate ' Coltend 2 linear beta ' d 4.6 d*coltend4
         0 4.6 0 0 d*dpm 2.3 2.3 d*coltend4*dpm 0 0
         2.3 2.3 0 0 0 0 ;
estimate ' Coltend 3 linear beta ' d 4.6 d*coltend4
         0 0 4.6 0 d*dpm 2.3 2.3 d*coltend4*dpm 0 0
         0 0 2.3 2.3 0 0 ;
estimate ' Coltend 4 linear beta ' d 4.6 d*coltend4
         0 0 0 4.6 d*dpm 2.3 2.3 d*coltend4*dpm 0 0
         0 0 0 0 2.3 2.3 ;
estimate ' 12 linear beta ' d 4.6 d*coltend4 1.15
         1.15 1.15 1.15 d*dpm 4.6 0 d*coltend4*dpm 1.15 0 1.15
         0 1.15 0 1.15 0 ;
estimate ' 26 linear beta ' d 4.6 d*coltend4 1.15
         1.15 1.15 1.15 d*dpm 0 4.6 d*coltend4*dpm 0 1.15 0
         1.15 0 1.15 0 1.15 ;

estimate ' Coltend 1 12 d 12 quadratic beta ' d2 37.4
         d2*coltend4 37.4 0 0 0 d2*dpm 37.4 0
         d2*coltend4*dpm 37.4 0 0 0 0 0 0 0 0
;

```

```

estimate '      Coltend 1      26      quadratic      beta      '      d2      37.4
          d2*coltend4      37.4      0      0      0      d2*dpm      0      37.4
          d2*coltend4*dpm      0      37.4      0      0      0      0      0
;
estimate '      Coltend 2      12      quadratic      beta      '      d2      37.4
          d2*coltend4      0      37.4      0      0      d2*dpm      37.4      0
          d2*coltend4*dpm      0      0      37.4      0      0      0      0      0
;
estimate '      Coltend 2      26      quadratic      beta      '      d2      37.4
          d2*coltend4      0      37.4      0      0      d2*dpm      0      37.4
          d2*coltend4*dpm      0      0      0      37.4      0      0      0      0
;
estimate '      Coltend3      12      quadratic      beta      '      d2      37.4
          d2*coltend4      0      0      37.4      0      d2*dpm      37.4      0
          d2*coltend4*dpm      0      0      0      0      0      37.4      0      0
;
estimate '      Coltend 3      26      quadratic      beta      '      d2      37.4
          d2*coltend4      0      0      37.4      0      d2*dpm      0      37.4
          d2*coltend4*dpm      0      0      0      0      0      0      37.4      0      0
;
estimate '      Coltend4      12      quadratic      beta      '      d2      37.4
          d2*coltend4      0      0      0      37.4      d2*dpm      37.4      0
          d2*coltend4*dpm      0      0      0      0      0      0      0      37.4      0
;
estimate '      Coltend 4      26      quadratic      beta      '      d2      37.4
          d2*coltend4      0      0      0      37.4      d2*dpm      0      37.4
          d2*coltend4*dpm      0      0      0      0      0      0      0      0      37.4
;
estimate '      Coltend 1      quadratic      beta      '      d2      37.4
          d2*coltend4      37.4      0      0      0      d2*dpm      18.7      18.7
          d2*coltend4*dpm      18.7      18.7      0      0      0      0      0      0      0
;
estimate '      Coltend 2      quadratic      beta      '      d2      37.4
          d2*coltend4      0      37.4      0      0      d2*dpm      18.7      18.7
          d2*coltend4*dpm      0      0      18.7      18.7      0      0      0      0      0
;
estimate '      Coltend 3      quadratic      beta      '      d2      37.4
          d2*coltend4      0      0      37.4      0      d2*dpm      18.7      18.7
          d2*coltend4*dpm      0      0      0      0      0      18.7      18.7      0      0
;
estimate '      Coltend 4      quadratic      beta      '      d2      37.4
          d2*coltend4      0      0      0      37.4      d2*dpm      18.7      18.7
          d2*coltend4*dpm      0      0      0      0      0      0      0      18.7      18.7
;
estimate '      12      quadratic      beta      '      d2      37.4      d2*coltend4
          9.35      9.35      9.35      9.35      d2*dpm      37.4      0      d2*coltend4*dpm      9.35
          0      9.35      0      9.35      0      9.35      0      ;
estimate '      26      quadratic      beta      '      d2      37.4      d2*coltend4
          9.35      9.35      9.35      9.35      d2*dpm      0      37.4      d2*coltend4*dpm      0
          9.35      0      9.35      0      9.35      0      9.35      ;
;
estimate '      Coltend 1 12 d      12      cubic      beta      '      d3      347.8      d3*coltend4
          347.8      0      0      0      d3*dpm      347.8      0      d3*coltend4*dpm      347.8
          0      0      0      0      0      0      0      ;

```

estimate	'	Coltend 1	26	cubic	beta	'	d3	347.8	d3*coltend4	
		347.8	0	0	0	d3*dpm	0	347.8	d3*coltend4*dpm	0
		347.8	0	0	0	0	0	0	;	
estimate	'	Coltend 2	12	cubic	beta	'	d3	347.8	d3*coltend4	
		0	347.8	0	0	d3*dpm	347.8	0	d3*coltend4*dpm	0
		0	347.8	0	0	0	0	0	;	
estimate	'	Coltend 2	26	cubic	beta	'	d3	347.8	d3*coltend4	
		0	347.8	0	0	d3*dpm	0	347.8	d3*coltend4*dpm	0
		0	0	347.8	0	0	0	0	;	
estimate	'	Coltend3	12	cubic	beta	'	d3	347.8	d3*coltend4	
		0	0	347.8	0	d3*dpm	347.8	0	d3*coltend4*dpm	0
		0	0	0	347.8	0	0	0	;	
estimate	'	Coltend 3	26	cubic	beta	'	d3	347.8	d3*coltend4	
		0	0	347.8	0	d3*dpm	0	347.8	d3*coltend4*dpm	0
		0	0	0	0	347.8	0	0	;	
estimate	'	Coltend4	12	cubic	beta	'	d3	347.8	d3*coltend4	
		0	0	0	347.8	d3*dpm	347.8	0	d3*coltend4*dpm	0
		0	0	0	0	0	347.8	0	;	
estimate	'	Coltend 4	26	cubic	beta	'	d3	347.8	d3*coltend4	
		0	0	0	347.8	d3*dpm	0	347.8	d3*coltend4*dpm	0
		0	0	0	0	0	0	347.8	;	
estimate	'	Coltend 1		cubic	beta	'	d3	347.8	d3*coltend4	
		347.8	0	0	0	d3*dpm	173.9	173.9	d3*coltend4*dpm	173.9
		173.9	0	0	0	0	0	0	;	
estimate	'	Coltend 2		cubic	beta	'	d3	347.8	d3*coltend4	
		0	347.8	0	0	d3*dpm	173.9	173.9	d3*coltend4*dpm	0
		0	173.9	173.9	0	0	0	0	;	
estimate	'	Coltend 3		cubic	beta	'	d3	347.8	d3*coltend4	
		0	0	347.8	0	d3*dpm	173.9	173.9	d3*coltend4*dpm	0
		0	0	0	173.9	173.9	0	0	;	
estimate	'	Coltend 4		cubic	beta	'	d3	347.8	d3*coltend4	
		0	0	0	347.8	d3*dpm	173.9	173.9	d3*coltend4*dpm	0
		0	0	0	0	0	173.9	173.9	;	
estimate	'		12	cubic	beta	'	d3	347.8	d3*coltend4	86.95
		86.95	86.95	86.95	d3*dpm	347.8	0	d3*coltend4*dpm	86.95	0
		86.95	0	86.95	0	86.95	0	;		
estimate	'		26	cubic	beta	'	d3	347.8	d3*coltend4	86.95
		86.95	86.95	86.95	d3*dpm	0	347.8	d3*coltend4*dpm	0	86.95
		0	86.95	0	86.95	0	86.95	;		
contrast	'	Coltend1 vs	Coltend2		Intercept	beta	'	Intercept	0	coltend4
		1	-1	0	dpm	0	0	coltend4*dpm	0.5	0.5
		-0.5	-0.5	0	0	0	0	;		
contrast	'	Coltend1 vs	Coltend3		Intercept	beta	'	Intercept	0	coltend4
		1	0	-1	dpm	0	0	coltend4*dpm	0.5	0.5
		0	0	-0.5	0	0	0	;		
contrast	'	Coltend1 vs	Coltend4		Intercept	beta	'	Intercept	0	coltend4
		1	0	0	dpm	0	0	coltend4*dpm	0.5	0.5
		0	0	0	-0.5	-0.5	;			
contrast	'	Coltend2 vs	Coltend3		Intercept	beta	'	Intercept	0	coltend4
		0	1	-1	dpm	0	0	coltend4*dpm	0	0
		0.5	0.5	-0.5	0	0	;			
contrast	'	Coltend2 vs	Coltend4		Intercept	beta	'	Intercept	0	coltend4
		0	1	0	dpm	0	0	coltend4*dpm	0	0
		0.5	0.5	0	0	-0.5	-0.5	;		

contrast'	Coltend3 vs	Coltend4	Intercept	beta	'	Intercept	0	coltend4
	0	0	-1	1	dpm	0	0	coltend4*dpm
	0	0	-0.5	-0.5	0.5	0.5	;	
contrast'	12 vs	26	Intercept	beta	'	Intercept	0	coltend4
	0	0	dpm	1	-1	coltend4*dpm	0.25	-0.25
	0.25	-0.25	0.25	-0.25	;		0.25	-0.25
contrast'	1_12	1_26	Intercept	beta	'	Intercept	0	coltend4
	0	0	dpm	1	-1	coltend4*dpm	1	-1
	0	0	0	0	;		0	0
contrast'	1_12	2_12	Intercept	beta	'	Intercept	0	coltend4
	0	0	dpm	0	0	coltend4*dpm	1	0
	0	0	0	0	;		-1	-1
contrast'	1_12	2_26	Intercept	beta	'	Intercept	0	coltend4
	0	0	dpm	1	-1	coltend4*dpm	1	0
	0	0	0	0	;		0	0
contrast'	1_12	3_12	Intercept	beta	'	Intercept	0	coltend4
	-1	0	dpm	0	0	coltend4*dpm	1	0
	-1	0	0	0	;		0	0
contrast'	1_12	3_26	Intercept	beta	'	Intercept	0	coltend4
	-1	0	dpm	1	-1	coltend4*dpm	1	0
	0	-1	0	0	;		0	0
contrast'	1_12	4_12	Intercept	beta	'	Intercept	0	coltend4
	0	-1	dpm	0	0	coltend4*dpm	1	0
	0	0	-1	0	;		0	0
contrast'	1_12	4_26	Intercept	beta	'	Intercept	0	coltend4
	0	-1	dpm	1	-1	coltend4*dpm	1	0
	0	0	0	-1	;		0	0
contrast'	1_26	2_12	Intercept	beta	'	Intercept	0	coltend4
	0	0	dpm	-1	1	coltend4*dpm	0	1
	0	0	0	0	;		-1	-1
contrast'	1_26	2_26	Intercept	beta	'	Intercept	0	coltend4
	0	0	dpm	0	0	coltend4*dpm	0	1
	0	0	0	0	;		0	0
contrast'	1_26	3_12	Intercept	beta	'	Intercept	0	coltend4
	-1	0	dpm	-1	1	coltend4*dpm	0	1
	-1	0	0	0	;		0	0
contrast'	1_26	3_26	Intercept	beta	'	Intercept	0	coltend4
	-1	0	dpm	0	0	coltend4*dpm	0	1
	0	-1	0	0	;		0	0
contrast'	1_26	4_12	Intercept	beta	'	Intercept	0	coltend4
	0	-1	dpm	-1	1	coltend4*dpm	0	1
	0	0	-1	0	;		0	0
contrast'	1_26	4_26	Intercept	beta	'	Intercept	0	coltend4
	0	-1	dpm	0	0	coltend4*dpm	0	1
	0	0	0	-1	;		0	0
contrast'	2_12	2_26	Intercept	beta	'	Intercept	0	coltend4
	0	0	dpm	1	-1	coltend4*dpm	0	0
	0	0	0	0	;		0	1
contrast'	2_12	3_12	Intercept	beta	'	Intercept	0	coltend4
	-1	0	dpm	0	0	coltend4*dpm	0	0
	-1	0	0	0	;		0	1
contrast'	2_12	3_26	Intercept	beta	'	Intercept	0	coltend4
	-1	0	dpm	1	-1	coltend4*dpm	0	0
	0	-1	0	0	;		0	1

contrast' 2_12	4_12		Intercept	beta	'	Intercept	0	coltend4	0	1
0	-1	dpm	0	0		coltend4*dpm	0	0	1	0
0	0	-1	0		;					
contrast' 2_12	4_26		Intercept	beta	'	Intercept	0	coltend4	0	1
0	-1	dpm	1	-1		coltend4*dpm	0	0	1	0
0	0	0	-1		;					
contrast' 2_26	3_12		Intercept	beta	'	Intercept	0	coltend4	0	1
-1	0	dpm	-1	1		coltend4*dpm	0	0	0	1
-1	0	0	0		;					
contrast' 2_26	3_26		Intercept	beta	'	Intercept	0	coltend4	0	1
-1	0	dpm	0	0		coltend4*dpm	0	0	0	1
0	-1	0	0		;					
contrast' 2_26	4_12		Intercept	beta	'	Intercept	0	coltend4	0	1
0	-1	dpm	-1	1		coltend4*dpm	0	0	0	1
0	0	-1	0		;					
contrast' 2_26	4_26		Intercept	beta	'	Intercept	0	coltend4	0	1
0	-1	dpm	0	0		coltend4*dpm	0	0	0	1
0	0	0	-1		;					
contrast' 3_12	3_26		Intercept	beta	'	Intercept	0	coltend4	0	0
0	0	dpm	1	-1		coltend4*dpm	0	0	0	0
1	-1	0	0		;					
contrast' 3_12	4_12		Intercept	beta	'	Intercept	0	coltend4	0	0
1	-1	dpm	0	0		coltend4*dpm	0	0	0	0
1	0	-1	0		;					
contrast' 3_12	4_26		Intercept	beta	'	Intercept	0	coltend4	0	0
1	-1	dpm	1	-1		coltend4*dpm	0	0	0	0
1	0	0	-1		;					
contrast' 3_26	4_12		Intercept	beta	'	Intercept	0	coltend4	0	0
1	-1	dpm	-1	1		coltend4*dpm	0	0	0	0
0	1	-1	0		;					
contrast' 3_26	4_26		Intercept	beta	'	Intercept	0	coltend4	0	0
1	-1	dpm	0	0		coltend4*dpm	0	0	0	0
0	1	0	-1		;					
contrast' 4_12	4_26		Intercept	beta	'	Intercept	0	coltend4	0	0
0	0	dpm	1	-1		coltend4*dpm	0	0	0	0
0	0	1	-1		;					
contrast' Coltend1 vs	Coltend2		linear	beta	'	d	0			
d*coltend4	4.6	-4.6	0	0		d*dpm	0	0	d*coltend4*dpm	
2.3	2.3	-2.3	-2.3	0		0	0	0		
contrast' Coltend1 vs	Coltend3		linear	beta	'	d	0			
d*coltend4	4.6	0	-4.6	0		d*dpm	0	0	d*coltend4*dpm	
2.3	2.3	0	0	-2.3		-2.3	0	0		
contrast' Coltend1 vs	Coltend4		linear	beta	'	d	0			
d*coltend4	4.6	0	0	-4.6		d*dpm	0	0	d*coltend4*dpm	
2.3	2.3	0	0	0		0	-2.3	-2.3		
contrast' Coltend2 vs	Coltend3		linear	beta	'	d	0			
d*coltend4	0	4.6	-4.6	0		d*dpm	0	0	d*coltend4*dpm	
0	0	2.3	2.3	-2.3		-2.3	0	0		
contrast' Coltend2 vs	Coltend4		linear	beta	'	d	0			
d*coltend4	0	4.6	0	-4.6		d*dpm	0	0	d*coltend4*dpm	
0	0	2.3	2.3	0		0	-2.3	-2.3		
contrast' Coltend3 vs	Coltend4		linear	beta	'	d	0			
d*coltend4	0	0	-4.6	4.6		d*dpm	0	0	d*coltend4*dpm	
0	0	0	0	-2.3		-2.3	2.3	2.3		

contrast' 12 vs	26		linear	beta	'	d	0	d*coltend4	0
	0	0	d*dpm	4.6	-4.6	d*coltend4*dpm	1.15	-1.15	1.15
	-1.15	1.15		1.15	-1.15				
contrast' 1_12	1_26		linear	beta	'	d	0	d*coltend4	0
	0	0	d*dpm	4.6	-4.6	d*coltend4*dpm	4.6	-4.6	0
	0	0		0	0				
contrast' 1_12	2_12		linear	beta	'	d	0	d*coltend4	4.6
	-4.6	0	d*dpm	0	0	d*coltend4*dpm	4.6	0	-4.6
	0	0		0	0				
contrast' 1_12	2_26		linear	beta	'	d	0	d*coltend4	4.6
	-4.6	0	d*dpm	4.6	-4.6	d*coltend4*dpm	4.6	0	0
	-4.6	0		0	0				
contrast' 1_12	3_12		linear	beta	'	d	0	d*coltend4	4.6
	0	-4.6	d*dpm	0	0	d*coltend4*dpm	4.6	0	0
	0	-4.6		0	0				
contrast' 1_12	3_26		linear	beta	'	d	0	d*coltend4	4.6
	0	-4.6	d*dpm	4.6	-4.6	d*coltend4*dpm	4.6	0	0
	0	0		0	0				
contrast' 1_12	4_12		linear	beta	'	d	0	d*coltend4	4.6
	0	0	d*dpm	0	0	d*coltend4*dpm	4.6	0	0
	0	-4.6		-4.6	0				
contrast' 1_12	4_26		linear	beta	'	d	0	d*coltend4	4.6
	0	0	d*dpm	4.6	-4.6	d*coltend4*dpm	4.6	0	0
	0	0		0	-4.6				
contrast' 1_26	2_12		linear	beta	'	d	0	d*coltend4	4.6
	-4.6	0	d*dpm	-4.6	4.6	d*coltend4*dpm	0	4.6	-4.6
	0	0		0	0				
contrast' 1_26	2_26		linear	beta	'	d	0	d*coltend4	4.6
	-4.6	0	d*dpm	0	0	d*coltend4*dpm	0	4.6	0
	-4.6	0		0	0				
contrast' 1_26	3_12		linear	beta	'	d	0	d*coltend4	4.6
	0	-4.6	d*dpm	-4.6	4.6	d*coltend4*dpm	0	4.6	0
	0	-4.6		0	0				
contrast' 1_26	3_26		linear	beta	'	d	0	d*coltend4	4.6
	0	-4.6	d*dpm	0	0	d*coltend4*dpm	0	4.6	0
	0	0		0	0				
contrast' 1_26	4_12		linear	beta	'	d	0	d*coltend4	4.6
	0	0	d*dpm	-4.6	4.6	d*coltend4*dpm	0	4.6	0
	0	0		-4.6	0				
contrast' 1_26	4_26		linear	beta	'	d	0	d*coltend4	4.6
	0	0	d*dpm	0	0	d*coltend4*dpm	0	4.6	0
	0	0		0	-4.6				
contrast' 2_12	2_26		linear	beta	'	d	0	d*coltend4	0
	0	0	d*dpm	4.6	-4.6	d*coltend4*dpm	0	0	4.6
	-4.6	0		0	0				
contrast' 2_12	3_12		linear	beta	'	d	0	d*coltend4	0
	4.6	-4.6	d*dpm	0	0	d*coltend4*dpm	0	0	4.6
	0	-4.6		0	0				
contrast' 2_12	3_26		linear	beta	'	d	0	d*coltend4	0
	4.6	-4.6	d*dpm	4.6	-4.6	d*coltend4*dpm	0	0	4.6
	0	0		0	0				
contrast' 2_12	4_12		linear	beta	'	d	0	d*coltend4	0
	4.6	0	d*dpm	0	0	d*coltend4*dpm	0	0	4.6
	0	0		-4.6	0				

```

contrast' 2_12 4_26 linear beta ' d 0 d*coltend4 0
4.6 0 -4.6 d*dpm 4.6 -4.6 d*coltend4*dpm 0 0 4.6
0 0 0 0 -4.6 ;
contrast' 2_26 3_12 linear beta ' d 0 d*coltend4 0
4.6 -4.6 0 d*dpm -4.6 4.6 d*coltend4*dpm 0 0 0
4.6 -4.6 0 0 0 ;
contrast' 2_26 3_26 linear beta ' d 0 d*coltend4 0
4.6 -4.6 0 d*dpm 0 0 d*coltend4*dpm 0 0 0
4.6 0 -4.6 0 0 ;
contrast' 2_26 4_12 linear beta ' d 0 d*coltend4 0
4.6 0 -4.6 d*dpm -4.6 4.6 d*coltend4*dpm 0 0 0
4.6 0 0 -4.6 0 ;
contrast' 2_26 4_26 linear beta ' d 0 d*coltend4 0
4.6 0 -4.6 d*dpm 0 0 d*coltend4*dpm 0 0 0
4.6 0 0 -4.6 ;
contrast' 3_12 3_26 linear beta ' d 0 d*coltend4 0
0 0 0 d*dpm 4.6 -4.6 d*coltend4*dpm 0 0 0
0 4.6 -4.6 0 0 ;
contrast' 3_12 4_12 linear beta ' d 0 d*coltend4 0
0 4.6 -4.6 d*dpm 0 0 d*coltend4*dpm 0 0 0
0 4.6 0 -4.6 0 ;
contrast' 3_12 4_26 linear beta ' d 0 d*coltend4 0
0 4.6 -4.6 d*dpm 4.6 -4.6 d*coltend4*dpm 0 0 0
0 4.6 0 0 -4.6 ;
contrast' 3_26 4_12 linear beta ' d 0 d*coltend4 0
0 4.6 -4.6 d*dpm -4.6 4.6 d*coltend4*dpm 0 0 0
0 0 4.6 -4.6 0 ;
contrast' 3_26 4_26 linear beta ' d 0 d*coltend4 0
0 4.6 -4.6 d*dpm 0 0 d*coltend4*dpm 0 0 0
0 0 4.6 0 -4.6 ;
contrast' 4_12 4_26 linear beta ' d 0 d*coltend4 0
0 0 0 d*dpm 4.6 -4.6 d*coltend4*dpm 0 0 0
0 0 0 4.6 -4.6 ;
contrast' Coltend1 vs Coltend2 quadratic beta ' d2 0
d2*coltend4 37.4 -37.4 0 0 d2*dpm 0 0
d2*coltend4*dpm 18.7 18.7 -18.7 -18.7 0 0 0 0
;
contrast' Coltend1 vs Coltend3 quadratic beta ' d2 0
d2*coltend4 37.4 0 -37.4 0 d2*dpm 0 0
d2*coltend4*dpm 18.7 18.7 0 0 -18.7 -18.7 0 0
;
contrast' Coltend1 vs Coltend4 quadratic beta ' d2 0
d2*coltend4 37.4 0 0 -37.4 d2*dpm 0 0
d2*coltend4*dpm 18.7 18.7 0 0 0 0 -18.7 -18.7
;
contrast' Coltend2 vs Coltend3 quadratic beta ' d2 0
d2*coltend4 0 37.4 -37.4 0 d2*dpm 0 0
d2*coltend4*dpm 0 0 18.7 18.7 -18.7 -18.7 0 0
;
contrast' Coltend2 vs Coltend4 quadratic beta ' d2 0
d2*coltend4 0 37.4 0 -37.4 d2*dpm 0 0
d2*coltend4*dpm 0 0 18.7 18.7 0 0 -18.7 -18.7
;
contrast' Coltend3 vs Coltend4 quadratic beta ' d2 0
d2*coltend4 0 0 -37.4 37.4 d2*dpm 0 0

```

```

d2*coltend4*dpm      0      0      0      0      -18.7  -18.7  18.7  18.7
;
contrast' 12 vs 26      quadratic      beta      '      d2      0      d2*coltend4
0      0      0      0      d2*dpm 37.4  -37.4  d2*coltend4*dpm      9.35
-9.35  9.35  -9.35  9.35  -9.35  9.35  -9.35
;
contrast' 1_12 1_26      quadratic      beta      '      d2      0      d2*coltend4
0      0      0      0      d2*dpm 37.4  -37.4  d2*coltend4*dpm      37.4
-37.4  0      0      0      0      0      0
;
contrast' 1_12 2_12      quadratic      beta      '      d2      0      d2*coltend4
37.4  -37.4  0      0      d2*dpm 0      0      d2*coltend4*dpm      37.4
0      -37.4  0      0      0      0      0
;
contrast' 1_12 2_26      quadratic      beta      '      d2      0      d2*coltend4
37.4  -37.4  0      0      d2*dpm 37.4  -37.4  d2*coltend4*dpm      37.4
0      0      -37.4  0      0      0      0
;
contrast' 1_12 3_12      quadratic      beta      '      d2      0      d2*coltend4
37.4  0      -37.4  0      d2*dpm 0      0      d2*coltend4*dpm      37.4
0      0      0      -37.4  0      0      0
;
contrast' 1_12 3_26      quadratic      beta      '      d2      0      d2*coltend4
37.4  0      -37.4  0      d2*dpm 37.4  -37.4  d2*coltend4*dpm      37.4
0      0      0      0      -37.4  0      0
;
contrast' 1_12 4_12      quadratic      beta      '      d2      0      d2*coltend4
37.4  0      0      -37.4  d2*dpm 0      0      d2*coltend4*dpm      37.4
0      0      0      0      0      -37.4  0
;
contrast' 1_12 4_26      quadratic      beta      '      d2      0      d2*coltend4
37.4  0      0      -37.4  d2*dpm 37.4  -37.4  d2*coltend4*dpm      37.4
0      0      0      0      0      0      -37.4
;
contrast' 1_26 2_12      quadratic      beta      '      d2      0      d2*coltend4
37.4  -37.4  0      0      d2*dpm -37.4  37.4  d2*coltend4*dpm      0
37.4  -37.4  0      0      0      0      0
;
contrast' 1_26 2_26      quadratic      beta      '      d2      0      d2*coltend4
37.4  -37.4  0      0      d2*dpm 0      0      d2*coltend4*dpm      0
37.4  0      -37.4  0      0      0      0
;
contrast' 1_26 3_12      quadratic      beta      '      d2      0      d2*coltend4
37.4  0      -37.4  0      d2*dpm -37.4  37.4  d2*coltend4*dpm      0
37.4  0      0      -37.4  0      0      0
;
contrast' 1_26 3_26      quadratic      beta      '      d2      0      d2*coltend4
37.4  0      -37.4  0      d2*dpm 0      0      d2*coltend4*dpm      0
37.4  0      0      -37.4  0      0      0
;
contrast' 1_26 4_12      quadratic      beta      '      d2      0      d2*coltend4
37.4  0      0      -37.4  d2*dpm -37.4  37.4  d2*coltend4*dpm      0
37.4  0      0      0      0      -37.4  0
;
contrast' 1_26 4_26      quadratic      beta      '      d2      0      d2*coltend4
37.4  0      0      -37.4  d2*dpm 0      0      d2*coltend4*dpm      0
37.4  0      0      0      0      0      -37.4
;
contrast' 2_12 2_26      quadratic      beta      '      d2      0      d2*coltend4
0      0      0      0      d2*dpm 37.4  -37.4  d2*coltend4*dpm      0
0      37.4  -37.4  0      0      0      0
;
contrast' 2_12 3_12      quadratic      beta      '      d2      0      d2*coltend4
0      37.4  -37.4  0      d2*dpm 0      0      d2*coltend4*dpm      0
0      37.4  0      -37.4  0      0      0
;
contrast' 2_12 3_26      quadratic      beta      '      d2      0      d2*coltend4
0      37.4  -37.4  0      d2*dpm 37.4  -37.4  d2*coltend4*dpm      0
0      37.4  0      0      -37.4  0      0
;
contrast' 2_12 4_12      quadratic      beta      '      d2      0      d2*coltend4
0      37.4  0      -37.4  d2*dpm 0      0      d2*coltend4*dpm      0
0      37.4  0      0      0      -37.4  0

```



```

contrast' 2_12 4_26 quadratic beta ' d2 0 d2*coltend4
0 37.4 0 -37.4 d2*dpm 37.4 -37.4 d2*coltend4*dpm 0
0 37.4 0 0 0 0 -37.4 ;
contrast' 2_26 3_12 quadratic beta ' d2 0 d2*coltend4
0 37.4 -37.4 0 d2*dpm -37.4 37.4 d2*coltend4*dpm 0
0 0 37.4 -37.4 0 0 0 ;
contrast' 2_26 3_26 quadratic beta ' d2 0 d2*coltend4
0 37.4 -37.4 0 d2*dpm 0 0 d2*coltend4*dpm 0
0 0 37.4 0 -37.4 0 0 ;
contrast' 2_26 4_12 quadratic beta ' d2 0 d2*coltend4
0 37.4 0 -37.4 d2*dpm -37.4 37.4 d2*coltend4*dpm 0
0 0 37.4 0 0 -37.4 0 ;
contrast' 2_26 4_26 quadratic beta ' d2 0 d2*coltend4
0 37.4 0 -37.4 d2*dpm 0 0 d2*coltend4*dpm 0
0 0 37.4 0 0 0 -37.4 ;
contrast' 3_12 3_26 quadratic beta ' d2 0 d2*coltend4
0 0 0 0 d2*dpm 37.4 -37.4 d2*coltend4*dpm 0
0 0 0 37.4 -37.4 0 0 ;
contrast' 3_12 4_12 quadratic beta ' d2 0 d2*coltend4
0 0 37.4 -37.4 d2*dpm 0 0 d2*coltend4*dpm 0
0 0 0 37.4 0 -37.4 0 ;
contrast' 3_12 4_26 quadratic beta ' d2 0 d2*coltend4
0 0 37.4 -37.4 d2*dpm 37.4 -37.4 d2*coltend4*dpm 0
0 0 0 37.4 0 0 -37.4 ;
contrast' 3_26 4_12 quadratic beta ' d2 0 d2*coltend4
0 0 37.4 -37.4 d2*dpm -37.4 37.4 d2*coltend4*dpm 0
0 0 0 0 37.4 -37.4 0 ;
contrast' 3_26 4_26 quadratic beta ' d2 0 d2*coltend4
0 0 37.4 -37.4 d2*dpm 0 0 d2*coltend4*dpm 0
0 0 0 0 37.4 0 -37.4 ;
contrast' 4_12 4_26 quadratic beta ' d2 0 d2*coltend4
0 0 0 0 d2*dpm 37.4 -37.4 d2*coltend4*dpm 0
0 0 0 0 0 37.4 -37.4 ;
contrast' Coltend1 vs Coltend2 cubic beta ' d3 0
d3*coltend4 347.8 -347.8 0 0 d3*dpm 0 0
d3*coltend4*dpm 173.9 173.9 -173.9 -173.9 0 0 0 0
;
contrast' Coltend1 vs Coltend3 cubic beta ' d3 0
d3*coltend4 347.8 0 -347.8 0 d3*dpm 0 0
d3*coltend4*dpm 173.9 173.9 0 0 -173.9 -173.9 0 0
;
contrast' Coltend1 vs Coltend4 cubic beta ' d3 0
d3*coltend4 347.8 0 0 -347.8 d3*dpm 0 0
d3*coltend4*dpm 173.9 173.9 0 0 0 0 -173.9 -173.9
;
contrast' Coltend2 vs Coltend3 cubic beta ' d3 0
d3*coltend4 0 347.8 -347.8 0 d3*dpm 0 0
d3*coltend4*dpm 0 0 173.9 173.9 -173.9 -173.9 0 0
;
contrast' Coltend2 vs Coltend4 cubic beta ' d3 0
d3*coltend4 0 347.8 0 -347.8 d3*dpm 0 0
d3*coltend4*dpm 0 0 173.9 173.9 0 0 -173.9 -173.9
;
contrast' Coltend3 vs Coltend4 cubic beta ' d3 0
d3*coltend4 0 0 -347.8 347.8 d3*dpm 0 0

```

	d3*coltend4*dpm	0	0	0	0	-173.9	-173.9	173.9	173.9
;									
contrast' 12 vs	26		cubic	beta	'	d3	0	d3*coltend4	0
	0	0	d3*dpm	347.8	-347.8	d3*coltend4*dpm	86.95	-86.95	
	86.95	-86.95	86.95	-86.95	86.95	-86.95	;		
contrast' 1_12	1_26		cubic	beta	'	d3	0	d3*coltend4	0
	0	0	d3*dpm	347.8	-347.8	d3*coltend4*dpm	347.8	-347.8	
	0	0	0	0	0	;			
contrast' 1_12	2_12		cubic	beta	'	d3	0	d3*coltend4	347.8
	-347.8	0	d3*dpm	0	0	d3*coltend4*dpm	347.8	0	
	-347.8	0	0	0	0	;			
contrast' 1_12	2_26		cubic	beta	'	d3	0	d3*coltend4	347.8
	-347.8	0	d3*dpm	347.8	-347.8	d3*coltend4*dpm	347.8	0	
	0	-347.8	0	0	0	;			
contrast' 1_12	3_12		cubic	beta	'	d3	0	d3*coltend4	347.8
	0	-347.8	d3*dpm	0	0	d3*coltend4*dpm	347.8	0	
	0	0	0	0	0	;			
contrast' 1_12	3_26		cubic	beta	'	d3	0	d3*coltend4	347.8
	0	-347.8	d3*dpm	347.8	-347.8	d3*coltend4*dpm	347.8	0	
	0	0	-347.8	0	0	;			
contrast' 1_12	4_12		cubic	beta	'	d3	0	d3*coltend4	347.8
	0	0	d3*dpm	0	0	d3*coltend4*dpm	347.8	0	
	0	-347.8	0	-347.8	0	;			
contrast' 1_12	4_26		cubic	beta	'	d3	0	d3*coltend4	347.8
	0	0	d3*dpm	347.8	-347.8	d3*coltend4*dpm	347.8	0	
	0	-347.8	0	0	-347.8	;			
contrast' 1_26	2_12		cubic	beta	'	d3	0	d3*coltend4	347.8
	-347.8	0	d3*dpm	-347.8	347.8	d3*coltend4*dpm	0	347.8	
	-347.8	0	0	0	0	;			
contrast' 1_26	2_26		cubic	beta	'	d3	0	d3*coltend4	347.8
	-347.8	0	d3*dpm	0	0	d3*coltend4*dpm	0	347.8	
	0	-347.8	0	0	0	;			
contrast' 1_26	3_12		cubic	beta	'	d3	0	d3*coltend4	347.8
	0	-347.8	d3*dpm	-347.8	347.8	d3*coltend4*dpm	0	347.8	
	0	0	0	0	0	;			
contrast' 1_26	3_26		cubic	beta	'	d3	0	d3*coltend4	347.8
	0	-347.8	d3*dpm	0	0	d3*coltend4*dpm	0	347.8	
	0	0	-347.8	0	0	;			
contrast' 1_26	4_12		cubic	beta	'	d3	0	d3*coltend4	347.8
	0	0	d3*dpm	-347.8	347.8	d3*coltend4*dpm	0	347.8	
	0	0	0	-347.8	0	;			
contrast' 1_26	4_26		cubic	beta	'	d3	0	d3*coltend4	347.8
	0	0	d3*dpm	0	0	d3*coltend4*dpm	0	347.8	
	0	0	0	0	-347.8	;			
contrast' 2_12	2_26		cubic	beta	'	d3	0	d3*coltend4	0
	0	0	d3*dpm	347.8	-347.8	d3*coltend4*dpm	0	0	
	347.8	-347.8	0	0	0	;			
contrast' 2_12	3_12		cubic	beta	'	d3	0	d3*coltend4	0
	347.8	-347.8	d3*dpm	0	0	d3*coltend4*dpm	0	0	
	347.8	0	-347.8	0	0	;			
contrast' 2_12	3_26		cubic	beta	'	d3	0	d3*coltend4	0
	347.8	-347.8	d3*dpm	347.8	-347.8	d3*coltend4*dpm	0	0	
	347.8	0	-347.8	0	0	;			
contrast' 2_12	4_12		cubic	beta	'	d3	0	d3*coltend4	0
	347.8	0	d3*dpm	0	0	d3*coltend4*dpm	0	0	
	347.8	0	0	-347.8	0	;			

```

contrast' 2_12 4_26 cubic beta ' d3 0 d3*coltend4 0
          347.8 0 -347.8 d3*dpm 347.8 -347.8 d3*coltend4*dpm 0 0
          347.8 0 0 0 0 -347.8 ;
contrast' 2_26 3_12 cubic beta ' d3 0 d3*coltend4 0
          347.8 -347.8 0 d3*dpm -347.8 347.8 d3*coltend4*dpm 0 0
          0 347.8 -347.8 0 0 0 ;
contrast' 2_26 3_26 cubic beta ' d3 0 d3*coltend4 0
          347.8 -347.8 0 d3*dpm 0 0 d3*coltend4*dpm 0 0
          0 347.8 0 -347.8 0 0 ;
contrast' 2_26 4_12 cubic beta ' d3 0 d3*coltend4 0
          347.8 0 -347.8 d3*dpm -347.8 347.8 d3*coltend4*dpm 0 0
          0 347.8 0 0 -347.8 0 ;
contrast' 2_26 4_26 cubic beta ' d3 0 d3*coltend4 0
          347.8 0 -347.8 d3*dpm 0 0 d3*coltend4*dpm 0 0
          0 347.8 0 0 -347.8 ;
contrast' 3_12 3_26 cubic beta ' d3 0 d3*coltend4 0
          0 0 0 d3*dpm 347.8 -347.8 d3*coltend4*dpm 0 0
          0 0 347.8 -347.8 0 0 ;
contrast' 3_12 4_12 cubic beta ' d3 0 d3*coltend4 0
          0 347.8 -347.8 d3*dpm 0 0 d3*coltend4*dpm 0 0
          0 0 347.8 0 -347.8 0 ;
contrast' 3_12 4_26 cubic beta ' d3 0 d3*coltend4 0
          0 347.8 -347.8 d3*dpm 347.8 -347.8 d3*coltend4*dpm 0 0
          0 0 347.8 0 0 -347.8 ;
contrast' 3_26 4_12 cubic beta ' d3 0 d3*coltend4 0
          0 347.8 -347.8 d3*dpm -347.8 347.8 d3*coltend4*dpm 0 0
          0 0 0 347.8 -347.8 0 ;
contrast' 3_26 4_26 cubic beta ' d3 0 d3*coltend4 0
          0 347.8 -347.8 d3*dpm 0 0 d3*coltend4*dpm 0 0
          0 0 0 347.8 0 -347.8 ;
contrast' 4_12 4_26 cubic beta ' d3 0 d3*coltend4 0
          0 0 0 d3*dpm 347.8 -347.8 d3*coltend4*dpm 0 0
          0 0 0 0 347.8 -347.8 ;

```

run;

```

data predval; set predval;
if cx <=599 then delete;
trt = catx('_', coltend4, dpm);
run;
proc sort data = predval; by coltend4 d; run;

```

```

proc means data = predval mean ;
by coltend4;
var pred;
OUTPUT OUT=cluster MEAN=;
run;

```

```

proc sgplot data=predval ;
title ' ';
series x = d y = pred/ group = trt markers name = "series";
*scatter x=d y=pred/ group = dcc2 name="fit" ;
axis label = "Day of display" values=(0 to 11 by 1) ;
yaxis label = "a* reflectance values" values = (0 to 50 by 5) ;
keylegend "series" / across = 3 noborder location = outside position = bottom ;
*keylegend "fit" / location=outside position=bottomleft;

```

```
run;
```

```
proc means data = predval mean ;  
by coltend4 d;  
var pred;  
OUTPUT OUT=cluster MEAN=;  
run;
```

```
proc sgplot data=cluster ;  
title ' ';  
series x = d y = pred/ group = coltend4 markers name = "series";  
*scatter x=d y=pred/ group = dcc2 name="fit" ;  
xaxis label = "Day of display" values=(0 to 11 by 1) ;  
yaxis label = "a* reflectance values" values = (0 to 50 by 5) ;  
keylegend "series" / across = 3 noborder location = outside position = bottom ;  
*keylegend "fit" / location=outside position=bottomleft;
```

```
run;
```

```
proc sort data = predval; by dpm d; run;
```

```
proc means data = predval mean ;  
by dpm ;  
var pred;  
OUTPUT OUT=dpm MEAN=;  
run;
```

```
proc means data = predval mean ;  
by dpm d;  
var pred;  
OUTPUT OUT=dpm MEAN=;  
run;
```

```
proc sgplot data=dpm ;  
title ' ';  
series x = d y = pred/ group = dpm markers name = "series";  
xaxis label = "Day of display" values=(0 to 11 by 1) ;  
yaxis label = "a* reflectance values" values = (0 to 50 by 5) ;  
keylegend "series" / across = 3 noborder location = outside position = bottom ;  
*keylegend "fit" / location=outside position=bottomleft;
```

```
run;
```

```
proc glimmix data = long ; *noprofile ;  
class STK_ID cx trip coltend4 dpm day1;  
model bstar = coltend4 dpm coltend4*dpm  
d coltend4*d dpm*d coltend4*dpm*d  
d2 coltend4*d2 dpm*d2 coltend4*dpm*d2  
d3 coltend4*d3 dpm*d3 coltend4*dpm*d3  
/ solution ddfm = kr ; * ;  
random trip(cx) ;
```

```

random day1/ TYPE = sp(pow) (day1) sub = STK_ID residual ; * ;
output out =predval predicted = pred;;
lsmeans coltend4*dpm/ e;
estimate '      Coltend 1 12 d  12  Interceptbeta  '      Intercept1      coltend4 1
          0      0      0      dpm  1      0      coltend4*dpm  1      0      0
          0      0      0      0      0      ;
estimate '      Coltend 1      26  Interceptbeta  '      Intercept1      coltend4 1
          0      0      0      dpm  0      1      coltend4*dpm  0      1      0
          0      0      0      0      0      ;
estimate '      Coltend 2      12  Interceptbeta  '      Intercept1      coltend4 0
          1      0      0      dpm  1      0      coltend4*dpm  0      0      1
          0      0      0      0      0      ;
estimate '      Coltend 2      26  Interceptbeta  '      Intercept1      coltend4 0
          1      0      0      dpm  0      1      coltend4*dpm  0      0      0
          1      0      0      0      0      ;
estimate '      Coltend3      12  Interceptbeta  '      Intercept1      coltend4 0
          0      1      0      dpm  1      0      coltend4*dpm  0      0      0
          0      1      0      0      0      ;
estimate '      Coltend 3      26  Interceptbeta  '      Intercept1      coltend4 0
          0      1      0      dpm  0      1      coltend4*dpm  0      0      0
          0      0      1      0      0      ;
estimate '      Coltend4      12  Interceptbeta  '      Intercept1      coltend4 0
          0      0      1      dpm  1      0      coltend4*dpm  0      0      0
          0      0      0      1      0      ;
estimate '      Coltend 4      26  Interceptbeta  '      Intercept1      coltend4 0
          0      0      1      dpm  0      1      coltend4*dpm  0      0      0
          0      0      0      0      1      ;
estimate '      Coltend 1      Interceptbeta  '      Intercept1      coltend4 1
          0      0      0      dpm  0.5  0.5  coltend4*dpm  0.5  0.5  0
          0      0      0      0      0      ;
estimate '      Coltend 2      Interceptbeta  '      Intercept1      coltend4 0
          1      0      0      dpm  0.5  0.5  coltend4*dpm  0      0      0.5
          0.5  0      0      0      0      ;
estimate '      Coltend 3      Interceptbeta  '      Intercept1      coltend4 0
          0      1      0      dpm  0.5  0.5  coltend4*dpm  0      0      0
          0      0.5  0.5  0      0      ;
estimate '      Coltend 4      Interceptbeta  '      Intercept1      coltend4 0
          0      0      1      dpm  0.5  0.5  coltend4*dpm  0      0      0
          0      0      0      0.5  0.5  ;
estimate '      12  Interceptbeta  '      Intercept1      coltend4 0.25  0.25
          0.25  0.25  dpm  1      0      coltend4*dpm  0.25  0      0.25  0
          0.25  0      0.25  0      ;
estimate '      26  Interceptbeta  '      Intercept1      coltend4 0.25  0.25
          0.25  0.25  dpm  0      1      coltend4*dpm  0      0.25  0      0.25
          0      0.25  0      0.25  ;

estimate '      Coltend 1 12 d  12  linear  beta  '      d      4.6  d*coltend4
          4.6  0      0      0      d*dpm  4.6  0      d*coltend4*dpm  4.6  0
          0      0      0      0      0      0      ;
estimate '      Coltend 1      26  linear  beta  '      d      4.6  d*coltend4
          4.6  0      0      0      d*dpm  0      4.6  d*coltend4*dpm  0      4.6
          0      0      0      0      0      0      ;

```

```

estimate '      Coltend 2      12      linear  beta      '      d      4.6      d*coltend4
          0      4.6      0      0      d*dpm  4.6      0      d*coltend4*dpm 0      0
          4.6      0      0      0      0      0      ;
estimate '      Coltend 2      26      linear  beta      '      d      4.6      d*coltend4
          0      4.6      0      0      d*dpm  0      4.6      d*coltend4*dpm 0      0
          0      4.6      0      0      0      0      ;
estimate '      Coltend3      12      linear  beta      '      d      4.6      d*coltend4
          0      0      4.6      0      d*dpm  4.6      0      d*coltend4*dpm 0      0
          0      0      4.6      0      0      0      ;
estimate '      Coltend 3      26      linear  beta      '      d      4.6      d*coltend4
          0      0      4.6      0      d*dpm  0      4.6      d*coltend4*dpm 0      0
          0      0      0      4.6      0      0      ;
estimate '      Coltend4      12      linear  beta      '      d      4.6      d*coltend4
          0      0      0      4.6      d*dpm  4.6      0      d*coltend4*dpm 0      0
          0      0      0      0      4.6      0      ;
estimate '      Coltend 4      26      linear  beta      '      d      4.6      d*coltend4
          0      0      0      4.6      d*dpm  0      4.6      d*coltend4*dpm 0      0
          0      0      0      0      0      4.6      ;
estimate '      Coltend 1      linear  beta      '      d      4.6      d*coltend4
          4.6      0      0      0      d*dpm  2.3      2.3      d*coltend4*dpm 2.3      2.3
          0      0      0      0      0      0      ;
estimate '      Coltend 2      linear  beta      '      d      4.6      d*coltend4
          0      4.6      0      0      d*dpm  2.3      2.3      d*coltend4*dpm 0      0
          2.3      2.3      0      0      0      0      ;
estimate '      Coltend 3      linear  beta      '      d      4.6      d*coltend4
          0      0      4.6      0      d*dpm  2.3      2.3      d*coltend4*dpm 0      0
          0      0      2.3      2.3      0      0      ;
estimate '      Coltend 4      linear  beta      '      d      4.6      d*coltend4
          0      0      0      4.6      d*dpm  2.3      2.3      d*coltend4*dpm 0      0
          0      0      0      0      2.3      2.3      ;
estimate '      12      linear  beta      '      d      4.6      d*coltend4      1.15
          1.15      1.15      1.15      d*dpm  4.6      0      d*coltend4*dpm 1.15      0      1.15
          0      1.15      0      1.15      0      ;
estimate '      26      linear  beta      '      d      4.6      d*coltend4      1.15
          1.15      1.15      1.15      d*dpm  0      4.6      d*coltend4*dpm 0      1.15      0
          1.15      0      1.15      0      1.15      ;

estimate '      Coltend 1 12 d      12      quadratic  beta      '      d2      37.4
          d2*coltend4      37.4      0      0      0      d2*dpm  37.4      0
          d2*coltend4*dpm      37.4      0      0      0      0      0      0      0
;
estimate '      Coltend 1      26      quadratic  beta      '      d2      37.4
          d2*coltend4      37.4      0      0      0      d2*dpm  0      37.4
          d2*coltend4*dpm      0      37.4      0      0      0      0      0      0
;
estimate '      Coltend 2      12      quadratic  beta      '      d2      37.4
          d2*coltend4      0      37.4      0      0      d2*dpm  37.4      0
          d2*coltend4*dpm      0      0      37.4      0      0      0      0      0
;
estimate '      Coltend 2      26      quadratic  beta      '      d2      37.4
          d2*coltend4      0      37.4      0      0      d2*dpm  0      37.4
          d2*coltend4*dpm      0      0      0      37.4      0      0      0      0
;

```

```

estimate '      Coltend3      12      quadratic      beta      '      d2      37.4
      d2*coltend4      0      0      37.4      0      d2*dpm 37.4      0
      d2*coltend4*dpm      0      0      0      0      0      37.4      0      0      0
;
estimate '      Coltend 3      26      quadratic      beta      '      d2      37.4
      d2*coltend4      0      0      37.4      0      d2*dpm 0      37.4
      d2*coltend4*dpm      0      0      0      0      0      0      37.4      0      0
;
estimate '      Coltend4      12      quadratic      beta      '      d2      37.4
      d2*coltend4      0      0      0      37.4      d2*dpm 37.4      0
      d2*coltend4*dpm      0      0      0      0      0      0      0      37.4      0
;
estimate '      Coltend 4      26      quadratic      beta      '      d2      37.4
      d2*coltend4      0      0      0      37.4      d2*dpm 0      37.4
      d2*coltend4*dpm      0      0      0      0      0      0      0      0      37.4
;
estimate '      Coltend 1      quadratic      beta      '      d2      37.4
      d2*coltend4      37.4      0      0      0      d2*dpm 18.7      18.7
      d2*coltend4*dpm      18.7      18.7      0      0      0      0      0      0      0
;
estimate '      Coltend 2      quadratic      beta      '      d2      37.4
      d2*coltend4      0      37.4      0      0      d2*dpm 18.7      18.7
      d2*coltend4*dpm      0      0      0      18.7      18.7      0      0      0      0
;
estimate '      Coltend 3      quadratic      beta      '      d2      37.4
      d2*coltend4      0      0      37.4      0      d2*dpm 18.7      18.7
      d2*coltend4*dpm      0      0      0      0      0      18.7      18.7      0      0
;
estimate '      Coltend 4      quadratic      beta      '      d2      37.4
      d2*coltend4      0      0      0      37.4      d2*dpm 18.7      18.7
      d2*coltend4*dpm      0      0      0      0      0      0      0      18.7      18.7
;
estimate '      12      quadratic      beta      '      d2      37.4      d2*coltend4
      9.35      9.35      9.35      9.35      d2*dpm 37.4      0      d2*coltend4*dpm      9.35
      0      9.35      0      9.35      0      9.35      0      ;
estimate '      26      quadratic      beta      '      d2      37.4      d2*coltend4
      9.35      9.35      9.35      9.35      d2*dpm 0      37.4      d2*coltend4*dpm      0
      9.35      0      9.35      0      9.35      0      9.35      ;
;
estimate '      Coltend 1 12 d      12      cubic      beta      '      d3      347.8      d3*coltend4
      347.8      0      0      0      d3*dpm 347.8      0      d3*coltend4*dpm      347.8
      0      0      0      0      0      0      0      ;
estimate '      Coltend 1      26      cubic      beta      '      d3      347.8      d3*coltend4
      347.8      0      0      0      d3*dpm 0      347.8      d3*coltend4*dpm      0
      347.8      0      0      0      0      0      0      ;
estimate '      Coltend 2      12      cubic      beta      '      d3      347.8      d3*coltend4
      0      347.8      0      0      d3*dpm 347.8      0      d3*coltend4*dpm      0
      0      347.8      0      0      0      0      0      ;
estimate '      Coltend 2      26      cubic      beta      '      d3      347.8      d3*coltend4
      0      347.8      0      0      d3*dpm 0      347.8      d3*coltend4*dpm      0
      0      0      347.8      0      0      0      0      ;
estimate '      Coltend3      12      cubic      beta      '      d3      347.8      d3*coltend4
      0      0      347.8      0      d3*dpm 347.8      0      d3*coltend4*dpm      0
      0      0      0      347.8      0      0      0      ;

```

```

estimate '      Coltend 3      26      cubic      beta      '      d3      347.8      d3*coltend4
          0      0      347.8      0      d3*dpm 0      347.8      d3*coltend4*dpm      0
          0      0      0      0      347.8      0      0      ;
estimate '      Coltend4      12      cubic      beta      '      d3      347.8      d3*coltend4
          0      0      0      347.8      d3*dpm 347.8      0      d3*coltend4*dpm      0
          0      0      0      0      0      347.8      0      ;
estimate '      Coltend 4      26      cubic      beta      '      d3      347.8      d3*coltend4
          0      0      0      347.8      d3*dpm 0      347.8      d3*coltend4*dpm      0
          0      0      0      0      0      0      347.8      ;
estimate '      Coltend 1      cubic      beta      '      d3      347.8      d3*coltend4
          347.8      0      0      0      d3*dpm 173.9      173.9      d3*coltend4*dpm      173.9
          173.9      0      0      0      0      0      0      ;
estimate '      Coltend 2      cubic      beta      '      d3      347.8      d3*coltend4
          0      347.8      0      0      d3*dpm 173.9      173.9      d3*coltend4*dpm      0
          0      173.9      173.9      0      0      0      0      ;
estimate '      Coltend 3      cubic      beta      '      d3      347.8      d3*coltend4
          0      0      347.8      0      d3*dpm 173.9      173.9      d3*coltend4*dpm      0
          0      0      0      173.9      173.9      0      0      ;
estimate '      Coltend 4      cubic      beta      '      d3      347.8      d3*coltend4
          0      0      0      347.8      d3*dpm 173.9      173.9      d3*coltend4*dpm      0
          0      0      0      0      0      173.9      173.9      ;
estimate '      12      cubic      beta      '      d3      347.8      d3*coltend4      86.95
          86.95      86.95      86.95      d3*dpm 347.8      0      d3*coltend4*dpm      86.95      0
          86.95      0      86.95      0      86.95      0      ;
estimate '      26      cubic      beta      '      d3      347.8      d3*coltend4      86.95
          86.95      86.95      86.95      d3*dpm 0      347.8      d3*coltend4*dpm      0      86.95
          0      86.95      0      86.95      0      86.95      ;
contrast' Coltend1 vs Coltend2      Interceptbeta      '      Intercept0      coltend4
          1      -1      0      0      dpm      0      0      coltend4*dpm      0.5      0.5
          -0.5      -0.5      0      0      0      0      ;
contrast' Coltend1 vs Coltend3      Interceptbeta      '      Intercept0      coltend4
          1      0      -1      0      dpm      0      0      coltend4*dpm      0.5      0.5
          0      0      -0.5      -0.5      0      0      ;
contrast' Coltend1 vs Coltend4      Interceptbeta      '      Intercept0      coltend4
          1      0      0      -1      dpm      0      0      coltend4*dpm      0.5      0.5
          0      0      0      0      -0.5      -0.5      ;
contrast' Coltend2 vs Coltend3      Interceptbeta      '      Intercept0      coltend4
          0      1      -1      0      dpm      0      0      coltend4*dpm      0      0
          0.5      0.5      -0.5      -0.5      0      0      ;
contrast' Coltend2 vs Coltend4      Interceptbeta      '      Intercept0      coltend4
          0      1      0      -1      dpm      0      0      coltend4*dpm      0      0
          0.5      0.5      0      0      -0.5      -0.5      ;
contrast' Coltend3 vs Coltend4      Interceptbeta      '      Intercept0      coltend4
          0      0      -1      1      dpm      0      0      coltend4*dpm      0      0
          0      0      -0.5      -0.5      0.5      0.5      ;
contrast' 12 vs 26      Interceptbeta      '      Intercept0      coltend4      0      0
          0      0      dpm      1      -1      coltend4*dpm      0.25      -0.25      0.25      -0.25
          0.25      -0.25      0.25      -0.25      ;
contrast' 1_12 1_26      Interceptbeta      '      Intercept0      coltend4      0      0
          0      0      dpm      1      -1      coltend4*dpm      1      -1      0      0
          0      0      0      0      ;
contrast' 1_12 2_12      Interceptbeta      '      Intercept0      coltend4      1      -1
          0      0      dpm      0      0      coltend4*dpm      1      0      -1      0
          0      0      0      0      ;

```



```

contrast' 1_12 2_26 Interceptbeta ' Intercept0 coltend4 1 -1
      0 0 dpm 1 -1 coltend4*dpm 1 0 0 -1
      0 0 0 0 ;
contrast' 1_12 3_12 Interceptbeta ' Intercept0 coltend4 1 0
      -1 0 dpm 0 0 coltend4*dpm 1 0 0 0
      -1 0 0 0 ;
contrast' 1_12 3_26 Interceptbeta ' Intercept0 coltend4 1 0
      -1 0 dpm 1 -1 coltend4*dpm 1 0 0 0
      0 -1 0 0 ;
contrast' 1_12 4_12 Interceptbeta ' Intercept0 coltend4 1 0
      0 -1 dpm 0 0 coltend4*dpm 1 0 0 0
      0 0 -1 0 ;
contrast' 1_12 4_26 Interceptbeta ' Intercept0 coltend4 1 0
      0 -1 dpm 1 -1 coltend4*dpm 1 0 0 0
      0 0 0 -1 ;
contrast' 1_26 2_12 Interceptbeta ' Intercept0 coltend4 1 -1
      0 0 dpm -1 1 coltend4*dpm 0 1 -1 0
      0 0 0 0 ;
contrast' 1_26 2_26 Interceptbeta ' Intercept0 coltend4 1 -1
      0 0 dpm 0 0 coltend4*dpm 0 1 0 -1
      0 0 0 0 ;
contrast' 1_26 3_12 Interceptbeta ' Intercept0 coltend4 1 0
      -1 0 dpm -1 1 coltend4*dpm 0 1 0 0
      -1 0 0 0 ;
contrast' 1_26 3_26 Interceptbeta ' Intercept0 coltend4 1 0
      -1 0 dpm 0 0 coltend4*dpm 0 1 0 0
      0 -1 0 0 ;
contrast' 1_26 4_12 Interceptbeta ' Intercept0 coltend4 1 0
      0 -1 dpm -1 1 coltend4*dpm 0 1 0 0
      0 0 -1 0 ;
contrast' 1_26 4_26 Interceptbeta ' Intercept0 coltend4 1 0
      0 -1 dpm 0 0 coltend4*dpm 0 1 0 0
      0 0 0 -1 ;
contrast' 2_12 2_26 Interceptbeta ' Intercept0 coltend4 0 0
      0 0 dpm 1 -1 coltend4*dpm 0 0 1 -1
      0 0 0 0 ;
contrast' 2_12 3_12 Interceptbeta ' Intercept0 coltend4 0 1
      -1 0 dpm 0 0 coltend4*dpm 0 0 1 0
      -1 0 0 0 ;
contrast' 2_12 3_26 Interceptbeta ' Intercept0 coltend4 0 1
      -1 0 dpm 1 -1 coltend4*dpm 0 0 1 0
      0 -1 0 0 ;
contrast' 2_12 4_12 Interceptbeta ' Intercept0 coltend4 0 1
      0 -1 dpm 0 0 coltend4*dpm 0 0 1 0
      0 0 -1 0 ;
contrast' 2_12 4_26 Interceptbeta ' Intercept0 coltend4 0 1
      0 -1 dpm 1 -1 coltend4*dpm 0 0 1 0
      0 0 0 -1 ;
contrast' 2_26 3_12 Interceptbeta ' Intercept0 coltend4 0 1
      -1 0 dpm -1 1 coltend4*dpm 0 0 0 1
      -1 0 0 0 ;
contrast' 2_26 3_26 Interceptbeta ' Intercept0 coltend4 0 1
      -1 0 dpm 0 0 coltend4*dpm 0 0 0 1
      0 -1 0 0 ;

```

contrast' 2_26	4_12		Intercept	beta	'	Intercept	0	coltend4	0	1
0	-1	dpm	-1	1		coltend4*dpm	0	0	0	1
0	0	-1	0		;					
contrast' 2_26	4_26		Intercept	beta	'	Intercept	0	coltend4	0	1
0	-1	dpm	0	0		coltend4*dpm	0	0	0	1
0	0	0	-1		;					
contrast' 3_12	3_26		Intercept	beta	'	Intercept	0	coltend4	0	0
0	0	dpm	1	-1		coltend4*dpm	0	0	0	0
1	-1	0	0		;					
contrast' 3_12	4_12		Intercept	beta	'	Intercept	0	coltend4	0	0
1	-1	dpm	0	0		coltend4*dpm	0	0	0	0
1	0	-1	0		;					
contrast' 3_12	4_26		Intercept	beta	'	Intercept	0	coltend4	0	0
1	-1	dpm	1	-1		coltend4*dpm	0	0	0	0
1	0	0	-1		;					
contrast' 3_26	4_12		Intercept	beta	'	Intercept	0	coltend4	0	0
1	-1	dpm	-1	1		coltend4*dpm	0	0	0	0
0	1	-1	0		;					
contrast' 3_26	4_26		Intercept	beta	'	Intercept	0	coltend4	0	0
1	-1	dpm	0	0		coltend4*dpm	0	0	0	0
0	1	0	-1		;					
contrast' 4_12	4_26		Intercept	beta	'	Intercept	0	coltend4	0	0
0	0	dpm	1	-1		coltend4*dpm	0	0	0	0
0	0	1	-1		;					
contrast' Coltend1 vs	Coltend2		linear	beta	'	d	0			
d*coltend4	4.6	-4.6	0	0		d*dpm	0	0	d*coltend4*dpm	
2.3	2.3	-2.3	-2.3	0		0	0	0		
contrast' Coltend1 vs	Coltend3		linear	beta	'	d	0			
d*coltend4	4.6	0	-4.6	0		d*dpm	0	0	d*coltend4*dpm	
2.3	2.3	0	0	-2.3		-2.3	0	0		
contrast' Coltend1 vs	Coltend4		linear	beta	'	d	0			
d*coltend4	4.6	0	0	-4.6		d*dpm	0	0	d*coltend4*dpm	
2.3	2.3	0	0	0		0	-2.3	-2.3		
contrast' Coltend2 vs	Coltend3		linear	beta	'	d	0			
d*coltend4	0	4.6	-4.6	0		d*dpm	0	0	d*coltend4*dpm	
0	0	2.3	2.3	-2.3		-2.3	0	0		
contrast' Coltend2 vs	Coltend4		linear	beta	'	d	0			
d*coltend4	0	4.6	0	-4.6		d*dpm	0	0	d*coltend4*dpm	
0	0	2.3	2.3	0		0	-2.3	-2.3		
contrast' Coltend3 vs	Coltend4		linear	beta	'	d	0			
d*coltend4	0	0	-4.6	4.6		d*dpm	0	0	d*coltend4*dpm	
0	0	0	0	-2.3		-2.3	2.3	2.3		
contrast' 12 vs	26		linear	beta	'	d	0	d*coltend4	0	
0	0	0	d*dpm	4.6		-4.6	d*coltend4*dpm	1.15	-1.15	1.15
-1.15	1.15	-1.15	1.15	-1.15						
contrast' 1_12	1_26		linear	beta	'	d	0	d*coltend4	0	
0	0	0	d*dpm	4.6		-4.6	d*coltend4*dpm	4.6	-4.6	0
0	0	0	0	0						
contrast' 1_12	2_12		linear	beta	'	d	0	d*coltend4	4.6	
-4.6	0	0	d*dpm	0		0	d*coltend4*dpm	4.6	0	-4.6
0	0	0	0	0						
contrast' 1_12	2_26		linear	beta	'	d	0	d*coltend4	4.6	
-4.6	0	0	d*dpm	4.6		-4.6	d*coltend4*dpm	4.6	0	0
-4.6	0	0	0	0						

contrast' 1_12	3_12		linear	beta	'	d	0	d*coltend4	4.6
0	-4.6	0	d*dpm	0	0	d*coltend4*dpm	4.6	0	0
0	-4.6	0	0	0	;				
contrast' 1_12	3_26		linear	beta	'	d	0	d*coltend4	4.6
0	-4.6	0	d*dpm	4.6	-4.6	d*coltend4*dpm	4.6	0	0
0	0	-4.6	0	0	;				
contrast' 1_12	4_12		linear	beta	'	d	0	d*coltend4	4.6
0	0	-4.6	d*dpm	0	0	d*coltend4*dpm	4.6	0	0
0	0	0	-4.6	0	;				
contrast' 1_12	4_26		linear	beta	'	d	0	d*coltend4	4.6
0	0	-4.6	d*dpm	4.6	-4.6	d*coltend4*dpm	4.6	0	0
0	0	0	0	-4.6	;				
contrast' 1_26	2_12		linear	beta	'	d	0	d*coltend4	4.6
-4.6	0	0	d*dpm	-4.6	4.6	d*coltend4*dpm	0	4.6	-4.6
0	0	0	0	0	;				
contrast' 1_26	2_26		linear	beta	'	d	0	d*coltend4	4.6
-4.6	0	0	d*dpm	0	0	d*coltend4*dpm	0	4.6	0
-4.6	0	0	0	0	;				
contrast' 1_26	3_12		linear	beta	'	d	0	d*coltend4	4.6
0	-4.6	0	d*dpm	-4.6	4.6	d*coltend4*dpm	0	4.6	0
0	-4.6	0	0	0	;				
contrast' 1_26	3_26		linear	beta	'	d	0	d*coltend4	4.6
0	-4.6	0	d*dpm	0	0	d*coltend4*dpm	0	4.6	0
0	0	-4.6	0	0	;				
contrast' 1_26	4_12		linear	beta	'	d	0	d*coltend4	4.6
0	0	-4.6	d*dpm	-4.6	4.6	d*coltend4*dpm	0	4.6	0
0	0	0	-4.6	0	;				
contrast' 1_26	4_26		linear	beta	'	d	0	d*coltend4	4.6
0	0	-4.6	d*dpm	0	0	d*coltend4*dpm	0	4.6	0
0	0	0	0	-4.6	;				
contrast' 2_12	2_26		linear	beta	'	d	0	d*coltend4	0
0	0	0	d*dpm	4.6	-4.6	d*coltend4*dpm	0	0	4.6
-4.6	0	0	0	0	;				
contrast' 2_12	3_12		linear	beta	'	d	0	d*coltend4	0
4.6	-4.6	0	d*dpm	0	0	d*coltend4*dpm	0	0	4.6
0	-4.6	0	0	0	;				
contrast' 2_12	3_26		linear	beta	'	d	0	d*coltend4	0
4.6	-4.6	0	d*dpm	4.6	-4.6	d*coltend4*dpm	0	0	4.6
0	0	-4.6	0	0	;				
contrast' 2_12	4_12		linear	beta	'	d	0	d*coltend4	0
4.6	0	-4.6	d*dpm	0	0	d*coltend4*dpm	0	0	4.6
0	0	0	-4.6	0	;				
contrast' 2_12	4_26		linear	beta	'	d	0	d*coltend4	0
4.6	0	-4.6	d*dpm	4.6	-4.6	d*coltend4*dpm	0	0	4.6
0	0	0	0	-4.6	;				
contrast' 2_26	3_12		linear	beta	'	d	0	d*coltend4	0
4.6	-4.6	0	d*dpm	-4.6	4.6	d*coltend4*dpm	0	0	0
4.6	-4.6	0	0	0	;				
contrast' 2_26	3_26		linear	beta	'	d	0	d*coltend4	0
4.6	-4.6	0	d*dpm	0	0	d*coltend4*dpm	0	0	0
4.6	0	-4.6	0	0	;				
contrast' 2_26	4_12		linear	beta	'	d	0	d*coltend4	0
4.6	0	-4.6	d*dpm	-4.6	4.6	d*coltend4*dpm	0	0	0
4.6	0	0	-4.6	0	;				

```

contrast' 2_26  4_26          linear  beta  '    d      0      d*coltend4  0
          4.6  0      -4.6  d*dpm  0      0      d*coltend4*dpm  0      0
          4.6  0      0      0      -4.6  ;
contrast' 3_12  3_26          linear  beta  '    d      0      d*coltend4  0
          0      0      0      d*dpm  4.6  -4.6  d*coltend4*dpm  0      0
          0      4.6  -4.6  0      0      ;
contrast' 3_12  4_12          linear  beta  '    d      0      d*coltend4  0
          0      4.6  -4.6  d*dpm  0      0      d*coltend4*dpm  0      0
          0      4.6  0      -4.6  0      ;
contrast' 3_12  4_26          linear  beta  '    d      0      d*coltend4  0
          0      4.6  -4.6  d*dpm  4.6  -4.6  d*coltend4*dpm  0      0
          0      4.6  0      0      -4.6  ;
contrast' 3_26  4_12          linear  beta  '    d      0      d*coltend4  0
          0      4.6  -4.6  d*dpm  -4.6  4.6  d*coltend4*dpm  0      0
          0      0      4.6  -4.6  0      ;
contrast' 3_26  4_26          linear  beta  '    d      0      d*coltend4  0
          0      4.6  -4.6  d*dpm  0      0      d*coltend4*dpm  0      0
          0      0      4.6  0      -4.6  ;
contrast' 4_12  4_26          linear  beta  '    d      0      d*coltend4  0
          0      0      0      d*dpm  4.6  -4.6  d*coltend4*dpm  0      0
          0      0      0      4.6  -4.6  ;
contrast' Coltend1 vs  Coltend2          quadratic  beta  '    d2  0
          d2*coltend4  37.4  -37.4  0      0      d2*dpm  0      0
          d2*coltend4*dpm  18.7  18.7  -18.7  -18.7  0      0      0      0
;
contrast' Coltend1 vs  Coltend3          quadratic  beta  '    d2  0
          d2*coltend4  37.4  0      -37.4  0      d2*dpm  0      0
          d2*coltend4*dpm  18.7  18.7  0      0      -18.7  -18.7  0      0
;
contrast' Coltend1 vs  Coltend4          quadratic  beta  '    d2  0
          d2*coltend4  37.4  0      0      -37.4  d2*dpm  0      0
          d2*coltend4*dpm  18.7  18.7  0      0      0      0      -18.7  -18.7
;
contrast' Coltend2 vs  Coltend3          quadratic  beta  '    d2  0
          d2*coltend4  0      37.4  -37.4  0      d2*dpm  0      0
          d2*coltend4*dpm  0      0      18.7  18.7  -18.7  -18.7  0      0
;
contrast' Coltend2 vs  Coltend4          quadratic  beta  '    d2  0
          d2*coltend4  0      37.4  0      -37.4  d2*dpm  0      0
          d2*coltend4*dpm  0      0      18.7  18.7  0      0      -18.7  -18.7
;
contrast' Coltend3 vs  Coltend4          quadratic  beta  '    d2  0
          d2*coltend4  0      0      -37.4  37.4  d2*dpm  0      0
          d2*coltend4*dpm  0      0      0      0      -18.7  -18.7  18.7  18.7
;
contrast' 12 vs  26          quadratic  beta  '    d2  0      d2*coltend4
          0      0      0      0      d2*dpm  37.4  -37.4  d2*coltend4*dpm  9.35
          -9.35  9.35  -9.35  9.35  -9.35  9.35  -9.35  ;
contrast' 1_12  1_26          quadratic  beta  '    d2  0      d2*coltend4
          0      0      0      0      d2*dpm  37.4  -37.4  d2*coltend4*dpm  37.4
          -37.4  0      0      0      0      0      0      ;
contrast' 1_12  2_12          quadratic  beta  '    d2  0      d2*coltend4
          37.4  -37.4  0      0      d2*dpm  0      0      d2*coltend4*dpm  37.4
          0      -37.4  0      0      0      0      0      ;

```

contrast' 1_12	2_26		quadratic	beta	'	d2	0	d2*coltend4
37.4	-37.4	0	0	d2*dpm	37.4	-37.4	d2*coltend4*dpm	37.4
0	0	-37.4	0	0	0	0	;	
contrast' 1_12	3_12		quadratic	beta	'	d2	0	d2*coltend4
37.4	0	-37.4	0	d2*dpm	0	0	d2*coltend4*dpm	37.4
0	0	0	-37.4	0	0	0	;	
contrast' 1_12	3_26		quadratic	beta	'	d2	0	d2*coltend4
37.4	0	-37.4	0	d2*dpm	37.4	-37.4	d2*coltend4*dpm	37.4
0	0	0	0	-37.4	0	0	;	
contrast' 1_12	4_12		quadratic	beta	'	d2	0	d2*coltend4
37.4	0	0	-37.4	d2*dpm	0	0	d2*coltend4*dpm	37.4
0	0	0	0	0	-37.4	0	;	
contrast' 1_12	4_26		quadratic	beta	'	d2	0	d2*coltend4
37.4	0	0	-37.4	d2*dpm	37.4	-37.4	d2*coltend4*dpm	37.4
0	0	0	0	0	0	-37.4	;	
contrast' 1_26	2_12		quadratic	beta	'	d2	0	d2*coltend4
37.4	-37.4	0	0	d2*dpm	-37.4	37.4	d2*coltend4*dpm	0
37.4	-37.4	0	0	0	0	0	;	
contrast' 1_26	2_26		quadratic	beta	'	d2	0	d2*coltend4
37.4	-37.4	0	0	d2*dpm	0	0	d2*coltend4*dpm	0
37.4	0	-37.4	0	0	0	0	;	
contrast' 1_26	3_12		quadratic	beta	'	d2	0	d2*coltend4
37.4	0	-37.4	0	d2*dpm	-37.4	37.4	d2*coltend4*dpm	0
37.4	0	0	-37.4	0	0	0	;	
contrast' 1_26	3_26		quadratic	beta	'	d2	0	d2*coltend4
37.4	0	-37.4	0	d2*dpm	0	0	d2*coltend4*dpm	0
37.4	0	0	0	-37.4	0	0	;	
contrast' 1_26	4_12		quadratic	beta	'	d2	0	d2*coltend4
37.4	0	0	-37.4	d2*dpm	-37.4	37.4	d2*coltend4*dpm	0
37.4	0	0	0	0	-37.4	0	;	
contrast' 1_26	4_26		quadratic	beta	'	d2	0	d2*coltend4
37.4	0	0	-37.4	d2*dpm	0	0	d2*coltend4*dpm	0
37.4	0	0	0	0	0	-37.4	;	
contrast' 2_12	2_26		quadratic	beta	'	d2	0	d2*coltend4
0	0	0	0	d2*dpm	37.4	-37.4	d2*coltend4*dpm	0
0	37.4	-37.4	0	0	0	0	;	
contrast' 2_12	3_12		quadratic	beta	'	d2	0	d2*coltend4
0	37.4	-37.4	0	d2*dpm	0	0	d2*coltend4*dpm	0
0	37.4	0	-37.4	0	0	0	;	
contrast' 2_12	3_26		quadratic	beta	'	d2	0	d2*coltend4
0	37.4	-37.4	0	d2*dpm	37.4	-37.4	d2*coltend4*dpm	0
0	37.4	0	0	-37.4	0	0	;	
contrast' 2_12	4_12		quadratic	beta	'	d2	0	d2*coltend4
0	37.4	0	-37.4	d2*dpm	0	0	d2*coltend4*dpm	0
0	37.4	0	0	0	-37.4	0	;	
contrast' 2_12	4_26		quadratic	beta	'	d2	0	d2*coltend4
0	37.4	0	-37.4	d2*dpm	37.4	-37.4	d2*coltend4*dpm	0
0	37.4	0	0	0	0	-37.4	;	
contrast' 2_26	3_12		quadratic	beta	'	d2	0	d2*coltend4
0	37.4	-37.4	0	d2*dpm	-37.4	37.4	d2*coltend4*dpm	0
0	0	37.4	-37.4	0	0	0	;	
contrast' 2_26	3_26		quadratic	beta	'	d2	0	d2*coltend4
0	37.4	-37.4	0	d2*dpm	0	0	d2*coltend4*dpm	0
0	0	37.4	0	-37.4	0	0	;	

```

contrast' 2_26 4_12 quadratic beta ' d2 0 d2*coltend4
0 37.4 0 -37.4 d2*dpm -37.4 37.4 d2*coltend4*dpm 0
0 0 37.4 0 0 -37.4 0 ;
contrast' 2_26 4_26 quadratic beta ' d2 0 d2*coltend4
0 37.4 0 -37.4 d2*dpm 0 0 d2*coltend4*dpm 0
0 0 37.4 0 0 0 -37.4 ;
contrast' 3_12 3_26 quadratic beta ' d2 0 d2*coltend4
0 0 0 0 d2*dpm 37.4 -37.4 d2*coltend4*dpm 0
0 0 0 37.4 -37.4 0 0 ;
contrast' 3_12 4_12 quadratic beta ' d2 0 d2*coltend4
0 0 37.4 -37.4 d2*dpm 0 0 d2*coltend4*dpm 0
0 0 0 37.4 0 -37.4 0 ;
contrast' 3_12 4_26 quadratic beta ' d2 0 d2*coltend4
0 0 37.4 -37.4 d2*dpm 37.4 -37.4 d2*coltend4*dpm 0
0 0 0 37.4 0 0 -37.4 ;
contrast' 3_26 4_12 quadratic beta ' d2 0 d2*coltend4
0 0 37.4 -37.4 d2*dpm -37.4 37.4 d2*coltend4*dpm 0
0 0 0 0 37.4 -37.4 0 ;
contrast' 3_26 4_26 quadratic beta ' d2 0 d2*coltend4
0 0 37.4 -37.4 d2*dpm 0 0 d2*coltend4*dpm 0
0 0 0 0 37.4 0 -37.4 ;
contrast' 4_12 4_26 quadratic beta ' d2 0 d2*coltend4
0 0 0 0 d2*dpm 37.4 -37.4 d2*coltend4*dpm 0
0 0 0 0 0 37.4 -37.4 ;
contrast' Coltend1 vs Coltend2 cubic beta ' d3 0
d3*coltend4 347.8 -347.8 0 0 d3*dpm 0 0
d3*coltend4*dpm 173.9 173.9 -173.9 -173.9 0 0 0 0
;
contrast' Coltend1 vs Coltend3 cubic beta ' d3 0
d3*coltend4 347.8 0 -347.8 0 d3*dpm 0 0
d3*coltend4*dpm 173.9 173.9 0 0 -173.9 -173.9 0 0
;
contrast' Coltend1 vs Coltend4 cubic beta ' d3 0
d3*coltend4 347.8 0 0 -347.8 d3*dpm 0 0
d3*coltend4*dpm 173.9 173.9 0 0 0 0 -173.9 -173.9
;
contrast' Coltend2 vs Coltend3 cubic beta ' d3 0
d3*coltend4 0 347.8 -347.8 0 d3*dpm 0 0
d3*coltend4*dpm 0 0 173.9 173.9 -173.9 -173.9 0 0
;
contrast' Coltend2 vs Coltend4 cubic beta ' d3 0
d3*coltend4 0 347.8 0 -347.8 d3*dpm 0 0
d3*coltend4*dpm 0 0 173.9 173.9 0 0 -173.9 -173.9
;
contrast' Coltend3 vs Coltend4 cubic beta ' d3 0
d3*coltend4 0 0 -347.8 347.8 d3*dpm 0 0
d3*coltend4*dpm 0 0 0 0 -173.9 -173.9 173.9 173.9
;
contrast' 12 vs 26 cubic beta ' d3 0 d3*coltend4 0
0 0 0 d3*dpm 347.8 -347.8 d3*coltend4*dpm 86.95 -86.95
86.95 -86.95 86.95 -86.95 86.95 -86.95 ;
contrast' 1_12 1_26 cubic beta ' d3 0 d3*coltend4 0
0 0 0 d3*dpm 347.8 -347.8 d3*coltend4*dpm 347.8 -347.8
0 0 0 0 0 ;

```

contrast' 1_12	2_12		cubic	beta	'	d3	0	d3*coltend4	347.8
	-347.8	0	d3*dpm	0	0	d3*coltend4*dpm	347.8	0	0
	-347.8	0	0	0	0	;			
contrast' 1_12	2_26		cubic	beta	'	d3	0	d3*coltend4	347.8
	-347.8	0	d3*dpm	347.8	-347.8	d3*coltend4*dpm	347.8	0	0
	0	-347.8	0	0	0	;			
contrast' 1_12	3_12		cubic	beta	'	d3	0	d3*coltend4	347.8
	0	-347.8	d3*dpm	0	0	d3*coltend4*dpm	347.8	0	0
	0	0	-347.8	0	0	;			
contrast' 1_12	3_26		cubic	beta	'	d3	0	d3*coltend4	347.8
	0	-347.8	d3*dpm	347.8	-347.8	d3*coltend4*dpm	347.8	0	0
	0	0	-347.8	0	0	;			
contrast' 1_12	4_12		cubic	beta	'	d3	0	d3*coltend4	347.8
	0	0	d3*dpm	0	0	d3*coltend4*dpm	347.8	0	0
	0	0	0	-347.8	0	;			
contrast' 1_12	4_26		cubic	beta	'	d3	0	d3*coltend4	347.8
	0	0	d3*dpm	347.8	-347.8	d3*coltend4*dpm	347.8	0	0
	0	0	0	0	-347.8	;			
contrast' 1_26	2_12		cubic	beta	'	d3	0	d3*coltend4	347.8
	-347.8	0	d3*dpm	-347.8	347.8	d3*coltend4*dpm	0	347.8	347.8
	-347.8	0	0	0	0	;			
contrast' 1_26	2_26		cubic	beta	'	d3	0	d3*coltend4	347.8
	-347.8	0	d3*dpm	0	0	d3*coltend4*dpm	0	347.8	347.8
	0	-347.8	0	0	0	;			
contrast' 1_26	3_12		cubic	beta	'	d3	0	d3*coltend4	347.8
	0	-347.8	d3*dpm	-347.8	347.8	d3*coltend4*dpm	0	347.8	347.8
	0	0	-347.8	0	0	;			
contrast' 1_26	3_26		cubic	beta	'	d3	0	d3*coltend4	347.8
	0	-347.8	d3*dpm	0	0	d3*coltend4*dpm	0	347.8	347.8
	0	0	-347.8	0	0	;			
contrast' 1_26	4_12		cubic	beta	'	d3	0	d3*coltend4	347.8
	0	0	d3*dpm	-347.8	347.8	d3*coltend4*dpm	0	347.8	347.8
	0	0	0	-347.8	0	;			
contrast' 1_26	4_26		cubic	beta	'	d3	0	d3*coltend4	347.8
	0	0	d3*dpm	0	0	d3*coltend4*dpm	0	347.8	347.8
	0	0	0	0	-347.8	;			
contrast' 2_12	2_26		cubic	beta	'	d3	0	d3*coltend4	0
	0	0	d3*dpm	347.8	-347.8	d3*coltend4*dpm	0	0	0
	347.8	-347.8	0	0	0	;			
contrast' 2_12	3_12		cubic	beta	'	d3	0	d3*coltend4	0
	347.8	-347.8	d3*dpm	0	0	d3*coltend4*dpm	0	0	0
	347.8	0	-347.8	0	0	;			
contrast' 2_12	3_26		cubic	beta	'	d3	0	d3*coltend4	0
	347.8	-347.8	d3*dpm	347.8	-347.8	d3*coltend4*dpm	0	0	0
	347.8	0	-347.8	0	0	;			
contrast' 2_12	4_12		cubic	beta	'	d3	0	d3*coltend4	0
	347.8	0	d3*dpm	0	0	d3*coltend4*dpm	0	0	0
	347.8	0	0	-347.8	0	;			
contrast' 2_12	4_26		cubic	beta	'	d3	0	d3*coltend4	0
	347.8	0	d3*dpm	347.8	-347.8	d3*coltend4*dpm	0	0	0
	347.8	0	0	0	-347.8	;			
contrast' 2_26	3_12		cubic	beta	'	d3	0	d3*coltend4	0
	347.8	-347.8	d3*dpm	-347.8	347.8	d3*coltend4*dpm	0	0	0
	0	347.8	-347.8	0	0	;			

```

contrast' 2_26 3_26 cubic beta ' d3 0 d3*coltend4 0
          347.8 -347.8 0 d3*dpm 0 0 d3*coltend4*dpm 0 0
          0 347.8 0 -347.8 0 0 ;
contrast' 2_26 4_12 cubic beta ' d3 0 d3*coltend4 0
          347.8 0 -347.8 d3*dpm -347.8 347.8 d3*coltend4*dpm 0 0
          0 347.8 0 0 -347.8 0 ;
contrast' 2_26 4_26 cubic beta ' d3 0 d3*coltend4 0
          347.8 0 -347.8 d3*dpm 0 0 d3*coltend4*dpm 0 0
          0 347.8 0 0 0 -347.8 ;
contrast' 3_12 3_26 cubic beta ' d3 0 d3*coltend4 0
          0 0 0 d3*dpm 347.8 -347.8 d3*coltend4*dpm 0 0
          0 0 347.8 -347.8 0 0 ;
contrast' 3_12 4_12 cubic beta ' d3 0 d3*coltend4 0
          0 347.8 -347.8 d3*dpm 0 0 d3*coltend4*dpm 0 0
          0 0 347.8 0 -347.8 0 ;
contrast' 3_12 4_26 cubic beta ' d3 0 d3*coltend4 0
          0 347.8 -347.8 d3*dpm 347.8 -347.8 d3*coltend4*dpm 0 0
          0 0 347.8 0 0 -347.8 ;
contrast' 3_26 4_12 cubic beta ' d3 0 d3*coltend4 0
          0 347.8 -347.8 d3*dpm -347.8 347.8 d3*coltend4*dpm 0 0
          0 0 0 347.8 -347.8 0 ;
contrast' 3_26 4_26 cubic beta ' d3 0 d3*coltend4 0
          0 347.8 -347.8 d3*dpm 0 0 d3*coltend4*dpm 0 0
          0 0 0 347.8 0 -347.8 ;
contrast' 4_12 4_26 cubic beta ' d3 0 d3*coltend4 0
          0 0 0 d3*dpm 347.8 -347.8 d3*coltend4*dpm 0 0
          0 0 0 0 347.8 -347.8 ;

```

```
run;
```

```

data predval; set predval;
if cx <=599 then delete;
trt = catx('_', coltend4, dpm);
run;
proc sort data = predval; by coltend4 d; run;

```

```

proc means data = predval mean ;
by coltend4;
var pred;
OUTPUT OUT=cluster MEAN=;
run;

```

```

proc sgplot data=predval ;
title ' ';
series x = d y = pred/ group = trt markers name = "series";
*scatter x=d y=pred/ group = dcc2 name="fit" ;
axis label = "Day of display" values=(0 to 11 by 1) ;
yaxis label = "b* reflectance values" values = (0 to 50 by 5) ;
keylegend "series" / across = 3 noborder location = outside position = bottom ;
*keylegend "fit" / location=outside position=bottomleft;

```

```
run;
```

```
proc means data = predval mean ;
```



```

by coltend4 d;
var pred;
OUTPUT OUT=cluster MEAN=;
run;

proc sgplot data=cluster ;
    title ' ';
series x = d y = pred/ group = coltend4 markers name = "series";
*scatter x=d y=pred/ group = dcc2 name="fit" ;
    xaxis label = "Day of display" values=(0 to 11 by 1) ;
    yaxis label = "b* reflectance values" values = (0 to 50 by 5) ;
keylegend "series" / across = 3 noborder location = outside position = bottom ;
*keylegend "fit" / location=outside position=bottomleft;

run;

proc sort data = predval; by dpm d; run;

proc means data = predval mean ;
by dpm ;
var pred;
OUTPUT OUT=dpm MEAN=;
run;

proc means data = predval mean ;
by dpm d;
var pred;
OUTPUT OUT=dpm MEAN=;
run;

proc sgplot data=dpm ;
    title ' ';
series x = d y = pred/ group = dpm markers name = "series";
    xaxis label = "Day of display" values=(0 to 11 by 1) ;
    yaxis label = "b* reflectance values" values = (0 to 50 by 5) ;
keylegend "series" / across = 3 noborder location = outside position = bottom ;
*keylegend "fit" / location=outside position=bottomleft;

run;

proc glimmix data = long ;          *noprofile ;
class STK_ID cx trip coltend4 dpm day1;
model ha = coltend4 dpm coltend4*dpm
d coltend4*d dpm*d coltend4*dpm*d
d2 coltend4*d2 dpm*d2 coltend4*dpm*d2
d3 coltend4*d3 dpm*d3 coltend4*dpm*d3
/ solution ddfm = kr ; * ;
random trip(cx) ;
random day1/ TYPE = sp(pow) (day1) sub = STK_ID residual ; * ;
output out =predval predicted = pred;;
lsmeans coltend4*dpm/ e;
estimate '          Coltend 1 12 d      12      Interceptbeta      '          Intercept1          coltend4 1
          0          0          0          dpm      1          0          coltend4*dpm      1          0          0
          0          0          0          0          0          ;

```

```

estimate '      Coltend 1      26      Interceptbeta      '      Intercept1      coltend4 1
          0      0      0      dpm      0      1      coltend4*dpm      0      1      0
          0      0      0      0      0      ;
estimate '      Coltend 2      12      Interceptbeta      '      Intercept1      coltend4 0
          1      0      0      dpm      1      0      coltend4*dpm      0      0      1
          0      0      0      0      0      ;
estimate '      Coltend 2      26      Interceptbeta      '      Intercept1      coltend4 0
          1      0      0      dpm      0      1      coltend4*dpm      0      0      0
          1      0      0      0      0      ;
estimate '      Coltend3      12      Interceptbeta      '      Intercept1      coltend4 0
          0      1      0      dpm      1      0      coltend4*dpm      0      0      0
          0      1      0      0      0      ;
estimate '      Coltend 3      26      Interceptbeta      '      Intercept1      coltend4 0
          0      1      0      dpm      0      1      coltend4*dpm      0      0      0
          0      0      1      0      0      ;
estimate '      Coltend4      12      Interceptbeta      '      Intercept1      coltend4 0
          0      0      1      dpm      1      0      coltend4*dpm      0      0      0
          0      0      0      1      0      ;
estimate '      Coltend 4      26      Interceptbeta      '      Intercept1      coltend4 0
          0      0      1      dpm      0      1      coltend4*dpm      0      0      0
          0      0      0      0      1      ;
estimate '      Coltend 1      Interceptbeta      '      Intercept1      coltend4 1
          0      0      0      dpm      0.5      0.5      coltend4*dpm      0.5      0.5      0
          0      0      0      0      0      ;
estimate '      Coltend 2      Interceptbeta      '      Intercept1      coltend4 0
          1      0      0      dpm      0.5      0.5      coltend4*dpm      0      0      0.5
          0.5      0      0      0      0      ;
estimate '      Coltend 3      Interceptbeta      '      Intercept1      coltend4 0
          0      1      0      dpm      0.5      0.5      coltend4*dpm      0      0      0
          0      0.5      0.5      0      0      ;
estimate '      Coltend 4      Interceptbeta      '      Intercept1      coltend4 0
          0      0      1      dpm      0.5      0.5      coltend4*dpm      0      0      0
          0      0      0      0.5      0.5      ;
estimate '      12      Interceptbeta      '      Intercept1      coltend4 0.25      0.25
          0.25      0.25      dpm      1      0      coltend4*dpm      0.25      0      0.25      0
          0.25      0      0.25      0      0      ;
estimate '      26      Interceptbeta      '      Intercept1      coltend4 0.25      0.25
          0.25      0.25      dpm      0      1      coltend4*dpm      0      0.25      0      0.25
          0      0.25      0      0.25      ;

estimate '      Coltend 1 12 d      12      linear      beta      '      d      4.6      d*coltend4
          4.6      0      0      0      d*dpm      4.6      0      d*coltend4*dpm      4.6      0
          0      0      0      0      0      0      ;
estimate '      Coltend 1      26      linear      beta      '      d      4.6      d*coltend4
          4.6      0      0      0      d*dpm      0      4.6      d*coltend4*dpm      0      4.6
          0      0      0      0      0      0      ;
estimate '      Coltend 2      12      linear      beta      '      d      4.6      d*coltend4
          0      4.6      0      0      d*dpm      4.6      0      d*coltend4*dpm      0      0
          4.6      0      0      0      0      0      ;
estimate '      Coltend 2      26      linear      beta      '      d      4.6      d*coltend4
          0      4.6      0      0      d*dpm      0      4.6      d*coltend4*dpm      0      0
          0      4.6      0      0      0      0      ;

```

```

estimate '      Coltend3      12      linear      beta      '      d      4.6      d*coltend4
0      0      4.6      0      d*dpm      4.6      0      d*coltend4*dpm      0      0
0      0      4.6      0      0      0      ;
estimate '      Coltend 3      26      linear      beta      '      d      4.6      d*coltend4
0      0      4.6      0      d*dpm      0      4.6      d*coltend4*dpm      0      0
0      0      0      4.6      0      0      ;
estimate '      Coltend4      12      linear      beta      '      d      4.6      d*coltend4
0      0      0      4.6      d*dpm      4.6      0      d*coltend4*dpm      0      0
0      0      0      0      4.6      0      ;
estimate '      Coltend 4      26      linear      beta      '      d      4.6      d*coltend4
0      0      0      4.6      d*dpm      0      4.6      d*coltend4*dpm      0      0
0      0      0      0      0      4.6      ;
estimate '      Coltend 1      linear      beta      '      d      4.6      d*coltend4
4.6      0      0      0      d*dpm      2.3      2.3      d*coltend4*dpm      2.3      2.3
0      0      0      0      0      0      ;
estimate '      Coltend 2      linear      beta      '      d      4.6      d*coltend4
0      4.6      0      0      d*dpm      2.3      2.3      d*coltend4*dpm      0      0
2.3      2.3      0      0      0      0      ;
estimate '      Coltend 3      linear      beta      '      d      4.6      d*coltend4
0      0      4.6      0      d*dpm      2.3      2.3      d*coltend4*dpm      0      0
0      0      2.3      2.3      0      0      ;
estimate '      Coltend 4      linear      beta      '      d      4.6      d*coltend4
0      0      0      4.6      d*dpm      2.3      2.3      d*coltend4*dpm      0      0
0      0      0      0      2.3      2.3      ;
estimate '      12      linear      beta      '      d      4.6      d*coltend4      1.15
1.15      1.15      1.15      d*dpm      4.6      0      d*coltend4*dpm      1.15      0      1.15
0      1.15      0      1.15      0      ;
estimate '      26      linear      beta      '      d      4.6      d*coltend4      1.15
1.15      1.15      1.15      d*dpm      0      4.6      d*coltend4*dpm      0      1.15      0
1.15      0      1.15      0      1.15      ;

estimate '      Coltend 1 12 d      12      quadratic      beta      '      d2      37.4
d2*coltend4      37.4      0      0      0      d2*dpm      37.4      0
d2*coltend4*dpm      37.4      0      0      0      0      0      0      0      0
;
estimate '      Coltend 1      26      quadratic      beta      '      d2      37.4
d2*coltend4      37.4      0      0      0      d2*dpm      0      37.4
d2*coltend4*dpm      0      37.4      0      0      0      0      0      0      0
;
estimate '      Coltend 2      12      quadratic      beta      '      d2      37.4
d2*coltend4      0      37.4      0      0      d2*dpm      37.4      0
d2*coltend4*dpm      0      0      37.4      0      0      0      0      0      0
;
estimate '      Coltend 2      26      quadratic      beta      '      d2      37.4
d2*coltend4      0      37.4      0      0      d2*dpm      0      37.4
d2*coltend4*dpm      0      0      0      37.4      0      0      0      0      0
;
estimate '      Coltend3      12      quadratic      beta      '      d2      37.4
d2*coltend4      0      0      37.4      0      d2*dpm      37.4      0
d2*coltend4*dpm      0      0      0      0      0      37.4      0      0      0
;
estimate '      Coltend 3      26      quadratic      beta      '      d2      37.4
d2*coltend4      0      0      37.4      0      d2*dpm      0      37.4

```

```

d2*coltend4*dpm      0      0      0      0      0      37.4      0      0
;
estimate '      Coltend4      12      quadratic      beta      '      d2      37.4
d2*coltend4      0      0      0      37.4      d2*dpm      37.4      0
d2*coltend4*dpm      0      0      0      0      0      0      37.4      0
;
estimate '      Coltend 4      26      quadratic      beta      '      d2      37.4
d2*coltend4      0      0      0      37.4      d2*dpm      0      37.4
d2*coltend4*dpm      0      0      0      0      0      0      0      37.4
;
estimate '      Coltend 1      quadratic      beta      '      d2      37.4
d2*coltend4      37.4      0      0      0      d2*dpm      18.7      18.7
d2*coltend4*dpm      18.7      18.7      0      0      0      0      0      0
;
estimate '      Coltend 2      quadratic      beta      '      d2      37.4
d2*coltend4      0      37.4      0      0      d2*dpm      18.7      18.7
d2*coltend4*dpm      0      0      18.7      18.7      0      0      0      0
;
estimate '      Coltend 3      quadratic      beta      '      d2      37.4
d2*coltend4      0      0      37.4      0      d2*dpm      18.7      18.7
d2*coltend4*dpm      0      0      0      0      0      18.7      18.7      0      0
;
estimate '      Coltend 4      quadratic      beta      '      d2      37.4
d2*coltend4      0      0      0      37.4      d2*dpm      18.7      18.7
d2*coltend4*dpm      0      0      0      0      0      0      0      18.7      18.7
;
estimate '      12      quadratic      beta      '      d2      37.4      d2*coltend4
9.35      9.35      9.35      9.35      d2*dpm      37.4      0      d2*coltend4*dpm      9.35
0      9.35      0      9.35      0      9.35      0      ;
estimate '      26      quadratic      beta      '      d2      37.4      d2*coltend4
9.35      9.35      9.35      9.35      d2*dpm      0      37.4      d2*coltend4*dpm      0
9.35      0      9.35      0      9.35      0      9.35      ;

estimate '      Coltend 1 12 d      12      cubic      beta      '      d3      347.8      d3*coltend4
347.8      0      0      0      d3*dpm      347.8      0      d3*coltend4*dpm      347.8
0      0      0      0      0      0      0      ;
estimate '      Coltend 1      26      cubic      beta      '      d3      347.8      d3*coltend4
347.8      0      0      0      d3*dpm      0      347.8      d3*coltend4*dpm      0
347.8      0      0      0      0      0      0      ;
estimate '      Coltend 2      12      cubic      beta      '      d3      347.8      d3*coltend4
0      347.8      0      0      d3*dpm      347.8      0      d3*coltend4*dpm      0
0      347.8      0      0      0      0      0      ;
estimate '      Coltend 2      26      cubic      beta      '      d3      347.8      d3*coltend4
0      347.8      0      0      d3*dpm      0      347.8      d3*coltend4*dpm      0
0      0      347.8      0      0      0      0      ;
estimate '      Coltend3      12      cubic      beta      '      d3      347.8      d3*coltend4
0      0      347.8      0      d3*dpm      347.8      0      d3*coltend4*dpm      0
0      0      0      347.8      0      0      0      ;
estimate '      Coltend 3      26      cubic      beta      '      d3      347.8      d3*coltend4
0      0      347.8      0      d3*dpm      0      347.8      d3*coltend4*dpm      0
0      0      0      0      347.8      0      0      ;
estimate '      Coltend4      12      cubic      beta      '      d3      347.8      d3*coltend4
0      0      0      347.8      d3*dpm      347.8      0      d3*coltend4*dpm      0
0      0      0      0      0      347.8      0      ;

```

estimate	'	Coltend 4	26	cubic	beta	'	d3	347.8	d3*coltend4	
	0	0	0	347.8	d3*dpm	0	347.8	d3*coltend4*dpm	0	
	0	0	0	0	0	0	347.8	;		
estimate	'	Coltend 1		cubic	beta	'	d3	347.8	d3*coltend4	
	347.8	0	0	0	d3*dpm	173.9	173.9	d3*coltend4*dpm	173.9	
	173.9	0	0	0	0	0	0	;		
estimate	'	Coltend 2		cubic	beta	'	d3	347.8	d3*coltend4	
	0	347.8	0	0	d3*dpm	173.9	173.9	d3*coltend4*dpm	0	
	0	173.9	173.9	0	0	0	0	;		
estimate	'	Coltend 3		cubic	beta	'	d3	347.8	d3*coltend4	
	0	0	347.8	0	d3*dpm	173.9	173.9	d3*coltend4*dpm	0	
	0	0	0	173.9	173.9	0	0	;		
estimate	'	Coltend 4		cubic	beta	'	d3	347.8	d3*coltend4	
	0	0	0	347.8	d3*dpm	173.9	173.9	d3*coltend4*dpm	0	
	0	0	0	0	0	173.9	173.9	;		
estimate	'	12		cubic	beta	'	d3	347.8	d3*coltend4	86.95
	86.95	86.95	86.95	d3*dpm	347.8	0	d3*coltend4*dpm	86.95	0	
	86.95	0	86.95	0	86.95	0	;			
estimate	'	26		cubic	beta	'	d3	347.8	d3*coltend4	86.95
	86.95	86.95	86.95	d3*dpm	0	347.8	d3*coltend4*dpm	0	86.95	
	0	86.95	0	86.95	0	86.95	;			
contrast	'	Coltend1 vs	Coltend2		Intercept	beta	'	Intercept	0	coltend4
	1	-1	0	0	dpm	0	0	coltend4*dpm	0.5	0.5
	-0.5	-0.5	0	0	0	0	;			
contrast	'	Coltend1 vs	Coltend3		Intercept	beta	'	Intercept	0	coltend4
	1	0	-1	0	dpm	0	0	coltend4*dpm	0.5	0.5
	0	0	-0.5	-0.5	0	0	;			
contrast	'	Coltend1 vs	Coltend4		Intercept	beta	'	Intercept	0	coltend4
	1	0	0	-1	dpm	0	0	coltend4*dpm	0.5	0.5
	0	0	0	0	-0.5	-0.5	;			
contrast	'	Coltend2 vs	Coltend3		Intercept	beta	'	Intercept	0	coltend4
	0	1	-1	0	dpm	0	0	coltend4*dpm	0	0
	0.5	0.5	-0.5	-0.5	0	0	;			
contrast	'	Coltend2 vs	Coltend4		Intercept	beta	'	Intercept	0	coltend4
	0	1	0	-1	dpm	0	0	coltend4*dpm	0	0
	0.5	0.5	0	0	-0.5	-0.5	;			
contrast	'	Coltend3 vs	Coltend4		Intercept	beta	'	Intercept	0	coltend4
	0	0	-1	1	dpm	0	0	coltend4*dpm	0	0
	0	0	-0.5	-0.5	0.5	0.5	;			
contrast	'	12 vs	26		Intercept	beta	'	Intercept	0	coltend4
	0	0	dpm	1	-1	coltend4*dpm	0.25	-0.25	0.25	-0.25
	0.25	-0.25	0.25	-0.25	;					
contrast	'	1_12	1_26		Intercept	beta	'	Intercept	0	coltend4
	0	0	dpm	1	-1	coltend4*dpm	1	-1	0	0
	0	0	0	0	;					
contrast	'	1_12	2_12		Intercept	beta	'	Intercept	0	coltend4
	0	0	dpm	0	0	coltend4*dpm	1	0	-1	0
	0	0	0	0	;					
contrast	'	1_12	2_26		Intercept	beta	'	Intercept	0	coltend4
	0	0	dpm	1	-1	coltend4*dpm	1	0	0	-1
	0	0	0	0	;					
contrast	'	1_12	3_12		Intercept	beta	'	Intercept	0	coltend4
	-1	0	dpm	0	0	coltend4*dpm	1	0	0	0
	-1	0	0	0	;					

contrast' 1_12	3_26		Intercept	beta	'	Intercept	0	coltend4	1	0
-1	0	dpm	1	-1		coltend4*dpm	1	0	0	0
0	-1	0	0		;					
contrast' 1_12	4_12		Intercept	beta	'	Intercept	0	coltend4	1	0
0	-1	dpm	0	0		coltend4*dpm	1	0	0	0
0	0	-1	0		;					
contrast' 1_12	4_26		Intercept	beta	'	Intercept	0	coltend4	1	0
0	-1	dpm	1	-1		coltend4*dpm	1	0	0	0
0	0	0	-1		;					
contrast' 1_26	2_12		Intercept	beta	'	Intercept	0	coltend4	1	-1
0	0	dpm	-1	1		coltend4*dpm	0	1	-1	0
0	0	0	0		;					
contrast' 1_26	2_26		Intercept	beta	'	Intercept	0	coltend4	1	-1
0	0	dpm	0	0		coltend4*dpm	0	1	0	-1
0	0	0	0		;					
contrast' 1_26	3_12		Intercept	beta	'	Intercept	0	coltend4	1	0
-1	0	dpm	-1	1		coltend4*dpm	0	1	0	0
-1	0	0	0		;					
contrast' 1_26	3_26		Intercept	beta	'	Intercept	0	coltend4	1	0
-1	0	dpm	0	0		coltend4*dpm	0	1	0	0
0	-1	0	0		;					
contrast' 1_26	4_12		Intercept	beta	'	Intercept	0	coltend4	1	0
0	-1	dpm	-1	1		coltend4*dpm	0	1	0	0
0	0	-1	0		;					
contrast' 1_26	4_26		Intercept	beta	'	Intercept	0	coltend4	1	0
0	-1	dpm	0	0		coltend4*dpm	0	1	0	0
0	0	0	-1		;					
contrast' 2_12	2_26		Intercept	beta	'	Intercept	0	coltend4	0	0
0	0	dpm	1	-1		coltend4*dpm	0	0	1	-1
0	0	0	0		;					
contrast' 2_12	3_12		Intercept	beta	'	Intercept	0	coltend4	0	1
-1	0	dpm	0	0		coltend4*dpm	0	0	1	0
-1	0	0	0		;					
contrast' 2_12	3_26		Intercept	beta	'	Intercept	0	coltend4	0	1
-1	0	dpm	1	-1		coltend4*dpm	0	0	1	0
0	-1	0	0		;					
contrast' 2_12	4_12		Intercept	beta	'	Intercept	0	coltend4	0	1
0	-1	dpm	0	0		coltend4*dpm	0	0	1	0
0	0	-1	0		;					
contrast' 2_12	4_26		Intercept	beta	'	Intercept	0	coltend4	0	1
0	-1	dpm	1	-1		coltend4*dpm	0	0	1	0
0	0	0	-1		;					
contrast' 2_26	3_12		Intercept	beta	'	Intercept	0	coltend4	0	1
-1	0	dpm	-1	1		coltend4*dpm	0	0	0	1
-1	0	0	0		;					
contrast' 2_26	3_26		Intercept	beta	'	Intercept	0	coltend4	0	1
-1	0	dpm	0	0		coltend4*dpm	0	0	0	1
0	-1	0	0		;					
contrast' 2_26	4_12		Intercept	beta	'	Intercept	0	coltend4	0	1
0	-1	dpm	-1	1		coltend4*dpm	0	0	0	1
0	0	-1	0		;					
contrast' 2_26	4_26		Intercept	beta	'	Intercept	0	coltend4	0	1
0	-1	dpm	0	0		coltend4*dpm	0	0	0	1
0	0	0	-1		;					

contrast' 3_12	3_26		Intercept	beta	'	Intercept	0	coltend4	0	0
0	0	dpm	1	-1		coltend4*dpm	0	0	0	0
1	-1	0	0		;					
contrast' 3_12	4_12		Intercept	beta	'	Intercept	0	coltend4	0	0
1	-1	dpm	0	0		coltend4*dpm	0	0	0	0
1	0	-1	0		;					
contrast' 3_12	4_26		Intercept	beta	'	Intercept	0	coltend4	0	0
1	-1	dpm	1	-1		coltend4*dpm	0	0	0	0
1	0	0	-1		;					
contrast' 3_26	4_12		Intercept	beta	'	Intercept	0	coltend4	0	0
1	-1	dpm	-1	1		coltend4*dpm	0	0	0	0
0	1	-1	0		;					
contrast' 3_26	4_26		Intercept	beta	'	Intercept	0	coltend4	0	0
1	-1	dpm	0	0		coltend4*dpm	0	0	0	0
0	1	0	-1		;					
contrast' 4_12	4_26		Intercept	beta	'	Intercept	0	coltend4	0	0
0	0	dpm	1	-1		coltend4*dpm	0	0	0	0
0	0	1	-1		;					
contrast' Coltend1 vs	Coltend2		linear	beta	'	d	0			
d*coltend4	4.6	-4.6	0			d*dpm	0	0	d*coltend4*dpm	
2.3	2.3	-2.3	-2.3	0		0	0	0	;	
contrast' Coltend1 vs	Coltend3		linear	beta	'	d	0			
d*coltend4	4.6	0	-4.6	0		d*dpm	0	0	d*coltend4*dpm	
2.3	2.3	0	0	-2.3		-2.3	0	0	;	
contrast' Coltend1 vs	Coltend4		linear	beta	'	d	0			
d*coltend4	4.6	0	0	-4.6		d*dpm	0	0	d*coltend4*dpm	
2.3	2.3	0	0	0		0	-2.3	-2.3	;	
contrast' Coltend2 vs	Coltend3		linear	beta	'	d	0			
d*coltend4	0	4.6	-4.6	0		d*dpm	0	0	d*coltend4*dpm	
0	0	2.3	2.3	-2.3		-2.3	0	0	;	
contrast' Coltend2 vs	Coltend4		linear	beta	'	d	0			
d*coltend4	0	4.6	0	-4.6		d*dpm	0	0	d*coltend4*dpm	
0	0	2.3	2.3	0		0	-2.3	-2.3	;	
contrast' Coltend3 vs	Coltend4		linear	beta	'	d	0			
d*coltend4	0	0	-4.6	4.6		d*dpm	0	0	d*coltend4*dpm	
0	0	0	0	-2.3		-2.3	2.3	2.3	;	
contrast' 12 vs	26		linear	beta	'	d	0	d*coltend4	0	
0	0	0	d*dpm	4.6		-4.6	d*coltend4*dpm	1.15	-1.15	1.15
-1.15	1.15	-1.15	1.15	-1.15		;				
contrast' 1_12	1_26		linear	beta	'	d	0	d*coltend4	0	
0	0	0	d*dpm	4.6		-4.6	d*coltend4*dpm	4.6	-4.6	0
0	0	0	0	0		;				
contrast' 1_12	2_12		linear	beta	'	d	0	d*coltend4	4.6	
-4.6	0	0	d*dpm	0		0	d*coltend4*dpm	4.6	0	-4.6
0	0	0	0	0		;				
contrast' 1_12	2_26		linear	beta	'	d	0	d*coltend4	4.6	
-4.6	0	0	d*dpm	4.6		-4.6	d*coltend4*dpm	4.6	0	0
-4.6	0	0	0	0		;				
contrast' 1_12	3_12		linear	beta	'	d	0	d*coltend4	4.6	
0	-4.6	0	d*dpm	0		0	d*coltend4*dpm	4.6	0	0
0	-4.6	0	0	0		;				
contrast' 1_12	3_26		linear	beta	'	d	0	d*coltend4	4.6	
0	-4.6	0	d*dpm	4.6		-4.6	d*coltend4*dpm	4.6	0	0
0	0	-4.6	0	0		;				

contrast' 1_12	4_12		linear	beta	'	d	0	d*coltend4	4.6
0	0	-4.6	d*dpm	0	0	d*coltend4*dpm	4.6	0	0
0	0	0	-4.6	0	;				
contrast' 1_12	4_26		linear	beta	'	d	0	d*coltend4	4.6
0	0	-4.6	d*dpm	4.6	-4.6	d*coltend4*dpm	4.6	0	0
0	0	0	0	-4.6	;				
contrast' 1_26	2_12		linear	beta	'	d	0	d*coltend4	4.6
-4.6	0	0	d*dpm	-4.6	4.6	d*coltend4*dpm	0	4.6	-4.6
0	0	0	0	0	;				
contrast' 1_26	2_26		linear	beta	'	d	0	d*coltend4	4.6
-4.6	0	0	d*dpm	0	0	d*coltend4*dpm	0	4.6	0
-4.6	0	0	0	0	;				
contrast' 1_26	3_12		linear	beta	'	d	0	d*coltend4	4.6
0	-4.6	0	d*dpm	-4.6	4.6	d*coltend4*dpm	0	4.6	0
0	-4.6	0	0	0	;				
contrast' 1_26	3_26		linear	beta	'	d	0	d*coltend4	4.6
0	-4.6	0	d*dpm	0	0	d*coltend4*dpm	0	4.6	0
0	0	-4.6	0	0	;				
contrast' 1_26	4_12		linear	beta	'	d	0	d*coltend4	4.6
0	0	-4.6	d*dpm	-4.6	4.6	d*coltend4*dpm	0	4.6	0
0	0	0	-4.6	0	;				
contrast' 1_26	4_26		linear	beta	'	d	0	d*coltend4	4.6
0	0	-4.6	d*dpm	0	0	d*coltend4*dpm	0	4.6	0
0	0	0	0	-4.6	;				
contrast' 2_12	2_26		linear	beta	'	d	0	d*coltend4	0
0	0	0	d*dpm	4.6	-4.6	d*coltend4*dpm	0	0	4.6
-4.6	0	0	0	0	;				
contrast' 2_12	3_12		linear	beta	'	d	0	d*coltend4	0
4.6	-4.6	0	d*dpm	0	0	d*coltend4*dpm	0	0	4.6
0	-4.6	0	0	0	;				
contrast' 2_12	3_26		linear	beta	'	d	0	d*coltend4	0
4.6	-4.6	0	d*dpm	4.6	-4.6	d*coltend4*dpm	0	0	4.6
0	0	-4.6	0	0	;				
contrast' 2_12	4_12		linear	beta	'	d	0	d*coltend4	0
4.6	0	-4.6	d*dpm	0	0	d*coltend4*dpm	0	0	4.6
0	0	0	-4.6	0	;				
contrast' 2_12	4_26		linear	beta	'	d	0	d*coltend4	0
4.6	0	-4.6	d*dpm	4.6	-4.6	d*coltend4*dpm	0	0	4.6
0	0	0	0	-4.6	;				
contrast' 2_26	3_12		linear	beta	'	d	0	d*coltend4	0
4.6	-4.6	0	d*dpm	-4.6	4.6	d*coltend4*dpm	0	0	0
4.6	-4.6	0	0	0	;				
contrast' 2_26	3_26		linear	beta	'	d	0	d*coltend4	0
4.6	-4.6	0	d*dpm	0	0	d*coltend4*dpm	0	0	0
4.6	0	-4.6	0	0	;				
contrast' 2_26	4_12		linear	beta	'	d	0	d*coltend4	0
4.6	0	-4.6	d*dpm	-4.6	4.6	d*coltend4*dpm	0	0	0
4.6	0	0	-4.6	0	;				
contrast' 2_26	4_26		linear	beta	'	d	0	d*coltend4	0
4.6	0	-4.6	d*dpm	0	0	d*coltend4*dpm	0	0	0
4.6	0	0	0	-4.6	;				
contrast' 3_12	3_26		linear	beta	'	d	0	d*coltend4	0
0	0	0	d*dpm	4.6	-4.6	d*coltend4*dpm	0	0	0
0	4.6	-4.6	0	0	;				


```

contrast' 3_12 4_12 linear beta ' d 0 d*coltend4 0
0 4.6 -4.6 d*dpm 0 0 d*coltend4*dpm 0 0 0
0 4.6 0 -4.6 0 ;
contrast' 3_12 4_26 linear beta ' d 0 d*coltend4 0
0 4.6 -4.6 d*dpm 4.6 -4.6 d*coltend4*dpm 0 0 0
0 4.6 0 0 -4.6 ;
contrast' 3_26 4_12 linear beta ' d 0 d*coltend4 0
0 4.6 -4.6 d*dpm -4.6 4.6 d*coltend4*dpm 0 0 0
0 0 4.6 -4.6 0 ;
contrast' 3_26 4_26 linear beta ' d 0 d*coltend4 0
0 4.6 -4.6 d*dpm 0 0 d*coltend4*dpm 0 0 0
0 0 4.6 0 -4.6 ;
contrast' 4_12 4_26 linear beta ' d 0 d*coltend4 0
0 0 0 d*dpm 4.6 -4.6 d*coltend4*dpm 0 0 0
0 0 0 4.6 -4.6 ;
contrast' Coltend1 vs Coltend2 quadratic beta ' d2 0
d2*coltend4 37.4 -37.4 0 0 d2*dpm 0 0
d2*coltend4*dpm 18.7 18.7 -18.7 -18.7 0 0 0
;
contrast' Coltend1 vs Coltend3 quadratic beta ' d2 0
d2*coltend4 37.4 0 -37.4 0 d2*dpm 0 0
d2*coltend4*dpm 18.7 18.7 0 0 -18.7 -18.7 0 0
;
contrast' Coltend1 vs Coltend4 quadratic beta ' d2 0
d2*coltend4 37.4 0 0 -37.4 d2*dpm 0 0
d2*coltend4*dpm 18.7 18.7 0 0 0 0 -18.7 -18.7
;
contrast' Coltend2 vs Coltend3 quadratic beta ' d2 0
d2*coltend4 0 37.4 -37.4 0 d2*dpm 0 0
d2*coltend4*dpm 0 0 18.7 18.7 -18.7 -18.7 0 0
;
contrast' Coltend2 vs Coltend4 quadratic beta ' d2 0
d2*coltend4 0 37.4 0 -37.4 d2*dpm 0 0
d2*coltend4*dpm 0 0 18.7 18.7 0 0 -18.7 -18.7
;
contrast' Coltend3 vs Coltend4 quadratic beta ' d2 0
d2*coltend4 0 0 -37.4 37.4 d2*dpm 0 0
d2*coltend4*dpm 0 0 0 0 -18.7 -18.7 18.7 18.7
;
contrast' 12 vs 26 quadratic beta ' d2 0 d2*coltend4
0 0 0 0 d2*dpm 37.4 -37.4 d2*coltend4*dpm 9.35
-9.35 9.35 -9.35 9.35 -9.35 9.35 -9.35 ;
contrast' 1_12 1_26 quadratic beta ' d2 0 d2*coltend4
0 0 0 0 d2*dpm 37.4 -37.4 d2*coltend4*dpm 37.4
-37.4 0 0 0 0 0 ;
contrast' 1_12 2_12 quadratic beta ' d2 0 d2*coltend4
37.4 -37.4 0 0 d2*dpm 0 0 d2*coltend4*dpm 37.4
0 -37.4 0 0 0 0 ;
contrast' 1_12 2_26 quadratic beta ' d2 0 d2*coltend4
37.4 -37.4 0 0 d2*dpm 37.4 -37.4 d2*coltend4*dpm 37.4
0 0 -37.4 0 0 0 ;
contrast' 1_12 3_12 quadratic beta ' d2 0 d2*coltend4
37.4 0 -37.4 0 d2*dpm 0 0 d2*coltend4*dpm 37.4
0 0 0 -37.4 0 0 ;

```

contrast' 1_12	3_26		quadratic	beta	'	d2	0	d2*coltend4
37.4	0	-37.4	0	d2*dpm	37.4	-37.4	d2*coltend4*dpm	37.4
0	0	0	0	-37.4	0	0	;	
contrast' 1_12	4_12		quadratic	beta	'	d2	0	d2*coltend4
37.4	0	0	-37.4	d2*dpm	0	0	d2*coltend4*dpm	37.4
0	0	0	0	0	-37.4	0	;	
contrast' 1_12	4_26		quadratic	beta	'	d2	0	d2*coltend4
37.4	0	0	-37.4	d2*dpm	37.4	-37.4	d2*coltend4*dpm	37.4
0	0	0	0	0	0	-37.4	;	
contrast' 1_26	2_12		quadratic	beta	'	d2	0	d2*coltend4
37.4	-37.4	0	0	d2*dpm	-37.4	37.4	d2*coltend4*dpm	0
37.4	-37.4	0	0	0	0	0	;	
contrast' 1_26	2_26		quadratic	beta	'	d2	0	d2*coltend4
37.4	-37.4	0	0	d2*dpm	0	0	d2*coltend4*dpm	0
37.4	0	-37.4	0	0	0	0	;	
contrast' 1_26	3_12		quadratic	beta	'	d2	0	d2*coltend4
37.4	0	-37.4	0	d2*dpm	-37.4	37.4	d2*coltend4*dpm	0
37.4	0	0	-37.4	0	0	0	;	
contrast' 1_26	3_26		quadratic	beta	'	d2	0	d2*coltend4
37.4	0	-37.4	0	d2*dpm	0	0	d2*coltend4*dpm	0
37.4	0	0	0	-37.4	0	0	;	
contrast' 1_26	4_12		quadratic	beta	'	d2	0	d2*coltend4
37.4	0	0	-37.4	d2*dpm	-37.4	37.4	d2*coltend4*dpm	0
37.4	0	0	0	0	-37.4	0	;	
contrast' 1_26	4_26		quadratic	beta	'	d2	0	d2*coltend4
37.4	0	0	-37.4	d2*dpm	0	0	d2*coltend4*dpm	0
37.4	0	0	0	0	0	-37.4	;	
contrast' 2_12	2_26		quadratic	beta	'	d2	0	d2*coltend4
0	0	0	0	d2*dpm	37.4	-37.4	d2*coltend4*dpm	0
0	37.4	-37.4	0	0	0	0	;	
contrast' 2_12	3_12		quadratic	beta	'	d2	0	d2*coltend4
0	37.4	-37.4	0	d2*dpm	0	0	d2*coltend4*dpm	0
0	37.4	0	-37.4	0	0	0	;	
contrast' 2_12	3_26		quadratic	beta	'	d2	0	d2*coltend4
0	37.4	-37.4	0	d2*dpm	37.4	-37.4	d2*coltend4*dpm	0
0	37.4	0	0	-37.4	0	0	;	
contrast' 2_12	4_12		quadratic	beta	'	d2	0	d2*coltend4
0	37.4	0	-37.4	d2*dpm	0	0	d2*coltend4*dpm	0
0	37.4	0	0	0	-37.4	0	;	
contrast' 2_12	4_26		quadratic	beta	'	d2	0	d2*coltend4
0	37.4	0	-37.4	d2*dpm	37.4	-37.4	d2*coltend4*dpm	0
0	37.4	0	0	0	0	-37.4	;	
contrast' 2_26	3_12		quadratic	beta	'	d2	0	d2*coltend4
0	37.4	-37.4	0	d2*dpm	-37.4	37.4	d2*coltend4*dpm	0
0	0	37.4	-37.4	0	0	0	;	
contrast' 2_26	3_26		quadratic	beta	'	d2	0	d2*coltend4
0	37.4	-37.4	0	d2*dpm	0	0	d2*coltend4*dpm	0
0	0	37.4	0	-37.4	0	0	;	
contrast' 2_26	4_12		quadratic	beta	'	d2	0	d2*coltend4
0	37.4	0	-37.4	d2*dpm	-37.4	37.4	d2*coltend4*dpm	0
0	0	37.4	0	0	-37.4	0	;	
contrast' 2_26	4_26		quadratic	beta	'	d2	0	d2*coltend4
0	37.4	0	-37.4	d2*dpm	0	0	d2*coltend4*dpm	0
0	0	37.4	0	0	0	-37.4	;	

```

contrast' 3_12 3_26 quadratic beta ' d2 0 d2*coltend4
0 0 0 0 d2*dpm 37.4 -37.4 d2*coltend4*dpm 0
0 0 0 37.4 -37.4 0 0 ;
contrast' 3_12 4_12 quadratic beta ' d2 0 d2*coltend4
0 0 37.4 -37.4 d2*dpm 0 0 d2*coltend4*dpm 0
0 0 0 37.4 0 -37.4 0 ;
contrast' 3_12 4_26 quadratic beta ' d2 0 d2*coltend4
0 0 37.4 -37.4 d2*dpm 37.4 -37.4 d2*coltend4*dpm 0
0 0 0 37.4 0 0 -37.4 ;
contrast' 3_26 4_12 quadratic beta ' d2 0 d2*coltend4
0 0 37.4 -37.4 d2*dpm -37.4 37.4 d2*coltend4*dpm 0
0 0 0 0 37.4 -37.4 0 ;
contrast' 3_26 4_26 quadratic beta ' d2 0 d2*coltend4
0 0 37.4 -37.4 d2*dpm 0 0 d2*coltend4*dpm 0
0 0 0 0 37.4 0 -37.4 ;
contrast' 4_12 4_26 quadratic beta ' d2 0 d2*coltend4
0 0 0 0 d2*dpm 37.4 -37.4 d2*coltend4*dpm 0
0 0 0 0 0 37.4 -37.4 ;
contrast' Coltend1 vs Coltend2 cubic beta ' d3 0
d3*coltend4 347.8 -347.8 0 0 d3*dpm 0 0
d3*coltend4*dpm 173.9 173.9 -173.9 -173.9 0 0 0
;
contrast' Coltend1 vs Coltend3 cubic beta ' d3 0
d3*coltend4 347.8 0 -347.8 0 d3*dpm 0 0
d3*coltend4*dpm 173.9 173.9 0 0 -173.9 -173.9 0 0
;
contrast' Coltend1 vs Coltend4 cubic beta ' d3 0
d3*coltend4 347.8 0 0 -347.8 d3*dpm 0 0
d3*coltend4*dpm 173.9 173.9 0 0 0 0 -173.9 -173.9
;
contrast' Coltend2 vs Coltend3 cubic beta ' d3 0
d3*coltend4 0 347.8 -347.8 0 d3*dpm 0 0
d3*coltend4*dpm 0 0 173.9 173.9 -173.9 -173.9 0 0
;
contrast' Coltend2 vs Coltend4 cubic beta ' d3 0
d3*coltend4 0 347.8 0 -347.8 d3*dpm 0 0
d3*coltend4*dpm 0 0 173.9 173.9 0 0 -173.9 -173.9
;
contrast' Coltend3 vs Coltend4 cubic beta ' d3 0
d3*coltend4 0 0 -347.8 347.8 d3*dpm 0 0
d3*coltend4*dpm 0 0 0 0 -173.9 -173.9 173.9 173.9
;
contrast' 12 vs 26 cubic beta ' d3 0 d3*coltend4 0
0 0 0 d3*dpm 347.8 -347.8 d3*coltend4*dpm 86.95 -86.95
86.95 -86.95 86.95 -86.95 86.95 -86.95 ;
contrast' 1_12 1_26 cubic beta ' d3 0 d3*coltend4 0
0 0 0 d3*dpm 347.8 -347.8 d3*coltend4*dpm 347.8 -347.8
0 0 0 0 ;
contrast' 1_12 2_12 cubic beta ' d3 0 d3*coltend4 347.8
-347.8 0 0 d3*dpm 0 0 d3*coltend4*dpm 347.8 0
-347.8 0 0 0 0 ;
contrast' 1_12 2_26 cubic beta ' d3 0 d3*coltend4 347.8
-347.8 0 0 d3*dpm 347.8 -347.8 d3*coltend4*dpm 347.8 0
0 -347.8 0 0 0 0 ;

```

contrast' 1_12	3_12		cubic	beta	'	d3	0	d3*coltend4	347.8
0	-347.8	0	d3*dpm	0	0	d3*coltend4*dpm	347.8	0	
0	0	-347.8	0	0	0	;			
contrast' 1_12	3_26		cubic	beta	'	d3	0	d3*coltend4	347.8
0	-347.8	0	d3*dpm	347.8	-347.8	d3*coltend4*dpm	347.8	0	
0	0	0	-347.8	0	0	;			
contrast' 1_12	4_12		cubic	beta	'	d3	0	d3*coltend4	347.8
0	0	-347.8	d3*dpm	0	0	d3*coltend4*dpm	347.8	0	
0	0	0	0	-347.8	0	;			
contrast' 1_12	4_26		cubic	beta	'	d3	0	d3*coltend4	347.8
0	0	-347.8	d3*dpm	347.8	-347.8	d3*coltend4*dpm	347.8	0	
0	0	0	0	0	-347.8	;			
contrast' 1_26	2_12		cubic	beta	'	d3	0	d3*coltend4	347.8
-347.8	0	0	d3*dpm	-347.8	347.8	d3*coltend4*dpm	0	347.8	
-347.8	0	0	0	0	0	;			
contrast' 1_26	2_26		cubic	beta	'	d3	0	d3*coltend4	347.8
-347.8	0	0	d3*dpm	0	0	d3*coltend4*dpm	0	347.8	
0	-347.8	0	0	0	0	;			
contrast' 1_26	3_12		cubic	beta	'	d3	0	d3*coltend4	347.8
0	-347.8	0	d3*dpm	-347.8	347.8	d3*coltend4*dpm	0	347.8	
0	0	-347.8	0	0	0	;			
contrast' 1_26	3_26		cubic	beta	'	d3	0	d3*coltend4	347.8
0	-347.8	0	d3*dpm	0	0	d3*coltend4*dpm	0	347.8	
0	0	0	-347.8	0	0	;			
contrast' 1_26	4_12		cubic	beta	'	d3	0	d3*coltend4	347.8
0	0	-347.8	d3*dpm	-347.8	347.8	d3*coltend4*dpm	0	347.8	
0	0	0	0	-347.8	0	;			
contrast' 1_26	4_26		cubic	beta	'	d3	0	d3*coltend4	347.8
0	0	-347.8	d3*dpm	0	0	d3*coltend4*dpm	0	347.8	
0	0	0	0	0	-347.8	;			
contrast' 2_12	2_26		cubic	beta	'	d3	0	d3*coltend4	0
0	0	0	d3*dpm	347.8	-347.8	d3*coltend4*dpm	0	0	
347.8	-347.8	0	0	0	0	;			
contrast' 2_12	3_12		cubic	beta	'	d3	0	d3*coltend4	0
347.8	-347.8	0	d3*dpm	0	0	d3*coltend4*dpm	0	0	
347.8	0	-347.8	0	0	0	;			
contrast' 2_12	3_26		cubic	beta	'	d3	0	d3*coltend4	0
347.8	-347.8	0	d3*dpm	347.8	-347.8	d3*coltend4*dpm	0	0	
347.8	0	0	-347.8	0	0	;			
contrast' 2_12	4_12		cubic	beta	'	d3	0	d3*coltend4	0
347.8	0	-347.8	d3*dpm	0	0	d3*coltend4*dpm	0	0	
347.8	0	0	0	-347.8	0	;			
contrast' 2_12	4_26		cubic	beta	'	d3	0	d3*coltend4	0
347.8	0	-347.8	d3*dpm	347.8	-347.8	d3*coltend4*dpm	0	0	
347.8	0	0	0	0	-347.8	;			
contrast' 2_26	3_12		cubic	beta	'	d3	0	d3*coltend4	0
347.8	-347.8	0	d3*dpm	-347.8	347.8	d3*coltend4*dpm	0	0	
0	347.8	-347.8	0	0	0	;			
contrast' 2_26	3_26		cubic	beta	'	d3	0	d3*coltend4	0
347.8	-347.8	0	d3*dpm	0	0	d3*coltend4*dpm	0	0	
0	347.8	0	-347.8	0	0	;			
contrast' 2_26	4_12		cubic	beta	'	d3	0	d3*coltend4	0
347.8	0	-347.8	d3*dpm	-347.8	347.8	d3*coltend4*dpm	0	0	
0	347.8	0	0	-347.8	0	;			

```

contrast' 2_26 4_26 cubic beta ' d3 0 d3*coltend4 0
          347.8 0 -347.8 d3*dpm 0 0 d3*coltend4*dpm 0 0
          0 347.8 0 0 0 -347.8 ;
contrast' 3_12 3_26 cubic beta ' d3 0 d3*coltend4 0
          0 0 0 d3*dpm 347.8 -347.8 d3*coltend4*dpm 0 0
          0 0 347.8 -347.8 0 0 ;
contrast' 3_12 4_12 cubic beta ' d3 0 d3*coltend4 0
          0 347.8 -347.8 d3*dpm 0 0 d3*coltend4*dpm 0 0
          0 0 347.8 0 -347.8 0 ;
contrast' 3_12 4_26 cubic beta ' d3 0 d3*coltend4 0
          0 347.8 -347.8 d3*dpm 347.8 -347.8 d3*coltend4*dpm 0 0
          0 0 347.8 0 0 -347.8 ;
contrast' 3_26 4_12 cubic beta ' d3 0 d3*coltend4 0
          0 347.8 -347.8 d3*dpm -347.8 347.8 d3*coltend4*dpm 0 0
          0 0 0 347.8 -347.8 0 ;
contrast' 3_26 4_26 cubic beta ' d3 0 d3*coltend4 0
          0 347.8 -347.8 d3*dpm 0 0 d3*coltend4*dpm 0 0
          0 0 0 347.8 0 -347.8 ;
contrast' 4_12 4_26 cubic beta ' d3 0 d3*coltend4 0
          0 0 0 d3*dpm 347.8 -347.8 d3*coltend4*dpm 0 0
          0 0 0 0 347.8 -347.8 ;

```

run;

```

data predval; set predval;
if cx <=599 then delete;
trt = catx('_', coltend4, dpm);
run;
proc sort data = predval; by coltend4 d; run;

```

```

proc means data = predval mean ;
by coltend4;
var pred;
OUTPUT OUT=cluster MEAN=;
run;

```

```

proc sgplot data=predval ;
title ' ';
series x = d y = pred/ group = trt markers name = "series";
*scatter x=d y=pred/ group = dcc2 name="fit" ;
axis label = "Day of display" values=(0 to 11 by 1) ;
yaxis label = "ha reflectance values" values = (0 to 50 by 5) ;
keylegend "series" / across = 3 noborder location = outside position = bottom ;
*keylegend "fit" / location=outside position=bottomleft;

```

run;

```

proc means data = predval mean ;
by coltend4 d;
var pred;
OUTPUT OUT=cluster MEAN=;
run;

```

```

proc sgplot data=cluster ;

```

```

        title ' ';
series x = d y = pred/ group = coltend4 markers name = "series";
*scatter x=d y=pred/ group = dcc2 name="fit" ;
        xaxis label = "Day of display" values=(0 to 11 by 1) ;
        yaxis label = "ha reflectance values" values = (0 to 50 by 5) ;
keylegend "series" / across = 3 noborder location = outside position = bottom ;
*keylegend "fit" / location=outside position=bottomleft;

```

```
run;
```

```
proc sort data = predval; by dpm d; run;
```

```
proc means data = predval mean ;
by dpm ;
var pred;
OUTPUT OUT=dpm MEAN=;
run;
```

```
proc means data = predval mean ;
by dpm d;
var pred;
OUTPUT OUT=dpm MEAN=;
run;
```

```
proc sgplot data=dpm ;
        title ' ';
series x = d y = pred/ group = dpm markers name = "series";
        xaxis label = "Day of display" values=(0 to 11 by 1) ;
        yaxis label = "ha reflectance values" values = (0 to 50 by 5) ;
keylegend "series" / across = 3 noborder location = outside position = bottom ;
*keylegend "fit" / location=outside position=bottomleft;

```

```
run;
```

```
proc glimmix data = long ;          *noprofile ;
class STK_ID cx trip coltend4 dpm day1;
model chr = coltend4 dpm coltend4*dpm
d coltend4*d dpm*d coltend4*dpm*d
d2 coltend4*d2 dpm*d2 coltend4*dpm*d2
d3 coltend4*d3 dpm*d3 coltend4*dpm*d3
/ solution ddfm = kr ; * ;
random trip(cx) ;
random day1/ TYPE = sp(pow) (day1) sub = STK_ID residual ; * ;
output out =predval predicted = pred;;
lsmeans coltend4*dpm/ e;

```

```

estimate '          Coltend 1 12 d      12      Interceptbeta      '          Intercept1      coltend4 1
           0          0          0      dpm      1          0      coltend4*dpm      1      0          0
           0          0          0          0          0          ;
estimate '          Coltend 1          26      Interceptbeta      '          Intercept1      coltend4 1
           0          0          0      dpm      0          1      coltend4*dpm      0      1          0
           0          0          0          0          0          ;
estimate '          Coltend 2          12      Interceptbeta      '          Intercept1      coltend4 0
           1          0          0      dpm      1          0      coltend4*dpm      0      0          1
           0          0          0          0          0          ;

```

```

estimate '      Coltend 2      26      Interceptbeta      '      Intercept1      coltend4 0
          1      0      0      dpm      0      1      coltend4*dpm      0      0      0
          1      0      0      0      0      ;
estimate '      Coltend3      12      Interceptbeta      '      Intercept1      coltend4 0
          0      1      0      dpm      1      0      coltend4*dpm      0      0      0
          0      1      0      0      0      ;
estimate '      Coltend 3      26      Interceptbeta      '      Intercept1      coltend4 0
          0      1      0      dpm      0      1      coltend4*dpm      0      0      0
          0      0      1      0      0      ;
estimate '      Coltend4      12      Interceptbeta      '      Intercept1      coltend4 0
          0      0      1      dpm      1      0      coltend4*dpm      0      0      0
          0      0      0      1      0      ;
estimate '      Coltend 4      26      Interceptbeta      '      Intercept1      coltend4 0
          0      0      1      dpm      0      1      coltend4*dpm      0      0      0
          0      0      0      0      1      ;
estimate '      Coltend 1      Interceptbeta      '      Intercept1      coltend4 1
          0      0      0      dpm      0.5      0.5      coltend4*dpm      0.5      0.5      0
          0      0      0      0      0      ;
estimate '      Coltend 2      Interceptbeta      '      Intercept1      coltend4 0
          1      0      0      dpm      0.5      0.5      coltend4*dpm      0      0      0.5
          0.5      0      0      0      0      ;
estimate '      Coltend 3      Interceptbeta      '      Intercept1      coltend4 0
          0      1      0      dpm      0.5      0.5      coltend4*dpm      0      0      0
          0      0.5      0.5      0      0      ;
estimate '      Coltend 4      Interceptbeta      '      Intercept1      coltend4 0
          0      0      1      dpm      0.5      0.5      coltend4*dpm      0      0      0
          0      0      0      0.5      0.5      ;
estimate '      12      Interceptbeta      '      Intercept1      coltend4 0.25      0.25
          0.25      0.25      dpm      1      0      coltend4*dpm      0.25      0      0.25      0
          0.25      0      0.25      0      0      ;
estimate '      26      Interceptbeta      '      Intercept1      coltend4 0.25      0.25
          0.25      0.25      dpm      0      1      coltend4*dpm      0      0.25      0      0.25
          0      0.25      0      0.25      0      ;

estimate '      Coltend 1 12 d      12      linear      beta      '      d      4.6      d*coltend4
          4.6      0      0      0      d*dpm      4.6      0      d*coltend4*dpm      4.6      0
          0      0      0      0      0      0      ;
estimate '      Coltend 1      26      linear      beta      '      d      4.6      d*coltend4
          4.6      0      0      0      d*dpm      0      4.6      d*coltend4*dpm      0      4.6
          0      0      0      0      0      0      ;
estimate '      Coltend 2      12      linear      beta      '      d      4.6      d*coltend4
          0      4.6      0      0      d*dpm      4.6      0      d*coltend4*dpm      0      0
          4.6      0      0      0      0      0      ;
estimate '      Coltend 2      26      linear      beta      '      d      4.6      d*coltend4
          0      4.6      0      0      d*dpm      0      4.6      d*coltend4*dpm      0      0
          0      4.6      0      0      0      0      ;
estimate '      Coltend3      12      linear      beta      '      d      4.6      d*coltend4
          0      0      4.6      0      d*dpm      4.6      0      d*coltend4*dpm      0      0
          0      0      4.6      0      0      0      ;
estimate '      Coltend 3      26      linear      beta      '      d      4.6      d*coltend4
          0      0      4.6      0      d*dpm      0      4.6      d*coltend4*dpm      0      0
          0      0      0      4.6      0      0      ;

```

```

estimate '      Coltend4      12      linear      beta      '      d      4.6      d*coltend4
          0      0      0      4.6      d*dpm      4.6      0      d*coltend4*dpm      0      0
          0      0      0      0      4.6      0      ;
estimate '      Coltend 4      26      linear      beta      '      d      4.6      d*coltend4
          0      0      0      4.6      d*dpm      0      4.6      d*coltend4*dpm      0      0
          0      0      0      0      0      4.6      ;
estimate '      Coltend 1      linear      beta      '      d      4.6      d*coltend4
          4.6      0      0      0      d*dpm      2.3      2.3      d*coltend4*dpm      2.3      2.3
          0      0      0      0      0      0      ;
estimate '      Coltend 2      linear      beta      '      d      4.6      d*coltend4
          0      4.6      0      0      d*dpm      2.3      2.3      d*coltend4*dpm      0      0
          2.3      2.3      0      0      0      0      ;
estimate '      Coltend 3      linear      beta      '      d      4.6      d*coltend4
          0      0      4.6      0      d*dpm      2.3      2.3      d*coltend4*dpm      0      0
          0      0      2.3      2.3      0      0      ;
estimate '      Coltend 4      linear      beta      '      d      4.6      d*coltend4
          0      0      0      4.6      d*dpm      2.3      2.3      d*coltend4*dpm      0      0
          0      0      0      0      2.3      2.3      ;
estimate '      12      linear      beta      '      d      4.6      d*coltend4      1.15
          1.15      1.15      1.15      d*dpm      4.6      0      d*coltend4*dpm      1.15      0      1.15
          0      1.15      0      1.15      0      ;
estimate '      26      linear      beta      '      d      4.6      d*coltend4      1.15
          1.15      1.15      1.15      d*dpm      0      4.6      d*coltend4*dpm      0      1.15      0
          1.15      0      1.15      0      1.15      ;

estimate '      Coltend 1 12 d      12      quadratic      beta      '      d2      37.4
          d2*coltend4      37.4      0      0      0      d2*dpm      37.4      0
          d2*coltend4*dpm      37.4      0      0      0      0      0      0      0      0
;
estimate '      Coltend 1      26      quadratic      beta      '      d2      37.4
          d2*coltend4      37.4      0      0      0      d2*dpm      0      37.4
          d2*coltend4*dpm      0      37.4      0      0      0      0      0      0      0
;
estimate '      Coltend 2      12      quadratic      beta      '      d2      37.4
          d2*coltend4      0      37.4      0      0      d2*dpm      37.4      0
          d2*coltend4*dpm      0      0      37.4      0      0      0      0      0      0
;
estimate '      Coltend 2      26      quadratic      beta      '      d2      37.4
          d2*coltend4      0      37.4      0      0      d2*dpm      0      37.4
          d2*coltend4*dpm      0      0      0      37.4      0      0      0      0      0
;
estimate '      Coltend3      12      quadratic      beta      '      d2      37.4
          d2*coltend4      0      0      37.4      0      d2*dpm      37.4      0
          d2*coltend4*dpm      0      0      0      0      0      37.4      0      0      0
;
estimate '      Coltend 3      26      quadratic      beta      '      d2      37.4
          d2*coltend4      0      0      37.4      0      d2*dpm      0      37.4
          d2*coltend4*dpm      0      0      0      0      0      0      37.4      0      0
;
estimate '      Coltend4      12      quadratic      beta      '      d2      37.4
          d2*coltend4      0      0      0      37.4      d2*dpm      37.4      0
          d2*coltend4*dpm      0      0      0      0      0      0      0      37.4      0
;

```



```

estimate '      Coltend 4      26      quadratic      beta      '      d2      37.4
          d2*coltend4      0      0      0      37.4      d2*dpm      0      37.4
          d2*coltend4*dpm      0      0      0      0      0      0      0      0      37.4
;
estimate '      Coltend 1      quadratic      beta      '      d2      37.4
          d2*coltend4      37.4      0      0      0      d2*dpm      18.7      18.7
          d2*coltend4*dpm      18.7      18.7      0      0      0      0      0      0      0
;
estimate '      Coltend 2      quadratic      beta      '      d2      37.4
          d2*coltend4      0      37.4      0      0      d2*dpm      18.7      18.7
          d2*coltend4*dpm      0      0      18.7      18.7      0      0      0      0      0
;
estimate '      Coltend 3      quadratic      beta      '      d2      37.4
          d2*coltend4      0      0      37.4      0      d2*dpm      18.7      18.7
          d2*coltend4*dpm      0      0      0      0      0      18.7      18.7      0      0
;
estimate '      Coltend 4      quadratic      beta      '      d2      37.4
          d2*coltend4      0      0      0      37.4      d2*dpm      18.7      18.7
          d2*coltend4*dpm      0      0      0      0      0      0      0      18.7      18.7
;
estimate '      12      quadratic      beta      '      d2      37.4      d2*coltend4
          9.35      9.35      9.35      9.35      d2*dpm      37.4      0      d2*coltend4*dpm      9.35
          0      9.35      0      9.35      0      9.35      0      ;
estimate '      26      quadratic      beta      '      d2      37.4      d2*coltend4
          9.35      9.35      9.35      9.35      d2*dpm      0      37.4      d2*coltend4*dpm      0
          9.35      0      9.35      0      9.35      0      9.35      ;
;
estimate '      Coltend 1 12 d      12      cubic      beta      '      d3      347.8      d3*coltend4
          347.8      0      0      0      d3*dpm      347.8      0      d3*coltend4*dpm      347.8
          0      0      0      0      0      0      0      ;
estimate '      Coltend 1      26      cubic      beta      '      d3      347.8      d3*coltend4
          347.8      0      0      0      d3*dpm      0      347.8      d3*coltend4*dpm      0
          347.8      0      0      0      0      0      0      ;
estimate '      Coltend 2      12      cubic      beta      '      d3      347.8      d3*coltend4
          0      347.8      0      0      d3*dpm      347.8      0      d3*coltend4*dpm      0
          0      347.8      0      0      0      0      0      ;
estimate '      Coltend 2      26      cubic      beta      '      d3      347.8      d3*coltend4
          0      347.8      0      0      d3*dpm      0      347.8      d3*coltend4*dpm      0
          0      0      347.8      0      0      0      0      ;
estimate '      Coltend3      12      cubic      beta      '      d3      347.8      d3*coltend4
          0      0      347.8      0      d3*dpm      347.8      0      d3*coltend4*dpm      0
          0      0      0      347.8      0      0      0      ;
estimate '      Coltend 3      26      cubic      beta      '      d3      347.8      d3*coltend4
          0      0      347.8      0      d3*dpm      0      347.8      d3*coltend4*dpm      0
          0      0      0      0      347.8      0      0      ;
estimate '      Coltend4      12      cubic      beta      '      d3      347.8      d3*coltend4
          0      0      0      347.8      d3*dpm      347.8      0      d3*coltend4*dpm      0
          0      0      0      0      0      347.8      0      ;
estimate '      Coltend 4      26      cubic      beta      '      d3      347.8      d3*coltend4
          0      0      0      347.8      d3*dpm      0      347.8      d3*coltend4*dpm      0
          0      0      0      0      0      0      347.8      ;
estimate '      Coltend 1      cubic      beta      '      d3      347.8      d3*coltend4
          347.8      0      0      0      d3*dpm      173.9      173.9      d3*coltend4*dpm      173.9
          173.9      0      0      0      0      0      0      ;

```

```

estimate '      Coltend 2      cubic beta '      d3      347.8      d3*coltend4
          0      347.8      0      0      d3*dpm 173.9      173.9      d3*coltend4*dpm      0
          0      173.9      173.9      0      0      0      0      ;
estimate '      Coltend 3      cubic beta '      d3      347.8      d3*coltend4
          0      0      347.8      0      d3*dpm 173.9      173.9      d3*coltend4*dpm      0
          0      0      0      173.9      173.9      0      0      ;
estimate '      Coltend 4      cubic beta '      d3      347.8      d3*coltend4
          0      0      0      347.8      d3*dpm 173.9      173.9      d3*coltend4*dpm      0
          0      0      0      0      0      173.9      173.9      ;
estimate '      12      cubic beta '      d3      347.8      d3*coltend4      86.95
          86.95      86.95      86.95      d3*dpm 347.8      0      d3*coltend4*dpm      86.95      0
          86.95      0      86.95      0      86.95      0      ;
estimate '      26      cubic beta '      d3      347.8      d3*coltend4      86.95
          86.95      86.95      86.95      d3*dpm 0      347.8      d3*coltend4*dpm      0      86.95
          0      86.95      0      86.95      0      86.95      ;
contrast' Coltend1 vs Coltend2      Interceptbeta '      Intercept0      coltend4
          1      -1      0      0      dpm      0      0      coltend4*dpm      0.5      0.5
          -0.5      -0.5      0      0      0      0      ;
contrast' Coltend1 vs Coltend3      Interceptbeta '      Intercept0      coltend4
          1      0      -1      0      dpm      0      0      coltend4*dpm      0.5      0.5
          0      0      -0.5      -0.5      0      0      ;
contrast' Coltend1 vs Coltend4      Interceptbeta '      Intercept0      coltend4
          1      0      0      -1      dpm      0      0      coltend4*dpm      0.5      0.5
          0      0      0      0      -0.5      -0.5      ;
contrast' Coltend2 vs Coltend3      Interceptbeta '      Intercept0      coltend4
          0      1      -1      0      dpm      0      0      coltend4*dpm      0      0
          0.5      0.5      -0.5      -0.5      0      0      ;
contrast' Coltend2 vs Coltend4      Interceptbeta '      Intercept0      coltend4
          0      1      0      -1      dpm      0      0      coltend4*dpm      0      0
          0.5      0.5      0      0      -0.5      -0.5      ;
contrast' Coltend3 vs Coltend4      Interceptbeta '      Intercept0      coltend4
          0      0      -1      1      dpm      0      0      coltend4*dpm      0      0
          0      0      -0.5      -0.5      0.5      0.5      ;
contrast' 12 vs 26      Interceptbeta '      Intercept0      coltend4      0      0
          0      0      dpm      1      -1      coltend4*dpm      0.25      -0.25      0.25      -0.25
          0.25      -0.25      0.25      -0.25      ;
contrast' 1_12 1_26      Interceptbeta '      Intercept0      coltend4      0      0
          0      0      dpm      1      -1      coltend4*dpm      1      -1      0      0
          0      0      0      0      ;
contrast' 1_12 2_12      Interceptbeta '      Intercept0      coltend4      1      -1
          0      0      dpm      0      0      coltend4*dpm      1      0      -1      0
          0      0      0      0      ;
contrast' 1_12 2_26      Interceptbeta '      Intercept0      coltend4      1      -1
          0      0      dpm      1      -1      coltend4*dpm      1      0      0      -1
          0      0      0      0      ;
contrast' 1_12 3_12      Interceptbeta '      Intercept0      coltend4      1      0
          -1      0      dpm      0      0      coltend4*dpm      1      0      0      0
          -1      0      0      0      ;
contrast' 1_12 3_26      Interceptbeta '      Intercept0      coltend4      1      0
          -1      0      dpm      1      -1      coltend4*dpm      1      0      0      0
          0      -1      0      0      ;
contrast' 1_12 4_12      Interceptbeta '      Intercept0      coltend4      1      0
          0      -1      dpm      0      0      coltend4*dpm      1      0      0      0
          0      0      -1      0      ;

```

contrast' 1_12	4_26		Intercept	beta	'	Intercept	0	coltend4	1	0
0	-1	dpm	1	-1		coltend4*dpm	1	0	0	0
0	0	0	-1		;					
contrast' 1_26	2_12		Intercept	beta	'	Intercept	0	coltend4	1	-1
0	0	dpm	-1	1		coltend4*dpm	0	1	-1	0
0	0	0	0		;					
contrast' 1_26	2_26		Intercept	beta	'	Intercept	0	coltend4	1	-1
0	0	dpm	0	0		coltend4*dpm	0	1	0	-1
0	0	0	0		;					
contrast' 1_26	3_12		Intercept	beta	'	Intercept	0	coltend4	1	0
-1	0	dpm	-1	1		coltend4*dpm	0	1	0	0
-1	0	0	0		;					
contrast' 1_26	3_26		Intercept	beta	'	Intercept	0	coltend4	1	0
-1	0	dpm	0	0		coltend4*dpm	0	1	0	0
0	-1	0	0		;					
contrast' 1_26	4_12		Intercept	beta	'	Intercept	0	coltend4	1	0
0	-1	dpm	-1	1		coltend4*dpm	0	1	0	0
0	0	-1	0		;					
contrast' 1_26	4_26		Intercept	beta	'	Intercept	0	coltend4	1	0
0	-1	dpm	0	0		coltend4*dpm	0	1	0	0
0	0	0	-1		;					
contrast' 2_12	2_26		Intercept	beta	'	Intercept	0	coltend4	0	0
0	0	dpm	1	-1		coltend4*dpm	0	0	1	-1
0	0	0	0		;					
contrast' 2_12	3_12		Intercept	beta	'	Intercept	0	coltend4	0	1
-1	0	dpm	0	0		coltend4*dpm	0	0	1	0
-1	0	0	0		;					
contrast' 2_12	3_26		Intercept	beta	'	Intercept	0	coltend4	0	1
-1	0	dpm	1	-1		coltend4*dpm	0	0	1	0
0	-1	0	0		;					
contrast' 2_12	4_12		Intercept	beta	'	Intercept	0	coltend4	0	1
0	-1	dpm	0	0		coltend4*dpm	0	0	1	0
0	0	-1	0		;					
contrast' 2_12	4_26		Intercept	beta	'	Intercept	0	coltend4	0	1
0	-1	dpm	1	-1		coltend4*dpm	0	0	1	0
0	0	0	-1		;					
contrast' 2_26	3_12		Intercept	beta	'	Intercept	0	coltend4	0	1
-1	0	dpm	-1	1		coltend4*dpm	0	0	0	1
-1	0	0	0		;					
contrast' 2_26	3_26		Intercept	beta	'	Intercept	0	coltend4	0	1
-1	0	dpm	0	0		coltend4*dpm	0	0	0	1
0	-1	0	0		;					
contrast' 2_26	4_12		Intercept	beta	'	Intercept	0	coltend4	0	1
0	-1	dpm	-1	1		coltend4*dpm	0	0	0	1
0	0	-1	0		;					
contrast' 2_26	4_26		Intercept	beta	'	Intercept	0	coltend4	0	1
0	-1	dpm	0	0		coltend4*dpm	0	0	0	1
0	0	0	-1		;					
contrast' 3_12	3_26		Intercept	beta	'	Intercept	0	coltend4	0	0
0	0	dpm	1	-1		coltend4*dpm	0	0	0	0
1	-1	0	0		;					
contrast' 3_12	4_12		Intercept	beta	'	Intercept	0	coltend4	0	0
1	-1	dpm	0	0		coltend4*dpm	0	0	0	0
1	0	-1	0		;					

contrast' 3_12	4_26		Intercept	beta	'	Intercept	0	coltend4	0	0
1	-1	dpm	1	-1		coltend4*dpm	0	0	0	0
1	0	0	-1		;					
contrast' 3_26	4_12		Intercept	beta	'	Intercept	0	coltend4	0	0
1	-1	dpm	-1	1		coltend4*dpm	0	0	0	0
0	1	-1	0		;					
contrast' 3_26	4_26		Intercept	beta	'	Intercept	0	coltend4	0	0
1	-1	dpm	0	0		coltend4*dpm	0	0	0	0
0	1	0	-1		;					
contrast' 4_12	4_26		Intercept	beta	'	Intercept	0	coltend4	0	0
0	0	dpm	1	-1		coltend4*dpm	0	0	0	0
0	0	1	-1		;					
contrast' Coltend1 vs	Coltend2		linear	beta	'	d	0			
d*coltend4	4.6	-4.6	0			d*dpm	0	0	d*coltend4*dpm	
2.3	2.3	-2.3	-2.3	0		0	0	0	;	
contrast' Coltend1 vs	Coltend3		linear	beta	'	d	0			
d*coltend4	4.6	0	-4.6	0		d*dpm	0	0	d*coltend4*dpm	
2.3	2.3	0	0	-2.3		-2.3	0	0	;	
contrast' Coltend1 vs	Coltend4		linear	beta	'	d	0			
d*coltend4	4.6	0	0	-4.6		d*dpm	0	0	d*coltend4*dpm	
2.3	2.3	0	0	0		0	-2.3	-2.3	;	
contrast' Coltend2 vs	Coltend3		linear	beta	'	d	0			
d*coltend4	0	4.6	-4.6	0		d*dpm	0	0	d*coltend4*dpm	
0	0	2.3	2.3	-2.3		-2.3	0	0	;	
contrast' Coltend2 vs	Coltend4		linear	beta	'	d	0			
d*coltend4	0	4.6	0	-4.6		d*dpm	0	0	d*coltend4*dpm	
0	0	2.3	2.3	0		0	-2.3	-2.3	;	
contrast' Coltend3 vs	Coltend4		linear	beta	'	d	0			
d*coltend4	0	0	-4.6	4.6		d*dpm	0	0	d*coltend4*dpm	
0	0	0	0	-2.3		-2.3	2.3	2.3	;	
contrast' 12 vs	26		linear	beta	'	d	0	d*coltend4	0	
0	0	0	d*dpm	4.6		-4.6	d*coltend4*dpm	1.15	-1.15	1.15
-1.15	1.15	-1.15	1.15	-1.15		;				
contrast' 1_12	1_26		linear	beta	'	d	0	d*coltend4	0	
0	0	0	d*dpm	4.6		-4.6	d*coltend4*dpm	4.6	-4.6	0
0	0	0	0	0		;				
contrast' 1_12	2_12		linear	beta	'	d	0	d*coltend4	4.6	
-4.6	0	0	d*dpm	0		0	d*coltend4*dpm	4.6	0	-4.6
0	0	0	0	0		;				
contrast' 1_12	2_26		linear	beta	'	d	0	d*coltend4	4.6	
-4.6	0	0	d*dpm	4.6		-4.6	d*coltend4*dpm	4.6	0	0
-4.6	0	0	0	0		;				
contrast' 1_12	3_12		linear	beta	'	d	0	d*coltend4	4.6	
0	-4.6	0	d*dpm	0		0	d*coltend4*dpm	4.6	0	0
0	-4.6	0	0	0		;				
contrast' 1_12	3_26		linear	beta	'	d	0	d*coltend4	4.6	
0	-4.6	0	d*dpm	4.6		-4.6	d*coltend4*dpm	4.6	0	0
0	0	-4.6	0	0		;				
contrast' 1_12	4_12		linear	beta	'	d	0	d*coltend4	4.6	
0	0	-4.6	d*dpm	0		0	d*coltend4*dpm	4.6	0	0
0	0	0	-4.6	0		;				
contrast' 1_12	4_26		linear	beta	'	d	0	d*coltend4	4.6	
0	0	-4.6	d*dpm	4.6		-4.6	d*coltend4*dpm	4.6	0	0
0	0	0	0	-4.6		;				

contrast' 1_26	2_12		linear	beta	'	d	0	d*coltend4	4.6
	-4.6	0	d*dpm	-4.6	4.6	d*coltend4*dpm	0	4.6	-4.6
	0	0	0	0	;				
contrast' 1_26	2_26		linear	beta	'	d	0	d*coltend4	4.6
	-4.6	0	d*dpm	0	0	d*coltend4*dpm	0	4.6	0
	-4.6	0	0	0	;				
contrast' 1_26	3_12		linear	beta	'	d	0	d*coltend4	4.6
	0	-4.6	d*dpm	-4.6	4.6	d*coltend4*dpm	0	4.6	0
	0	-4.6	0	0	;				
contrast' 1_26	3_26		linear	beta	'	d	0	d*coltend4	4.6
	0	-4.6	d*dpm	0	0	d*coltend4*dpm	0	4.6	0
	0	0	0	0	;				
contrast' 1_26	4_12		linear	beta	'	d	0	d*coltend4	4.6
	0	0	d*dpm	-4.6	4.6	d*coltend4*dpm	0	4.6	0
	0	0	-4.6	0	;				
contrast' 1_26	4_26		linear	beta	'	d	0	d*coltend4	4.6
	0	0	d*dpm	0	0	d*coltend4*dpm	0	4.6	0
	0	0	0	-4.6	;				
contrast' 2_12	2_26		linear	beta	'	d	0	d*coltend4	0
	0	0	d*dpm	4.6	-4.6	d*coltend4*dpm	0	0	4.6
	-4.6	0	0	0	;				
contrast' 2_12	3_12		linear	beta	'	d	0	d*coltend4	0
	4.6	-4.6	d*dpm	0	0	d*coltend4*dpm	0	0	4.6
	0	-4.6	0	0	;				
contrast' 2_12	3_26		linear	beta	'	d	0	d*coltend4	0
	4.6	-4.6	d*dpm	4.6	-4.6	d*coltend4*dpm	0	0	4.6
	0	0	0	0	;				
contrast' 2_12	4_12		linear	beta	'	d	0	d*coltend4	0
	4.6	0	d*dpm	0	0	d*coltend4*dpm	0	0	4.6
	0	0	-4.6	0	;				
contrast' 2_12	4_26		linear	beta	'	d	0	d*coltend4	0
	4.6	0	d*dpm	4.6	-4.6	d*coltend4*dpm	0	0	4.6
	0	0	0	-4.6	;				
contrast' 2_26	3_12		linear	beta	'	d	0	d*coltend4	0
	4.6	-4.6	d*dpm	-4.6	4.6	d*coltend4*dpm	0	0	0
	4.6	-4.6	0	0	;				
contrast' 2_26	3_26		linear	beta	'	d	0	d*coltend4	0
	4.6	-4.6	d*dpm	0	0	d*coltend4*dpm	0	0	0
	4.6	0	0	0	;				
contrast' 2_26	4_12		linear	beta	'	d	0	d*coltend4	0
	4.6	0	d*dpm	-4.6	4.6	d*coltend4*dpm	0	0	0
	4.6	0	-4.6	0	;				
contrast' 2_26	4_26		linear	beta	'	d	0	d*coltend4	0
	4.6	0	d*dpm	0	0	d*coltend4*dpm	0	0	0
	4.6	0	0	-4.6	;				
contrast' 3_12	3_26		linear	beta	'	d	0	d*coltend4	0
	0	0	d*dpm	4.6	-4.6	d*coltend4*dpm	0	0	0
	0	4.6	0	0	;				
contrast' 3_12	4_12		linear	beta	'	d	0	d*coltend4	0
	0	4.6	d*dpm	0	0	d*coltend4*dpm	0	0	0
	0	4.6	-4.6	0	;				
contrast' 3_12	4_26		linear	beta	'	d	0	d*coltend4	0
	0	4.6	d*dpm	4.6	-4.6	d*coltend4*dpm	0	0	0
	0	4.6	0	-4.6	;				

```

contrast' 3_26 4_12 linear beta ' d 0 d*coltend4 0
0 4.6 -4.6 d*dpm -4.6 4.6 d*coltend4*dpm 0 0 0
0 0 4.6 -4.6 0 ;
contrast' 3_26 4_26 linear beta ' d 0 d*coltend4 0
0 4.6 -4.6 d*dpm 0 0 d*coltend4*dpm 0 0 0
0 0 4.6 0 -4.6 ;
contrast' 4_12 4_26 linear beta ' d 0 d*coltend4 0
0 0 0 d*dpm 4.6 -4.6 d*coltend4*dpm 0 0 0
0 0 0 4.6 -4.6 ;
contrast' Coltend1 vs Coltend2 quadratic beta ' d2 0
d2*coltend4 37.4 -37.4 0 0 d2*dpm 0 0
d2*coltend4*dpm 18.7 18.7 -18.7 -18.7 0 0 0
;
contrast' Coltend1 vs Coltend3 quadratic beta ' d2 0
d2*coltend4 37.4 0 -37.4 0 d2*dpm 0 0
d2*coltend4*dpm 18.7 18.7 0 0 -18.7 -18.7 0 0
;
contrast' Coltend1 vs Coltend4 quadratic beta ' d2 0
d2*coltend4 37.4 0 0 -37.4 d2*dpm 0 0
d2*coltend4*dpm 18.7 18.7 0 0 0 -18.7 -18.7
;
contrast' Coltend2 vs Coltend3 quadratic beta ' d2 0
d2*coltend4 0 37.4 -37.4 0 d2*dpm 0 0
d2*coltend4*dpm 0 0 18.7 18.7 -18.7 -18.7 0 0
;
contrast' Coltend2 vs Coltend4 quadratic beta ' d2 0
d2*coltend4 0 37.4 0 -37.4 d2*dpm 0 0
d2*coltend4*dpm 0 0 18.7 18.7 0 0 -18.7 -18.7
;
contrast' Coltend3 vs Coltend4 quadratic beta ' d2 0
d2*coltend4 0 0 -37.4 37.4 d2*dpm 0 0
d2*coltend4*dpm 0 0 0 0 -18.7 -18.7 18.7 18.7
;
contrast' 12 vs 26 quadratic beta ' d2 0 d2*coltend4
0 0 0 0 d2*dpm 37.4 -37.4 d2*coltend4*dpm 9.35
-9.35 9.35 -9.35 9.35 -9.35 9.35 -9.35 ;
contrast' 1_12 1_26 quadratic beta ' d2 0 d2*coltend4
0 0 0 0 d2*dpm 37.4 -37.4 d2*coltend4*dpm 37.4
-37.4 0 0 0 0 ;
contrast' 1_12 2_12 quadratic beta ' d2 0 d2*coltend4
37.4 -37.4 0 0 d2*dpm 0 0 d2*coltend4*dpm 37.4
0 -37.4 0 0 0 0 ;
contrast' 1_12 2_26 quadratic beta ' d2 0 d2*coltend4
37.4 -37.4 0 0 d2*dpm 37.4 -37.4 d2*coltend4*dpm 37.4
0 0 -37.4 0 0 0 ;
contrast' 1_12 3_12 quadratic beta ' d2 0 d2*coltend4
37.4 0 -37.4 0 d2*dpm 0 0 d2*coltend4*dpm 37.4
0 0 0 -37.4 0 0 ;
contrast' 1_12 3_26 quadratic beta ' d2 0 d2*coltend4
37.4 0 -37.4 0 d2*dpm 37.4 -37.4 d2*coltend4*dpm 37.4
0 0 0 0 -37.4 0 0 ;
contrast' 1_12 4_12 quadratic beta ' d2 0 d2*coltend4
37.4 0 0 -37.4 d2*dpm 0 0 d2*coltend4*dpm 37.4
0 0 0 0 0 -37.4 0 ;

```

contrast' 1_12	4_26		quadratic	beta	'	d2	0	d2*coltend4
37.4	0	0	-37.4	d2*dpm	37.4	-37.4	d2*coltend4*dpm	37.4
0	0	0	0	0	0	-37.4		
contrast' 1_26	2_12		quadratic	beta	'	d2	0	d2*coltend4
37.4	-37.4	0	0	d2*dpm	-37.4	37.4	d2*coltend4*dpm	0
37.4	-37.4	0	0	0	0	0		
contrast' 1_26	2_26		quadratic	beta	'	d2	0	d2*coltend4
37.4	-37.4	0	0	d2*dpm	0	0	d2*coltend4*dpm	0
37.4	0	-37.4	0	0	0	0		
contrast' 1_26	3_12		quadratic	beta	'	d2	0	d2*coltend4
37.4	0	-37.4	0	d2*dpm	-37.4	37.4	d2*coltend4*dpm	0
37.4	0	0	-37.4	0	0	0		
contrast' 1_26	3_26		quadratic	beta	'	d2	0	d2*coltend4
37.4	0	-37.4	0	d2*dpm	0	0	d2*coltend4*dpm	0
37.4	0	0	0	-37.4	0	0		
contrast' 1_26	4_12		quadratic	beta	'	d2	0	d2*coltend4
37.4	0	0	-37.4	d2*dpm	-37.4	37.4	d2*coltend4*dpm	0
37.4	0	0	0	0	-37.4	0		
contrast' 1_26	4_26		quadratic	beta	'	d2	0	d2*coltend4
37.4	0	0	-37.4	d2*dpm	0	0	d2*coltend4*dpm	0
37.4	0	0	0	0	0	-37.4		
contrast' 2_12	2_26		quadratic	beta	'	d2	0	d2*coltend4
0	0	0	0	d2*dpm	37.4	-37.4	d2*coltend4*dpm	0
0	37.4	-37.4	0	0	0	0		
contrast' 2_12	3_12		quadratic	beta	'	d2	0	d2*coltend4
0	37.4	-37.4	0	d2*dpm	0	0	d2*coltend4*dpm	0
0	37.4	0	-37.4	0	0	0		
contrast' 2_12	3_26		quadratic	beta	'	d2	0	d2*coltend4
0	37.4	-37.4	0	d2*dpm	37.4	-37.4	d2*coltend4*dpm	0
0	37.4	0	0	-37.4	0	0		
contrast' 2_12	4_12		quadratic	beta	'	d2	0	d2*coltend4
0	37.4	0	-37.4	d2*dpm	0	0	d2*coltend4*dpm	0
0	37.4	0	0	0	-37.4	0		
contrast' 2_12	4_26		quadratic	beta	'	d2	0	d2*coltend4
0	37.4	0	-37.4	d2*dpm	37.4	-37.4	d2*coltend4*dpm	0
0	37.4	0	0	0	0	-37.4		
contrast' 2_26	3_12		quadratic	beta	'	d2	0	d2*coltend4
0	37.4	-37.4	0	d2*dpm	-37.4	37.4	d2*coltend4*dpm	0
0	0	37.4	-37.4	0	0	0		
contrast' 2_26	3_26		quadratic	beta	'	d2	0	d2*coltend4
0	37.4	-37.4	0	d2*dpm	0	0	d2*coltend4*dpm	0
0	0	37.4	0	-37.4	0	0		
contrast' 2_26	4_12		quadratic	beta	'	d2	0	d2*coltend4
0	37.4	0	-37.4	d2*dpm	-37.4	37.4	d2*coltend4*dpm	0
0	0	37.4	0	0	-37.4	0		
contrast' 2_26	4_26		quadratic	beta	'	d2	0	d2*coltend4
0	37.4	0	-37.4	d2*dpm	0	0	d2*coltend4*dpm	0
0	0	37.4	0	0	0	-37.4		
contrast' 3_12	3_26		quadratic	beta	'	d2	0	d2*coltend4
0	0	0	0	d2*dpm	37.4	-37.4	d2*coltend4*dpm	0
0	0	0	37.4	-37.4	0	0		
contrast' 3_12	4_12		quadratic	beta	'	d2	0	d2*coltend4
0	0	37.4	-37.4	d2*dpm	0	0	d2*coltend4*dpm	0
0	0	0	37.4	0	-37.4	0		

```

contrast' 3_12 4_26 quadratic beta ' d2 0 d2*coltend4
0 0 37.4 -37.4 d2*dpm 37.4 -37.4 d2*coltend4*dpm 0
0 0 0 37.4 0 0 -37.4 ;
contrast' 3_26 4_12 quadratic beta ' d2 0 d2*coltend4
0 0 37.4 -37.4 d2*dpm -37.4 37.4 d2*coltend4*dpm 0
0 0 0 0 37.4 -37.4 0 ;
contrast' 3_26 4_26 quadratic beta ' d2 0 d2*coltend4
0 0 37.4 -37.4 d2*dpm 0 0 d2*coltend4*dpm 0
0 0 0 0 37.4 0 -37.4 ;
contrast' 4_12 4_26 quadratic beta ' d2 0 d2*coltend4
0 0 0 0 d2*dpm 37.4 -37.4 d2*coltend4*dpm 0
0 0 0 0 0 37.4 -37.4 ;
contrast' Coltend1 vs Coltend2 cubic beta ' d3 0
d3*coltend4 347.8 -347.8 0 0 d3*dpm 0 0
d3*coltend4*dpm 173.9 173.9 -173.9 -173.9 0 0 0 0
;
contrast' Coltend1 vs Coltend3 cubic beta ' d3 0
d3*coltend4 347.8 0 -347.8 0 d3*dpm 0 0
d3*coltend4*dpm 173.9 173.9 0 0 -173.9 -173.9 0 0
;
contrast' Coltend1 vs Coltend4 cubic beta ' d3 0
d3*coltend4 347.8 0 0 -347.8 d3*dpm 0 0
d3*coltend4*dpm 173.9 173.9 0 0 0 0 -173.9 -173.9
;
contrast' Coltend2 vs Coltend3 cubic beta ' d3 0
d3*coltend4 0 347.8 -347.8 0 d3*dpm 0 0
d3*coltend4*dpm 0 0 173.9 173.9 -173.9 -173.9 0 0
;
contrast' Coltend2 vs Coltend4 cubic beta ' d3 0
d3*coltend4 0 347.8 0 -347.8 d3*dpm 0 0
d3*coltend4*dpm 0 0 173.9 173.9 0 0 -173.9 -173.9
;
contrast' Coltend3 vs Coltend4 cubic beta ' d3 0
d3*coltend4 0 0 -347.8 347.8 d3*dpm 0 0
d3*coltend4*dpm 0 0 0 0 -173.9 -173.9 173.9 173.9
;
contrast' 12 vs 26 cubic beta ' d3 0 d3*coltend4 0
0 0 0 d3*dpm 347.8 -347.8 d3*coltend4*dpm 86.95 -86.95
86.95 -86.95 86.95 -86.95 86.95 -86.95 ;
contrast' 1_12 1_26 cubic beta ' d3 0 d3*coltend4 0
0 0 0 d3*dpm 347.8 -347.8 d3*coltend4*dpm 347.8 -347.8
0 0 0 0 0 ;
contrast' 1_12 2_12 cubic beta ' d3 0 d3*coltend4 347.8
-347.8 0 0 d3*dpm 0 0 d3*coltend4*dpm 347.8 0
-347.8 0 0 0 0 0 ;
contrast' 1_12 2_26 cubic beta ' d3 0 d3*coltend4 347.8
-347.8 0 0 d3*dpm 347.8 -347.8 d3*coltend4*dpm 347.8 0
0 -347.8 0 0 0 0 ;
contrast' 1_12 3_12 cubic beta ' d3 0 d3*coltend4 347.8
0 -347.8 0 d3*dpm 0 0 d3*coltend4*dpm 347.8 0
0 0 -347.8 0 0 0 ;
contrast' 1_12 3_26 cubic beta ' d3 0 d3*coltend4 347.8
0 -347.8 0 d3*dpm 347.8 -347.8 d3*coltend4*dpm 347.8 0
0 0 0 -347.8 0 0 ;

```


contrast' 1_12	4_12		cubic	beta	'	d3	0	d3*coltend4	347.8
0	0	-347.8	d3*dpm	0	0	d3*coltend4*dpm	347.8	0	
0	0	0	0	-347.8	0	;			
contrast' 1_12	4_26		cubic	beta	'	d3	0	d3*coltend4	347.8
0	0	-347.8	d3*dpm	347.8	-347.8	d3*coltend4*dpm	347.8	0	
0	0	0	0	0	-347.8	;			
contrast' 1_26	2_12		cubic	beta	'	d3	0	d3*coltend4	347.8
-347.8	0	0	d3*dpm	-347.8	347.8	d3*coltend4*dpm	0	347.8	
-347.8	0	0	0	0	0	;			
contrast' 1_26	2_26		cubic	beta	'	d3	0	d3*coltend4	347.8
-347.8	0	0	d3*dpm	0	0	d3*coltend4*dpm	0	347.8	
0	-347.8	0	0	0	0	;			
contrast' 1_26	3_12		cubic	beta	'	d3	0	d3*coltend4	347.8
0	-347.8	0	d3*dpm	-347.8	347.8	d3*coltend4*dpm	0	347.8	
0	0	-347.8	0	0	0	;			
contrast' 1_26	3_26		cubic	beta	'	d3	0	d3*coltend4	347.8
0	-347.8	0	d3*dpm	0	0	d3*coltend4*dpm	0	347.8	
0	0	0	-347.8	0	0	;			
contrast' 1_26	4_12		cubic	beta	'	d3	0	d3*coltend4	347.8
0	0	-347.8	d3*dpm	-347.8	347.8	d3*coltend4*dpm	0	347.8	
0	0	0	0	-347.8	0	;			
contrast' 1_26	4_26		cubic	beta	'	d3	0	d3*coltend4	347.8
0	0	-347.8	d3*dpm	0	0	d3*coltend4*dpm	0	347.8	
0	0	0	0	0	-347.8	;			
contrast' 2_12	2_26		cubic	beta	'	d3	0	d3*coltend4	0
0	0	0	d3*dpm	347.8	-347.8	d3*coltend4*dpm	0	0	
347.8	-347.8	0	0	0	0	;			
contrast' 2_12	3_12		cubic	beta	'	d3	0	d3*coltend4	0
347.8	-347.8	0	d3*dpm	0	0	d3*coltend4*dpm	0	0	
347.8	0	-347.8	0	0	0	;			
contrast' 2_12	3_26		cubic	beta	'	d3	0	d3*coltend4	0
347.8	-347.8	0	d3*dpm	347.8	-347.8	d3*coltend4*dpm	0	0	
347.8	0	0	-347.8	0	0	;			
contrast' 2_12	4_12		cubic	beta	'	d3	0	d3*coltend4	0
347.8	0	-347.8	d3*dpm	0	0	d3*coltend4*dpm	0	0	
347.8	0	0	0	-347.8	0	;			
contrast' 2_12	4_26		cubic	beta	'	d3	0	d3*coltend4	0
347.8	0	-347.8	d3*dpm	347.8	-347.8	d3*coltend4*dpm	0	0	
347.8	0	0	0	0	-347.8	;			
contrast' 2_26	3_12		cubic	beta	'	d3	0	d3*coltend4	0
347.8	-347.8	0	d3*dpm	-347.8	347.8	d3*coltend4*dpm	0	0	
0	347.8	-347.8	0	0	0	;			
contrast' 2_26	3_26		cubic	beta	'	d3	0	d3*coltend4	0
347.8	-347.8	0	d3*dpm	0	0	d3*coltend4*dpm	0	0	
0	347.8	0	-347.8	0	0	;			
contrast' 2_26	4_12		cubic	beta	'	d3	0	d3*coltend4	0
347.8	0	-347.8	d3*dpm	-347.8	347.8	d3*coltend4*dpm	0	0	
0	347.8	0	0	-347.8	0	;			
contrast' 2_26	4_26		cubic	beta	'	d3	0	d3*coltend4	0
347.8	0	-347.8	d3*dpm	0	0	d3*coltend4*dpm	0	0	
0	347.8	0	0	0	-347.8	;			
contrast' 3_12	3_26		cubic	beta	'	d3	0	d3*coltend4	0
0	0	0	d3*dpm	347.8	-347.8	d3*coltend4*dpm	0	0	
0	0	347.8	-347.8	0	0	;			

```

contrast' 3_12 4_12 cubic beta ' d3 0 d3*coltend4 0
          0 347.8 -347.8 d3*dpm 0 0 d3*coltend4*dpm 0 0
          0 0 347.8 0 -347.8 0 ;
contrast' 3_12 4_26 cubic beta ' d3 0 d3*coltend4 0
          0 347.8 -347.8 d3*dpm 347.8 -347.8 d3*coltend4*dpm 0 0
          0 0 347.8 0 0 -347.8 ;
contrast' 3_26 4_12 cubic beta ' d3 0 d3*coltend4 0
          0 347.8 -347.8 d3*dpm -347.8 347.8 d3*coltend4*dpm 0 0
          0 0 0 347.8 -347.8 0 ;
contrast' 3_26 4_26 cubic beta ' d3 0 d3*coltend4 0
          0 347.8 -347.8 d3*dpm 0 0 d3*coltend4*dpm 0 0
          0 0 0 347.8 0 -347.8 ;
contrast' 4_12 4_26 cubic beta ' d3 0 d3*coltend4 0
          0 0 0 d3*dpm 347.8 -347.8 d3*coltend4*dpm 0 0
          0 0 0 0 347.8 -347.8 ;

```

```
run;
```

```

data predval; set predval;
if cx <=599 then delete;
trt = catx('_', coltend4, dpm);
run;
proc sort data = predval; by coltend4 d; run;

```

```

proc means data = predval mean ;
by coltend4;
var pred;
OUTPUT OUT=cluster MEAN=;
run;

```

```

proc sgplot data=predval ;
title ' ';
series x = d y = pred/ group = trt markers name = "series";
*scatter x=d y=pred/ group = dcc2 name="fit" ;
axis label = "Day of display" values=(0 to 11 by 1) ;
yaxis label = "chr reflectance values" values = (0 to 50 by 5) ;
keylegend "series" / across = 3 noborder location = outside position = bottom ;
*keylegend "fit" / location=outside position=bottomleft;

```

```
run;
```

```

proc means data = predval mean ;
by coltend4 d;
var pred;
OUTPUT OUT=cluster MEAN=;
run;

```

```

proc sgplot data=cluster ;
title ' ';
series x = d y = pred/ group = coltend4 markers name = "series";
*scatter x=d y=pred/ group = dcc2 name="fit" ;
axis label = "Day of display" values=(0 to 11 by 1) ;
yaxis label = "chr reflectance values" values = (0 to 50 by 5) ;
keylegend "series" / across = 3 noborder location = outside position = bottom ;

```

```

*keylegend "fit" / location=outside position=bottomleft;

run;

proc sort data = predval; by dpm d; run;

proc means data = predval mean ;
by dpm ;
var pred;
OUTPUT OUT=dpm MEAN=;
run;

proc means data = predval mean ;
by dpm d;
var pred;
OUTPUT OUT=dpm MEAN=;
run;

proc sgplot data=dpm ;
title ' ';
series x = d y = pred/ group = dpm markers name = "series";
axis label = "Day of display" values=(0 to 11 by 1) ;
yaxis label = "chr reflectance values" values = (0 to 50 by 5) ;
keylegend "series" / across = 3 noborder location = outside position = bottom ;
*keylegend "fit" / location=outside position=bottomleft;

run;

proc glimmix data = long ; *noprofile ;
class STK_ID cx trip coltend4 dpm day1;
model de = coltend4 dpm coltend4*dpm
d coltend4*d dpm*d coltend4*dpm*d
d2 coltend4*d2 dpm*d2 coltend4*dpm*d2
d3 coltend4*d3 dpm*d3 coltend4*dpm*d3
/ solution ddfm = kr ; * ;
random trip(cx) ;
random day1/ TYPE = sp(pow) (day1) sub = STK_ID residual ; * ;
output out =predval predicted = pred;;
lsmeans coltend4*dpm/ e;
estimate ' Coltend 1 12 d 12 Interceptbeta ' Intercept1 coltend4 1
0 0 0 dpm 1 0 coltend4*dpm 1 0 0
0 0 0 0 0 ;
estimate ' Coltend 1 26 Interceptbeta ' Intercept1 coltend4 1
0 0 0 dpm 0 1 coltend4*dpm 0 1 0
0 0 0 0 0 ;
estimate ' Coltend 2 12 Interceptbeta ' Intercept1 coltend4 0
1 0 0 dpm 1 0 coltend4*dpm 0 0 1
0 0 0 0 0 ;
estimate ' Coltend 2 26 Interceptbeta ' Intercept1 coltend4 0
1 0 0 dpm 0 1 coltend4*dpm 0 0 0
1 0 0 0 0 ;
estimate ' Coltend3 12 Interceptbeta ' Intercept1 coltend4 0
0 1 0 dpm 1 0 coltend4*dpm 0 0 0
0 1 0 0 0 ;

```

```

estimate '      Coltend 3      26      Interceptbeta      '      Intercept1      coltend4 0
          0      1      0      dpm      0      1      coltend4*dpm      0      0      0
          0      0      1      0      0      ;
estimate '      Coltend4      12      Interceptbeta      '      Intercept1      coltend4 0
          0      0      1      dpm      1      0      coltend4*dpm      0      0      0
          0      0      0      1      0      ;
estimate '      Coltend 4      26      Interceptbeta      '      Intercept1      coltend4 0
          0      0      1      dpm      0      1      coltend4*dpm      0      0      0
          0      0      0      0      1      ;
estimate '      Coltend 1      Interceptbeta      '      Intercept1      coltend4 1
          0      0      0      dpm      0.5      0.5      coltend4*dpm      0.5      0.5      0
          0      0      0      0      0      ;
estimate '      Coltend 2      Interceptbeta      '      Intercept1      coltend4 0
          1      0      0      dpm      0.5      0.5      coltend4*dpm      0      0      0.5
          0.5      0      0      0      0      ;
estimate '      Coltend 3      Interceptbeta      '      Intercept1      coltend4 0
          0      1      0      dpm      0.5      0.5      coltend4*dpm      0      0      0
          0      0.5      0.5      0      0      ;
estimate '      Coltend 4      Interceptbeta      '      Intercept1      coltend4 0
          0      0      1      dpm      0.5      0.5      coltend4*dpm      0      0      0
          0      0      0      0.5      0.5      ;
estimate '      12      Interceptbeta      '      Intercept1      coltend4 0.25      0.25
          0.25      0.25      dpm      1      0      coltend4*dpm      0.25      0      0.25      0
          0.25      0      0.25      0      0      ;
estimate '      26      Interceptbeta      '      Intercept1      coltend4 0.25      0.25
          0.25      0.25      dpm      0      1      coltend4*dpm      0      0.25      0      0.25
          0      0.25      0      0.25      0      ;

estimate '      Coltend 1 12 d      12      linear      beta      '      d      4.6      d*coltend4
          4.6      0      0      0      d*dpm      4.6      0      d*coltend4*dpm      4.6      0
          0      0      0      0      0      0      ;
estimate '      Coltend 1      26      linear      beta      '      d      4.6      d*coltend4
          4.6      0      0      0      d*dpm      0      4.6      d*coltend4*dpm      0      4.6
          0      0      0      0      0      0      ;
estimate '      Coltend 2      12      linear      beta      '      d      4.6      d*coltend4
          0      4.6      0      0      d*dpm      4.6      0      d*coltend4*dpm      0      0
          4.6      0      0      0      0      0      ;
estimate '      Coltend 2      26      linear      beta      '      d      4.6      d*coltend4
          0      4.6      0      0      d*dpm      0      4.6      d*coltend4*dpm      0      0
          0      4.6      0      0      0      0      ;
estimate '      Coltend3      12      linear      beta      '      d      4.6      d*coltend4
          0      0      4.6      0      d*dpm      4.6      0      d*coltend4*dpm      0      0
          0      0      4.6      0      0      0      ;
estimate '      Coltend 3      26      linear      beta      '      d      4.6      d*coltend4
          0      0      4.6      0      d*dpm      0      4.6      d*coltend4*dpm      0      0
          0      0      0      4.6      0      0      ;
estimate '      Coltend4      12      linear      beta      '      d      4.6      d*coltend4
          0      0      0      4.6      d*dpm      4.6      0      d*coltend4*dpm      0      0
          0      0      0      4.6      0      0      ;
estimate '      Coltend 4      26      linear      beta      '      d      4.6      d*coltend4
          0      0      0      4.6      d*dpm      0      4.6      d*coltend4*dpm      0      0
          0      0      0      0      0      4.6      ;

```

```

estimate '      Coltend 1      linear beta '      d      4.6      d*coltend4
      4.6      0      0      0      d*dpm 2.3      2.3      d*coltend4*dpm 2.3      2.3
      0      0      0      0      0      0      ;
estimate '      Coltend 2      linear beta '      d      4.6      d*coltend4
      0      4.6      0      0      d*dpm 2.3      2.3      d*coltend4*dpm 0      0
      2.3      2.3      0      0      0      0      ;
estimate '      Coltend 3      linear beta '      d      4.6      d*coltend4
      0      0      4.6      0      d*dpm 2.3      2.3      d*coltend4*dpm 0      0
      0      0      2.3      2.3      0      0      ;
estimate '      Coltend 4      linear beta '      d      4.6      d*coltend4
      0      0      0      4.6      d*dpm 2.3      2.3      d*coltend4*dpm 0      0
      0      0      0      0      2.3      2.3      ;
estimate '      12      linear beta '      d      4.6      d*coltend4      1.15
      1.15      1.15      1.15      d*dpm 4.6      0      d*coltend4*dpm 1.15      0      1.15
      0      1.15      0      1.15      0      ;
estimate '      26      linear beta '      d      4.6      d*coltend4      1.15
      1.15      1.15      1.15      d*dpm 0      4.6      d*coltend4*dpm 0      1.15      0
      1.15      0      1.15      0      1.15      ;

```

```

estimate '      Coltend 1 12 d      12      quadratic beta '      d2      37.4
      d2*coltend4      37.4      0      0      0      d2*dpm 37.4      0
      d2*coltend4*dpm      37.4      0      0      0      0      0      0      0
;
estimate '      Coltend 1      26      quadratic beta '      d2      37.4
      d2*coltend4      37.4      0      0      0      d2*dpm 0      37.4
      d2*coltend4*dpm      0      37.4      0      0      0      0      0      0
;
estimate '      Coltend 2      12      quadratic beta '      d2      37.4
      d2*coltend4      0      37.4      0      0      d2*dpm 37.4      0
      d2*coltend4*dpm      0      0      37.4      0      0      0      0      0
;
estimate '      Coltend 2      26      quadratic beta '      d2      37.4
      d2*coltend4      0      37.4      0      0      d2*dpm 0      37.4
      d2*coltend4*dpm      0      0      0      37.4      0      0      0      0
;
estimate '      Coltend3      12      quadratic beta '      d2      37.4
      d2*coltend4      0      0      37.4      0      d2*dpm 37.4      0
      d2*coltend4*dpm      0      0      0      0      0      37.4      0      0
;
estimate '      Coltend 3      26      quadratic beta '      d2      37.4
      d2*coltend4      0      0      37.4      0      d2*dpm 0      37.4
      d2*coltend4*dpm      0      0      0      0      0      0      37.4      0
;
estimate '      Coltend4      12      quadratic beta '      d2      37.4
      d2*coltend4      0      0      0      37.4      d2*dpm 37.4      0
      d2*coltend4*dpm      0      0      0      0      0      0      0      37.4      0
;
estimate '      Coltend 4      26      quadratic beta '      d2      37.4
      d2*coltend4      0      0      0      37.4      d2*dpm 0      37.4
      d2*coltend4*dpm      0      0      0      0      0      0      0      0      37.4
;
estimate '      Coltend 1      quadratic beta '      d2      37.4
      d2*coltend4      37.4      0      0      0      d2*dpm 18.7      18.7

```

```

d2*coltend4*dpm      18.7  18.7  0    0    0    0    0    0    0
;
estimate '          Coltend 2          quadratic  beta  '    d2    37.4
d2*coltend4    0    37.4  0    0    d2*dpm 18.7  18.7
d2*coltend4*dpm  0    0    18.7  18.7  0    0    0    0    0
;
estimate '          Coltend 3          quadratic  beta  '    d2    37.4
d2*coltend4    0    0    37.4  0    d2*dpm 18.7  18.7
d2*coltend4*dpm  0    0    0    0    0    18.7  18.7  0    0
;
estimate '          Coltend 4          quadratic  beta  '    d2    37.4
d2*coltend4    0    0    0    37.4  d2*dpm 18.7  18.7
d2*coltend4*dpm  0    0    0    0    0    0    0    18.7  18.7
;
estimate '          12    quadratic  beta  '    d2    37.4  d2*coltend4
9.35  9.35  9.35  9.35  d2*dpm 37.4  0    d2*coltend4*dpm  9.35
0    9.35  0    9.35  0    9.35  0    ;
estimate '          26    quadratic  beta  '    d2    37.4  d2*coltend4
9.35  9.35  9.35  9.35  d2*dpm 0    37.4  d2*coltend4*dpm  0
9.35  0    9.35  0    9.35  0    9.35  ;

estimate '          Coltend 1 12 d 12    cubic  beta  '    d3    347.8  d3*coltend4
347.8  0    0    0    d3*dpm 347.8  0    d3*coltend4*dpm  347.8
0    0    0    0    0    0    0    ;
estimate '          Coltend 1 26    cubic  beta  '    d3    347.8  d3*coltend4
347.8  0    0    0    d3*dpm 0    347.8  d3*coltend4*dpm  0
347.8  0    0    0    0    0    0    ;
estimate '          Coltend 2 12    cubic  beta  '    d3    347.8  d3*coltend4
0    347.8  0    0    d3*dpm 347.8  0    d3*coltend4*dpm  0
0    347.8  0    0    0    0    0    ;
estimate '          Coltend 2 26    cubic  beta  '    d3    347.8  d3*coltend4
0    347.8  0    0    d3*dpm 0    347.8  d3*coltend4*dpm  0
0    0    347.8  0    0    0    0    ;
estimate '          Coltend3 12    cubic  beta  '    d3    347.8  d3*coltend4
0    0    347.8  0    d3*dpm 347.8  0    d3*coltend4*dpm  0
0    0    0    347.8  0    0    0    ;
estimate '          Coltend 3 26    cubic  beta  '    d3    347.8  d3*coltend4
0    0    347.8  0    d3*dpm 0    347.8  d3*coltend4*dpm  0
0    0    0    0    347.8  0    0    ;
estimate '          Coltend4 12    cubic  beta  '    d3    347.8  d3*coltend4
0    0    0    347.8  d3*dpm 347.8  0    d3*coltend4*dpm  0
0    0    0    0    0    347.8  0    ;
estimate '          Coltend 4 26    cubic  beta  '    d3    347.8  d3*coltend4
0    0    0    347.8  d3*dpm 0    347.8  d3*coltend4*dpm  0
0    0    0    0    0    0    347.8  ;
estimate '          Coltend 1 12    cubic  beta  '    d3    347.8  d3*coltend4
347.8  0    0    0    d3*dpm 173.9  173.9  d3*coltend4*dpm  173.9
173.9  0    0    0    0    0    0    ;
estimate '          Coltend 2 12    cubic  beta  '    d3    347.8  d3*coltend4
0    347.8  0    0    d3*dpm 173.9  173.9  d3*coltend4*dpm  0
0    173.9  173.9  0    0    0    0    ;
estimate '          Coltend 3 12    cubic  beta  '    d3    347.8  d3*coltend4
0    0    347.8  0    d3*dpm 173.9  173.9  d3*coltend4*dpm  0
0    0    0    173.9  173.9  0    0    ;

```

```

estimate '      Coltend 4      cubic beta '      d3      347.8      d3*coltend4
          0      0      0      347.8      d3*dpm 173.9      173.9      d3*coltend4*dpm      0
          0      0      0      0      0      173.9      173.9      ;
estimate '      12      cubic beta '      d3      347.8      d3*coltend4      86.95
          86.95      86.95      86.95      d3*dpm 347.8      0      d3*coltend4*dpm      86.95      0
          86.95      0      86.95      0      86.95      0      ;
estimate '      26      cubic beta '      d3      347.8      d3*coltend4      86.95
          86.95      86.95      86.95      d3*dpm 0      347.8      d3*coltend4*dpm      0      86.95
          0      86.95      0      86.95      0      86.95      ;
contrast' Coltend1 vs      Coltend2      Interceptbeta '      Intercept0      coltend4
          1      -1      0      0      dpm      0      0      coltend4*dpm      0.5      0.5
          -0.5      -0.5      0      0      0      0      ;
contrast' Coltend1 vs      Coltend3      Interceptbeta '      Intercept0      coltend4
          1      0      -1      0      dpm      0      0      coltend4*dpm      0.5      0.5
          0      0      -0.5      -0.5      0      0      ;
contrast' Coltend1 vs      Coltend4      Interceptbeta '      Intercept0      coltend4
          1      0      0      -1      dpm      0      0      coltend4*dpm      0.5      0.5
          0      0      0      0      -0.5      -0.5      ;
contrast' Coltend2 vs      Coltend3      Interceptbeta '      Intercept0      coltend4
          0      1      -1      0      dpm      0      0      coltend4*dpm      0      0
          0.5      0.5      -0.5      -0.5      0      0      ;
contrast' Coltend2 vs      Coltend4      Interceptbeta '      Intercept0      coltend4
          0      1      0      -1      dpm      0      0      coltend4*dpm      0      0
          0.5      0.5      0      0      -0.5      -0.5      ;
contrast' Coltend3 vs      Coltend4      Interceptbeta '      Intercept0      coltend4
          0      0      -1      1      dpm      0      0      coltend4*dpm      0      0
          0      0      -0.5      -0.5      0.5      0.5      ;
contrast' 12 vs      26      Interceptbeta '      Intercept0      coltend4 0      0
          0      0      dpm      1      -1      coltend4*dpm      0.25      -0.25      0.25      -0.25
          0.25      -0.25      0.25      -0.25      ;
contrast' 1_12      1_26      Interceptbeta '      Intercept0      coltend4 0      0
          0      0      dpm      1      -1      coltend4*dpm      1      -1      0      0
          0      0      0      0      ;
contrast' 1_12      2_12      Interceptbeta '      Intercept0      coltend4 1      -1
          0      0      dpm      0      0      coltend4*dpm      1      0      -1      0
          0      0      0      0      ;
contrast' 1_12      2_26      Interceptbeta '      Intercept0      coltend4 1      -1
          0      0      dpm      1      -1      coltend4*dpm      1      0      0      -1
          0      0      0      0      ;
contrast' 1_12      3_12      Interceptbeta '      Intercept0      coltend4 1      0
          -1      0      dpm      0      0      coltend4*dpm      1      0      0      0
          -1      0      0      0      ;
contrast' 1_12      3_26      Interceptbeta '      Intercept0      coltend4 1      0
          -1      0      dpm      1      -1      coltend4*dpm      1      0      0      0
          0      -1      0      0      ;
contrast' 1_12      4_12      Interceptbeta '      Intercept0      coltend4 1      0
          0      -1      dpm      0      0      coltend4*dpm      1      0      0      0
          0      0      -1      0      ;
contrast' 1_12      4_26      Interceptbeta '      Intercept0      coltend4 1      0
          0      -1      dpm      1      -1      coltend4*dpm      1      0      0      0
          0      0      0      -1      ;
contrast' 1_26      2_12      Interceptbeta '      Intercept0      coltend4 1      -1
          0      0      dpm      -1      1      coltend4*dpm      0      1      -1      0
          0      0      0      0      ;

```

contrast' 1_26	2_26		Intercept	beta	'	Intercept	0	coltend4	1	-1
0	0	dpm	0	0		coltend4*dpm	0	1	0	-1
0	0	0	0	;						
contrast' 1_26	3_12		Intercept	beta	'	Intercept	0	coltend4	1	0
-1	0	dpm	-1	1		coltend4*dpm	0	1	0	0
-1	0	0	0	;						
contrast' 1_26	3_26		Intercept	beta	'	Intercept	0	coltend4	1	0
-1	0	dpm	0	0		coltend4*dpm	0	1	0	0
0	-1	0	0	;						
contrast' 1_26	4_12		Intercept	beta	'	Intercept	0	coltend4	1	0
0	-1	dpm	-1	1		coltend4*dpm	0	1	0	0
0	0	-1	0	;						
contrast' 1_26	4_26		Intercept	beta	'	Intercept	0	coltend4	1	0
0	-1	dpm	0	0		coltend4*dpm	0	1	0	0
0	0	0	-1	;						
contrast' 2_12	2_26		Intercept	beta	'	Intercept	0	coltend4	0	0
0	0	dpm	1	-1		coltend4*dpm	0	0	1	-1
0	0	0	0	;						
contrast' 2_12	3_12		Intercept	beta	'	Intercept	0	coltend4	0	1
-1	0	dpm	0	0		coltend4*dpm	0	0	1	0
-1	0	0	0	;						
contrast' 2_12	3_26		Intercept	beta	'	Intercept	0	coltend4	0	1
-1	0	dpm	1	-1		coltend4*dpm	0	0	1	0
0	-1	0	0	;						
contrast' 2_12	4_12		Intercept	beta	'	Intercept	0	coltend4	0	1
0	-1	dpm	0	0		coltend4*dpm	0	0	1	0
0	0	-1	0	;						
contrast' 2_12	4_26		Intercept	beta	'	Intercept	0	coltend4	0	1
0	-1	dpm	1	-1		coltend4*dpm	0	0	1	0
0	0	0	-1	;						
contrast' 2_26	3_12		Intercept	beta	'	Intercept	0	coltend4	0	1
-1	0	dpm	-1	1		coltend4*dpm	0	0	0	1
-1	0	0	0	;						
contrast' 2_26	3_26		Intercept	beta	'	Intercept	0	coltend4	0	1
-1	0	dpm	0	0		coltend4*dpm	0	0	0	1
0	-1	0	0	;						
contrast' 2_26	4_12		Intercept	beta	'	Intercept	0	coltend4	0	1
0	-1	dpm	-1	1		coltend4*dpm	0	0	0	1
0	0	-1	0	;						
contrast' 2_26	4_26		Intercept	beta	'	Intercept	0	coltend4	0	1
0	-1	dpm	0	0		coltend4*dpm	0	0	0	1
0	0	0	-1	;						
contrast' 3_12	3_26		Intercept	beta	'	Intercept	0	coltend4	0	0
0	0	dpm	1	-1		coltend4*dpm	0	0	0	0
1	-1	0	0	;						
contrast' 3_12	4_12		Intercept	beta	'	Intercept	0	coltend4	0	0
1	-1	dpm	0	0		coltend4*dpm	0	0	0	0
1	0	-1	0	;						
contrast' 3_12	4_26		Intercept	beta	'	Intercept	0	coltend4	0	0
1	-1	dpm	1	-1		coltend4*dpm	0	0	0	0
1	0	0	-1	;						
contrast' 3_26	4_12		Intercept	beta	'	Intercept	0	coltend4	0	0
1	-1	dpm	-1	1		coltend4*dpm	0	0	0	0
0	1	-1	0	;						

contrast'	3_26	4_26		Intercept	beta	'	Intercept	0	coltend4	0	0
	1	-1	dpm	0	0		coltend4*dpm	0	0	0	0
	0	1	0	-1		;					
contrast'	4_12	4_26		Intercept	beta	'	Intercept	0	coltend4	0	0
	0	0	dpm	1	-1		coltend4*dpm	0	0	0	0
	0	0	1	-1		;					
contrast'	Coltend1 vs	Coltend2		linear	beta	'	d	0			
	d*coltend4	4.6	-4.6	0	0		d*dpm	0	0	d*coltend4*dpm	
	2.3	2.3	-2.3	-2.3	0		0	0	0		;
contrast'	Coltend1 vs	Coltend3		linear	beta	'	d	0			
	d*coltend4	4.6	0	-4.6	0		d*dpm	0	0	d*coltend4*dpm	
	2.3	2.3	0	0	-2.3		-2.3	0	0		;
contrast'	Coltend1 vs	Coltend4		linear	beta	'	d	0			
	d*coltend4	4.6	0	0	-4.6		d*dpm	0	0	d*coltend4*dpm	
	2.3	2.3	0	0	0		-2.3	-2.3			;
contrast'	Coltend2 vs	Coltend3		linear	beta	'	d	0			
	d*coltend4	0	4.6	-4.6	0		d*dpm	0	0	d*coltend4*dpm	
	0	0	2.3	2.3	-2.3		-2.3	0	0		;
contrast'	Coltend2 vs	Coltend4		linear	beta	'	d	0			
	d*coltend4	0	4.6	0	-4.6		d*dpm	0	0	d*coltend4*dpm	
	0	0	2.3	2.3	0		0	-2.3	-2.3		;
contrast'	Coltend3 vs	Coltend4		linear	beta	'	d	0			
	d*coltend4	0	0	-4.6	4.6		d*dpm	0	0	d*coltend4*dpm	
	0	0	0	0	-2.3		-2.3	2.3	2.3		;
contrast'	12 vs	26		linear	beta	'	d	0	d*coltend4	0	
	0	0	0	d*dpm	4.6		-4.6	d*coltend4*dpm	1.15	-1.15	1.15
	-1.15	1.15	-1.15	1.15	-1.15						;
contrast'	1_12	1_26		linear	beta	'	d	0	d*coltend4	0	
	0	0	0	d*dpm	4.6		-4.6	d*coltend4*dpm	4.6	-4.6	0
	0	0	0	0	0						;
contrast'	1_12	2_12		linear	beta	'	d	0	d*coltend4	4.6	
	-4.6	0	0	d*dpm	0		0	d*coltend4*dpm	4.6	0	-4.6
	0	0	0	0	0						;
contrast'	1_12	2_26		linear	beta	'	d	0	d*coltend4	4.6	
	-4.6	0	0	d*dpm	4.6		-4.6	d*coltend4*dpm	4.6	0	0
	-4.6	0	0	0	0						;
contrast'	1_12	3_12		linear	beta	'	d	0	d*coltend4	4.6	
	0	-4.6	0	d*dpm	0		0	d*coltend4*dpm	4.6	0	0
	0	-4.6	0	0	0						;
contrast'	1_12	3_26		linear	beta	'	d	0	d*coltend4	4.6	
	0	-4.6	0	d*dpm	4.6		-4.6	d*coltend4*dpm	4.6	0	0
	0	0	-4.6	0	0						;
contrast'	1_12	4_12		linear	beta	'	d	0	d*coltend4	4.6	
	0	0	-4.6	d*dpm	0		0	d*coltend4*dpm	4.6	0	0
	0	0	0	-4.6	0						;
contrast'	1_12	4_26		linear	beta	'	d	0	d*coltend4	4.6	
	0	0	-4.6	d*dpm	4.6		-4.6	d*coltend4*dpm	4.6	0	0
	0	0	0	0	-4.6						;
contrast'	1_26	2_12		linear	beta	'	d	0	d*coltend4	4.6	
	-4.6	0	0	d*dpm	-4.6		4.6	d*coltend4*dpm	0	4.6	-4.6
	0	0	0	0	0						;
contrast'	1_26	2_26		linear	beta	'	d	0	d*coltend4	4.6	
	-4.6	0	0	d*dpm	0		0	d*coltend4*dpm	0	4.6	0
	-4.6	0	0	0	0						;

contrast' 1_26	3_12		linear	beta	'	d	0	d*coltend4	4.6
0	-4.6	0	d*dpm	-4.6	4.6	d*coltend4*dpm	0	4.6	0
0	-4.6	0	0	0	;				
contrast' 1_26	3_26		linear	beta	'	d	0	d*coltend4	4.6
0	-4.6	0	d*dpm	0	0	d*coltend4*dpm	0	4.6	0
0	0	-4.6	0	0	;				
contrast' 1_26	4_12		linear	beta	'	d	0	d*coltend4	4.6
0	0	-4.6	d*dpm	-4.6	4.6	d*coltend4*dpm	0	4.6	0
0	0	0	-4.6	0	;				
contrast' 1_26	4_26		linear	beta	'	d	0	d*coltend4	4.6
0	0	-4.6	d*dpm	0	0	d*coltend4*dpm	0	4.6	0
0	0	0	0	-4.6	;				
contrast' 2_12	2_26		linear	beta	'	d	0	d*coltend4	0
0	0	0	d*dpm	4.6	-4.6	d*coltend4*dpm	0	0	4.6
-4.6	0	0	0	0	;				
contrast' 2_12	3_12		linear	beta	'	d	0	d*coltend4	0
4.6	-4.6	0	d*dpm	0	0	d*coltend4*dpm	0	0	4.6
0	-4.6	0	0	0	;				
contrast' 2_12	3_26		linear	beta	'	d	0	d*coltend4	0
4.6	-4.6	0	d*dpm	4.6	-4.6	d*coltend4*dpm	0	0	4.6
0	0	-4.6	0	0	;				
contrast' 2_12	4_12		linear	beta	'	d	0	d*coltend4	0
4.6	0	-4.6	d*dpm	0	0	d*coltend4*dpm	0	0	4.6
0	0	0	-4.6	0	;				
contrast' 2_12	4_26		linear	beta	'	d	0	d*coltend4	0
4.6	0	-4.6	d*dpm	4.6	-4.6	d*coltend4*dpm	0	0	4.6
0	0	0	0	-4.6	;				
contrast' 2_26	3_12		linear	beta	'	d	0	d*coltend4	0
4.6	-4.6	0	d*dpm	-4.6	4.6	d*coltend4*dpm	0	0	0
4.6	-4.6	0	0	0	;				
contrast' 2_26	3_26		linear	beta	'	d	0	d*coltend4	0
4.6	-4.6	0	d*dpm	0	0	d*coltend4*dpm	0	0	0
4.6	0	-4.6	0	0	;				
contrast' 2_26	4_12		linear	beta	'	d	0	d*coltend4	0
4.6	0	-4.6	d*dpm	-4.6	4.6	d*coltend4*dpm	0	0	0
4.6	0	0	-4.6	0	;				
contrast' 2_26	4_26		linear	beta	'	d	0	d*coltend4	0
4.6	0	-4.6	d*dpm	0	0	d*coltend4*dpm	0	0	0
4.6	0	0	0	-4.6	;				
contrast' 3_12	3_26		linear	beta	'	d	0	d*coltend4	0
0	0	0	d*dpm	4.6	-4.6	d*coltend4*dpm	0	0	0
0	4.6	-4.6	0	0	;				
contrast' 3_12	4_12		linear	beta	'	d	0	d*coltend4	0
0	4.6	-4.6	d*dpm	0	0	d*coltend4*dpm	0	0	0
0	4.6	0	-4.6	0	;				
contrast' 3_12	4_26		linear	beta	'	d	0	d*coltend4	0
0	4.6	-4.6	d*dpm	4.6	-4.6	d*coltend4*dpm	0	0	0
0	4.6	0	0	-4.6	;				
contrast' 3_26	4_12		linear	beta	'	d	0	d*coltend4	0
0	4.6	-4.6	d*dpm	-4.6	4.6	d*coltend4*dpm	0	0	0
0	0	4.6	-4.6	0	;				
contrast' 3_26	4_26		linear	beta	'	d	0	d*coltend4	0
0	4.6	-4.6	d*dpm	0	0	d*coltend4*dpm	0	0	0
0	0	4.6	0	-4.6	;				

```

contrast' 4_12  4_26          linear  beta  '    d    0    d*coltend4  0
          0    0    0    d*dpm  4.6  -4.6  d*coltend4*dpm 0    0    0
          0    0    0    4.6  -4.6  ;
contrast' Coltend1 vs  Coltend2          quadratic  beta  '    d2  0
          d2*coltend4  37.4  -37.4  0    0    d2*dpm 0    0
          d2*coltend4*dpm  18.7  18.7  -18.7  -18.7  0    0    0
;
contrast' Coltend1 vs  Coltend3          quadratic  beta  '    d2  0
          d2*coltend4  37.4  0    -37.4  0    d2*dpm 0    0
          d2*coltend4*dpm  18.7  18.7  0    0    -18.7  -18.7  0    0
;
contrast' Coltend1 vs  Coltend4          quadratic  beta  '    d2  0
          d2*coltend4  37.4  0    0    -37.4  d2*dpm 0    0
          d2*coltend4*dpm  18.7  18.7  0    0    0    0    -18.7  -18.7
;
contrast' Coltend2 vs  Coltend3          quadratic  beta  '    d2  0
          d2*coltend4  0    37.4  -37.4  0    d2*dpm 0    0
          d2*coltend4*dpm  0    0    18.7  18.7  -18.7  -18.7  0    0
;
contrast' Coltend2 vs  Coltend4          quadratic  beta  '    d2  0
          d2*coltend4  0    37.4  0    -37.4  d2*dpm 0    0
          d2*coltend4*dpm  0    0    18.7  18.7  0    0    -18.7  -18.7
;
contrast' Coltend3 vs  Coltend4          quadratic  beta  '    d2  0
          d2*coltend4  0    0    -37.4  37.4  d2*dpm 0    0
          d2*coltend4*dpm  0    0    0    0    -18.7  -18.7  18.7  18.7
;
contrast' 12 vs  26          quadratic  beta  '    d2  0    d2*coltend4
          0    0    0    0    d2*dpm 37.4  -37.4  d2*coltend4*dpm  9.35
          -9.35  9.35  -9.35  9.35  -9.35  9.35  -9.35  ;
contrast' 1_12  1_26          quadratic  beta  '    d2  0    d2*coltend4
          0    0    0    0    d2*dpm 37.4  -37.4  d2*coltend4*dpm  37.4
          -37.4  0    0    0    0    0    0    ;
contrast' 1_12  2_12          quadratic  beta  '    d2  0    d2*coltend4
          37.4  -37.4  0    0    d2*dpm 0    0    d2*coltend4*dpm  37.4
          0    -37.4  0    0    0    0    0    ;
contrast' 1_12  2_26          quadratic  beta  '    d2  0    d2*coltend4
          37.4  -37.4  0    0    d2*dpm 37.4  -37.4  d2*coltend4*dpm  37.4
          0    0    -37.4  0    0    0    0    ;
contrast' 1_12  3_12          quadratic  beta  '    d2  0    d2*coltend4
          37.4  0    -37.4  0    d2*dpm 0    0    d2*coltend4*dpm  37.4
          0    0    0    -37.4  0    0    0    ;
contrast' 1_12  3_26          quadratic  beta  '    d2  0    d2*coltend4
          37.4  0    -37.4  0    d2*dpm 37.4  -37.4  d2*coltend4*dpm  37.4
          0    0    0    0    -37.4  0    0    ;
contrast' 1_12  4_12          quadratic  beta  '    d2  0    d2*coltend4
          37.4  0    0    -37.4  d2*dpm 0    0    d2*coltend4*dpm  37.4
          0    0    0    0    0    -37.4  0    ;
contrast' 1_12  4_26          quadratic  beta  '    d2  0    d2*coltend4
          37.4  0    0    -37.4  d2*dpm 37.4  -37.4  d2*coltend4*dpm  37.4
          0    0    0    0    0    0    -37.4  ;
contrast' 1_26  2_12          quadratic  beta  '    d2  0    d2*coltend4
          37.4  -37.4  0    0    d2*dpm -37.4  37.4  d2*coltend4*dpm  0
          37.4  -37.4  0    0    0    0    0    ;

```

contrast' 1_26	2_26		quadratic	beta	'	d2	0	d2*coltend4
	37.4	-37.4	0	0	d2*dpm	0	0	d2*coltend4*dpm
	37.4	0	-37.4	0	0	0	0	;
contrast' 1_26	3_12		quadratic	beta	'	d2	0	d2*coltend4
	37.4	0	-37.4	0	d2*dpm	-37.4	37.4	d2*coltend4*dpm
	37.4	0	0	-37.4	0	0	0	;
contrast' 1_26	3_26		quadratic	beta	'	d2	0	d2*coltend4
	37.4	0	-37.4	0	d2*dpm	0	0	d2*coltend4*dpm
	37.4	0	0	0	-37.4	0	0	;
contrast' 1_26	4_12		quadratic	beta	'	d2	0	d2*coltend4
	37.4	0	0	-37.4	d2*dpm	-37.4	37.4	d2*coltend4*dpm
	37.4	0	0	0	0	-37.4	0	;
contrast' 1_26	4_26		quadratic	beta	'	d2	0	d2*coltend4
	37.4	0	0	-37.4	d2*dpm	0	0	d2*coltend4*dpm
	37.4	0	0	0	0	0	-37.4	;
contrast' 2_12	2_26		quadratic	beta	'	d2	0	d2*coltend4
	0	0	0	0	d2*dpm	37.4	-37.4	d2*coltend4*dpm
	0	37.4	-37.4	0	0	0	0	;
contrast' 2_12	3_12		quadratic	beta	'	d2	0	d2*coltend4
	0	37.4	-37.4	0	d2*dpm	0	0	d2*coltend4*dpm
	0	37.4	0	-37.4	0	0	0	;
contrast' 2_12	3_26		quadratic	beta	'	d2	0	d2*coltend4
	0	37.4	-37.4	0	d2*dpm	37.4	-37.4	d2*coltend4*dpm
	0	37.4	0	0	-37.4	0	0	;
contrast' 2_12	4_12		quadratic	beta	'	d2	0	d2*coltend4
	0	37.4	0	-37.4	d2*dpm	0	0	d2*coltend4*dpm
	0	37.4	0	0	0	-37.4	0	;
contrast' 2_12	4_26		quadratic	beta	'	d2	0	d2*coltend4
	0	37.4	0	-37.4	d2*dpm	37.4	-37.4	d2*coltend4*dpm
	0	37.4	0	0	0	0	-37.4	;
contrast' 2_26	3_12		quadratic	beta	'	d2	0	d2*coltend4
	0	37.4	-37.4	0	d2*dpm	-37.4	37.4	d2*coltend4*dpm
	0	0	37.4	-37.4	0	0	0	;
contrast' 2_26	3_26		quadratic	beta	'	d2	0	d2*coltend4
	0	37.4	-37.4	0	d2*dpm	0	0	d2*coltend4*dpm
	0	0	37.4	0	-37.4	0	0	;
contrast' 2_26	4_12		quadratic	beta	'	d2	0	d2*coltend4
	0	37.4	0	-37.4	d2*dpm	-37.4	37.4	d2*coltend4*dpm
	0	0	37.4	0	0	-37.4	0	;
contrast' 2_26	4_26		quadratic	beta	'	d2	0	d2*coltend4
	0	37.4	0	-37.4	d2*dpm	0	0	d2*coltend4*dpm
	0	0	37.4	0	0	0	-37.4	;
contrast' 3_12	3_26		quadratic	beta	'	d2	0	d2*coltend4
	0	0	0	0	d2*dpm	37.4	-37.4	d2*coltend4*dpm
	0	0	0	37.4	-37.4	0	0	;
contrast' 3_12	4_12		quadratic	beta	'	d2	0	d2*coltend4
	0	0	37.4	-37.4	d2*dpm	0	0	d2*coltend4*dpm
	0	0	0	37.4	0	-37.4	0	;
contrast' 3_12	4_26		quadratic	beta	'	d2	0	d2*coltend4
	0	0	37.4	-37.4	d2*dpm	37.4	-37.4	d2*coltend4*dpm
	0	0	0	37.4	0	0	-37.4	;
contrast' 3_26	4_12		quadratic	beta	'	d2	0	d2*coltend4
	0	0	37.4	-37.4	d2*dpm	-37.4	37.4	d2*coltend4*dpm
	0	0	0	0	37.4	-37.4	0	;

```

contrast' 3_26 4_26 quadratic beta ' d2 0 d2*coltend4
0 0 37.4 -37.4 d2*dpm 0 0 d2*coltend4*dpm 0
0 0 0 0 37.4 0 -37.4 ;
contrast' 4_12 4_26 quadratic beta ' d2 0 d2*coltend4
0 0 0 0 d2*dpm 37.4 -37.4 d2*coltend4*dpm 0
0 0 0 0 0 37.4 -37.4 ;
contrast' Coltend1 vs Coltend2 cubic beta ' d3 0
d3*coltend4 347.8 -347.8 0 0 d3*dpm 0 0
d3*coltend4*dpm 173.9 173.9 -173.9 -173.9 0 0 0 0
;
contrast' Coltend1 vs Coltend3 cubic beta ' d3 0
d3*coltend4 347.8 0 -347.8 0 d3*dpm 0 0
d3*coltend4*dpm 173.9 173.9 0 0 -173.9 -173.9 0 0
;
contrast' Coltend1 vs Coltend4 cubic beta ' d3 0
d3*coltend4 347.8 0 0 -347.8 d3*dpm 0 0
d3*coltend4*dpm 173.9 173.9 0 0 0 0 -173.9 -173.9
;
contrast' Coltend2 vs Coltend3 cubic beta ' d3 0
d3*coltend4 0 347.8 -347.8 0 d3*dpm 0 0
d3*coltend4*dpm 0 0 173.9 173.9 -173.9 -173.9 0 0
;
contrast' Coltend2 vs Coltend4 cubic beta ' d3 0
d3*coltend4 0 347.8 0 -347.8 d3*dpm 0 0
d3*coltend4*dpm 0 0 173.9 173.9 0 0 -173.9 -173.9
;
contrast' Coltend3 vs Coltend4 cubic beta ' d3 0
d3*coltend4 0 0 -347.8 347.8 d3*dpm 0 0
d3*coltend4*dpm 0 0 0 0 -173.9 -173.9 173.9 173.9
;
contrast' 12 vs 26 cubic beta ' d3 0 d3*coltend4 0
0 0 0 d3*dpm 347.8 -347.8 d3*coltend4*dpm 86.95 -86.95
86.95 -86.95 86.95 -86.95 86.95 -86.95 ;
contrast' 1_12 1_26 cubic beta ' d3 0 d3*coltend4 0
0 0 0 d3*dpm 347.8 -347.8 d3*coltend4*dpm 347.8 -347.8
0 0 0 0 0 ;
contrast' 1_12 2_12 cubic beta ' d3 0 d3*coltend4 347.8
-347.8 0 0 d3*dpm 0 0 d3*coltend4*dpm 347.8 0
-347.8 0 0 0 0 ;
contrast' 1_12 2_26 cubic beta ' d3 0 d3*coltend4 347.8
-347.8 0 0 d3*dpm 347.8 -347.8 d3*coltend4*dpm 347.8 0
0 -347.8 0 0 0 ;
contrast' 1_12 3_12 cubic beta ' d3 0 d3*coltend4 347.8
0 -347.8 0 d3*dpm 0 0 d3*coltend4*dpm 347.8 0
0 0 -347.8 0 0 ;
contrast' 1_12 3_26 cubic beta ' d3 0 d3*coltend4 347.8
0 -347.8 0 d3*dpm 347.8 -347.8 d3*coltend4*dpm 347.8 0
0 0 0 -347.8 0 ;
contrast' 1_12 4_12 cubic beta ' d3 0 d3*coltend4 347.8
0 0 -347.8 d3*dpm 0 0 d3*coltend4*dpm 347.8 0
0 0 0 0 -347.8 ;
contrast' 1_12 4_26 cubic beta ' d3 0 d3*coltend4 347.8
0 0 -347.8 d3*dpm 347.8 -347.8 d3*coltend4*dpm 347.8 0
0 0 0 0 0 -347.8 ;

```

contrast' 1_26	2_12		cubic	beta	'	d3	0	d3*coltend4	347.8
	-347.8	0	d3*dpm	-347.8	347.8	d3*coltend4*dpm	0	347.8	
	-347.8	0	0	0	0	;			
contrast' 1_26	2_26		cubic	beta	'	d3	0	d3*coltend4	347.8
	-347.8	0	d3*dpm	0	0	d3*coltend4*dpm	0	347.8	
	0	-347.8	0	0	0	;			
contrast' 1_26	3_12		cubic	beta	'	d3	0	d3*coltend4	347.8
	0	-347.8	d3*dpm	-347.8	347.8	d3*coltend4*dpm	0	347.8	
	0	0	0	0	0	;			
contrast' 1_26	3_26		cubic	beta	'	d3	0	d3*coltend4	347.8
	0	-347.8	d3*dpm	0	0	d3*coltend4*dpm	0	347.8	
	0	0	-347.8	0	0	;			
contrast' 1_26	4_12		cubic	beta	'	d3	0	d3*coltend4	347.8
	0	0	d3*dpm	-347.8	347.8	d3*coltend4*dpm	0	347.8	
	0	0	0	-347.8	0	;			
contrast' 1_26	4_26		cubic	beta	'	d3	0	d3*coltend4	347.8
	0	0	d3*dpm	0	0	d3*coltend4*dpm	0	347.8	
	0	0	0	0	-347.8	;			
contrast' 2_12	2_26		cubic	beta	'	d3	0	d3*coltend4	0
	0	0	d3*dpm	347.8	-347.8	d3*coltend4*dpm	0	0	
	347.8	-347.8	0	0	0	;			
contrast' 2_12	3_12		cubic	beta	'	d3	0	d3*coltend4	0
	347.8	-347.8	d3*dpm	0	0	d3*coltend4*dpm	0	0	
	347.8	0	0	0	0	;			
contrast' 2_12	3_26		cubic	beta	'	d3	0	d3*coltend4	0
	347.8	-347.8	d3*dpm	347.8	-347.8	d3*coltend4*dpm	0	0	
	347.8	0	-347.8	0	0	;			
contrast' 2_12	4_12		cubic	beta	'	d3	0	d3*coltend4	0
	347.8	0	d3*dpm	0	0	d3*coltend4*dpm	0	0	
	347.8	0	0	-347.8	0	;			
contrast' 2_12	4_26		cubic	beta	'	d3	0	d3*coltend4	0
	347.8	0	d3*dpm	347.8	-347.8	d3*coltend4*dpm	0	0	
	347.8	0	0	0	-347.8	;			
contrast' 2_26	3_12		cubic	beta	'	d3	0	d3*coltend4	0
	347.8	-347.8	d3*dpm	-347.8	347.8	d3*coltend4*dpm	0	0	
	0	347.8	0	0	0	;			
contrast' 2_26	3_26		cubic	beta	'	d3	0	d3*coltend4	0
	347.8	-347.8	d3*dpm	0	0	d3*coltend4*dpm	0	0	
	0	347.8	0	-347.8	0	;			
contrast' 2_26	4_12		cubic	beta	'	d3	0	d3*coltend4	0
	347.8	0	d3*dpm	-347.8	347.8	d3*coltend4*dpm	0	0	
	0	347.8	0	-347.8	0	;			
contrast' 2_26	4_26		cubic	beta	'	d3	0	d3*coltend4	0
	347.8	0	d3*dpm	0	0	d3*coltend4*dpm	0	0	
	0	347.8	0	0	-347.8	;			
contrast' 3_12	3_26		cubic	beta	'	d3	0	d3*coltend4	0
	0	0	d3*dpm	347.8	-347.8	d3*coltend4*dpm	0	0	
	0	0	347.8	-347.8	0	;			
contrast' 3_12	4_12		cubic	beta	'	d3	0	d3*coltend4	0
	0	347.8	d3*dpm	0	0	d3*coltend4*dpm	0	0	
	0	0	347.8	0	-347.8	;			
contrast' 3_12	4_26		cubic	beta	'	d3	0	d3*coltend4	0
	0	347.8	d3*dpm	347.8	-347.8	d3*coltend4*dpm	0	0	
	0	0	347.8	0	-347.8	;			

```

contrast' 3_26 4_12 cubic beta ' d3 0 d3*coltend4 0
          0 347.8 -347.8 d3*dpm -347.8 347.8 d3*coltend4*dpm 0 0
          0 0 0 347.8 -347.8 0 ;
contrast' 3_26 4_26 cubic beta ' d3 0 d3*coltend4 0
          0 347.8 -347.8 d3*dpm 0 0 d3*coltend4*dpm 0 0
          0 0 0 347.8 0 -347.8 ;
contrast' 4_12 4_26 cubic beta ' d3 0 d3*coltend4 0
          0 0 0 d3*dpm 347.8 -347.8 d3*coltend4*dpm 0 0
          0 0 0 0 347.8 -347.8 ;

```

```
run;
```

```

data predval; set predval;
if cx <=599 then delete;
trt = catx('_', coltend4, dpm);
run;
proc sort data = predval; by coltend4 d; run;

```

```

proc means data = predval mean ;
by coltend4;
var pred;
OUTPUT OUT=cluster MEAN=;
run;

```

```

proc sgplot data=predval ;
title ' ';
series x = d y = pred/ group = trt markers name = "series";
*scatter x=d y=pred/ group = dcc2 name="fit" ;
axis label = "Day of display" values=(0 to 11 by 1) ;
yaxis label = "de reflectance values" values = (0 to 30 by 5) ;
keylegend "series" / across = 3 noborder location = outside position = bottom ;
*keylegend "fit" / location=outside position=bottomleft;

```

```
run;
```

```

proc means data = predval mean ;
by coltend4 d;
var pred;
OUTPUT OUT=cluster MEAN=;
run;

```

```

proc sgplot data=cluster ;
title ' ';
series x = d y = pred/ group = coltend4 markers name = "series";
*scatter x=d y=pred/ group = dcc2 name="fit" ;
axis label = "Day of display" values=(0 to 11 by 1) ;
yaxis label = "de reflectance values" values = (0 to 30 by 5) ;
keylegend "series" / across = 3 noborder location = outside position = bottom ;
*keylegend "fit" / location=outside position=bottomleft;

```

```
run;
```

```
proc sort data = predval; by dpm d; run;
```

```

proc means data = predval mean ;
by dpm ;
var pred;
OUTPUT OUT=dpm MEAN=;
run;

proc means data = predval mean ;
by dpm d;
var pred;
OUTPUT OUT=dpm MEAN=;
run;

proc sgplot data=dpm ;
title ' ';
series x = d y = pred/ group = dpm markers name = "series";
xaxis label = "Day of display" values=(0 to 11 by 1) ;
yaxis label = "de reflectance values" values = (0 to 30 by 5) ;
keylegend "series" / across = 3 noborder location = outside position = bottom ;
*keylegend "fit" / location=outside position=bottomleft;

run;

ods trace on;

proc corr data= metdata;
var aLstar_00 astar_00 aLstar_11 astar_11 OT SSF desmin sarc;
with NORA OC TMYO phd2 ph solcarb insolcarb gly glu g6p malate lactate typei typeii;
ods output Pearsoncorr=corr;
run;
*****;
ods trace on;
data d12; set metdata;
if dpm = 26 then delete;
run;
ods trace on;
data d26; set metdata;
if dpm = 12 then delete;
run;

proc princomp data = d12 out = prins11c outstat = prinstatc plot = pattern(ncomp = 2) plot =
SCORE(NCOMP=2) ;
ID coltend4;
var
aLstar_11 astar_11 bstar_11 de_11 ha_11 chr_11 OT SSF desmin sarc
;
ods output eigenvectors = EV; *(Keep = Muscle Effect AGE QG Estimate Stderr rename= (Estimate =
M_JUI StdErr = S_JUI ));
ods output PatternPlot= ppv;
ods output ScorePlot = SP;
run;
proc sort data = SP;
by L1; run;
proc sgplot data=SP ;
styleattrs datacontrastcolors=(black gold gray maroon)

```



```

datasymbols=(circlefilled squarefilled trianglefilled starfilled);
title ' ';
scatter x = Prin1 y = Prin2/ group = L1 name = "series";
        xaxis label = "Component 1" values=(-5 to 10 by 0.2) ;
        yaxis label = "Component 2" values = (-5 to 5 by 0.2) ;
        reflate 0 / axis = x transparency = 0.5;
        reflate 0 / axis = y transparency = 0.5;
keylegend "series" / across = 4 noborder location = outside position = bottom ;
*keylegend "fit" / location=outside position=bottomleft;
run;

proc corr data = prins11c;
with NORA OC TMYO phd2 ph solcarb insolcarb gly glu g6p malate lactate typei typeii;
var Prin1 Prin2;
ods output PearsonCorr = corr;
run;

proc sgplot data=corr ;
title ' ';
scatter x = Prin1 y = Prin2/ datalabel =variable;
        xaxis label = "Component 1" values=(-1 to 1 by 0.2);
        yaxis label = "Component 2" values = (-1 to 1 by 0.2);
        reflate 0 / axis = x transparency = 0.5;
        reflate 0 / axis = y transparency = 0.5;
keylegend "series" / across = 3 noborder location = outside position = bottom ;
*keylegend "fit" / location=outside position=bottomleft;
run;

proc princomp data = d26 out = prins11c outstat = prinstatc plot = pattern(ncomp = 2) plot =
SCORE(NCOMP=2) ;
ID coltend4;
var
        aLstar_11 astar_11 bstar_11 de_11 ha_11 chr_11 OT SSF desmin sarc
;
ods output eigenvectors = EV; *(Keep = Muscle Effect AGE QG Estimate Stderr rename= (Estimate =
M_JUI StdErr = S_JUI ));
ods output PatternPlot= ppv;
ods output ScorePlot = SP;
run;
proc sort data = SP;
by L1; run;
proc sgplot data=SP ;
styleattrs datacontrastcolors=(black gold gray maroon)
datasymbols=(circlefilled squarefilled trianglefilled starfilled);
title ' ';
scatter x = Prin1 y = Prin2/ group = L1 name = "series";
        xaxis label = "Component 1" values=(-5 to 10 by 0.2) ;
        yaxis label = "Component 2" values = (-5 to 5 by 0.2) ;
        reflate 0 / axis = x transparency = 0.5;
        reflate 0 / axis = y transparency = 0.5;
keylegend "series" / across = 4 noborder location = outside position = bottom ;
*keylegend "fit" / location=outside position=bottomleft;
run;

proc corr data = prins11c;

```

```

with NORA OC TMYO phd2 ph solcarb insolcarb gly glu g6p malate lactate typei typeii;
var Prin1 Prin2;
ods output PearsonCorr = corr;
run;

proc sgplot data=corr ;
    title ' ';
scatter x = Prin1 y = Prin2/ datalabel =variable;
        xaxis label = "Component 1" values=(-1 to 1 by 0.2);
    yaxis label = "Component 2" values = (-1 to 1 by 0.2);
    refline 0 / axis = x transparency = 0.5;
    refline 0 / axis = y transparency = 0.5;
    keylegend "series" / across = 3 noborder location = outside position = bottom ;
    *keylegend "fit" / location=outside position=bottomleft;
run;

ods trace on;
proc corr data= d12;
var aLstar_00 astar_00 aLstar_11 astar_11 OT SSF desmin sarc;
with NORA OC TMYO PHD2 PH SOLCARB INSOLCARB GLY GLU G6P LACTATE MALATE
TYPEI TYPEII;
ods ouput pearsoncorr=corr12;
run;

ods trace on;
proc corr data= d26;
var aLstar_00 astar_00 aLstar_11 astar_11 OT SSF desmin sarc;
with NORA OC TMYO PHD2 PH SOLCARB INSOLCARB GLY GLU G6P LACTATE MALATE
TYPEI TYPEII;
ods ouput pearsoncorr=corr26;
run;

ods trace on;
proc glimmix data=metdata;
class trip coltend4 dpm cx;
model ot = dpm coltend4 dpm*coltend4 / ddfm=kr;
random trip(cx);
lsmeans dpm coltend4 dpm*coltend4/diff lines;
run;

ods trace on;
proc glimmix data=metdata;
class trip coltend4 dpm cx;
model ssf= dpm coltend4 dpm*coltend4 / ddfm=kr;
random trip(cx);
lsmeans dpm coltend4 dpm*coltend4/diff lines;
run;

ods trace on;
proc glimmix data=metdata;
class trip coltend4 dpm cx;
model sarc= dpm coltend4 dpm*coltend4 / ddfm=kr;
random trip(cx);

```

```

lsmeans dpm coltend4 dpm*coltend4/diff lines;
run;
ods trace on;

proc glimmix data=metdata;
class trip coltend4 dpm cx;
model desmin= dpm coltend4 dpm*coltend4 / ddfm=kr;
random trip(cx);
lsmeans dpm coltend4 dpm*coltend4/diff lines;
run;

ods trace on;
proc glimmix data=metdata;
class trip coltend4 dpm cx;
model tmyo= dpm coltend4 dpm*coltend4 / ddfm=kr;
random trip(cx);
lsmeans dpm coltend4 dpm*coltend4/diff lines;
run;

/*running all metabolic data */

ods trace on;
proc glimmix data=metdata;
class trip coltend4 dpm cx;
model bloom= dpm coltend4 dpm*coltend4 / ddfm=kr;
random trip(cx);
lsmeans dpm coltend4 dpm*coltend4/diff lines;
run;

/*
ods trace on;
proc glimmix data=metdata;
class trip coltend4 dpm cx;
model deox= dpm coltend4 dpm*coltend4 / ddfm=kr;
random trip*coltend4;
lsmeans dpm coltend4 dpm*coltend4/diff lines;
run;
*/
ods trace on;
proc glimmix data=metdata;
class trip coltend4 dpm cx;
model oc= dpm coltend4 dpm*coltend4 / ddfm=kr;
random trip(cx);
lsmeans dpm coltend4 dpm*coltend4/diff lines;
run;

ods trace on;
proc glimmix data=metdata;
class trip coltend4 dpm cx;
model imf= dpm coltend4 dpm*coltend4 / ddfm=kr;
random trip(cx);
lsmeans dpm coltend4 dpm*coltend4/diff lines;
run;

ods trace on;

```

```

proc glimmix data=metdata;
class trip coltend4 dpm cx;
model prm= dpm coltend4 dpm*coltend4 / ddfm=kr;
random trip(cx);
lsmeans dpm coltend4 dpm*coltend4/diff lines;
run;

```

```

ods trace on;
proc glimmix data=metdata;
class trip coltend4 dpm cx;
model nora= dpm coltend4 dpm*coltend4 / ddfm=kr;
random trip(cx);
lsmeans dpm coltend4 dpm*coltend4/diff lines;
run;

```

```

ods trace on;
proc glimmix data=metdata;
class trip coltend4 dpm cx;
model phd2= dpm coltend4 dpm*coltend4 / ddfm=kr;
random trip(cx);
lsmeans dpm coltend4 dpm*coltend4/diff lines;
run;

```

```

ods trace on;
proc glimmix data=metdata;
class trip coltend4 dpm cx;
model ph= dpm coltend4 dpm*coltend4 / ddfm=kr;
random trip(cx);
lsmeans dpm coltend4 dpm*coltend4/diff lines;
run;

```

```

ods trace on;
proc glimmix data=metdata;
class trip coltend4 dpm cx;
model solcarb= dpm coltend4 dpm*coltend4 / ddfm=kr;
random trip(cx);
lsmeans dpm coltend4 dpm*coltend4/diff lines;
run;

```

```

ods trace on;
proc glimmix data=metdata;
class trip coltend4 dpm cx;
model insolcarb= dpm coltend4 dpm*coltend4 / ddfm=kr;
random trip(cx);
lsmeans dpm coltend4 dpm*coltend4/diff lines;
run;

```

```

ods trace on;
proc glimmix data=metdata;
class trip coltend4 dpm cx;
model gly= dpm coltend4 dpm*coltend4 / ddfm=kr;
random trip(cx);
lsmeans dpm coltend4 dpm*coltend4/diff lines;
run;

```

```

ods trace on;

```

```

proc glimmix data=metdata;
class trip coltend4 dpm cx;
model glu= dpm coltend4 dpm*coltend4 / ddfm=kr;
random trip(cx);
lsmeans dpm coltend4 dpm*coltend4/diff lines;
run;

ods trace on;
proc glimmix data=metdata;
class trip coltend4 dpm cx;
model g6p= dpm coltend4 dpm*coltend4 / ddfm=kr;
random trip(cx);
lsmeans dpm coltend4 dpm*coltend4/diff lines;
run;

ods trace on;
proc glimmix data=metdata;
class trip coltend4 dpm cx;
model lactate= dpm coltend4 dpm*coltend4 / ddfm=kr;
random trip(cx);
lsmeans dpm coltend4 dpm*coltend4/diff lines;
run;

ods trace on;
proc glimmix data=metdata;
class trip coltend4 dpm cx;
model malate= dpm coltend4 dpm*coltend4 / ddfm=kr;
random trip(cx);
lsmeans dpm coltend4 dpm*coltend4/diff lines;
run;

ods trace on;
proc glimmix data=metdata;
class trip coltend4 dpm cx;
model typei= dpm coltend4 dpm*coltend4 / ddfm=kr;
random trip(cx);
lsmeans dpm coltend4 dpm*coltend4/diff lines;
run;

ods trace on;
proc glimmix data=metdata;
class trip coltend4 dpm cx;
model typeii= dpm coltend4 dpm*coltend4 / ddfm=kr;
random trip(cx);
lsmeans dpm coltend4 dpm*coltend4/diff lines;
run;

```

Appendix C. SAS input for Chapter 4

```
ods trace on;
proc glimmix data=metdata;
class trip flav3 dpm cx;
model ot = dpm flav3 dpm*flav3 / ddfm=kr;
random trip*flav3;
lsmeans dpm flav3 dpm*flav3/diff lines;
run;
```

```
ods trace on;
proc glimmix data=metdata;
class trip flav3 dpm cx;
model juice= dpm flav3 dpm*flav3 / ddfm=kr;
random trip*flav3;
lsmeans dpm flav3 dpm*flav3/diff lines;
run;
```

```
ods trace on;
proc glimmix data=metdata;
class trip flav3 dpm cx;
model beef= dpm flav3 dpm*flav3 / ddfm=kr;
random trip*flav3;
lsmeans dpm flav3 dpm*flav3/diff lines;
run;
ods trace on;
```

```
proc glimmix data=metdata;
class trip flav3 dpm cx;
model bloody= dpm flav3 dpm*flav3 / ddfm=kr;
random trip*flav3;
lsmeans dpm flav3 dpm*flav3/diff lines;
run;
```

```
ods trace on;
proc glimmix data=metdata;
class trip flav3 dpm cx;
model brown= dpm flav3 dpm*flav3 / ddfm=kr;
random trip*flav3;
lsmeans dpm flav3 dpm*flav3/diff lines;
run;
```

```
ods trace on;
proc glimmix data=metdata;
class trip flav3 dpm cx;
model fat= dpm flav3 dpm*flav3 / ddfm=kr;
random trip*flav3;
lsmeans dpm flav3 dpm*flav3/diff lines;
run;
```

```
ods trace on;
proc glimmix data=metdata;
class trip flav3 dpm cx;
model metallic= dpm flav3 dpm*flav3 / ddfm=kr;
random trip*flav3;
```

```
lsmeans dpm flav3 dpm*flav3/diff lines;  
run;
```

```
ods trace on;  
proc glimmix data=metdata;  
class trip flav3 dpm cx;  
model liver= dpm flav3 dpm*flav3 / ddfm=kr;  
random trip*flav3;  
lsmeans dpm flav3 dpm*flav3/diff lines;  
run;
```

```
ods trace on;  
proc glimmix data=metdata;  
class trip flav3 dpm cx;  
model umami= dpm flav3 dpm*flav3 / ddfm=kr;  
random trip*flav3;  
lsmeans dpm flav3 dpm*flav3/diff lines;  
run;
```

```
ods trace on;  
proc glimmix data=metdata;  
class trip flav3 dpm cx;  
model sweet= dpm flav3 dpm*flav3 / ddfm=kr;  
random trip*flav3;  
lsmeans dpm flav3 dpm*flav3/diff lines;  
run;
```

```
ods trace on;  
proc glimmix data=metdata;  
class trip flav3 dpm cx;  
model sor= dpm flav3 dpm*flav3 / ddfm=kr;  
random trip*flav3;  
lsmeans dpm flav3 dpm*flav3/diff lines;  
run;
```

```
ods trace on;  
proc glimmix data=metdata;  
class trip flav3 dpm cx;  
model salt= dpm flav3 dpm*flav3 / ddfm=kr;  
random trip*flav3;  
lsmeans dpm flav3 dpm*flav3/diff lines;  
run;
```

```
ods trace on;  
proc glimmix data=metdata;  
class trip flav3 dpm cx;  
model bitter= dpm flav3 dpm*flav3 / ddfm=kr;  
random trip*flav3;  
lsmeans dpm flav3 dpm*flav3/diff lines;  
run;
```

```
ods trace on;  
proc glimmix data=metdata;  
class trip flav3 dpm cx;  
model rancid= dpm flav3 dpm*flav3 / ddfm=kr;  
random trip*flav3;
```

```

lsmeans dpm flav3 dpm*flav3/diff lines;
run;

ods trace on;
proc glimmix data=metdata;
class trip flav3 dpm cx;
model heatedoil= dpm flav3 dpm*flav3 / ddfm=kr;
random trip*flav3;
lsmeans dpm flav3 dpm*flav3/diff lines;
run;

ods trace on;
proc glimmix data=metdata;
class trip flav3 dpm cx;
model chem= dpm flav3 dpm*flav3 / ddfm=kr;
random trip*flav3;
lsmeans dpm flav3 dpm*flav3/diff lines;
run;

ods trace on;
proc glimmix data=metdata;
class trip flav3 dpm cx;
model musty= dpm flav3 dpm*flav3 / ddfm=kr;
random trip*flav3;
lsmeans dpm flav3 dpm*flav3/diff lines;
run;

ods trace on;
proc glimmix data=metdata;
class trip flav3 dpm cx;
model spoiled= dpm flav3 dpm*flav3 / ddfm=kr;
random trip*flav3;
lsmeans dpm flav3 dpm*flav3/diff lines;
run;

ods trace on;
proc glimmix data=metdata;
class trip flav3 dpm cx;
model butter= dpm flav3 dpm*flav3 / ddfm=kr;
random trip*flav3;
lsmeans dpm flav3 dpm*flav3/diff lines;
run;

ods trace on;
proc glimmix data=metdata;
class trip flav3 dpm cx;
model beef= dpm flav3 dpm*flav3 / ddfm=kr;
random trip*flav3;
lsmeans dpm flav3 dpm*flav3/diff lines;
run;

/*running all metabolic data with andy defined clusters*/

ods trace on;
proc glimmix data=metdata;

```



```
class trip flav3 dpm cx;
model deox= dpm flav3 dpm*flav3 / ddfm=kr;
random trip*flav3;
lsmeans dpm flav3 dpm*flav3/diff lines;
run;
```

```
ods trace on;
proc glimmix data=metdata;
class trip flav3 dpm cx;
model oc= dpm flav3 dpm*flav3 / ddfm=kr;
random trip*flav3;
lsmeans dpm flav3 dpm*flav3/diff lines;
run;
```

```
ods trace on;
proc glimmix data=metdata;
class trip flav3 dpm cx;
model imf= dpm flav3 dpm*flav3 / ddfm=kr;
random trip*flav3;
lsmeans dpm flav3 dpm*flav3/diff lines;
run;
```

```
ods trace on;
proc glimmix data=metdata;
class trip flav3 dpm cx;
model prm= dpm flav3 dpm*flav3 / ddfm=kr;
random trip*flav3;
lsmeans dpm flav3 dpm*flav3/diff lines;
run;
```

```
ods trace on;
proc glimmix data=metdata;
class trip flav3 dpm cx;
model nora= dpm flav3 dpm*flav3 / ddfm=kr;
random trip*flav3;
lsmeans dpm flav3 dpm*flav3/diff lines;
run;
```

```
ods trace on;
proc glimmix data=metdata;
class trip flav3 dpm cx;
model phd2= dpm flav3 dpm*flav3 / ddfm=kr;
random trip*flav3;
lsmeans dpm flav3 dpm*flav3/diff lines;
run;
```

```
ods trace on;
proc glimmix data=metdata;
class trip flav3 dpm cx;
model ph= dpm flav3 dpm*flav3 / ddfm=kr;
random trip*flav3;
lsmeans dpm flav3 dpm*flav3/diff lines;
run;
```

```
ods trace on;
proc glimmix data=metdata;
```

```
class trip flav3 dpm cx;  
model solcarb= dpm flav3 dpm*flav3 / ddfm=kr;  
random trip*flav3;  
lsmeans dpm flav3 dpm*flav3/diff lines;  
run;
```

```
ods trace on;  
proc glimmix data=metdata;  
class trip flav3 dpm cx;  
model insolcarb= dpm flav3 dpm*flav3 / ddfm=kr;  
random trip*flav3;  
lsmeans dpm flav3 dpm*flav3/diff lines;  
run;
```

```
ods trace on;  
proc glimmix data=metdata;  
class trip flav3 dpm cx;  
model gly= dpm flav3 dpm*flav3 / ddfm=kr;  
random trip*flav3;  
lsmeans dpm flav3 dpm*flav3/diff lines;  
run;
```

```
ods trace on;  
proc glimmix data=metdata;  
class trip flav3 dpm cx;  
model glu= dpm flav3 dpm*flav3 / ddfm=kr;  
random trip*flav3;  
lsmeans dpm flav3 dpm*flav3/diff lines;  
run;
```

```
ods trace on;  
proc glimmix data=metdata;  
class trip flav3 dpm cx;  
model g6p= dpm flav3 dpm*flav3 / ddfm=kr;  
random trip*flav3;  
lsmeans dpm flav3 dpm*flav3/diff lines;  
run;
```

```
ods trace on;  
proc glimmix data=metdata;  
class trip flav3 dpm cx;  
model lactate= dpm flav3 dpm*flav3 / ddfm=kr;  
random trip*flav3;  
lsmeans dpm flav3 dpm*flav3/diff lines;  
run;
```

```
ods trace on;  
proc glimmix data=metdata;  
class trip flav3 dpm cx;  
model malate= dpm flav3 dpm*flav3 / ddfm=kr;  
random trip*flav3;  
lsmeans dpm flav3 dpm*flav3/diff lines;  
run;
```

```
ods trace on;  
proc glimmix data=metdata;
```

```

class trip flav3 dpm cx;
model typeii= dpm flav3 dpm*flav3 / ddfm=kr;
random trip*flav3;
lsmeans dpm flav3 dpm*flav3/diff lines;
run;

```

```

ods trace on;
proc glimmix data=metdata;
class trip flav3 dpm cx;
model typei= dpm flav3 dpm*flav3 / ddfm=kr;
random trip*flav3;
lsmeans dpm flav3 dpm*flav3/diff lines;
run;

```

```

ods trace on;
proc print;
run;

```

```

ods trace on;
proc glimmix data=metdata;
class trip flav3 dpm cx;
model bloom= dpm flav3 dpm*flav3 / ddfm=kr;
random trip*flav3;
lsmeans dpm flav3 dpm*flav3/diff lines;
run;

```

```

ods trace on;
proc corr data=metdata;
var ot juice beef brown bloody fat metallic liver umami sweet sor salt bitter rancid heatedoil chem musty
spoiled butter;
ods output pearsoncorr=flav;
run;

```

```

ods trace on;
proc corr data=metdata;
var bloom deox oc nora imf prm phd2 ph solcarb insolcarb gly glu g6p lactate malate typeii typei;
ods output pearsoncorr=met;
run;

```

```

ods trace on;
proc corr data=metdata;
var bloom deox oc nora imf prm phd2 ph solcarb insolcarb gly glu g6p lactate malate typeii typei;
with ot juice beef brown bloody fat metallic liver umami sweet sor salt bitter rancid heatedoil chem musty
spoiled butter;
ods output pearsoncorr=metflav;
run;

```

```

ods trace on;
proc corr data=metdata;
var bloom deox oc nora imf prm phd2 ph solcarb insolcarb gly glu g6p lactate malate typeii typei ot juice
beef brown bloody fat metallic liver umami sweet sor salt bitter rancid heatedoil chem musty spoiled
butter;
ods output pearsoncorr=allmetflav;
run;

```

```

data d12; set metdata;
if dpm = 26 then delete;
run;

data d26; set metdata;
if dpm = 12 then delete;
run;

proc princomp data = d12 out = prins11c outstat = prinstatc plot = pattern(ncomp = 2) plot =
SCORE(NCOMP=2) ;
ID flav3;
var
    beef brown bloody metallic liver umami
    sweet sor bitter rancid
    heatedoil musty spoiled butter
;
ods output eigenvectors = EV; *(Keep = Muscle Effect AGE QG Estimate Stderr rename= (Estimate =
M_JUI StdErr = S_JUI ));
ods output PatternPlot= ppv;
ods output ScorePlot = SP;
run;
proc sort data = SP;
by L1; run;
proc sgplot data=SP ;
styleattrs datacontrastcolors=(black gold gray)
datasymbols=(circlefilled squarefilled trianglefilled);
title ' ';
scatter x = Prin1 y = Prin2/ group = L1 name = "series";
axis label = "Component 1" values=(-5 to 10 by 0.2) ;
axis label = "Component 2" values = (-5 to 5 by 0.2) ;
refline 0 / axis = x transparency = 0.5;
refline 0 / axis = y transparency = 0.5;
keylegend "series" / across = 3 noborder location = outside position = bottom ;
*keylegend "fit" / location=outside position=bottomleft;
run;

proc corr data = prins11c;
with OC NORA
TMYO pHd2 pH SOLCARB INSOLCARB GLY GLU G6P
LACTATE MALATE TYPEI TYPEII;
var Prin1 Prin2;
ods output PearsonCorr = corr;
run;

proc sgplot data=corr ;
title ' ';
scatter x = Prin1 y = Prin2/ datalabel =variable;
axis label = "Component 1" values=(-1 to 1 by 0.2);
axis label = "Component 2" values = (-1 to 1 by 0.2);
refline 0 / axis = x transparency = 0.5;
refline 0 / axis = y transparency = 0.5;
keylegend "series" / across = 3 noborder location = outside position = bottom ;
*keylegend "fit" / location=outside position=bottomleft;
run;

```

```

proc princomp data = d26 out = prins11c outstat = prinstatc plot = pattern(ncomp = 2) plot =
SCORE(NCOMP=2) ;
ID flav3;
var
    beef brown bloody metallic liver umami
    sweet sor bitter rancid
    heatedoil musty spoiled butter
;
ods output eigenvectors = EV; *(Keep = Muscle Effect AGE QG Estimate Stderr rename= (Estimate =
M_JUI StdErr = S_JUI ));
ods output PatternPlot= ppv;
ods output ScorePlot = SP;
run;

```

```

proc sort data = SP;
by L1; run;
proc sgplot data=SP ;
styleattrs datacontrastcolors=(black gold gray)
datasymbols=(circlefilled squarefilled trianglefilled);
title ' ';
scatter x = Prin1 y = Prin2/ group = L1 name = "series";
    xaxis label = "Component 1" values=(-5 to 10 by 0.2) ;
    yaxis label = "Component 2" values = (-5 to 5 by 0.2) ;
    refline 0 / axis = x transparency = 0.5;
    refline 0 / axis = y transparency = 0.5;
keylegend "series" / across = 3 noborder location = outside position = bottom ;
*keylegend "fit" / location=outside position=bottomleft;
run;

```

```

proc corr data = prins11c;
with OC NORA
TMYO pHd2 pH SOLCARB INSOLCARB GLY GLU G6P
LACTATE MALATE TYPEI TYPEII;
var Prin1 Prin2;
ods output PearsonCorr = corr;
run;

```

```

proc sgplot data=corr ;
title ' ';
scatter x = Prin1 y = Prin2/ datalabel =variable;
    xaxis label = "Component 1" values=(-1 to 1 by 0.2);
    yaxis label = "Component 2" values = (-1 to 1 by 0.2);
    refline 0 / axis = x transparency = 0.5;
    refline 0 / axis = y transparency = 0.5;
keylegend "series" / across = 3 noborder location = outside position = bottom ;
*keylegend "fit" / location=outside position=bottomleft;
run;

```

Appendix D Materials and Methods

Objective Color Determination

- 1) Fresh meat samples were removed from coolers and immediately transported to the research lab for analysis.
- 2) Hunter MiniScan 45/0 colorimeter was equipped with a 25 mm aperture and a D65 light source.
- 3) Standardize the colorimeter using the supplied black and white standardizing discs.
- 4) Take product surface reading through polyvinyl chloride overwrap in three different locations.
- 5) Using the colorimeter, save the calculated average of all three readings for objective color values (L^* , a^* , b^*).

Calculated Percentage Myoglobin Concentrations

- 1) Equip the Hunter MiniScan 45/0 colorimeter with a 25 mm aperture.
- 2) Standardize the colorimeter using the supplied black and white standardizing discs.
- 3) Take product surface reading through polyvinyl chloride overwrap in three different locations
- 4) Using the colorimeter, save the calculated average of all three readings for objective color values (L^* , a^* , b^*).
- 5) After average objective color readings are saved, use the following equations to calculate myoglobin concentrations via isobetic wavelengths.
 - a. $A = \log 1/R$
 - b. $\%MMb = \{1.395 - [(A_{572} - A_{730}) / (A_{525} - A_{730})]\} \times 100$
 - c. $\%DMb = \{2.375 \times [(A_{473} - A_{730}) / (A_{525} - A_{730})]\} \times 100$
 - d. $\%MbO_2 = 100 - (\%MMb + \%DMb)$

pH Determination

- 1) 5 g of fresh meat sample was homogenized with 50 ml of DI water for 30 seconds.
- 2) After homogenization, pH of homogenate was determined using a benchtop pH probe.
- 3) pH was measured in duplicate on each sample and values were averaged to determine overall sample pH.

Polytron Info:

Polytron 10-35 GT, Kinematica, Bohemia, New York

Extraction Protocol

Solutions:

2 M Hydrochloric Acid (HCl)

- Measure out 330 ml of 12 M stock HCl with a 1000 ml glass graduated cylinder
- Add HCl to ~800 ml d.d. H₂O (do NOT add water to acid!)
- QS to 2000 ml with d.d. H₂O in a 2000 ml volumetric flask

5.4 M Potassium Hydroxide (KOH)

- Weigh out 30.3 g KOH into a 150 ml beaker
- Dissolve in ~60 ml of d.d. H₂O
- QS to 100 ml with d.d. H₂O in a 100 ml volumetric flask

Materials:

- 1000 ml glass graduated cylinder
- 2000 ml volumetric flask
- 150 ml beaker
- 100 ml volumetric flask
- 50 ml conical centrifuge tubes
- Scale
- Polytron homogenizer
- Centrifuge JA-17 Rotor
- Pipet Aid
- Disposable 10 ml pipette tip
- 50 ml tubes
- 1000 µl pipette and tips

Deproteinization – neutralization method

- 1) Weigh out 0.5 g of powdered raw tissue into a 50 ml conical centrifuge tube
 - Be sure to record the actual weight of the sample
- 2) Add 10 ml 2 M HCl to the 50 ml conical centrifuge tube with the sample
- 3) Homogenize sample with Polytron (speed ~6) for 15 seconds
- 4) Incubate in fridge (2-4 °C) for 15 minutes
- 5) Centrifuge at 30,000 x G for 20 minutes with JA-17 rotor (can fit 14 samples in rotor at a time)
- 6) Pour supernatant in a 50 ml tube and neutralize the sample with 3.5 ml of 5.4 M KOH (pH is a little over 7, but varies per sample); discard pellet – don't need
 - Note: some extracts are clear and some are opaque

- 7) Use neutralized supernatant for the glucose/glucose-6-phosphate, lactate, and malate assays. Also use the neutralized supernatant to hydrolyze the samples for the glycogen assay

Glucose/G6P Assay Protocol

Solutions:

1 N Potassium Hydroxide (KOH)

- Weigh out 5.611 g KOH into a 150 ml beaker
- Dissolve in ~50 ml of d.d. H₂O
- Bring volume up to 100 ml in a 100 ml volumetric flask

0.3 M Triethanolamine buffer (0.3 M TRA; 3 mM MgSO₄; pH 7.5)

- Weigh out 5.6 g Triethanolamine hydrochloride into a 150 ml beaker
- Weigh out 740 mg Magnesium Sulfate Heptahydrate (MgSO₄•7 H₂O) into the same 150 ml beaker
- Dissolve in ~50 ml d.d. H₂O
- Add ~6 ml 1 N KOH (I added 8 ml) to adjust the pH to 7.5
- QS to 100 ml with d.d. H₂O in a 100 ml volumetric flask

ATP (Adenosine triphosphate)/NADP (Nicotinamide adenine dinucleotide phosphate) (150 mM ATP; 12 mM NADP)

- Weigh out 455 mg ATP
- Weigh out 50 mg NADP
- Dissolve in 5 ml 0.3 M Triethanolamine buffer in a 15 ml tube

3.2 M Ammonium Sulfate (422.85 g/L)

- Weigh out 8.46 g Ammonium Sulfate
- Dissolve in 20 mL of d.d. H₂O in 50 ml tube

Glucose-6-Phosphate dehydrogenase (4 IU/sample)

- 41 µl in 1 ml of 3.2 M Ammonium Sulfate in 2 ml plastic tube with cap

Hexokinase

- Whole container (1000 IU) in 20 mL of 3.2 M Ammonium Sulfate in 50 ml tube

Materials:

- 150 ml beaker
- 100 ml volumetric flask
- 50 ml tube
- 15 ml tube
- 2 ml plastic tube with cap
- Vortex
- 13 mm x 100 mm glass test tubes
- Test tube racks

- 1.5 ml microcentrifuge tubes and racks
- 1000 μ l pipette and tips
- 200 μ l pipette and tips
- Repeater pipette
 - 0.5 ml repeater pipette tip
 - 100 μ l repeater pipette tips
 - 10 μ l repeater pipette tips
- 96-well plates
- Immulon 1B assembly strips

Glucose and G-6-P Assay:

- 1) Label the glass test tubes with standard and sample IDs
- 2) Add 200 μ l glucose standard + 200 μ l glucose-6-phosphate standard to the same corresponding concentration test tube (this will go through the reaction)
 - For the glucose-6-phosphate standard, I took 0.0282 g glucose-6-phosphate into 100 ml of d.d. H₂O to get 1 mmol glucose-6-phosphate standard
 - To make the right dilution use, using a 100 μ l repeater pipette tips, in 1.5 ml microcentrifuge tubes:
 - 1 – 1 ml 1 mmol g6p standard
 - 0.9 – 0.9 ml 1 mmol g6p standard, 0.1 ml HCl/KOH
 - 0.6 – 0.6 ml 1 mmol g6p standard, 0.4 ml HCl/KOH
 - 0.3 – 0.3 ml 1 mmol g6p standard, 0.7 ml HCl/KOH
 - 0 – 1 ml HCl/KOH
 - For the glucose standard, I took 1.8 ml glucose standard solution into 10 ml of the TEA buffer to get 1 mmol glucose standard
 - To make the right dilutions we did, using a 100 μ l repeater pipette tips, in 1.5 ml microcentrifuge tubes:
 - 1 – 1 ml 1 mmol glucose standard
 - 0.9 – 0.9 ml 1 mmol glucose standard, 0.1 ml HCl/KOH
 - 0.6 – 0.6 ml 1 mmol glucose standard, 0.4 ml HCl/KOH
 - 0.3 – 0.3 ml 1 mmol glucose standard, 0.7 ml HCl/KOH
 - 0 – 1 ml HCl/KOH
- 3) Add 400 μ l sample to the test tube, using the 1000 μ l pipette set to 400
 - Use a new tip for each sample
- 4) Add 200 μ l of ATP/NADP solution to each test tube, using the 100 μ l repeater pipette tips set to 2
- 5) Add 1700 μ l of 0.3 M triethanolamine (TEA) buffer to each test tube, using both the 0.5 ml repeater pipette tip set to 3 and the 100 μ l repeater pipette tip set to 2
- 6) Vortex test tubes

- 7) Prepare a 96-well plate with a corresponding number of wells to the number of samples and standards you have, in triplicate (use the Immulon 1B assembly strips)
- 8) Take 210 μ l aliquots, in triplicate, to a 96-well plate, use the 200 μ l pipette set to 210
- 9) Read absorbance at 340 nm on a 96-well plate reader (OD1)
- 10) Add 40 μ l Glucose-6-phosphate dehydrogenase to each tube, using the 10 μ l repeater pipette tip set to 4
- 11) Vortex test tubes
- 12) Incubate at room temperature for 20 minutes
- 13) Vortex test tubes
- 14) Take 210 μ l aliquots, in triplicate, to a 96-well plate, use the 200 μ l pipette set to 210
- 15) Read absorbance at 340 nm on a 96-well plate reader (OD2)
- 16) Add 40 μ l of Hexokinase solution, using the 10 μ l repeater pipette tip set to 4
- 17) Vortex test tubes
- 18) Incubate at room temperature for 20 minutes
- 19) Vortex test tubes
- 20) Take 210 μ l aliquots, in triplicate, to a 96-well plate, use the 200 μ l pipette set to 210
- 21) Read absorbance at 340 nm on a 96-well plate reader (OD3)
- 22) Glucose-6-phosphate absorbance = OD2 – OD1
- 23) Glucose absorbance = OD3 – OD2

Notes:

- When using the repeater pipette, shoot out the first volume because it won't be accurate
- The glucose/g6p standard slope is around 2

Lactate Assay Protocol

Solutions:

0.4 M Hydrazine, 0.5 M Glycine Buffer (Lactate Reaction Buffer) pH 9.0

- Weigh out 11.4 g Glycine into a 600 ml beaker
- Add 25 ml Hydrazine hydrate into the same 600 ml beaker
- Dissolve in 200 ml d.d. H₂O
- pH to 9.0 with 2 M HCl
- Bring volume up to 300 ml with d.d. H₂O with a 500 ml graduated cylinder

NAD (Nicotinamide adenine dinucleotide hydrate)

- Weigh out 150 mg NAD
- Dissolve in 5 ml d.d. H₂O in 15 ml tube

Lactate dehydrogenase (~5 mg suspension; 20 IU/ml)

- Add 50 µl lactate dehydrogenase into 1 ml of the Lactate Reaction Buffer in 2 ml plastic tube with cap

2 M Hydrochloric Acid (HCl)

- Measure out 330 ml of 12 M stock HCl with a 1000 ml glass graduated cylinder
- Add HCl to ~800 ml d.d. H₂O (do NOT add water to acid!)
- QS to 2000 ml with d.d. H₂O in a 2000 ml volumetric flask

5.4 M Potassium Hydroxide (KOH)

- Weigh out 30.3 g KOH into a 400 ml beaker
- Dissolve in ~60 ml of d.d. H₂O
- QS to 100 ml with d.d. H₂O in 100 ml volumetric flask

HCl/KOH solution

- Add 10 ml 2 M HCl to 50 ml tube
- Add 3.5 ml 5.4 M KOH in the same tube

Materials:

- 600 ml beaker
- 400 ml beaker
- 500 ml graduated cylinder
- 50 ml tube
- 15 ml tube
- 2 ml plastic tube with cap
- 1000 ml glass graduated cylinder
- 2000 ml volumetric flask
- 100 ml volumetric flask

- Vortex
- 25° C Water Bath
- 13 mm x 100 mm glass test tube
- Test tube racks
- 1.5 ml microcentrifuge tubes and rack
- 200 µl pipette and tips
- 100 µl pipette and tips
- Repeater pipette
 - 1 ml repeater pipette tip
 - 100 µl repeater pipette tips
 - 50 µl repeater pipette tip
 - 10 µl repeater pipette tip
- 96-well plates
- Immulon 1B assembly strips

Lactate Assay

- 1) Turn on 25 °C water bath
- 2) Label the glass test tubes with standard and sample IDs
- 3) For the lactate standard curve, add 200 µl of lactate standard to the test tube (this will go through the reaction)
 - For the lactate standard, I took 2 ml 5 mmol lactate standard into 5 ml Lactate Reaction buffer to get 2 mmol lactate standard
 - To get the right dilutions, using a 100 µl repeater pipette tip, in 1.5 ml microcentrifuge tubes:
 - 2: 1 ml 2 mmol lactate standard
 - 1.4: 0.7 ml 2 mmol lactate standard, 0.3 ml HCl/KOH
 - 1: 0.5 ml 2 mmol lactate standard, 0.5 ml HCl/KOH
 - 0.4: 0.2 ml 2 mmol lactate standard, 0.8 ml HCl/KOH
 - 0: 1 ml HCl/KOH
- 4) For the samples, add 50 µl of the sample to a test tube, using the 100 µl pipette set to 50
 - Use a new tip for each sample
- 5) Add 150 µl of HCl/KOH solution to just the sample test tubes (so the sample volume adds up to 200 µl – same as the standard), using the 50 µl repeater pipette tip set to 3
- 6) Add 200 µl Nicotinamide adenine dinucleotide hydrate (NAD) solution to each test tube, using the 100 µl repeater pipette tip set to 2
- 7) Add 3000 µl of Lactate Reaction Buffer to each test tube, using the 1 ml repeater pipette tip set to 3
- 8) Vortex test tubes

- 9) Prepare a 96-well plate with a corresponding number of wells to the number of samples and standards you have, in triplicate (use the Immulon 1 B assembly strips)
- 10) Take 210 μ l aliquots, in triplicate, to a 96-well plate, use the 200 μ l pipette set to 210
- 11) Read absorbance at 340 nm on a 96-well plate reader (OD1)
- 12) Add 40 μ l of the lactate dehydrogenase solution to each test tube, using the 10 μ l repeater pipette tip set to 4
- 13) Vortex test tubes
- 14) Incubate in a 25 °C water bath for 2 hours
- 15) Vortex test tubes
- 16) Take 210 μ l aliquots, in triplicate, to a 96-well plate, use the 200 μ l pipette set to 210
- 17) Read absorbance at 340 nm on a 96-well plate reader (OD2)
- 18) Absorbance for lactate = OD2 – OD1

Notes:

- When using the repeater pipette, shoot out the first volume because it won't be accurate
- The lactate standard slope is around 7.8

Malate Assay Protocol

Solutions:

0.4 M Hydrazine, 0.5 M Glycine Buffer (Reaction Buffer) pH 9.0

- Weigh out 11.4 g Glycine into a 600 ml beaker
- Add 25 ml Hydrazine hydrate into the same 600 ml beaker
- Dissolve in 200 ml d.d. H₂O
- pH to 9.0 with 2 M HCl
- Bring volume up to 300 ml with d.d. H₂O with a 500 ml graduated cylinder

NAD (Nicotinamide adenine dinucleotide hydrate)

- Weigh out 150 mg NAD
- Dissolve in 5 ml d.d. H₂O in 15 ml tube

Malate dehydrogenase (40 U/ml)

- Add whole container malate dehydrogenase into 5 ml of the Lactate Reaction Buffer in 15 ml tube

2 M Hydrochloric Acid (HCl)

- Measure out 330 ml of 12 M stock HCl with a 1000 ml glass graduated cylinder
- Add HCl to ~800 ml d.d. H₂O (do NOT add water to acid!)
- QS to 2000 ml with d.d. H₂O in a 2000 ml volumetric flask

5.4 M Potassium Hydroxide (KOH)

- Weigh out 30.3 g KOH into a 400 ml beaker
- Dissolve in ~60 ml of d.d. H₂O
- QS to 100 ml with d.d. H₂O in 100 ml volumetric flask

HCl/KOH solution

- Add 10 ml 2 M HCl to 50 ml tube
- Add 3.5 ml 5.4 M KOH in the same tube

Materials:

- 600 ml beaker
- 400 ml beaker
- 500 ml graduated cylinder
- 50 ml tube
- 15 ml tube
- 1000 ml glass graduated cylinder
- 2000 ml volumetric flask
- 100 ml volumetric flask

- Vortex
- 25° C Water Bath
- 13 mm x 100 mm glass test tube
- Test tube racks
- 2.5 ml microcentrifuge tubes and rack
- 200 µl pipette and tips
- 100 µl pipette and tips
- Repeater pipette
 - 1 ml repeater pipette tip
 - 100 µl repeater pipette tips
 - 50 µl repeater pipette tip
 - 10 µl repeater pipette tip
- 96-well plates
- Immulon 1B assembly strips

Malate Assay

19) Turn on 25 °C water bath

20) Label the glass test tubes with standard and sample IDs

21) For the malate standard curve, add 200 µl of malate standard to the test tube (this will go through the reaction)

- For the malate standard, I took 0.027 g L-malic acid into 100 ml d.d. H₂O to get a 2 mmol malate standard (Or 0.013 g L-malic acid into 100 ml d.d. H₂O to get a 1 mmol malate standard)
 - To get the right dilutions, using a 100 µl repeater pipette tip, in 2.5 ml microcentrifuge tubes:
 - 2: 1 ml 2 mmol malate standard
 - 1.4: 0.7 ml 2 mmol malate standard, 0.3 ml HCl/KOH
 - 1: 0.5 ml 2 mmol malate standard, 0.5 ml HCl/KOH
 - 0.4: 0.2 ml 2 mmol malate standard, 0.8 ml HCl/KOH
 - 0: 1 ml HCl/KOH
 - OR
 - 1: 1 ml 1 mmol malate standard
 - 0.9: 0.9 ml 1 mmol malate standard, 0.1 ml HCl/KOH
 - 0.6: 0.6 ml 1 mmol malate standard, 0.4 ml HCl/KOH
 - 0.3: 0.3 ml 1 mmol malate standard, 0.7 ml HCl/KOH
 - 0: 1 ml HCl/KOH

22) For the samples, add 50 µl of the sample to a test tube, using the 100 µl pipette set to 50

- Use a new tip for each sample
- Or try 100 µl of the sample to a test tube
- Or 200 µl of the sample to a test tube

- 23) Add 150 μl of HCl/KOH solution to just the sample test tubes (so the sample volume adds up to 200 μl – same as the standard), using the 50 μl repeater pipette tip set to 3
 - Use 100 μl of HCl/KOH solution if adding 100 μl of sample
 - Use no HCl/KOH solution if using full 200 μl of sample
- 24) Add 200 μl Nicotinamide adenine dinucleotide hydrate (NAD) solution to each test tube, using the 100 μl repeater pipette tip set to 2
- 25) Add 3000 μl of Reaction Buffer to each test tube, using the 1 ml repeater pipette tip set to 3
- 26) Vortex test tubes
- 27) Prepare a 96-well plate with a corresponding number of wells to the number of samples and standards you have, in triplicate (use the Immulon 1 B assembly strips)
- 28) Take 210 μl aliquots, in triplicate, to a 96-well plate, use the 200 μl pipette set to 210
- 29) Read absorbance at 340 nm on a 96-well plate reader (OD1)
- 30) Add 40 μl of the lactate dehydrogenase solution to each test tube, using the 10 μl repeater pipette tip set to 4
- 31) Vortex test tubes
- 32) Incubate in a 25 °C water bath for 2 hours
- 33) Vortex test tubes
- 34) Take 210 μl aliquots, in triplicate, to a 96-well plate, use the 200 μl pipette set to 210
- 35) Read absorbance at 340 nm on a 96-well plate reader (OD2)
- 36) Absorbance for malate = OD2 – OD1

Notes:

When using the repeater pipette, shoot out the first volume because it won't be accurate

Measurement of Muscle pH

Reagents:

Iodoacetate /KCl Solution

5 mM Iodoacetic Acid (1.04 g/liter) (CAS 305-53-3)

150 mM KCl (11.18 g/liter) (CAS 7447-40-7)

Adjust pH to 7.0 with very dilute HCl or NaOH (this is VERY sensitive). Be careful when adjusting the pH

Procedure:

- 1.) Calibrate the pH meter used for meat homogenates using 2 standards
- 2.) All measurements are done at room temperature
- 3.) Using a polytron, homogenize 2.5 g muscle sample in 25 ml IAA/KCl solution for 10 seconds at half speed.
- 4.) Measure pH of suspension

Metmyoglobin Reducing Activity

- 1) Steaks surface were removed for evaluation.
- 2) Two (TB) or three (SM) center portions were removed from steak surface.
- 3) Samples were placed in individual weigh boats and submerged in sodium nitrite solution for 20 minutes.
- 4) After incubation, samples were individually vacuum packaged and objective color was measured in triplicate on each sample with a HunterLab MiniScan 45/0.
- 5) Samples were left at room temperature for 2 h.
- 6) After 2 h, objective color was taken in triplicate on each sample.
- 7) MRA was calculated using the following equation.

Solutions:

6 g of Sodium Nitrite- Fisher Chemical S347-500

2 L Water

Slice Shear Force

- 1.) Thaw frozen steaks for a minimum of 24 to 26 hours. Internal temperature of steaks should be between 2 and 5 °C. Cook steaks to an internal temperature of 71°C using a belt grill.
- 2.) Using a thermocouple probe, monitor internal steak temperature and record highest temperature reached.
- 3.) After recording final temperature, remove a 1-cm x 5 cm slice from the lateral end of each steak parallel to the muscle fibers
- 4.) Place the 5 cm long section into the slice box centered on the two 45° slots with the angle of the slots aligned with the muscle fiber angle
- 5.) Insert the double bladed knife into the slots at the back and make two parallel cuts simultaneously through the length of the 5 cm long section.
- 6.) The 1 cm thick x 5 cm long slice is placed in the testing machine so that the blade shears perpendicular to the muscle fibers along the 5cm dimension of the slice.
- 7.) The slice blade should be 1.1684 mm thick with the cutting edge beveled to a half round. The spacers creating the gap for the blade should be 20.828 mm thick. The crosshead speed should be 500 mm/min for Instron Universal Testing Machines.

Data should be captured by instrument software on the computer running the instrument and values should be hand recorded in case of computer failure.

Sarcomere Length

- 1.) If powdering cooked slice, trim hard cooked edges from both sides of the slice
- 2.) Dice sample finely and snap freeze in liquid nitrogen. After freezing, pulverize samples in pre-cooled Waring blender to a fine powder. Keep powder frozen while transferring to a pre-cooled conical.
- 3.) Before starting sarcomere length determination, ensure the microscope stage is properly set. The top of a microscope slide on top of the stage should be 10 cm from the top of the base of the ring stand where the paper that the bands will be marked is located.
- 4.) Place a small amount of powdered tissue on a microscope slide. Add a drop of 0.2 M Sucrose to moisten the powder.
- 5.) Place the microscope slide on the stage below the laser so that the beam passes through the sample. Move the slide around until you find different diffraction patterns. Measure the distance (mm) between the two first order diffraction bands. Divide the value by 2 and plug into the equation of Cross et al. (1981). To calculate sarcomere length

Measurements can be measured with a ruler or scanned into a computer and measured with image analysis software.

$$\text{sarcomere length, } \mu\text{m} = \frac{0.6328 \times D \times \sqrt{\left(\frac{T}{D}\right)^2 + 1}}{T}$$

0.2 M Sucrose in 0.1M NaHPO₄ buffer:

Na₂HPO₄ (mw 141.96) 10.18g/liter

NaH₂PO₄ (mw 137.99) 3.91g/liter

Sucrose 68.46g/liter

Dissolve in dd water, pH to 7.2 and bring up to volume.

Store at 4°C

Protein Degradation in Muscle Extract Using the Protein Simple WES System

Solutions for Sample Extraction

Tris-EDTA Buffer, pH 8.3

50 mM Tris 6.06g/liter

10mM EDTA 3.72g/liter

Adjust pH to 8.3, qs to 1 liter. Store at 4°C

10% SDS

SDS 5g/500ml

0.5 M Tris, pH 6.8

Tris 12g/200mL

Adjust pH to 6.8 with HCl, qs to 200 ml. Filter and store at 4°C

2X Treatment Buffer, pH 6.8

0.125 M Tris – 2.5 ml of 0.5M Tris

4% SDS -- 4.0 ml of 10% SDS

20% Glycerol- 2.0 ml

H₂O -- 0.5 ml

9.0ml

pH 6.8. Store at Room Temperature

Sample Preparation

1) Homogenize 1 g of sample in 10 volumes (10 ml) of TRIS-EDTA buffer for 20 seconds with polytron at 4. Immediately remove a 0.5 ml aliquot and transfer to a 1.5 ml microcentrifuge tube

2) Add 0.5 ml of 2X treatment buffer. Mix well with vortex mixer

- 3) Heat samples in a 50°C water bath for 20 min. Repeat mixing using a pipetman that has been fitted with a pipet tip that has had the tip snipped off. Reheat samples for 5 min. Nucleic acids may be stringy and viscous but pipetting will help shear them.
- 4) Centrifuge for 20 min in an Eppendorf 5414 C centrifuge at max speed to pellet insoluble material (pellet should be small or undetectable)
- 5) Determine protein concentration of the supernatant (diluted 1:5 with 1x treatment buffer) using the thermoscientific pierce micro-BCA protein assay in a 96 well plate. Do in triplicate using a new tip for each well.

To each well add: 10 ul sample

Or

10 ul (4, 2, 1, 0.5, 0 mg/ml BSA)

Add 200 ul of BCA reagent and incubate at 37°C for 30 min. Read plate on microplate reader at 562. Run standard curve for each plate and use standard curve to calculate protein values.

- 6) Record total protein values and enter into WES Spreadsheet that is used to set up the assay. Once entered the spreadsheet will determine dilutions needed for sample protein and antibodies for running the assay.

Protein Simple Kits Used:

SM-W004 12-130 kDa Jess or Wes Separation Module, 8x25 Capillary cartridges

DM-001 Anti-Rabbit detection module

DM-002 Anti-Mouse detection module

WES Assay

- 1) Run a 0h sample at least 3-4 reps on the WES Assay Plate and spread those throughout the plate.
- 2) Set up the WES assay using the Master WES template. This will automatically calculate how much reagent you need as well as the dilutions for sample and antibodies.
- 3) Turn on WES computer and instrument and run an instrument check scan. Proceed if scan is passed.
- 4) Import assay template or data into computer
- 5) Proteins

Desmin Concentration of sample 0.3 mg/ml

Primary antibody Rabbit monoclonal Desmin clone RM234 (Novus)

Primary antibody dilution 1:50

Secondary antibody Anti-Rabbit (WES Kit) Dilution is Neat

Assay

1) Make 0.1x sample buffer (WES kit)

2) Dilute samples to the first dilution step only (the intermediate step). Do not take to final volume at this point.

3) Separation module preparation

Follow the card that is supplied with the kit. Prepare standard packet reagents and

Store on ice

-DTT

-Fluorescent Master Mix

- Biotinylated Ladder

4) Dilute primary antibody and store on ice

5) Final sample dilutions and preparation

-Transfer sample from intermediate dilution (using 4 ul) to a 0.5 ml microcentrifuge tube. Add 5x master mix. Mix sample with vortex mixer

6) Denature your samples using a 95°C block heater for 5 min. Vortex again after heating.

7) Using the Eppendorf microcentrifuge at max speed, spin samples briefly (15 seconds)

8) Prepare HRP solution by combining 200ul peroxide and 200ul luminol supplied in WES kit

9) Pipette your plate following the kit insert instructions. Plate from bottom to top. Always keep lid on between reagents.

10) Centrifuge plates at 2500 rpm for 5 minutes at room temp.

11) Add 500ul of wash buffer to the first three rows of wells below the sample rows

12) Run plate

Literature Cited

- Abraham, A., J. W. Dillwith, G. G. Mafi, D. L. VanOverbeke, and R. Ramanathan. 2017. Metabolite profile differences between beef longissimus and psoas muscles during display. *Meat and Muscle Biology*. 1:18–27. doi:10.22175/mmb2016.12.0007.
- Abril, M., M. M. Campo, A. Öneç, C. Sañudo, P. Albertí, and A. I. Negueruela. 2001. Beef colour evolution as a function of ultimate pH. *Meat Science*. 58:69–78. doi:10.1016/S0309-1740(00)00133-9.
- Adhikari, K., E. Chambers IV, R. Miller, L. Vazquez-Araujo, N. Bhumiratana, and C. Philip. 2011. Development of a lexicon for beef flavor in intact muscle. *Journal of Sensory Studies*. 26. doi:10.1111/j.1745-459X.2011.00356.x.
- Allen, K. E., and D. P. Cornforth. 2006. Myoglobin oxidation in a model system as affected by nonheme iron and iron chelating agents. *Journal of Agricultural and Food Chemistry*. 54:10134–10140. doi:10.1021/jf0623182.
- Amaral, A. B., M. V. da Silva, and S. C. da S. Lannes. 2018. Lipid oxidation in meat: mechanisms and protective factors – a review. *Food Science and Technology*. 38. doi:10.1590/fst.32518.
- AMSA. 2012. Meat Color Measurement Guidelines. Am. Meat Sci. Assoc. Champaign, IL.
- Anderson, M. J., S. M. Lonergan, C. A. Fedler, K. J. Prusa, J. M. Binning, and E. Huff-Lonergan. 2012a. Profile of biochemical traits influencing tenderness of muscles from the beef round. *Meat Science*. 91:247–254. doi:10.1016/j.meatsci.2012.01.022.
- Anderson, M. J., S. M. Lonergan, and E. Huff-Lonergan. 2012b. Myosin light chain 1 release from myofibrillar fraction during postmortem aging is a potential indicator of proteolysis and tenderness of beef. *Meat Science*. 90:345–351. doi:10.1016/j.meatsci.2011.07.021.
- Anderson, M. J., S. M. Lonergan, and E. Huff-Lonergan. 2014. Differences in phosphorylation of phosphoglucosmutase 1 in beef steaks from the longissimus dorsi with high or low star probe values. *Meat Science*. 96:379–384. doi:10.1016/j.meatsci.2013.07.017.
- Antonelo, D., J. F. M. Gómez, N. R. B. Cônsolo, M. Beline, L. A. Colnago, W. Schilling, X. Zhang, S. P. Suman, D. E. Gerrard, J. C. C. Balieiro, and S. L. Silva. 2020. Metabolites and metabolic pathways correlated with beef tenderness. *Meat and Muscle Biology*. 4:1–9. doi:10.22175/mmb.10854.

- Apaoblaza, A., A. Galaz, P. Strobel, A. Ramírez-Reveco, N. Jeréz-Timaure, and C. Gallo. 2015. Glycolytic potential and activity of adenosine monophosphate kinase (AMPK), glycogen phosphorylase (GP) and glycogen debranching enzyme (GDE) in steer carcasses with normal (<5.8) or high (>5.9) 24h pH determined in *M. longissimus dorsi*. *Meat Science*. 101:83–89. doi:10.1016/j.meatsci.2014.11.008.
- Arihara, K., R. G. Cassens, M. L. Greaser, J. B. Luchansky, and P. E. Mozdziak. 1995. Localization of metmyoglobin-reducing enzyme (NADH-cytochrome b5 reductase) system components in bovine skeletal muscle. *Meat Science*. 39:205–213. doi:10.1016/0309-1740(94)P1821-C.
- Ashmore, C. R. 1974. Phenotypic expression of muscle fiber types and some implications to meat quality. *Journal of Animal Science*. 38. doi:10.2527/jas1974.3851158x.
- Ashmore, C. R., L. Doerr, G. Foster, and F. Carroll. 1971. Respiration of mitochondria isolated from dark-cutting beef. *Journal of Animal Science*. 33. doi:10.2527/jas1971.333574x.
- Ashmore, C. R., W. Parker, and L. Doerr. 1972. Respiration of mitochondria isolated from dark-cutting beef: postmortem changes. *Journal of Animal Science*. 34:46–48. doi:10.2527/jas1972.34146x.
- Ayala, A., M. F. Muñoz, and S. Argüelles. 2014. Lipid peroxidation: Production, metabolism, and signaling mechanisms of malondialdehyde and 4-hydroxy-2-nonenal. *Oxidative Medicine and Cellular Longevity*. 2014. doi:10.1155/2014/360438.
- Baron, C. P., and H. J. Andersen. 2002. Myoglobin-induced lipid oxidation. A review. *Journal of Agricultural and Food Chemistry*. 50. doi:10.1021/jf011394w.
- Baron, C. P., S. Jacobsen, and P. P. Purslow. 2004. Cleavage of desmin by cysteine proteases: Calpains and cathepsin B. *Meat Science*. 68:447–456. doi:10.1016/j.meatsci.2004.03.019.
- Bate-Smith, E. C., and J. R. Bendall. 1947. Rigor mortis and adenosine-triphosphate. *The Journal of Physiology*. 106:177–185. doi:10.1113/jphysiol.1947.sp004202.
- Batzer, O. F., A. T. Santoro, M. C. Tan, W. A. Landmann, and B. S. Schweigert. 1960. Meat flavor chemistry, precursors of beef flavor. *Journal of Agricultural and Food Chemistry*. 8. doi:10.1021/jf60112a023.
- Bekhit, A. E. D., and C. Faustman. 2005. Metmyoglobin reducing activity. *Meat Science*. 71:407–439. doi:10.1016/j.meatsci.2005.04.032.

- Bekhit, A. E. D., G. H. Geesink, J. D. Morton, and R. Bickerstaffe. 2001. Metmyoglobin reducing activity and colour stability of ovine longissimus muscle. *Meat Science*. 57:427–435. doi:10.1016/S0309-1740(00)00121-2.
- Beline, M., J. F. M. Gómez, D. S. Antonelo, J. Silva, V. L. M. Buarque, N. R. B. Cònsolo, P. R. Leme, S. K. Matarneh, D. E. Gerrard, and S. L. Silva. 2020. Muscle fiber type, postmortem metabolism, and meat quality of Nellore cattle with different post-weaning growth potential. *Livestock Science*. 244:104348. doi:10.1016/j.livsci.2020.104348.
- Bendall, J. R. 1973. Postmortem Changes in Muscle. In: *The Structure and Function of Muscle*. Elsevier.
- Bernard, C., I. Cassar-Malek, M. le Cunff, H. Dubroeuq, G. Renand, and J.-F. Hocquette. 2007. New indicators of beef sensory quality revealed by expression of specific genes. *Journal of Agricultural and Food Chemistry*. 55. doi:10.1021/jf063372l.
- Bhat, Z. F., J. D. Morton, S. L. Mason, and A. E. D. A. Bekhit. 2018. Role of calpain system in meat tenderness: A review. *Food Science and Human Wellness*. 7:196–204. doi:10.1016/j.fshw.2018.08.002.
- Blackstock, J. C. 1989. Carbohydrate metabolism. In: *Guide to Biochemistry*. Elsevier.
- van Boekel, M. A. J. S. 2006. Formation of flavour compounds in the Maillard reaction. *Biotechnology Advances*. 24:230–233. doi:10.1016/j.biotechadv.2005.11.004.
- Boleman, S. J., S. L. Boleman, R. K. Miller, J. F. Taylor, H. R. Cross, T. L. Wheeler, M. Koochmarai, S. D. Shackelford, M. F. Miller, R. L. West, D. D. Johnson, and J. W. Savell. 1997. Consumer evaluation of beef of known categories of tenderness. *Journal of Animal Science*. 75. doi:10.2527/1997.7561521x.
- Brown, W. D., and H. E. Snyder. 1969. Nonenzymatic reduction and oxidation of myoglobin and hemoglobin by nicotinamide adenine dinucleotides and flavins. *Journal of Biological Chemistry*. 244:6702–6706. doi:10.1016/s0021-9258(18)63463-5.
- Calkins, C. R., T. R. Dutson, G. C. Smith, Z. L. Carpenter, and G. W. Davis. 1981. Relationship of fiber type composition to marbling and tenderness of bovine muscle. *Journal of Food Science*. 46. doi:10.1111/j.1365-2621.1981.tb15331.x.
- Callahan, Z. D., K. E. Belk, R. K. Miller, J. B. Morgan, and C. L. Lorenzen. 2013. Combining two proven mechanical tenderness measurements in one steak. *Journal of Animal Science*. 91. doi:10.2527/jas.2013-6539.
- Callahan, Z. D., J. V. Cooper, and C. L. Lorenzen. 2017. Aging condition and retail display lighting impact retail display life and lipid oxidation of beef biceps

- femoris steaks. *Meat and Muscle Biology*. 3:265–275.
doi:10.22175/mmb2019.02.0005.
- Camou, J. P., J. A. Marchello, V. F. Thompson, S. W. Mares, and D. E. Goll. 2007. Effect of postmortem storage on activity of μ - and m-calpain in five bovine muscles. *Journal of Animal Science*. 85:2670–2681. doi:10.2527/jas.2007-0164.
- Canto, A. C. V. C. S., B. R. C. Costa-Lima, S. P. Suman, M. L. G. Monteiro, F. M. Viana, A. P. A. A. Salim, M. N. Nair, T. J. P. Silva, and C. A. Conte-Junior. 2016. Color attributes and oxidative stability of longissimus lumborum and psoas major muscles from Nellore bulls. *Meat Science*. 121:19–26.
doi:10.1016/j.meatsci.2016.05.015.
- Canto, A. C. V. C. S., S. P. Suman, M. N. Nair, S. Li, G. Rentfrow, C. M. Beach, T. J. P. Silva, T. L. Wheeler, S. D. Shackelford, A. Grayson, R. O. McKeith, and D. A. King. 2015. Differential abundance of sarcoplasmic proteome explains animal effect on beef Longissimus lumborum color stability. *Meat Science*. 102:90–98.
doi:10.1016/j.meatsci.2014.11.011.
- Cao, J., W. Sun, G. Zhou, X. Xu, Z. Peng, and Z. Hu. 2010. Morphological and biochemical assessment of apoptosis in different skeletal muscles of bulls during conditioning. *Journal of Animal Science*. 88. doi:10.2527/jas.2009-2412.
- Carlson, K. B., K. J. Prusa, C. A. Fedler, E. M. Steadham, A. C. Outhouse, D. A. King, E. Huff-Lonergan, and S. M. Lonergan. 2017. Postmortem protein degradation is a key contributor to fresh pork loin tenderness¹²³. *Journal of Animal Science*. 95. doi:10.2527/jas.2016.1032.
- Chauhan, S. S., and E. M. England. 2018. Postmortem glycolysis and glycogenolysis: insights from species comparisons. *Meat Science*. 144:118–126.
doi:10.1016/j.meatsci.2018.06.021.
- Chauhan, S. S., M. N. LeMaster, D. L. Clark, M. K. Foster, C. E. Miller, and E. M. England. 2019. Glycolysis and pH decline terminate prematurely in oxidative muscles despite the presence of excess glycogen. *Meat and Muscle Biology*. 3:254–264. doi:10.22175/mmb2019.02.0006.
- Cheah, K. S., and A. M. Cheah. 1971. Post-mortem changes in structure and function of ox muscle mitochondria. 1. Electron microscopic and polarographic investigations. *Journal of Bioenergetics*. 2. doi:10.1007/BF01648923.
- Chen, Q., J. Huang, F. Huang, M. Huang, and G. Zhou. 2014. Influence of oxidation on the susceptibility of purified desmin to degradation by μ -calpain, caspase-3 and -6. *Food Chemistry*. 150:220–226. doi:10.1016/j.foodchem.2013.10.149.
- Chikuni, K., M. Oe, K. Sasaki, M. Shibata, I. Nakajima, K. Ojikma, and S. Muroya. 2010. Effects of muscle type on beef taste-traits assessed by an electric sensing system. *Animal Science Journal*. 81. doi:10.1111/j.1740-0929.2010.00773.x.

- Cho, S., G. Kang, P. N. Seong, B. Park, and S. M. Kang. 2015. Effect of slaughter age on the antioxidant enzyme activity, color, and oxidative stability of Korean Hanwoo (*Bos taurus coreanae*) cow beef. *Meat Science*. 108:44–49. doi:10.1016/j.meatsci.2015.05.018.
- Choe, E., and D. B. Min. 2006. Mechanisms and factors for edible oil oxidation. *Comprehensive Reviews in Food Science and Food Safety*. 5. doi:10.1111/j.1541-4337.2006.00009.x.
- Choi, Y. M., Y. C. Ryu, and B. C. Kim. 2007. Influence of myosin heavy- and light chain isoforms on early postmortem glycolytic rate and pork quality. *Meat Science*. 76:281–288. doi:10.1016/j.meatsci.2006.11.009.
- Chriki, S., G. E. Gardner, C. Jurie, B. Picard, D. Micol, J. P. Brun, L. Journaux, and J. F. Hocquette. 2012. Cluster analysis application identifies muscle characteristics of importance for beef tenderness. *BMC Biochemistry*. 13. doi:10.1186/1471-2091-13-29.
- Chun, C. K. Y., W. Wu, A. A. Welter, T. G. O’Quinn, G. Magnin-Bissel, D. L. Boyle, and M. D. Chao. 2020. A preliminary investigation of the contribution of different tenderness factors to beef loin, tri-tip and heel tenderness. *Meat Science*. 170:108247. doi:10.1016/j.meatsci.2020.108247.
- Colle, M. J., J. A. Nasados, J. M. Rogers, D. M. Kerby, M. M. Colle, J. B. van Buren, R. P. Richard, G. K. Murdoch, C. J. Williams, and M. E. Doumit. 2018. Strategies to improve beef tenderness by activating calpain-2 earlier postmortem. *Meat Science*. 135. doi:10.1016/j.meatsci.2017.08.008.
- Cônsolo, N. R. B., A. F. Rosa, L. C. G. S. Barbosa, P. H. Maclean, A. Higuera-Padilla, L. A. Colnago, and E. A. L. Titto. 2021. Preliminary study on the characterization of Longissimus lumborum dark cutting meat in Angus × Nellore crossbreed cattle using NMR-based metabolomics. *Meat Science*. 172:108350. doi:10.1016/j.meatsci.2020.108350.
- Cooper, J. V., S. P. Suman, B. R. Wiegand, L. Schumacher, and C. L. Lorenzen. 2017. Light source influences color stability and lipid oxidation in steaks from low color stability beef muscle. *Meat and Muscle Biology*. 1:149–156. doi:10.22175/mmb2017.06.0029.
- Cooper, J. V., S. P. Suman, B. R. Wiegand, L. Schumacher, and C. L. Lorenzen. 2018. Impact of light source on color and lipid oxidative stabilities from a moderately color-stable beef muscle during retail display. *Meat and Muscle Biology*. 2:102–110. doi:10.22175/mmb2017.07.0040.
- Cooper, J. V., B. R. Wiegand, A. B. Koc, L. Schumacher, I. Grün, and C. L. Lorenzen. 2016. Impact of contemporary light sources on oxidation of fresh ground beef. *Journal of Animal Science*. 94. doi:10.2527/jas.2016-0728.

- Cross, H. R., R. Moen, and M. S. Stanfield. 1978. Training and testing of judges for sensory analysis of meat quality. *Food Technology*. 32:48–54.
- Cross, H. R., R. L. West, and T. R. Dutson. 1981. Comparison of methods for measuring sarcomere length in beef semitendinosus muscle. *Meat Science*. 5:261–266. doi:10.1016/0309-1740(81)90016-4.
- Cruzen, S. M., P. V. R. Paulino, S. M. Lonergan, and E. Huff-Lonergan. 2014. Postmortem proteolysis in three muscles from growing and mature beef cattle. *Meat Science*. 96:854–861. doi:10.1016/j.meatsci.2013.09.021.
- D'Alessandro, A., S. Rinalducci, C. Marrocco, V. Zolla, F. Napolitano, and L. Zolla. 2012. Love me tender: An Omics window on the bovine meat tenderness network. *Journal of Proteomics*. 75:4360–4380. doi:10.1016/j.jprot.2012.02.013.
- Dang, D. S., J. F. Buhler, K. J. Thornton, J. F. Legako, and S. K. Matarneh. 2020. Myosin heavy chain isoform and metabolic profile differ in beef steaks varying in tenderness. *Meat Science*. 170:108266. doi:10.1016/j.meatsci.2020.108266.
- Degens, H., A. K. Swisher, Y. F. Heijdra, P. M. Siu, P. N. Richard Dekhuijzen, and S. E. Alway. 2007. Apoptosis and Id2 expression in diaphragm and soleus muscle from the emphysematous hamster. *American Journal of Physiology-Regulatory, Integrative and Comparative Physiology*. 293. doi:10.1152/ajpregu.00046.2007.
- Denzer, M. L., C. Mowery, H. Comstock, N. B. Maheswarappa, G. G. Mafi, D. L. VanOverbeke, and R. Ramanathan. 2020. Characterization of the cofactors involved in non-enzymatic metmyoglobin/methemoglobin reduction in vitro. *Meat and Muscle Biology*. 4:7–10. doi:10.22175/mmb.9507.
- Devine, C. E., N. M. Wahlgren, and E. Tornberg. 1999. Effect of rigor temperature on muscle shortening and tenderisation of restrained and unrestrained beef m. longissimus thoracicus et lumborum. *Meat Science*. 51. doi:10.1016/S0309-1740(98)00098-9.
- Domínguez, R., M. Pateiro, M. Gagaoua, F. J. Barba, W. Zhang, and J. M. Lorenzo. 2019. A comprehensive review on lipid oxidation in meat and meat products. *Antioxidants*. 8. doi:10.3390/antiox8100429.
- Dransfield, E. 1994. Modelling Post-mortem tenderisation -- V: Inactivation of calpains. *Meat Science*. 37:391–409.
- Elroy, N. N., J. Rogers, G. G. Mafi, D. L. VanOverbeke, S. D. Hartson, and R. Ramanathan. 2015. Species-specific effects on non-enzymatic metmyoglobin reduction in vitro. *Meat Science*. 105:108–113. doi:10.1016/j.meatsci.2015.03.010.
- England, E. M., S. K. Matarneh, R. M. Mitacek, A. Abraham, R. Ramanathan, J. C. Wicks, H. Shi, T. L. Scheffler, E. M. Oliver, E. T. Helm, and D. E. Gerrard. 2018.

- Presence of oxygen and mitochondria in skeletal muscle early postmortem. *Meat Science*. 139:97–106. doi:10.1016/j.meatsci.2017.12.008.
- England, E. M., S. K. Matarneh, T. L. Scheffler, C. Wachet, and D. E. Gerrard. 2014. PH inactivation of phosphofructokinase arrests postmortem glycolysis. *Meat Science*. 98:850–857. doi:10.1016/j.meatsci.2014.07.019.
- England, E. M., T. L. Scheffler, S. C. Kasten, S. K. Matarneh, and D. E. Gerrard. 2013. Exploring the unknowns involved in the transformation of muscle to meat. *Meat Science*. 95:837–843. doi:10.1016/j.meatsci.2013.04.031.
- Estévez, M. 2011. Protein carbonyls in meat systems: A review. *Meat Science*. 89:259–279. doi:10.1016/j.meatsci.2011.04.025.
- Estévez, M., and M. Heinonen. 2010. Effect of Phenolic Compounds on the Formation of α -Amino adipic and γ -Glutamic Semialdehydes from Myofibrillar Proteins Oxidized by Copper, Iron, and Myoglobin. *Journal of Agricultural and Food Chemistry*. 58. doi:10.1021/jf903757h.
- Estévez, M., P. Kylli, E. Puolanne, R. Kivikari, and M. Heinonen. 2008. Fluorescence spectroscopy as a novel approach for the assessment of myofibrillar protein oxidation in oil-in-water emulsions. *Meat Science*. 80:1290–1296. doi:10.1016/j.meatsci.2008.06.004.
- Estévez, M., S. Ventanas, and M. Heinonen. 2011. Formation of Strecker aldehydes between protein carbonyls - α -Amino adipic and γ -glutamic semialdehydes - and leucine and isoleucine. *Food Chemistry*. 128:1051–1057. doi:10.1016/j.foodchem.2011.04.012.
- Etherington, D. J. 1984. The Contribution of Proteolytic Enzymes to Postmortem Changes in Muscle. *Journal of Animal Science*. 59. doi:10.2527/jas1984.5961644x.
- Faustman, C., and R. Cassens. 1990. The biochemical basis for discoloration in fresh meat: A review. *Journal of Muscle Foods*. 1. doi:10.1111/j.1745-4573.1990.tb00366.x.
- Faustman, C., D. C. Liebler, T. D. McClure, and Q. Sun. 1999. α,β -Unsaturated aldehydes accelerate oxymyoglobin oxidation. *Journal of Agricultural and Food Chemistry*. 47. doi:10.1021/jf990016c.
- Faustman, C., Q. Sun, R. Mancini, and S. P. Suman. 2010. Myoglobin and lipid oxidation interactions: Mechanistic bases and control. *Meat Science*. 86:86–94. doi:10.1016/j.meatsci.2010.04.025.
- Faustman, C., M. C. Yin, and D. B. Nadeau. 1992. Color stability, lipid stability, and nutrient composition of red and white veal. *Journal of Food Science*. 57:302–304.

- Ferguson, D. M., and D. E. Gerrard. 2014. Regulation of post-mortem glycolysis in ruminant muscle. *Animal Production Science*. 54:464–481. doi:10.1071/AN13088.
- Ferguson, D. M., and R. D. Warner. 2008. Have we underestimated the impact of pre-slaughter stress on meat quality in ruminants? *Meat Science*. 80:12–19. doi:10.1016/j.meatsci.2008.05.004.
- Foraker, B. A., D. Gredell, J. F. Legako, R. D. Stevens, J. D. Tatum, K. E. Belk, and D. R. Woerner. 2020. Flavor, Tenderness, and Related Chemical Changes of Aged Beef Strip Loins. *Meat and Muscle Biology*. 4:1–18. doi:10.22175/mmb.11115.
- Gagaoua, M., J. Hughes, E. M. C. Terlouw, R. D. Warner, P. P. Purslow, J. M. Lorenzo, and B. Picard. 2020. Proteomic biomarkers of beef colour. *Trends in Food Science and Technology*. 101:234–252. doi:10.1016/j.tifs.2020.05.005.
- Gagaoua, M., E. M. C. Terlouw, A. M. Mullen, D. Franco, R. D. Warner, J. M. Lorenzo, P. P. Purslow, D. Gerrard, D. L. Hopkins, D. Troy, and B. Picard. 2021. Molecular signatures of beef tenderness: Underlying mechanisms based on integromics of protein biomarkers from multi-platform proteomics studies. *Meat Science*. 172:108311. doi:10.1016/j.meatsci.2020.108311.
- Gardner, K., and J. F. Legako. 2018. Volatile flavor compounds vary by beef product type and degree of doneness. *Journal of Animal Science*. 96. doi:10.1093/jas/sky287.
- Geesink, G. H., and M. Koohmaraie. 1999. Postmortem proteolysis and calpain/calpastatin activity in callipyge and normal lamb biceps femoris during extended postmortem storage. *Journal of Animal Science*. 77:1490–1501. doi:10.2527/1999.7761490x.
- George, P., and C. J. Stratmann. 1952. The oxidation of myoglobin to metmyoglobin by oxygen. 2. The relation between the first order rate constant and the partial pressure of oxygen. *The Biochemical journal*. 51:418–425. doi:10.1042/bj0510418.
- Girard, I., J. L. Aalhus, J. A. Basarab, I. L. Larsen, and H. L. Bruce. 2012. Modification of beef quality through steer age at slaughter, breed cross and growth promotants. *Canadian Journal of Animal Science*. 92. doi:10.4141/cjas2012-001.
- Goñi, M. V., M. J. Beriain, G. Indurain, and K. Insausti. 2007. Predicting longissimus dorsi texture characteristics in beef based on early post-mortem colour measurements. *Meat Science*. 76. doi:10.1016/j.meatsci.2006.10.012.
- Grayson, A. L., S. D. Shackelford, D. A. King, R. O. McKeith, R. K. Miller, and T. L. Wheeler. 2016. The effects of degree of dark cutting on tenderness and sensory attributes of beef. *Journal of Animal Science*. 94. doi:10.2527/jas.2016-0388.

- Greene, B. E., and T. H. Cumuze. 1982. Relationship Between TBA Numbers and Inexperienced Panelists' Assessments of Oxidized Flavor in Cooked Beef. *Journal of Food Science*. 47. doi:10.1111/j.1365-2621.1982.tb11025.x.
- Greene, B. E., and L. G. Price. 1975. Oxidation-induced color and flavor changes in meat. *Journal of Agricultural and Food Chemistry*. 23. doi:10.1021/jf60198a014.
- Hammelman, J. E., B. C. Bowker, A. L. Grant, J. C. Forrest, A. P. Schinckel, and D. E. Gerrard. 2003. Early postmortem electrical stimulation simulates PSE pork development. *Meat Science*. 63:69–77. doi:10.1016/S0309-1740(02)00057-8.
- Hedrick, H. B., J. B. Boillot, D. E. Brady, and H. D. Naumann. 1959. Etiology of dark-cutting beef. *Research Bulletin 717*. Columbia, MO. Available from: <https://hdl.handle.net/10355/53718>
- Hocquette, J.-F., S. Lehnert, W. Barendse, I. Cassar-Malek, and B. Picard. 2007. Recent advances in cattle functional genomics and their application to beef quality. *Animal*. 1:159–173. doi:10.1017/S1751731107658042.
- Hornstein, I., and P. F. Crowe. 1960. Meat Flavor Chemistry, Flavor Studies on Beef and Pork. *Journal of Agricultural and Food Chemistry*. 8. doi:10.1021/jf60112a022.
- Hornstein, I., P. F. Crowe, and W. L. Sulzbacher. 1960. Flavor Chemistry, Constituents of Meat Flavor: Beef. *Journal of Agricultural and Food Chemistry*. 8. doi:10.1021/jf60107a017.
- Huang, F., M. Huang, G. Zhou, X. Xu, and M. Xue. 2011. In Vitro Proteolysis of Myofibrillar Proteins from Beef Skeletal Muscle by Caspase-3 and Caspase-6. *Journal of Agricultural and Food Chemistry*. 59. doi:10.1021/jf202129r.
- Huff Lonergan, E., W. Zhang, and S. M. Lonergan. 2010. Biochemistry of postmortem muscle - Lessons on mechanisms of meat tenderization. *Meat Science*. 86:184–195. doi:10.1016/j.meatsci.2010.05.004.
- Huff-Lonergan, E., T. Mitsuhashi, D. D. Beekman, F. C. Parrish, D. G. Olson, and R. M. Robson. 1996. Proteolysis of specific muscle structural proteins by mu-calpain at low pH and temperature is similar to degradation in postmortem bovine muscle. *Journal of Animal Science*. 74. doi:10.2527/1996.745993x.
- Huff-Lonergan, Elisabeth, T. Mitsuhashi, D. D. Beekman, F. C. Parrish, D. G. Olson, and R. M. Robson. 1996. Proteolysis of Specific Muscle Structural Proteins by μ -Calpain at Low pH and Temperature is Similar to Degradation in Postmortem Bovine Muscle. *Journal of Animal Science*. 74:993–1008. doi:10.2527/1996.745993x.
- Huff-Lonergan, E., F. C. Parrish, and R. M. Robson. 1995. Effects of postmortem aging time, animal age, and sex on degradation of titin and nebulin in bovine longissimus muscle. *Journal of Animal Science*. 73. doi:10.2527/1995.7341064x.

- Hughes, J., F. Clarke, P. Purslow, and R. Warner. 2017. High pH in beef longissimus thoracis reduces muscle fibre transverse shrinkage and light scattering which contributes to the dark colour. *Food Research International*. 101:228–238. doi:10.1016/j.foodres.2017.09.003.
- Hunt, M. C., and H. B. Hedrick. 1977. Profile of Fiber Types and Related Properties of Five Bovine Muscles. *Journal of Food Science*. 42. doi:10.1111/j.1365-2621.1977.tb01535.x.
- Hwang, Y. H., G. D. Kim, J. Y. Jeong, S. J. Hur, and S. T. Joo. 2010. The relationship between muscle fiber characteristics and meat quality traits of highly marbled Hanwoo (Korean native cattle) steers. *Meat Science*. 86:456–461. doi:10.1016/j.meatsci.2010.05.034.
- Jacob, R. 2020. Implications of the variation in bloom properties of red meat: A review. *Meat Science*. 162:108040. doi:10.1016/j.meatsci.2019.108040.
- Jeremiah, L. E., T. A.K.W., and L. L. Gibson. 1991. The usefulness of muscle color and pH for segregating beef carcasses into tenderness groups. *Meat Science*. 30. doi:10.1016/0309-1740(91)90001-7.
- Ji, J. R., and K. Takahashi. 2006. Changes in concentration of sarcoplasmic free calcium during post-mortem ageing of meat. *Meat Science*. 73:395–403. doi:10.1016/j.meatsci.2005.09.010.
- Joseph, P., S. P. Suman, G. Rentfrow, S. Li, and C. M. Beach. 2012. Proteomics of Muscle-Specific Beef Color Stability. *Journal of Agricultural and Food Chemistry*. 60. doi:10.1021/jf204188v.
- Kassambara, A., and F. Mundt. 2020. Factoextra: Extract and visualize the results of multivariate data. Available from: <http://www.sthda.com/english/rpkgs/factoextra>
- Ke, Y., R. M. Mitacek, A. Abraham, G. G. Mafi, D. L. VanOverbeke, U. DeSilva, and R. Ramanathan. 2017. Effects of Muscle-Specific Oxidative Stress on Cytochrome c Release and Oxidation–Reduction Potential Properties. *Journal of Agricultural and Food Chemistry*. 65. doi:10.1021/acs.jafc.7b01735.
- Kemp, C. M., R. G. Bardsley, and T. Parr. 2006. Changes in caspase activity during the postmortem conditioning period and its relationship to shear force in porcine longissimus muscle1. *Journal of Animal Science*. 84. doi:10.2527/jas.2006-163.
- Kemp, C. M., D. A. King, S. D. Shackelford, T. L. Wheeler, and M. Koohmaraie. 2009. The caspase proteolytic system in callipyge and normal lambs in longissimus, semimembranosus, and infraspinatus muscles during postmortem storage. *Journal of Animal Science*. 87. doi:10.2527/jas.2009-1790.
- Kemp, C. M., and T. Parr. 2012. Advances in apoptotic mediated proteolysis in meat tenderisation. *Meat Science*. 92:252–259. doi:10.1016/j.meatsci.2012.03.013.

- Kemp, C. M., P. L. Sensky, R. G. Bardsley, P. J. Buttery, and T. Parr. 2010. Tenderness – An enzymatic view. *Meat Science*. 84. doi:10.1016/j.meatsci.2009.06.008.
- Kerth, C. R., and R. K. Miller. 2015. Beef flavor: a review from chemistry to consumer. *Journal of the Science of Food and Agriculture*. 95. doi:10.1002/jsfa.7204.
- Khan, M. I., C. Jo, and M. R. Tariq. 2015. Meat flavor precursors and factors influencing flavor precursors-A systematic review. *Meat Science*. 110:278–284. doi:10.1016/j.meatsci.2015.08.002.
- Kim, Y. H. B., D. Ma, D. Setyabrata, M. M. Farouk, S. M. Lonergan, E. Huff-Lonergan, and M. C. Hunt. 2018. Understanding postmortem biochemical processes and post-harvest aging factors to develop novel smart-aging strategies. *Meat Science*. 144:74–90. doi:10.1016/j.meatsci.2018.04.031.
- King, D. A., S. D. Shackelford, C. D. Broeckling, J. E. Prenni, K. E. Belk, and T. L. Wheeler. 2019. Metabolomic Investigation of Tenderness and Aging Response in Beef Longissimus Steaks. *Meat and Muscle Biology*. 3:76–89. doi:10.22175/mmb2018.09.0027.
- King, D. A., S. D. Shackelford, A. B. Rodriguez, and T. L. Wheeler. 2011a. Effect of time of measurement on the relationship between metmyoglobin reducing activity and oxygen consumption to instrumental measures of beef longissimus color stability. *Meat Science*. 87:26–32. doi:10.1016/j.meatsci.2010.08.013.
- King, D. A., S. D. Shackelford, and T. L. Wheeler. 2011b. Relative contributions of animal and muscle effects to variation in beef lean color stability. *Journal of Animal Science*. 89. doi:10.2527/jas.2010-3595.
- King, D. A., S. D. Shackelford, T. L. Wheeler, K. D. Pfeiffer, J. M. Mehaffey, M. F. Miller, R. Nickelson, and M. Koohmaraie. 2009. Consumer acceptance and steak cutting yields of beef top sirloin and knuckle subprimals. *Meat Science*. 83:782–787. doi:10.1016/j.meatsci.2009.08.021.
- King, D. A., S. Shackelford, and T. Wheeler. 2021. Postmortem Aging Time and Marbling Class Effects on Flavor of Three Muscles From Beef Top Loin and Top Sirloin Subprimals. *Meat and Muscle Biology*. 5:1–12. doi:10.22175/mmb.10939.
- Klont, R. E., L. Brocks, and G. Eikelenboom. 1998. Muscle fibre type and meat quality. *Meat Science*. 49:S219–S229. doi:10.1016/S0309-1740(98)90050-X.
- Koohmaraie, M. 1992. The role of Ca²⁺-dependent proteases (calpains) in post mortem proteolysis and meat tenderness. *Biochimie*. 74:239–245. doi:10.1016/0300-9084(92)90122-U.
- Koohmaraie, M. 1994. Muscle proteinases and meat aging. *Meat Science*. 36:93–104. doi:10.1016/0309-1740(94)90036-1.

- Koohmaraie, M. 1996. Biochemical factors regulating the toughening and tenderization processes of meat. *Meat Science*. 43:193–201. doi:10.1016/0309-1740(96)00065-4.
- Koohmaraie, M., and G. H. Geesink. 2006. Contribution of postmortem muscle biochemistry to the delivery of consistent meat quality with particular focus on the calpain system. *Meat Science*. 74. doi:10.1016/j.meatsci.2006.04.025.
- Koohmaraie, M., M. P. Kent, S. D. Shackelford, E. Veiseth, and T. L. Wheeler. 2002. Meat tenderness and muscle growth: Is there any relationship? In: *Meat Science*. Vol. 62. Elsevier. p. 345–352.
- Koutsidis, G., J. S. Elmore, M. J. Oruna-Concha, M. M. Campo, J. D. Wood, and D. S. Mottram. 2008. Water-soluble precursors of beef flavour: I. Effect of diet and breed. *Meat Science*. 79:124–130. doi:10.1016/j.meatsci.2007.08.008.
- Kuffi, K. D., S. Lescouhier, B. M. Nicolai, S. de Smet, A. Geeraerd, and P. Verboven. 2018. Modelling postmortem evolution of pH in beef M. biceps femoris under two different cooling regimes. *Journal of Food Science and Technology*. 55. doi:10.1007/s13197-017-2925-9.
- Lametsch, R., S. Lonergan, and E. Huff-Lonergan. 2008. Disulfide bond within μ -calpain active site inhibits activity and autolysis. *Biochimica et Biophysica Acta - Proteins and Proteomics*. 1784:1215–1221. doi:10.1016/j.bbapap.2008.04.018.
- Lana, A., and L. Zolla. 2016. Proteolysis in meat tenderization from the point of view of each single protein: A proteomic perspective. *Journal of Proteomics*. 147:85–97. doi:10.1016/j.jprot.2016.02.011.
- Larick, D. K., H. B. Hedrick, M. E. Bailey, J. E. Williams, D. L. Hancock, G. B. Garner, and R. E. Morrow. 1987. Flavor Constituents of Beef as Influenced by Forage- and Grain-Feeding. *Journal of Food Science*. 52:245–251. doi:10.1111/j.1365-2621.1987.tb06585.x.
- Ledward, D. A. 1985. Post-slaughter influences on the formation of metmyoglobin in beef muscles. *Meat Science*. 15. doi:10.1016/0309-1740(85)90034-8.
- Lefaucheur, L. 2010. A second look into fibre typing - Relation to meat quality. *Meat Science*. 84:257–270. doi:10.1016/j.meatsci.2009.05.004.
- Legako, J. F., J. C. Brooks, T. G. O’Quinn, T. D. J. Hagan, R. Polkinghorne, L. J. Farmer, and M. F. Miller. 2015. Consumer palatability scores and volatile beef flavor compounds of five USDA quality grades and four muscles. *Meat Science*. 100:291–300. doi:10.1016/j.meatsci.2014.10.026.
- Listrat, A., M. Gagaoua, J. Normand, D. Gruffat, D. Andueza, G. Mairesse, B. Mourot, G. Chesneau, C. Gobert, and B. Picard. 2020. Contribution of connective tissue components, muscle fibres and marbling to beef tenderness variability in

- longissimus thoracis, rectus abdominis, semimembranosus and semitendinosus muscles. *Journal of the Science of Food and Agriculture*. 100. doi:10.1002/jsfa.10275.
- Listrat, A., B. Leuret, I. Louveau, T. Astruc, M. Bonnet, L. Lefaucheur, B. Picard, and J. Bugeon. 2016. How Muscle Structure and Composition Influence Meat and Flesh Quality. *The Scientific World Journal*. 2016. doi:10.1155/2016/3182746.
- Liu, H. H., Y. Q. Wan, and G. L. Zou. 2006. Redox reactions and enzyme-like activities of immobilized myoglobin in aqueous/organic mixtures. *Journal of Electroanalytical Chemistry*. 594:111–117. doi:10.1016/j.jelechem.2006.05.027.
- Locker, R. H., and C. J. Hagyard. 1963. A cold shortening effect in beef muscles. *Journal of the Science of Food and Agriculture*. 14. doi:10.1002/jsfa.2740141103.
- Lomiwes, D., M. M. Farouk, E. Wiklund, and O. A. Young. 2014a. Small heat shock proteins and their role in meat tenderness: A review. *Meat Science*. 96:26–40. doi:10.1016/j.meatsci.2013.06.008.
- Lomiwes, D., M. M. Farouk, G. Wu, and O. A. Young. 2014b. The development of meat tenderness is likely to be compartmentalised by ultimate pH. *Meat Science*. 96:646–651. doi:10.1016/j.meatsci.2013.08.022.
- Lomiwes, D., S. M. Hurst, P. Dobbie, D. A. Frost, R. D. Hurst, O. A. Young, and M. M. Farouk. 2014c. The protection of bovine skeletal myofibrils from proteolytic damage post mortem by small heat shock proteins. *Meat Science*. 97:548–557. doi:10.1016/j.meatsci.2014.03.016.
- Lorenzen, C. L., C. R. Calkins, M. D. Green, R. K. Miller, J. B. Morgan, and B. E. Wasser. 2010. Efficacy of performing Warner-Bratzler and slice shear force on the same beef steak following rapid cooking. *Meat Science*. 85:792–794. doi:10.1016/j.meatsci.2010.03.030.
- Lucherik, L. W., T. G. O’Quinn, J. F. Legako, R. J. Rathmann, J. C. Brooks, and M. F. Miller. 2016. Consumer and trained panel evaluation of beef strip steaks of varying marbling and enhancement levels cooked to three degrees of doneness. *Meat Science*. 122:145–154. doi:10.1016/J.MEATSCI.2016.08.005.
- Lund, M. N., M. S. Hviid, and L. H. Skibsted. 2007. The combined effect of antioxidants and modified atmosphere packaging on protein and lipid oxidation in beef patties during chill storage. *Meat Science*. 76:226–233. doi:10.1016/j.meatsci.2006.11.003.
- Lynch, M. P., and C. Faustman. 2000. Effect of Aldehyde Lipid Oxidation Products on Myoglobin. *Journal of Agricultural and Food Chemistry*. 48. doi:10.1021/jf990732e.

- Maccougall, D. B. 1970. Characteristics of the appearance of meat I. —The luminous absorption, scatter and internal transmittance of the lean of bacon manufactured from normal and pale pork. *Journal of the Science of Food and Agriculture*. 21. doi:10.1002/jsfa.2740211107.
- Maddock, K. R., E. Huff-Lonergan, L. J. Rowe, and S. M. Lonergan. 2005. Effect of pH and ionic strength on μ - and m-calpain inhibition by calpastatin1. *Journal of Animal Science*. 83. doi:10.2527/2005.8361370x.
- Madhavi, D. L., and C. E. Carpenter. 1993. Aging and Processing Affect Color, Metmyoglobin Reductase and Oxygen Consumption of Beef Muscles. *Journal of Food Science*. 58. doi:10.1111/j.1365-2621.1993.tb06083.x.
- Malheiros, J. M., C. P. Braga, R. A. Grove, F. A. Ribeiro, C. R. Calkins, J. Adamec, and L. A. L. Chardulo. 2019. Influence of oxidative damage to proteins on meat tenderness using a proteomics approach. *Meat Science*. 148:64–71. doi:10.1016/j.meatsci.2018.08.016.
- Maltin, C. A., K. D. Sinclair, P. D. Warriss, C. M. Grant, A. D. Porter, M. I. Delday, and C. C. Warkup. 1998. The effects of age at slaughter, genotype and finishing system on the biochemical properties, muscle fibre type characteristics and eating quality of bull beef from suckled calves. *Animal Science*. 66. doi:10.1017/S1357729800009462.
- Mancini, R. A., and M. C. Hunt. 2005. Current research in meat color. In: *Meat Science*. Vol. 71. Elsevier. p. 100–121.
- Mancini, R. A., and R. Ramanathan. 2014. Effects of postmortem storage time on color and mitochondria in beef. *Meat Science*. 98:65–70. doi:10.1016/j.meatsci.2014.04.007.
- Marino, R., M. Albenzio, A. della Malva, A. Santillo, P. Loizzo, and A. Sevi. 2013. Proteolytic pattern of myofibrillar protein and meat tenderness as affected by breed and aging time. *Meat Science*. 95:281–287. doi:10.1016/j.meatsci.2013.04.009.
- Marsh, B. B. 1954. Rigor mortis in beef. *Journal of the Science of Food and Agriculture*. 5. doi:10.1002/jsfa.2740050202.
- Martínez-Reyes, I., and N. S. Chandel. 2020. Mitochondrial TCA cycle metabolites control physiology and disease. *Nature Communications*. 11. doi:10.1038/s41467-019-13668-3.
- Martins, S. I. F. S., and M. A. J. S. van Boekel. 2005. Kinetics of the glucose/glycine Maillard reaction pathways: Influences of pH and reactant initial concentrations. *Food Chemistry*. 92:437–448. doi:10.1016/j.foodchem.2004.08.013.

- Matarneh, S. K., C. N. Yen, J. Bodmer, S. W. El-Kadi, and D. E. Gerrard. 2021. Mitochondria influence glycolytic and tricarboxylic acid cycle metabolism under postmortem simulating conditions. *Meat Science*. 172:108316. doi:10.1016/j.meatsci.2020.108316.
- Matarneh, S. K., C. N. Yen, J. M. Elgin, M. Beline, S. da Luz e Silva, J. C. Wicks, E. M. England, R. A. Dalloul, M. E. Persia, I. I. Omara, H. Shi, and D. E. Gerrard. 2018. Phosphofructokinase and mitochondria partially explain the high ultimate pH of broiler pectoralis major muscle. *Poultry Science*. 97:1808–1817. doi:10.3382/ps/pex455.
- McCormick, R. J. 1994. The flexibility of the collagen compartment of muscle. *Meat Science*. 36. doi:10.1016/0309-1740(94)90035-3.
- McKeith, R. O., D. A. King, A. L. Grayson, S. D. Shackelford, K. B. Gehring, J. W. Savell, and T. L. Wheeler. 2016. Mitochondrial abundance and efficiency contribute to lean color of dark cutting beef. *Meat Science*. 116:165–173. doi:10.1016/j.meatsci.2016.01.016.
- McKenna, D. R., P. D. Mies, B. E. Baird, K. D. Pfeiffer, J. W. Ellebracht, and J. W. Savell. 2005. Biochemical and physical factors affecting discoloration characteristics of 19 bovine muscles. *Meat Science*. 70:665–682. doi:10.1016/j.meatsci.2005.02.016.
- Melody, J. L., S. M. Lonergan, L. J. Rowe, T. W. Huiatt, M. S. Mayes, and E. Huff-Lonergan. 2004. Early postmortem biochemical factors influence tenderness and water-holding capacity of three porcine muscles¹. *Journal of Animal Science*. 82. doi:10.2527/2004.8241195x.
- Miller, M. F., M. A. Carr, C. B. Ramsey, K. L. Crockett, and L. C. Hoover. 2001. Consumer thresholds for establishing the value of beef tenderness. *Journal of Animal Science*. 79. doi:10.2527/2001.79123062x.
- Mitacek, R. M., A. R. English, G. G. Mafi, D. L. VanOverbeke, and R. Ramanathan. 2018. Modified Atmosphere Packaging Improves Surface Color of Dark-Cutting Beef. *Meat and Muscle Biology*. 2:57–63. doi:10.22175/mmb2017.04.0023.
- Mitacek, R. M., Y. Ke, J. E. Prenni, R. Jadeja, D. L. VanOverbeke, G. G. Mafi, and R. Ramanathan. 2019. Mitochondrial Degeneration, Depletion of NADH, and Oxidative Stress Decrease Color Stability of Wet-Aged Beef Longissimus Steaks. *Journal of Food Science*. 84. doi:10.1111/1750-3841.14396.
- Morzell, M., P. Gatellier, T. Sayd, M. Renner, and E. Laville. 2006. Chemical oxidation decreases proteolytic susceptibility of skeletal muscle myofibrillar proteins. *Meat Science*. 73:536–543. doi:10.1016/j.meatsci.2006.02.005.
- Mottram, D. S. 1998. Flavour formation in meat and meat products: a review. *Food Chemistry*. 62. doi:10.1016/S0308-8146(98)00076-4.

- Nair, M. N., S. Li, C. M. Beach, G. Rentfrow, and S. P. Suman. 2018a. Changes in the Sarcoplasmic Proteome of Beef Muscles with Differential Color Stability during Postmortem Aging. *Meat and Muscle Biology*. 2:1–17. doi:10.22175/mmb2017.07.0037.
- Nair, M. N., S. Li, C. Beach, G. Rentfrow, and S. P. Suman. 2018b. Intramuscular Variations in Color and Sarcoplasmic Proteome of Beef during Postmortem Aging. *Meat and Muscle Biology*. 2:92–101. doi:10.22175/mmb2017.11.0055.
- Neely, T. R., C. L. Lorenzen, R. K. Miller, J. D. Tatum, J. W. Wise, J. F. Taylor, M. J. Buyck, J. O. Reagan, and J. W. Savell. 1998. Beef customer satisfaction: role of cut, USDA quality grade, and city on in-home consumer ratings. *Journal of Animal Science*. 76. doi:10.2527/1998.7641027x.
- Nowak, D. 2011. Enzymes in tenderization of meat - the system of calpains and other systems - a review. *Polish Journal of Food and Nutrition Sciences*. 61:231–237. doi:10.2478/v10222-011-0025-5.
- Nyquist, K. M., T. G. O’Quinn, L. N. Drey, L. W. Lucher, J. C. Brooks, M. F. Miller, and J. F. Legako. 2018. Palatability of beef chuck, loin, and round muscles from three USDA quality grades¹. *Journal of Animal Science*. 96:4276–4292. doi:10.1093/jas/sky305.
- Olson, B. A., E. A. Rice, L. L. Prill, L. N. Drey, J. M. Gonzalez, J. L. Vipham, M. D. Chao, and T. G. O’Quinn. 2019. Evaluation of Beef Top Sirloin Steaks of Four Quality Grades Cooked to Three Degrees of Doneness. *Meat and Muscle Biology*. 3:399–410. doi:10.22175/mmb2019.07.0022.
- O’Quinn, T. G., J. F. Legako, J. C. Brooks, and M. F. Miller. 2018. Evaluation of the contribution of tenderness, juiciness, and flavor to the overall consumer beef eating experience. *Translational Animal Science*. 2. doi:10.1093/tas/txx008.
- Ordway, G. A., and D. J. Garry. 2004. Myoglobin: an essential hemoprotein in striated muscle. *Journal of Experimental Biology*. 207. doi:10.1242/jeb.01172.
- Ouali, A., M. Gagaoua, Y. Boudida, S. Becila, A. Boudjellal, C. H. Herrera-Mendez, and M. A. Sentandreu. 2013. Biomarkers of meat tenderness: Present knowledge and perspectives in regards to our current understanding of the mechanisms involved. *Meat Science*. 95:854–870. doi:10.1016/j.meatsci.2013.05.010.
- Page, J. K., D. M. Wulf, and T. R. Schwotzer. 2001. A survey of beef muscle color and pH. *Journal of Animal Science*. 79:678–687. doi:10.2527/2001.793678x.
- Park, D., Y. L. Xiong, A. L. Alderton, and T. Ooizumi. 2006. Biochemical Changes in Myofibrillar Protein Isolates Exposed to Three Oxidizing Systems. *Journal of Agricultural and Food Chemistry*. 54. doi:10.1021/jf0531813.

- Picard, B., C. Barboiron, D. Chadeyron, and C. Jurie. 2011. Protocol for high-resolution electrophoresis separation of myosin heavy chain isoforms in bovine skeletal muscle. *Electrophoresis*. 32:1804–1806. doi:10.1002/elps.201100118.
- Picard, B., and M. Gagaoua. 2017. Proteomic Investigations of Beef Tenderness. In: *Proteomics in Food Science*. Elsevier.
- Picard, B., and M. Gagaoua. 2020. Meta-proteomics for the discovery of protein biomarkers of beef tenderness: An overview of integrated studies. *Food Research International*. 127:108739. doi:10.1016/j.foodres.2019.108739.
- Picard, B., M. Gagaoua, D. Micol, I. Cassar-Malek, J.-F. Hocquette, and C. E. M. Terlouw. 2014. Inverse Relationships between Biomarkers and Beef Tenderness According to Contractile and Metabolic Properties of the Muscle. *Journal of Agricultural and Food Chemistry*. 62. doi:10.1021/jf501528s.
- Picard, M., K. Csukly, M.-E. Robillard, R. Godin, A. Ascah, C. Bourcier-Lucas, and Y. Burelle. 2008. Resistance to Ca²⁺ -induced opening of the permeability transition pore differs in mitochondria from glycolytic and oxidative muscles. *American Journal of Physiology-Regulatory, Integrative and Comparative Physiology*. 295. doi:10.1152/ajpregu.90357.2008.
- Picard, M., R. T. Hepple, and Y. Burelle. 2012. Mitochondrial functional specialization in glycolytic and oxidative muscle fibers: tailoring the organelle for optimal function. *American Journal of Physiology-Cell Physiology*. 302. doi:10.1152/ajpcell.00368.2011.
- Ponce, J., J. C. Brooks, and J. F. Legako. 2019. Consumer Liking and Descriptive Flavor Attributes of M. Longissimus Lumborum and M. Gluteus Medius Beef Steaks Held in Varied Packaging Systems. *Meat and Muscle Biology*. 3:158–170. doi:10.22175/mmb2018.12.0041.
- Ponnampalam, E. N., D. L. Hopkins, H. Bruce, D. Li, G. Baldi, and A. E. Bekhit. 2017. Causes and Contributing Factors to “Dark Cutting” Meat: Current Trends and Future Directions: A Review. *Comprehensive Reviews in Food Science and Food Safety*. 16. doi:10.1111/1541-4337.12258.
- Pösö, A. R., and E. Puolanne. 2005. Carbohydrate metabolism in meat animals. In: *Meat Science*. Vol. 70. Elsevier Ltd. p. 423–434.
- Promeyrat, A., T. Sayd, E. Laville, C. Chambon, B. Lebreton, and Ph. Gatellier. 2011. Early post-mortem sarcoplasmic proteome of porcine muscle related to protein oxidation. *Food Chemistry*. 127. doi:10.1016/j.foodchem.2011.01.108.
- Przybylski, W., P. Vernin, and G. Monin. 1994. Relationship between glycolytic potential and ultimate pH in bovine, porcine and ovine muscles. *Journal of Muscle Foods*. 5. doi:10.1111/j.1745-4573.1994.tb00534.x.

- Purslow, P. P., M. Gagaoua, and R. D. Warner. 2021. Insights on meat quality from combining traditional studies and proteomics. *Meat Science*. 174:108423. doi:10.1016/j.meatsci.2020.108423.
- R Core Team. 2020. R: A language and environment for statistical computing. Available from: <https://www.R-project.org/>.
- Ramanathan, R., F. Kiyimba, J. Gonzalez, G. Mafi, and U. DeSilva. 2020a. Impact of Up- and Downregulation of Metabolites and Mitochondrial Content on pH and Color of the Longissimus Muscle from Normal-pH and Dark-Cutting Beef. *Journal of Agricultural and Food Chemistry*. 68. doi:10.1021/acs.jafc.0c01884.
- Ramanathan, R., and R. A. Mancini. 2018. Role of Mitochondria in Beef Color: A Review. *Meat and Muscle Biology*. 2:309. doi:10.22175/mmb2018.05.0013.
- Ramanathan, R., R. A. Mancini, G. A. Dady, and C. B. van Buiten. 2013. Effects of succinate and pH on cooked beef color. *Meat Science*. 93:888–892. doi:10.1016/j.meatsci.2012.12.007.
- Ramanathan, R., R. A. Mancini, and M. R. Konda. 2009. Effects of Lactate on Beef Heart Mitochondrial Oxygen Consumption and Muscle Darkening. *Journal of Agricultural and Food Chemistry*. 57. doi:10.1021/jf802933p.
- Ramanathan, R., R. A. Mancini, and N. B. Maheswarappa. 2010. Effects of Lactate on Bovine Heart Mitochondria-Mediated Metmyoglobin Reduction. *Journal of Agricultural and Food Chemistry*. 58. doi:10.1021/jf1002842.
- Ramanathan, R., R. A. Mancini, S. P. Suman, and C. M. Beach. 2014. Covalent binding of 4-hydroxy-2-nonenal to lactate dehydrogenase decreases nadh formation and metmyoglobin reducing activity. *Journal of Agricultural and Food Chemistry*. 62:2112–2117. doi:10.1021/jf404900y.
- Ramanathan, R., R. A. Mancini, S. P. Suman, and M. E. Cantino. 2012. Effects of 4-hydroxy-2-nonenal on beef heart mitochondrial ultrastructure, oxygen consumption, and metmyoglobin reduction. *Meat Science*. 90:564–571. doi:10.1016/j.meatsci.2011.09.017.
- Ramanathan, R., M. N. Nair, Y. Wang, S. Li, C. M. Beach, R. A. Mancini, K. Belskie, and S. P. Suman. 2021. Differential abundance of mitochondrial proteome influences the color stability of beef longissimus lumborum and psoas major muscles. *Meat and Muscle Biology*. 5:1–16. doi:10.22175/mmb.11705.
- Ramanathan, R., S. P. Suman, and C. Faustman. 2020b. Biomolecular Interactions Governing Fresh Meat Color in Post-mortem Skeletal Muscle: A Review. *Journal of Agricultural and Food Chemistry*. 68. doi:10.1021/acs.jafc.9b08098.

- Renand, G., B. Picard, C. Touraille, P. Berge, and J. Lepetit. 2001. Relationships between muscle characteristics and meat quality traits of young Charolais bulls. *Meat Science*. 59:49–60. doi:10.1016/S0309-1740(01)00051-1.
- Resconi, V., A. Escudero, and M. Campo. 2013. The Development of Aromas in Ruminant Meat. *Molecules*. 18. doi:10.3390/molecules18066748.
- Rosell, C. M., M. Flores, and F. Toldrá. 1996. Myoglobin as an Endogenous Inhibitor of Proteolytic Muscle Enzymes. *Journal of Agricultural and Food Chemistry*. 44. doi:10.1021/jf9601022.
- Rowe, L. J., K. R. Maddock, S. M. Lonergan, and E. Huff-Lonergan. 2004. Influence of early postmortem protein oxidation on beef quality. *Journal of Animal Science*. 82. doi:10.2527/2004.823785x.
- Salim, A. P. A. A., S. P. Suman, A. C. V. C. S. Canto, B. R. C. Costa-Lima, F. M. Viana, M. L. G. Monteiro, T. J. P. Silva, and C. A. Conte-Junior. 2019. Muscle-specific color stability in fresh beef from grain-finished *Bos indicus* cattle. *Asian-Australasian Journal of Animal Sciences*. 32. doi:10.5713/ajas.18.0531.
- Scheffler, T. L., and D. E. Gerrard. 2007. Mechanisms controlling pork quality development: The biochemistry controlling postmortem energy metabolism. *Meat Science*. 77:7–16. doi:10.1016/j.meatsci.2007.04.024.
- Scheffler, T. L., S. K. Matarneh, E. M. England, and D. E. Gerrard. 2015. Mitochondria influence postmortem metabolism and pH in an in vitro model. *Meat Science*. 110:118–125. doi:10.1016/j.meatsci.2015.07.007.
- Schenkel, L. C., and M. Bakovic. 2014. Formation and Regulation of Mitochondrial Membranes. *International Journal of Cell Biology*. 2014. doi:10.1155/2014/709828.
- Schiaffino, S., and C. Reggiani. 1996. Molecular diversity of myofibrillar proteins: gene regulation and functional significance. *Physiological Reviews*. 76. doi:10.1152/physrev.1996.76.2.371.
- Scopes, R. K. 1974. Studies with a reconstituted muscle glycolytic system. The rate and extent of glycolysis in simulated post-mortem conditions. *Biochemical Journal*. 142. doi:10.1042/bj1420079.
- Seideman, S. C., H. R. Cross, G. C. Smith, and P. R. Durland. 1984. Factors associated with fresh meat color: A review. *Journal of Food Quality*. 6. doi:10.1111/j.1745-4557.1984.tb00826.x.
- Setyabrata, D., B. R. Cooper, T. J. P. Sobreira, J. F. Legako, S. Martini, and Y. H. B. Kim. 2021. Elucidating mechanisms involved in flavor generation of dry-aged beef loins using metabolomics approach. *Food Research International*. 139:109969. doi:10.1016/j.foodres.2020.109969.

- Seyfert, M., R. A. Mancini, M. C. Hunt, J. Tang, C. Faustman, and M. Garcia. 2006. Color stability, reducing activity, and cytochrome c oxidase activity of five bovine muscles. *Journal of Agricultural and Food Chemistry*. 54:8919–8925. doi:10.1021/jf061657s.
- Shackelford, S. D., M. Koohmaraie, L. v. Cundiff, K. E. Gregory, G. A. Rohrer, and J. W. Savell. 1994. Heritabilities and phenotypic and genetic correlations for bovine postrigor calpastatin activity, intramuscular fat content, Warner-Bratzler shear force, retail product yield, and growth rate. *Journal of Animal Science*. 72. doi:10.2527/1994.724857x.
- Shackelford, S. D., T. L. Wheeler, D. A. King, and M. Koohmaraie. 2012. Field testing of a system for online classification of beef carcasses for longissimus tenderness using visible and near-infrared reflectance spectroscopy. *Journal of Animal Science*. 90:978–988. doi:10.2527/jas.2011-4167.
- Shackelford, S. D., T. L. Wheeler, and M. Koohmaraie. 1999. Evaluation of slice shear force as an objective method of assessing beef longissimus tenderness. *Journal of Animal Science*. 77. doi:10.2527/1999.77102693x.
- Shackelford, S. D., T. L. Wheeler, and M. Koohmaraie. 2003. On-line prediction of yield grade, longissimus muscle area, preliminary yield grade, adjusted preliminary yield grade, and marbling score using the MARC beef carcass image analysis system. *Journal of Animal Science*. 81. doi:10.2527/2003.811150x.
- Shackelford, S. D., T. L. Wheeler, M. K. Meade, J. O. Reagan, B. L. Byrnes, and M. Koohmaraie. 2001. Consumer impressions of Tender Select beef. *Journal of Animal Science*. 79. doi:10.2527/2001.79102605x.
- Sitz, B. M., C. R. Calkins, D. M. Feuz, W. J. Umberger, and K. M. Eskridge. 2005. Consumer sensory acceptance and value of domestic, Canadian, and Australian grass-fed beef steaks. *Journal of Animal Science*. 83. doi:10.2527/2005.83122863x.
- Stetzer, A. J., E. Tucker, F. K. McKeith, and M. S. Brewer. 2007. Quality Changes in Beef Complexus, Serratus Ventralis, Vastus Lateralis, Vastus Medialis, and Longissimus Dorsi Muscles Enhanced Prior to Aging. *Journal of Food Science*. 73. doi:10.1111/j.1750-3841.2007.00582.x.
- Suman, S. P., C. Faustman, S. L. Stamer, and D. C. Liebler. 2006. Redox Instability Induced by 4-Hydroxy-2-nonenal in Porcine and Bovine Myoglobins at pH 5.6 and 4 °C. *Journal of Agricultural and Food Chemistry*. 54. doi:10.1021/jf052811y.
- Suman, Surendranath P., M. C. Hunt, M. N. Nair, and G. Rentfrow. 2014. Improving beef color stability: Practical strategies and underlying mechanisms. *Meat Science*. 98. doi:10.1016/j.meatsci.2014.06.032.

- Suman, S. P., and P. Joseph. 2013. Myoglobin Chemistry and Meat Color. *Annual Review of Food Science and Technology*. 4:79–99. doi:10.1146/annurev-food-030212-182623.
- Suman, S. P., G. Rentfrow, M. N. Nair, and P. Joseph. 2014. Proteomics of muscle- and species-specificity in meat color stability. *Journal of Animal Science*. 92. doi:10.2527/jas.2013-7277.
- Tang, J., C. Faustman, T. A. Hoagland, R. A. Mancini, M. Seyfert, and M. C. Hunt. 2005a. Postmortem oxygen consumption by mitochondria and its effects on myoglobin form and stability. *Journal of Agricultural and Food Chemistry*. 53:1223–1230. doi:10.1021/jf048646o.
- Tang, J., C. Faustman, R. A. Mancini, M. Seyfert, and M. C. Hunt. 2005b. Mitochondrial reduction of metmyoglobin: Dependence on the electron transport chain. *Journal of Agricultural and Food Chemistry*. 53:5449–5455. doi:10.1021/jf050092h.
- Toldrá, F., and M. Flores. 2000. The use of muscle enzymes as predictors of pork meat quality. *Food Chemistry*. 69:387–395. doi:10.1016/S0308-8146(00)00052-2.
- Trinderup, C. H., and Y. H. B. Kim. 2015. Fresh meat color evaluation using a structured light imaging system. *Food Research International*. 71:100–107. doi:10.1016/J.FoodRes.2015.02.013.
- USDA. 2017. USDA A.M. Service (Ed.), United States standards for grades of carcass beef, United States Department of Agriculture, Washington, DC.
- Vasta, V., and A. Priolo. 2006. Ruminant fat volatiles as affected by diet. A review. *Meat Science*. 73:218–228. doi:10.1016/j.meatsci.2005.11.017.
- Vierck, K. R., J. F. Legako, J. K. Kim, B. Johnson, and J. C. Brooks. 2020. Determination of Package and Muscle-Type Influence on Proteolysis, Beef-Flavor-Contributing Free Amino Acids, Final Beef Flavor, and Tenderness. *Meat and Muscle Biology*. 4:1–14. doi:10.22175/mmb.10933.
- Vierck, K. R., K. v. McKillip, T. G. O’Quinn, and J. F. Legako. 2019. The Impact of Enhancement, Degree of Doneness, and USDA Quality Grade on Beef Flavor Development. *Meat and Muscle Biology*. 3:299–312. doi:10.22175/mmb2019.05.0014.
- Vierck, K. R., T. G. O’Quinn, J. A. Noel, T. A. Houser, E. A. E. Boyle, and J. M. Gonzalez. 2018. Effects of Marbling Texture on Muscle Fiber and Collagen Characteristics. *Meat and Muscle Biology*. 2:75–82. doi:10.22175/mmb2017.10.0054.
- Volle, B., D. Dutaud, and A. Ouali. 1999. Myoglobin inhibition of most protease activities measured with fluorescent substrates is an artifact! *Meat Science*. 52. doi:10.1016/S0309-1740(98)00151-X.

- Wang, Y., S. Li, G. Rentfrow, J. Chen, H. Zhu, and S. P. Suman. 2021. Myoglobin Post-Translational Modifications Influence Color Stability of Beef Longissimus Lumborum. *Meat and Muscle Biology*. 5:1–21. doi:10.22175/mmb.11689.
- Warner, R. D., F. R. Dunshea, E. N. Ponnampalam, and J. J. Cottrell. 2005. Effects of nitric oxide and oxidation in vivo and postmortem on meat tenderness. In: *Meat Science*. Vol. 71. Elsevier. p. 205–217.
- Warner, R. D., P. L. Greenwood, D. W. Pethick, and D. M. Ferguson. 2010. Genetic and environmental effects on meat quality. *Meat Science*. 86:171–183. doi:10.1016/j.meatsci.2010.04.042.
- Warriss, P. D., S. C. Kestin, C. S. Young, E. A. Bevis, and S. N. Brown. 1990. Effect of preslaughter transport on carcass yield and indices of meat quality in sheep. *Journal of the Science of Food and Agriculture*. 51. doi:10.1002/jsfa.2740510408.
- Watanabe, A., C. C. Daly, and C. E. Devine. 1996. The effects of the ultimate pH of meat on tenderness changes during ageing. *Meat Science*. 42:67–78. doi:10.1016/0309-1740(95)00012-7.
- Watanabe, A., G. Kamada, M. Imanari, N. Shiba, M. Yonai, and T. Muramoto. 2015. Effect of aging on volatile compounds in cooked beef. *Meat Science*. 107:12–19. doi:10.1016/j.meatsci.2015.04.004.
- Werkhoff, P., J. Bruening, R. Emberger, M. Guentert, M. Koepsel, W. Kuhn, and H. Surburg. 1990. Isolation and characterization of volatile sulfur-containing meat flavor components in model systems. *Journal of Agricultural and Food Chemistry*. 38. doi:10.1021/jf00093a041.
- Weston, A. R., R. W. Rogers, and T. G. Althen. 2002. Review: The Role of Collagen in Meat Tenderness. *The Professional Animal Scientist*. 18. doi:10.15232/S1080-7446(15)31497-2.
- Wheeler, T. L., S. D. Shackelford, and M. Koohmaraie. 1998. Cooking and palatability traits of beef longissimus steaks cooked with a belt grill or an open hearth electric broiler. *Journal of Animal Science*. 76:2805–2810. doi:10.2527/1998.76112805x.
- White, A., A. O’Sullivan, E. E. O’Neill, and D. J. Troy. 2006. Manipulation of the pre-rigor phase to investigate the significance of proteolysis and sarcomere length in determining the tenderness of bovine *M. longissimus dorsi*. *Meat Science*. 73:204–208. doi:10.1016/j.meatsci.2005.11.022.
- Wicks, J., M. Beline, J. F. M. Gomez, S. Luzardo, S. L. Silva, and D. Gerrard. 2019. Muscle Energy Metabolism, Growth, and Meat Quality in Beef Cattle. *Agriculture*. 9. doi:10.3390/agriculture9090195.
- Wismer-Pederson, J. 1959. Quality of Pork in Relation to Rate of pH Change Post Mortem. *Journal of Food Science*. 24. doi:10.1111/j.1365-2621.1959.tb17325.x.

- Wittenberg, J. B., and B. A. Wittenberg. 2003. Myoglobin function reassessed. *Journal of Experimental Biology*. 206. doi:10.1242/jeb.00243.
- Wright, S. A., P. Ramos, D. D. Johnson, J. M. Scheffler, M. A. Elzo, R. G. Mateescu, A. L. Bass, C. C. Carr, and T. L. Scheffler. 2018. Brahman genetics influence muscle fiber properties, protein degradation, and tenderness in an Angus-Brahman multibreed herd. *Meat Science*. 135:84–93. doi:10.1016/j.meatsci.2017.09.006.
- Wu, S., X. Luo, X. Yang, D. L. Hopkins, Y. Mao, and Y. Zhang. 2020. Understanding the development of color and color stability of dark cutting beef based on mitochondrial proteomics. *Meat Science*. 163. doi:10.1016/j.meatsci.2020.108046.
- Wulf, D. M., R. S. Emmett, J. M. Leheska, and S. J. Moeller. 2002. Relationships among glycolytic potential, dark cutting (dark, firm, and dry) beef, and cooked beef palatability¹. *Journal of Animal Science*. 80. doi:10.2527/2002.8071895x.
- Wulf, D. M., S. F. O'Connor, J. D. Tatum, and G. C. Smith. 1997. Using objective measures of muscle color to predict beef longissimus tenderness. *Journal of Animal Science*. 75. doi:10.2527/1997.753684x.
- Wulf, D. M., and J. K. Page. 2000. Using measurements of muscle color, pH, and electrical impedance to augment the current USDA beef quality grading standards and improve the accuracy and precision of sorting carcasses into palatability groups. *Journal of Animal Science*. 78. doi:10.2527/2000.78102595x.
- Wulf, D. M., J. D. Tatum, R. D. Green, J. B. Morgan, B. L. Golden, and G. C. Smith. 1996. Genetic influences on beef longissimus palatability in charolais- and limousin-sired steers and heifers. *Journal of Animal Science*. 74. doi:10.2527/1996.74102394x.
- Wyrwicz, J., M. Moczowska, M. Kurek, A. Stelmasiak, A. Półtorak, and A. Wierzbicka. 2016. Influence of 21 days of vacuum-aging on color, bloom development, and WBSF of beef semimembranosus. *Meat Science*. 122:48–54. doi:10.1016/j.meatsci.2016.07.018.
- Yancey, E. J., M. E. Dikeman, K. A. Hachmeister, E. Chambers, and G. A. Milliken. 2005. Flavor characterization of top-blade, top-sirloin, and tenderloin steaks as affected by pH, maturity, and marbling^{1,2,3}. *Journal of Animal Science*. 83. doi:10.2527/2005.83112618x.
- Yin, S., C. Faustman, N. Tatiyaborworntham, R. Ramanathan, N. B. Maheswarappa, R. A. Mancini, P. Joseph, S. P. Suman, and Q. Sun. 2011. Species-Specific Myoglobin Oxidation. *Journal of Agricultural and Food Chemistry*. 59. doi:10.1021/jf202844t.
- Yong, H. I., M. Han, H.-J. Kim, J.-Y. Suh, and C. Jo. 2018. Mechanism Underlying Green Discolouration of Myoglobin Induced by Atmospheric Pressure Plasma.

Scientific Reports. 8:9790-undefined. doi:10.1038/s41598-018-28096-4. Available from: www.nature.com/scientificreports/

- Yu, Q., X. Tian, L. Shao, X. Li, and R. Dai. 2019. Targeted metabolomics to reveal muscle-specific energy metabolism between bovine longissimus lumborum and psoas major during early postmortem periods. *Meat Science*. 156:166–173. doi:10.1016/j.meatsci.2019.05.029.
- Yu, Q., W. Wu, X. Tian, F. Jia, L. Xu, R. Dai, and X. Li. 2017. Comparative proteomics to reveal muscle-specific beef color stability of Holstein cattle during post-mortem storage. *Food Chemistry*. 229:769–778. doi:10.1016/j.foodchem.2017.03.004.
- Zakrys, P. I., M. G. O’Sullivan, P. Allen, and J. P. Kerry. 2009. Consumer acceptability and physiochemical characteristics of modified atmosphere packed beef steaks. *Meat Science*. 81:720–725. doi:10.1016/j.meatsci.2008.10.024.
- Zakrys-Waliwander, P. I., M. G. O’Sullivan, E. E. O’Neill, and J. P. Kerry. 2012. The effects of high oxygen modified atmosphere packaging on protein oxidation of bovine M. longissimus dorsi muscle during chilled storage. *Food Chemistry*. 131:527–532. doi:10.1016/J.FOODCHEM.2011.09.017.
- Zeece, M. G., and K. Katoh. 1989. Cathepsin D and its effects on myofibrillar proteins: A review. *Journal of Food Biochemistry*. 13. doi:10.1111/j.1745-4514.1989.tb00391.x.
- Zhang, J., D. Ma, and Y. H. B. Kim. 2020. Mitochondrial apoptosis and proteolytic changes of myofibrillar proteins in two different pork muscles during aging. *Food Chemistry*. 319:126571. doi:10.1016/j.foodchem.2020.126571.
- Zhang, Y. min, D. L. Hopkins, X. xiao Zhao, R. van de Ven, Y. wei Mao, L. xian Zhu, G. xing Han, and X. Luo. 2018. Characterisation of pH decline and meat color development of beef carcasses during the early postmortem period in a Chinese beef cattle abattoir. *Journal of Integrative Agriculture*. 17:1691–1695. doi:10.1016/S2095-3119(17)61890-2.

Vita

Jade Victoria Cooper was born in Norman, Oklahoma on December 15, 1993, and spent the majority of her life living in southwest Oklahoma, in a town called Chickasha. Jade graduated from Chickasha High School in May of 2011 after spending years showing cattle and hogs and competitively public speaking in FFA; Jade decided to pursue a food science degree at Oklahoma State University.

While at Oklahoma State, Jade was under the guidance of Dr. Deb VanOverbeke, who introduced Jade to meat science. After discovering her passion for the industry, Jade decided to continue her education with a master's degree in animal science. Jade was introduced to Dr. Carol Lorenzen by Dr. VanOverbeke. After completing a summer internship at the University of Missouri in Dr. Lorenzen's lab, Jade was accepted to complete an M.S. program beginning the following Spring semester. Jade graduated from Oklahoma State in December of 2014 and began her M.S. at the University of Missouri in January of 2015 under Dr. Lorenzen.

After completing her master's program with Dr. Lorenzen in May of 2017, Jade spent six months working as the HACCP Coordinator at Jennings Premium Meats in New Franklin, MO. She returned to Dr. Lorenzen's lab in January of 2018 to begin a Ph.D. program. Jade has spent the last year and a half of her Ph.D. program at the US Meat Animal Research Center in Clay Center, NE working in Dr. Andy King's lab.